Dispersion relations in magnetized plasmas

Adrien Fontaine

▶ **To cite this version:**

Adrien Fontaine. Dispersion relations in magnetized plasmas. Mathematical Physics [math-ph]. Université de Rennes, 2017. English. NNT : 2017REN1S029 . tel-01646853

HAL Id: tel-01646853
https://theses.hal.science/tel-01646853

Submitted on 23 Nov 2017

HAL is a multi-disciplinary open access archive for the deposit and dissemination of scientific research documents, whether they are published or not. The documents may come from teaching and research institutions in France or abroad, or from public or private research centers.

L'archive ouverte pluridisciplinaire **HAL**, est destinée au dépôt et à la diffusion de documents scientifiques de niveau recherche, publiés ou non, émanant des établissements d'enseignement et de recherche français ou étrangers, des laboratoires publics ou privés.

ANNÉE 2017

UNIVERSITÉ DE RENNES 1

UNIVERSITE BRETAGNE LOIRE

THÈSE / UNIVERSITÉ DE RENNES 1
sous le sceau de l'Université Bretagne Loire

pour le grade de

DOCTEUR DE L'UNIVERSITÉ DE RENNES 1

Mention : Mathématiques et applications

École doctorale MATISSE

présentée par

Adrien Fontaine

préparée à l'unité de recherche UMR 6625 du CNRS : IRMAR
Institut de Recherche Mathématiques de Rennes
U.F.R de Mathématiques

Relations de dispersion dans les plasmas magnétisés

Thèse soutenue à Rennes
le 04/07/2017

devant le jury composé de :

Anne NOURI
Professeure, Univ. Marseille / rapportrice

Zied AMMARI
Maître de conférence, Univ. Rennes 1 / examinateur

Guy MÉTIVIER
Professeur, Univ. Bordeaux 1 / examinateur

Miguel RODRIGUES
Professeur, Univ. Rennes 1 / examinateur

Frédéric ROUSSET
Professeur, Univ. Paris IX / examinateur

Christophe CHEVERRY
Professeur, Univ. Rennes 1/ directeur de thèse

À Georges et Marie-Thérèse

REMERCIEMENTS

En premier lieu, je tiens à remercier mon directeur de thèse, Christophe Cheverry, pour m'avoir fait découvrir le monde de la recherche, pour tout le temps qu'il m'a consacré au cours des trois dernières années, et pour sa relecture minutieuse de mes différentes productions. Et je le prie de bien vouloir m'excuser si certains mots se retrouvent malheureusement coupés à la fin d'une ligne dans ces remerciements.

Je tiens à remercier Alain Brizard et Anne Nouri, pour avoir accepté la lourde tache de rapporteurs. Leurs remarques ont sans aucun doute contribué à améliorer la qualité de ce mémoire de thèse. Je remercie également Guy Métivier, Frédéric Rousset, Miguel Rodrigues et Zied Ammari qui m'ont fait le plaisir de venir compléter mon jury.

La bonne ambiance qui règne au sein de l'IRMAR en fait un lieu où il est très agréable de travailler. Aussi, je voudrais remercier vivement les équipes de l'IRMAR tant du côté de la recherche que du côté administratif. Un grand merci à Marie-Aude, Chantal, Hélène, Xhensila, Carole, Nicole, Emmanuelle, pour avoir toujours su garder leur calme devant mon incapacité chronique à faire face aux affres de l'administration. Merci également à tous les chercheurs (et même les algébristes!) avec qui j'ai pu partager un café, un thé ou une discussion. Je remercie également les équipes de l'ENS, et en particulier Arnaud Debussche pour m'avoir encouragé à aller jusqu'au bout.

L'enseignement aura été pour moi une véritable bouffée d'air quand je me perdais dans les articles de physique totalement abscons, et les calculs sans fin. Je remercie très sincèrement Benoît Cadre pour m'avoir donné l'opportunité de faire mes enseignements à l'ENS Rennes. Je remercie également Thibaut Deheuvels de m'avoir fait participer à la préparation à l'agrégation. J'ai pris beaucoup de plaisir à passer du côté obscur de la force, lors des oraux blancs. Enfin, un immense merci à Karine Beauchard. Assurer l'enseignement d'EVNCD à ses côtés a été un vrai plaisir. Mais bien au delà de ça, elle a été un soutien indéfectible au cours de ces trois années. Je l'ai écoutée, je n'ai RIEN LÂCHÉ!! Ses qualités humaines et pédagogiques resteront un exemple pour moi dans ma carrière d'enseignant.

La thèse marque la fin d'un long cheminement. Aussi, je souhaite remercier tous ceux qui m'ont accompagné le long de cette route. Mr Andrieux, qui m'a appris que l'on pouvait appeler un carré autrement que ABCD. Mr Raymond, qui m'a démontré le théorème de Pythagore (la première démonstration de ma vie!). Mme Mouchard, qui m'aura fait aimer l'analyse et détester les statistiques. Mr Braconnier, grâce à qui je ne suis pas prêt d'oublier mes formules de trigo. Grégoire Taviot, qui m'aura appris que "Diviser par zéro, c'est mal!" (il aura fallu attendre la sup pour que je comprenne ça...). Stéphane Legros, qui en plus de m'avoir appris le Théorème de Cantor-Bernstein, m'a donné l'exemple du professeur que je voulais devenir. Jean-Claude Sikorav, qui malgré ses efforts, n'a pas su me faire renoncer à l'axiome du choix. Séverine Rigot, grâce à qui je sais parfaitement justifier qu'une fonction est mesurable. Michel Pierre, dont j'aimerais garder la même

joie à transmettre les mathématiques tout au long de ma carrière. François Castella, qui m'aura appris qu'une fonction peut être un type à qui on a envie de casser la gueule. Et bien d'autres encore, qui ont contribué de près ou de loin, à faire de moi le mathématicien que je suis aujourd'hui.

Je tiens également à remercier mes amis de Rennes et d'ailleurs. Le groupe de tarot (dont le simple nom m'ennuie déjà), avec qui on passe toujours des super moments. Les amis de toujours, Paul, Simon, Clémence et Juliette. Olivier, dont la traîtrise nantaise a encore du mal à passer. Anaïs et Quentin, dont l'amitié m'est très chère. Merci d'avoir écouter tous mes déboires sans jamais vous plaindre! Merci aux amis de la promo maths2011 qui ont désormais quitté Rennes mais que j'ai toujours beaucoup de plaisir à revoir: Tristan et Pauline, dont l'hospitalité n'est plus à prouver, et Jean-Jérôme, pour son amour de la côte de boeuf. Merci aux compagnons d'infortune de l'agrégation: PAM, Clément et Florentin.

Et puis il y a tous les doctorants matheux de Rennes. Mes cobureaux successifs: Valentin qui aura été là jusqu'au bout et que je suis désolé d'abandonner pour les derniers mois, Loïc qui a fui le soleil de Rennes pour les nuages marseillais, et Joackim, le nouveau, devenu mon coach course à pied personnel. Et puis il y a les autres, qui sont là depuis plus ou moins longtemps! Coralie et Basile, évidemment! Merci pour le canapé! Ceux qui sont déjà partis: Hélène, Julie, Arnaud, Ophélie, Jean-Phi, Salomé, Tristan, Florian, Richard, Charles, Damien. Les anciens, Vincent, Yvan, Blandine (qui m'a mis une sacré pression pour le pot de thèse), Alexandre B., Alexandre L. M., Mac, Maxime, Romain, Pierig, Nestor, Federico, Clément, Hélène, Cyril, Grégory, Tristan, Olivier. Et les nouveaux, Kévin, Simon (coach assistant), Florian, Camille, Adrien, Ninon, Arnaud, Zoïs, Thi, Tho.

Je devrais sans doute dire quelque chose pour Axel, car il a été un véritable ami pendant ces trois ans! Mais, il m'a aussi fait perdre énormément de temps pendant cette thèse, entre les entraînements triathlon, les pauses café, et les soirées ciné. À défaut, merci pour *Moon*. Il est cool ce film.

Merci, évidemment, à Roger, pour le 18ème.

Je remercie également ma deuxième famille. Marc et Anne-Cécile, qui m'ont accueilli avec beaucoup de gentillesse et de générosité. Et puis évidemment, Nathan, Clémentine et Wandrille, qui n'ont de beauf que le titre. Merci aussi à Mathilde, qui a gentiment accepté de venir vider notre frigo plusieurs fois par semaine, pendant sa période rennaise.

Je remercie bien évidemment mes parents. Pour m'avoir toujours encouragé dans la voie que j'avais suivie. Et puis avant tout pour leur amour. Merci à mon frère Pierre, et à ma soeur Adèle, d'être là même quand ils ne sont pas là. Merci à mes grands parents, qui ont suivi mon parcours avec toute l'attention et l'affection qui les caractérisent.

Enfin à Marine, qui m'a permis de dormir 10 minutes de plus tous les matins en me préparant le petit déjeuner. Merci aussi pour sa patience, son soutien et son amour. Cette thèse lui doit bien plus que je ne pourrais l'exprimer ici.

"Finish it? Why would I want to finish it?"

FIGURE A. W. B. Perk. New Yorker Cartoons.

Contents

Index of notations

Notations introduced in Chapter 3

CHAPTER 1

Introduction

Ce travail porte sur l'analyse mathématique des *variétés caractéristiques* qui, dans les régimes de fréquence électron cyclotron, sont associées au système dit de Vlasov-Maxwell relativiste, qui est un système d'équations aux dérivées partielles non linéaires.

On présente ci-dessous en trois parties les principaux thèmes abordés dans ce document. Dans la Partie 1.1, on évoque le contexte physique général, à savoir les plasmas froids et chauds magnétisés vus sous l'angle de la théorie cinétique. Dans la Partie 1.2, on introduit de manière élémentaire la notion de *relation de dispersion*, et on l'illustre par des exemples. Dans la Partie 1.3, on décrit l'organisation du texte ; on expose les principaux résultats qui ont été obtenus ; et on évoque quelques perspectives.

1.1. Présentation générale

1.1.1. **Contexte physique.** Un plasma désigne un gaz ionisé constitué généralement d'ions, d'électrons, et éventuellement de particules neutres. Le terme plasma a été introduit par le chimiste et physicien américain Irving Langmuir en 1928, par analogie avec le plasma sanguin. À la différence d'un gaz, constitué de particules neutres, un plasma est sensible à l'action d'un champ électromagnétique. D'une part, le mouvement des particules chargées est déterminé par le champ électromagnétique, via la force électrique et la force de Lorentz. D'autre part, le champ électromagnétique peut lui-même être induit ou impacté par les mouvements de ces particules, via les densités de charge et de courant.

Un plasma peut être obtenu en chauffant un gaz à une température suffisamment élevée, afin d'en ioniser les particules. Pour cette raison et sans doute aussi parce qu'ils sont peu présents dans l'environnement terrestre, les plasmas sont souvent considérés comme relevant d'un quatrième état de la matière. Pour autant, on estime que la presque totalité de la matière baryonique de l'univers se retrouve à l'état de plasma. Les plasmas sont en effet les constituants de base des étoiles, du vent solaire, des magnétosphères, de la foudre, etc. Aujourd'hui, ils sont aussi utilisés dans de nombreuses applications industrielles, une des plus importantes étant la tentative de production d'énergie au moyen de la fusion thermonucléaire contrôlée.

Les électrons ont une masse très inférieure à celle des ions. Ils sont à peu près deux milles fois plus légers. Ils peuvent donc plus facilement atteindre des niveaux d'énergie élevés. Il s'ensuit que la température des électrons est supérieure à celle des ions et des particules neutres. On parle alors de plasmas *froids*. En revanche, les plasmas *chauds* sont ceux pour lesquels la température des électrons est similaire à celle des ions.

La plupart des plasmas, qu'ils soient froids ou chauds, sont *magnétisés*. Autrement dit, ils sont sous l'influence d'un champ magnétique extérieur $\mathbf{B}_e(\mathbf{x})$, souvent inhomogène. La magnétosphère et la surface du soleil, qui sont soumis respectivement aux champs magnétiques de la Terre et du Soleil, entrent dans cette catégorie. De même, les dispositifs de type Tokamak ou Stellarator visent à confiner les plasmas par l'action d'un champ magnétique extérieur qui varie notablement en fonction de la position spatiale. C'est ce principe qui guide la filière (non inertielle) de production d'énergie par fusion nucléaire. Dans tous les cas, la présence d'un champ magnétique externe n'est pas sans conséquences. Sous l'effet de la force de Lorentz, les ions et les électrons se déplacent le long des lignes de champ selon des mouvements complexes [4, 5]. De plus, le champ magnétique extérieur influence profondément la façon dont les ondes électromagnétiques (qu'elles soient émises ou induites) se propagent. *Expliquer comment est l'objectif principal de cette thèse.*

On s'intéressera dans un premier temps à un exemple typique de plasma froid magnétisé: les ceintures de Van-Allen. Découvertes en 1958 par le physicien américain James Van Allen, il s'agit de zones toroïdales de la magnétosphère (dessinées sur la Figure 1) contenant une densité importante de particules chargées (certaines provenant du vent solaire). Ces particules sont maintenues en place par le champ magnétique terrestre. L'interaction de ces particules avec la haute atmosphère est par exemple responsable des aurores boréales. Un autre phénomène observé au niveau des ceintures de Van Allen est l'apparition des ondes de sifflement, qualifiées de *whistler waves* en anglais. Ces ondes qui sont de très basses fréquences (quelques kHz) sont parfois générées par la foudre. Elles se propagent dans la magnétosphère selon des processus compliqués qui peuvent donner lieu à des phénomènes d'échos [4]. La modélisation des plasmas froids magnétisés est le thème abordé dans le Chapitre 2, au travers de l'exemple des ceintures de Van Allen. L'accent sera mis sur l'*impact des variations du champ magnétique terrestre* sur la propagation des ondes.

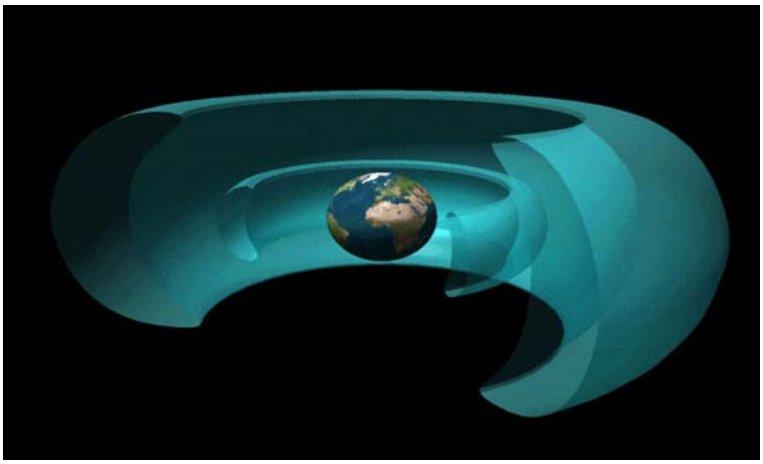

FIGURE 1.
Les ceintures de Van Allen: un exemple de plasma froid magnétisé.

On considère ensuite les plasmas chauds magnétisés via le cas typique des plasmas de tokamak. Un tokamak est une chambre toroïdale contenant un plasma dans lequel on espère réaliser la fusion des particules légères pour former des particules plus lourdes, et ainsi produire de l'énergie. L'idée est alors d'utiliser un champ magnétique intense pour confiner le plasma loin des parois de la chambre, afin d'éviter toute dégradation du matériau. Les plasmas de tokamak ont fait et font toujours l'objet de très nombreuses recherches. On peut notamment citer le projet du réacteur ITER, actuellement en construction près de Cadarache. Dans un tokamak, les ondes électromagnétiques (utilisées pour le chauffage du plasma ou en réflectométrie) interagissent avec les faisceaux de particules chargées, selon un processus dit de résonance électron cyclotron. L'objectif du Chapitre 3, entre autres choses, est de mener une analyse fine et rigoureuse de l'*impact des interactions onde-particule* sur la propagation des ondes.

1.1.2. **Théorie cinétique.** Il existe trois approches principales pour l'étude des plasmas. Selon les circonstances, trois niveaux différents d'approximation peuvent être utilisés: d'abord la description *microscopique*, ensuite la théorie *cinétique*, et enfin l'approche *fluide*. Le modèle *microscopique* prend en compte le mouvement de chaque particule chargée via l'application des Équations Fondamentales de la Dynamique. Ensuite, partant du système d'équations différentielles ordinaires ainsi obtenu, des travaux en physique statistique font le lien vers une description *cinétique* du plasma. Le principe est alors de décrire la répartition des particules de type $\alpha \in \{1, \cdots, N\}$ via une fonction de distribution $\mathrm{f}_\alpha(\mathbf{t}, \mathbf{x}, \mathbf{p})$ donnant le nombre de particules ayant à l'instant $\mathbf{t}$ la position $\mathbf{x}$ et le moment $\mathbf{p}$. L'évolution temporelle de $\mathrm{f}_\alpha(\cdot)$ est alors déterminée par l'équation de Vlasov:

$$\partial_{\mathbf{t}} \mathrm{f}_\alpha + \mathbf{v}_\alpha(\mathbf{p}) \cdot \nabla_{\mathbf{x}} \mathrm{f}_\alpha + e_\alpha \left[\mathbf{E}(\mathbf{t}, \mathbf{x}) + \mathbf{v}_\alpha(\mathbf{p}) \times \big(\mathbf{B}(\mathbf{t}, \mathbf{x}) + \mathbf{B}_e(\mathbf{x}) \big) \right] \cdot \nabla_{\mathbf{p}} \mathrm{f}_\alpha = 0 \,, \tag{1.1.1}$$

où e_α désigne la charge de l'espèce α. Dans le cadre d'un modèle relativiste, la vitesse $\mathbf{v}_\alpha$ de la particule α est liée au moment $\mathbf{p}$ via:

$$\frac{\mathbf{v}_\alpha(\mathbf{p})}{c_0} = \frac{\mathbf{p}}{m_\alpha \, c_0} \left(1 + \frac{|\mathbf{p}|^2}{m_\alpha^2 \, c_0^2} \right)^{-1/2} , \qquad \frac{\mathbf{p}(\mathbf{v}_\alpha)}{m_\alpha \, c_0} = \frac{\mathbf{v}_\alpha}{c_0} \left(1 - \frac{|\mathbf{v}_\alpha|^2}{c_0^2} \right)^{-1/2} , \tag{1.1.2}$$

où m_α correspond à la masse de la particule α et c_0 à la vitesse de la lumière. Le champ électromagnétique auto-induit $(\mathbf{E}, \mathbf{B})(\cdot)$ est quant à lui soumis aux équations de Maxwell:

$$\partial_{\mathbf{t}} \mathbf{E} - c_0^2 \, \nabla_{\mathbf{x}} \times \mathbf{B} = - \epsilon_0^{-1} \, \jmath(\mathrm{f}_\alpha) \,, \qquad \nabla_{\mathbf{x}} \cdot \mathbf{E} = \epsilon_0^{-1} \, \rho(\mathrm{f}_\alpha) \,, \tag{1.1.3a}$$

$$\partial_{\mathbf{t}} \mathbf{B} + \nabla_{\mathbf{x}} \times \mathbf{E} = 0 \,, \qquad \nabla_{\mathbf{x}} \cdot \mathbf{B} = 0 \,, \tag{1.1.3b}$$

avec ϵ_0 qui désigne la permittivité du vide. La densité de charge ρ et la densité de courant $\jmath$ sont données par:

$$\begin{aligned} \rho(\mathrm{f}_\alpha)(\mathbf{t}, \mathbf{x}) &:= \sum_{\alpha=1}^{N} \int_{\mathbb{R}^3} e_\alpha \; \mathrm{f}_\alpha(\mathbf{t}, \mathbf{x}, \mathbf{p}) \; d\mathbf{p} \,, \\ \jmath(\mathrm{f}_\alpha)(\mathbf{t}, \mathbf{x}) &:= \sum_{\alpha=1}^{N} \int_{\mathbb{R}^3} e_\alpha \; \mathbf{v}_\alpha(\mathbf{p}) \; \mathrm{f}_\alpha(\mathbf{t}, \mathbf{x}, \mathbf{p}) \; d\mathbf{p} \,. \end{aligned} \tag{1.1.4}$$

L'équation de Vlasov a été obtenue par le physicien russe Anatoly Vlasov en 1938, voir [29]. Les équations de Maxwell (1.1.3) ont été synthétisées vers 1865 par James Clerk Maxwell, puis remaniées par Oliver Heaviside. La combinaison de (1.1.1), (1.1.2), (1.1.3) et de (1.1.4) est ce qui forme le *système de Vlasov-Maxwell relativiste*. La théorie de l'existence de solutions pour ce système a une très longue histoire. Pour avoir une vision globale du sujet, on peut se reporter au livre [20]. Parmi les nombreuses références, on peut citer le résultat remarquable [12] obtenu en 1988 par Robert Glassey et Jack Schaeffer.

1.1.3. **Relations de dispersion.** Les relations de dispersion apparaissent lors de l'étude des équations aux dérivées partielles modélisant la propagation d'ondes. Afin d'en expliquer le principe, on s'intéresse dans ce paragraphe à l'EDP linéaire d'ordre 1 en temps:

$$\partial_{\mathbf{t}} u + \sum_{|\beta|\leq m} A_\beta(\mathbf{t},\mathbf{x})\,\partial_\beta u \;=\; B(\mathbf{t},\mathbf{x})\,u\,, \tag{1.1.5}$$

dont l'inconnue est la fonction:

$$\begin{array}{rccc} u & : & \mathbb{R}_+\times\mathbb{R}^d & \to & \mathbb{C}^N \\ & & (\mathbf{t},\mathbf{x}) & \mapsto & u(\mathbf{t},\mathbf{x})\,. \end{array}$$

Au niveau de l'équation (1.1.5), les β sont des multi-indices (avec les notations usuelles sur la longueur d'un multi-indice et sur l'opérateur de dérivation ∂_β), tandis que les $A_\beta(\mathbf{t},\mathbf{x})$ et $B(\mathbf{t},\mathbf{x})$ sont des matrices de taille $N\times N$. La plupart des modèles établissent un lien entre les quantités $\jmath(\cdot)$ et $\mathbf{E}(\cdot)$ via un *tenseur de conductivité* σ, opérateur tel que :

$$\jmath(\mathbf{t},\mathbf{x}) = (\sigma\,\mathbf{E})(\mathbf{t},\mathbf{x})\,. \tag{1.1.6}$$

Lorsque de plus σ agit simplement par la multiplication d'une matrice $\sigma(\mathbf{t},\mathbf{x})$, on voit que les équations de Maxwell:

$$\partial_{\mathbf{t}}\mathbf{E} - c_0^2\,\nabla_{\mathbf{x}}\times\mathbf{B} = -\,\epsilon_0^{-1}\,\sigma\,\mathbf{E}\,, \tag{1.1.7a}$$

$$\partial_{\mathbf{t}}\mathbf{B} + \nabla_{\mathbf{x}}\times\mathbf{E} = 0\,, \tag{1.1.7b}$$

s'écrivent sous la forme (1.1.5) avec $u = {}^t(\mathbf{E}\,,\,\mathbf{B}) \in \mathbb{R}^3\times\mathbb{R}^3$. Dans la Partie 1.2 de cette introduction, on donne un aperçu de configurations qui sont issues de choix physiquement pertinents du tenseur de conductivité σ.

Lorsque toutes les matrices $A_\beta(\cdot)$ et $B(\cdot)$ sont des fonctions constantes, on peut chercher à construire des solutions particulières de (1.1.5) sous la forme d'*ondes planes progressives monochromatiques*, OPPM en abrégé.

Définition 1.1.1. *Une onde plane progressive monochromatique (OPPM) est une fonction $u(\mathbf{t},\mathbf{x})$ de la forme:*

$$u(\mathbf{t},\mathbf{x}) := U\,\exp(i\,(\xi\cdot\mathbf{x}+\tau\,\mathbf{t}))\,,\qquad U\in\mathbb{C}^N\setminus\{0\}\,. \tag{1.1.8}$$

Le vecteur $\xi\in\mathbb{R}^d$ est le vecteur d'onde ; le réel $\tau\in\mathbb{R}$ est la fréquence de l'onde.

Remarque: Dans la plupart des livres de physique des plasmas [2, 9, 23, 24], le vecteur d'onde est noté $\mathbf{k}$ et la fréquence $-\omega$. Tout au long du texte, on préferera la notation ξ et τ, usuelle en Optique Géométrique [3].

La notion de relation de dispersion apparaît clairement lorsqu'il s'agit d'ajuster ξ et τ de façon à ce que la fonction $u(\cdot)$ de (1.1.8) soit solution de (1.1.5).

Définition 1.1.2. *Le symbole (à valeurs matricielles) de l'EDP (1.1.5) est la fonction:*

$$\chi : (\mathbb{R}\times\mathbb{R}^d)\times(\mathbb{R}\times\mathbb{R}^d) \longrightarrow M_N(\mathbb{C}) \quad (\mathbf{t},\mathbf{x},\tau,\xi) \longmapsto \chi(\mathbf{t},\mathbf{x},\tau,\xi)\,, \tag{1.1.9}$$

où $\chi(\mathbf{t},\mathbf{x},\cdot)$ est le polynôme:

$$\chi(\mathbf{t},\mathbf{x},\tau,\xi) := i\,\tau\,Id + \sum_{|\beta|\le m} (i\,\xi)^\beta\, A_\beta(\mathbf{t},\mathbf{x}) - B(\mathbf{t},\mathbf{x})\,. \tag{1.1.10}$$

On appelle relation de dispersion liant $\mathbf{t}$, $\mathbf{x}$, τ et ξ la condition:

$$\det\chi(\mathbf{t},\mathbf{x},\tau,\xi) = 0\,. \tag{1.1.11}$$

Si u est une OPPM, on a l'équivalence entre:

$$\partial_{\mathbf{t}}u + \sum_{|\beta|\le m} A_\beta(\mathbf{t},\mathbf{x})\,\partial_\beta u = B(\mathbf{t},\mathbf{x})\,u \quad\Longleftrightarrow\quad \chi(\mathbf{t},\mathbf{x},\tau,\xi)\,U = 0\,.$$

Cette dernière équation admet une solution U non nulle si et seulement si $(\mathbf{t},\mathbf{x},\tau,\xi)$ vérifie la relation de dispersion (1.1.11). On peut à présent introduire :

Définition 1.1.3. *La variété caractéristique associée à (1.1.5) est définie par:*

$$\mathscr{V} := \{\,(\mathbf{t},\mathbf{x},\tau,\xi)\in(\mathbb{R}\times\mathbb{R}^d)\times(\mathbb{R}\times\mathbb{R}^d)\,;\,\det\chi(\mathbf{t},\mathbf{x},\tau,\xi)=0\,\}\,. \tag{1.1.12}$$

Il peut arriver que $\mathscr{V}$, localement ou globalement, puisse être vue comme le graphe en τ d'une fonction $\lambda(\cdot)$ de variables $\mathbf{t}$, $\mathbf{x}$ et ξ parcourant un ouvert Ω. Autrement dit:

$$\{\,(\mathbf{t},\mathbf{x},\lambda(\mathbf{t},\mathbf{x},\xi),\xi)\in(\mathbb{R}\times\mathbb{R}^d)\times(\mathbb{R}\times\mathbb{R}^d)\,;\,(\mathbf{t},\mathbf{x},\xi)\in\Omega\,\}\subset\mathscr{V}\,.$$

Dans ce cas, le point $(\mathbf{t},\mathbf{x})$ étant fixé, la fonction $\lambda(\cdot)$ établit un lien entre la pulsation τ et le vecteur d'onde ξ de l'OPPM. Par extension, on parle encore de relation de dispersion en ce qui concerne $\lambda(\cdot)$. À partir des relations de dispersion ou de $\mathscr{V}$, on peut déterminer les notions de *vitesse de groupe*, de *vitesse de phase*, d'*EDP dispersive*, etc. On pourra par exemple consulter [3] pour une présentation détaillée de ces notions ainsi que de nombreux exemples. Dans les Chapitres 2 et 3, sur la base de considérations réalistes quant au choix des paramètres physiques, on *met en valeur des versions convenablement adimensionnées du système de Vlasov-Maxwell relativiste pour en extraire les variétés caractéristiques qui sont associées aux plasmas froids et chauds magnétisés.*

Les relations de dispersion ont été très étudiées en physique des plasmas, historiquement d'abord dans le cas froid [1, 11, 13, 14] puis dans le cas chaud [2, 9, 16, 24, 27]. Cela s'explique par le fait qu'elles interviennent dans une grande diversité de contextes (de l'astrophysique aux plasmas de laboratoire), et qu'elles sont cruciales pour comprendre la plupart des phénomènes. Elles apportent de nombreuses informations sur la propagation des ondes. Elles permettent de tracer les rayons de l'optique géométrique [26], d'obtenir l'indice de réfraction d'un milieu, de détecter d'éventuels effets tunnel, de percevoir des mécanismes de conversion de modes, de calculer les résonances de type onde-onde, etc.

Interprétées dans le cas où ξ et τ sont complexes, elles peuvent aussi indiquer si une onde se trouve amplifiée ou amortie, ...

Malgré l'abondance de travaux sur le sujet, les relations de dispersion font toujours l'objet de nombreuses recherches actuelles, voir les articles récents [7, 10, 17, 19, 21, 25, 30, 31] pour n'en citer que quelques uns. En effet, la situation est riche. Plusieurs angles d'approche peuvent être retenus. Les études peuvent être relativistes ou non ; elles peuvent balayer toutes les directions de propagation ou n'en sélectionner que quelques unes ; elles peuvent incorporer les variations en espace du champ magnétique extérieur $\mathbf{B}_e(\cdot)$ ou se restreindre au seul cas des coefficients constants, etc. *Le but de cette thèse est d'aboutir à une synthèse de ces différents aspects. Il est aussi d'apporter un éclairage nouveau sur les effets des inhomogénéités du champ magnétique et sur le rôle des résonances électron cyclotron.*

1.2. Panorama des relations de dispersion

Comme expliqué précédemment, on peut chercher à identifier les solutions des équations de Maxwell (1.1.7) sous la forme d'OPPM:

$$\mathbf{E}(\mathbf{t},\mathbf{x}) := \mathbf{E}_0 \exp\big(i\,(\xi\cdot\mathbf{x}+\tau\,t)\big)\,, \qquad \mathbf{B}(\mathbf{t},\mathbf{x}) := \mathbf{B}_0 \exp\big(i\,(\xi\cdot\mathbf{x}+\tau\,t)\big)\,. \tag{1.2.1}$$

Selon le contenu de $\sigma(\cdot)$, les relations de dispersion et la variété caractéristique peuvent prendre des formes très différentes. L'ensemble $\mathscr{V}$ étant un sous-ensemble de $\mathbb{R}^4\times\mathbb{R}^4$, il n'est pas possible d'en fournir une représentation graphique. En revanche, la position $(\mathbf{t},\mathbf{x},\tau)$ étant fixée, on peut dessiner l'ensemble $\boldsymbol{\mathcal{V}}(\mathbf{t},\mathbf{x},\tau) := \{\,\xi\in\mathbb{R}^3\,;\,(\mathbf{t},\mathbf{x},\tau,\xi)\in\mathscr{V}\,\}$. Dans ce qui suit, on commence par examiner quelques situations simples, bien connues, pour ensuite évoquer les situations plus compliquées qui motivent ce document.

1.2.1. **Propagation dans le vide.** On examine ici le cas le plus élémentaire, celui d'une onde électromagnétique qui se propage dans le vide. Dans ce contexte, on a $\rho=0$ et $\jmath=0$ (c'est à dire $\sigma\equiv 0$). Appliquées à une OPPM telle que (1.2.1), les équations de Maxwell (1.1.7) se réduisent à:

$$\tau\,\mathbf{E}_0 - c_0^2\,\xi\times\mathbf{B}_0 = 0\,, \qquad \xi\cdot\mathbf{E}_0 = 0\,, \tag{1.2.2a}$$

$$\tau\,\mathbf{B}_0 + \xi\times\mathbf{E}_0 = 0\,, \qquad \xi\cdot\mathbf{B}_0 = 0\,. \tag{1.2.2b}$$

En combinant (1.2.2a) et (1.2.2b), on obtient facilement:

$$\chi(\tau,\xi)\,\mathbf{E}_0 = 0\,, \qquad \chi(\tau,\xi) := \big(\tau^2 - |\xi|^2\,c_0^2\big)\,Id\,.$$

Cette équation a une solution non nulle $\mathbf{E}_0$ si et seulement si $\tau^2 = |\xi|^2\,c_0^2$. Cette condition donne la relation de dispersion dans le vide. On a:

$$\boldsymbol{\mathcal{V}}(\mathbf{t},\mathbf{x},\tau) \equiv \boldsymbol{\mathcal{V}}_v(\tau) := \{\,\xi\in\mathbb{R}^3\,;\,|\xi|^2 = c_0^{-2}\,\tau^2\,\}\,.$$

Comme indiqué sur la Figure 3, il s'agit d'une sphère de rayon $c_0^{-1}\,\tau$. Cela implique que l'onde se propage dans toutes les directions à la même vitesse c_0. Le système d'équations (1.2.2) montre aussi que le triplet $(\mathbf{E}_0,\mathbf{B}_0,\xi)$ forme une base orthogonale directe. De plus, les champs $\mathbf{E}_0(\cdot)$ et $\mathbf{B}_0(\cdot)$ ont une variation sinusoïdale en espace, voir la Figure 2.

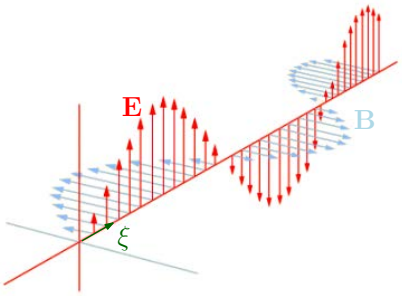

FIGURE 2.
Polarisation de $\mathbf{E}(\cdot)$ et de $\mathbf{B}(\cdot)$.

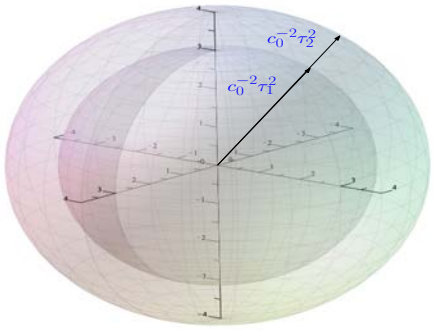

FIGURE 3.
L'ensemble $\mathbf{V}_v(\tau)$ pour deux valeurs $\tau_1 < \tau_2$.

1.2.2. **Propagation dans un plasma non magnétisé.** On s'intéresse dans ce paragraphe à la propagation d'une onde électromagnétique plane progressive monochromatique dans un plasma. Dans un modèle classique relativiste (à grande échelle), il est parfois considéré que la force magnétique extérieure est négligeable. On peut alors considérer que $\jmath$ et $\mathbf{E}$ sont liés par un tenseur de conductivité scalaire σ qui agit comme un multiplicateur de Fourier, au sens où:

$$\hat{\jmath} = \sigma\, \hat{\mathbf{E}}\,, \qquad \sigma(\mathbf{t},\mathbf{x},\tau,\xi) \equiv \sigma(\tau) := -\,i\, \sum_{\alpha=1}^{N} \frac{n_\alpha\, e_\alpha^2}{m_\alpha\, \tau}\,, \tag{1.2.3}$$

où n_α, e_α et m_α désignent respectivement la densité, la charge et la masse de l'espèce α. En interprétant (1.1.7) côté Fourier, on obtient:

$$\chi(\mathbf{t},\mathbf{x},\tau,\xi) \equiv \chi_p(\tau,\xi) := (\tau^2 - \tau_p^2 - |\xi|^2\, c_0^2)\; Id\,, \qquad \tau_p := \left(\epsilon_0^{-1} \sum_{\alpha=1}^{N} \frac{n_\alpha\, e_\alpha^2}{m_\alpha}\right)^{1/2}.$$

La relation de dispersion associée est de type Klein-Gordon. Elle s'écrit:

$$|\xi|^2\, c_0^2 = \tau^2 - \tau_p^2\,. \tag{1.2.4}$$

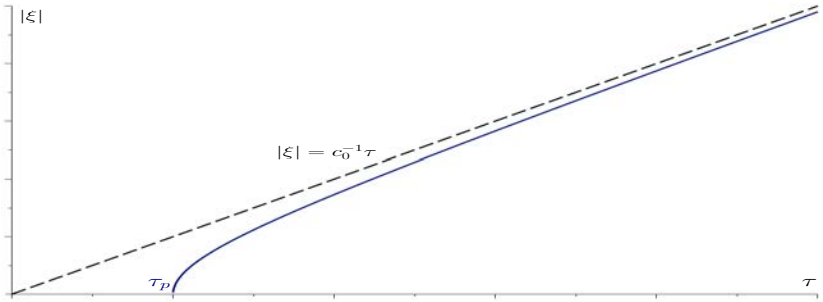

FIGURE 4. Évolution de $|\xi|$ en fonction de τ.

L'équation (1.2.4) a une solution $(\tau,\xi)\in\mathbb{R}^4$ si et seulement si $\tau\geq\tau_p$. En deçà de la *fréquence de coupure* τ_p qu'on peut visualiser sur la Figure 4, une OPPM ne peut pas se propager. En revanche, pour $\tau\geq\tau_p$, on récupère:

$$\boldsymbol{\mathcal{V}}(\mathbf{t},\mathbf{x},\tau)\equiv\boldsymbol{\mathcal{V}}_p(\tau):=\left\{\,\xi\in\mathbb{R}^3\,;\,|\xi|^2=c_0^{-2}\,(\tau^2-\tau_p^2)\,\right\}.$$

On obtient encore une sphère. Cependant, comme le montre la Figure 4 qui trace l'évolution de $|\xi|$ en fonction de τ, la relation liant le rayon de la sphère à la fréquence temporelle n'est plus linéaire. Le milieu est dispersif. Comme pour le vide, le trièdre $(\mathbf{E},\mathbf{B},\xi)$ est direct. Par ailleurs, pour $\tau\gg\tau_p$, la relation de dispersion devient $|\xi|\sim c_0^{-1}\,\tau$. Ainsi, pour les très hautes fréquences, le comportement du plasma se rapproche de celui du vide.

Sous l'action d'un champ magnétique extérieur, l'accès au tenseur de conductivité σ s'avère beaucoup plus délicat. En effet, pour bien comprendre l'origine même de σ, il convient de remonter au niveau du système de Vlasov-Maxwell relativiste. Se pose alors la question de savoir comment on peut déduire du modèle cinétique (1.1.1)-(1.1.2)-(1.1.3)-(1.1.4) un objet macroscopique (parce qu'agissant sur des fonctions de $\mathbf{t}$ et de $\mathbf{x}$) tel que σ. *L'extraction et la description de σ fait l'objet des deux Théorèmes principaux de ce document.* On se contente dans ce qui suit d'illustrer par des dessins la richesse des géométries impliquées.

1.2.3. **Influence d'un champ magnétique extérieur sur un plasma froid.** On donne ici un avant-goût des résultats qui seront énoncés et démontrés dans le Chapitre 2. Sans trop rentrer dans les détails, le but est de mettre en valeur l'influence du champ magnétique extérieur sur la topologie de la variété caractéristique d'un plasma froid. Dans cette analyse, un paramètre adimensionné important est la *fréquence électron cyclotron* ε^{-1} dont la taille augmente avec l'intensité du champ magnétique, voir (2.2.48) pour une définition précise.

Selon le régime de fréquence considéré, la variété caractéristique associée aux plasmas froids magnétisés peut prendre des formes variées. On distinguera deux régimes principaux: celui des hautes et très hautes fréquences (Paragraphe 1.2.3.1) pour lequel $\tau\gg\varepsilon^{-1}$, et pour lequel l'ensemble $\boldsymbol{\mathcal{V}}(\cdot,\tau)$ ressemble à ce que l'on a déjà rencontré dans les paragraphes 1.2.1 et 1.2.2 ; celui des basses fréquences (Paragraphe 1.2.3.2) pour lequel $\tau\sim\varepsilon^{-1}$, et pour lequel les choses sont radicalement différentes. La lecture de ce qui suit peut être avantageusement complétée par celle de l'Appendice B, ne serait-ce que pour les dessins.

1.2.3.1. *Excursion dans le régime des hautes et très hautes fréquences.* Pour des fréquences qui sont élevées par rapport à ε^{-1}, l'ensemble $\boldsymbol{\mathcal{V}}(\mathbf{x},\tau)$ n'est plus d'un seul tenant comme c'était le cas dans les deux parties 1.2.1 et 1.2.2 précédentes. Au contraire, il est composé de deux composantes connexes notées $\boldsymbol{\mathcal{V}}_o(\mathbf{x},\tau)$ et $\boldsymbol{\mathcal{V}}_x(\mathbf{x},\tau)$, appelées respectivement *sphère ordinaire* et *sphère extraordinaire* (même s'il s'agit dans la pratique de sphéroïdes). Ce partage de $\boldsymbol{\mathcal{V}}(\mathbf{x},\tau)$ en deux correspond au dédoublement d'une valeur propre multiple et se traduit expérimentalement par l'apparition de deux types d'ondes: les ondes ordinaires et les ondes extraordinaires. Les ensembles $\boldsymbol{\mathcal{V}}_o(\mathbf{x},\tau)$ et $\boldsymbol{\mathcal{V}}_x(\mathbf{x},\tau)$ sont homéomorphes à une sphère. Par ailleurs, dans le régime des très hautes fréquences, ils se retrouvent presque confondus avec $\boldsymbol{\mathcal{V}}_v(\tau)$: pour les très hautes fréquences, l'influence du champ magnétique recouvre un caractère perturbatif.

Pour des fréquences un peu plus basses, la séparation entre la sphère ordinaire et la sphère extraordinaire devient plus marquée. Par ailleurs, la distinction avec la sphère $\mathbf{V}_v(\tau)$ est aussi plus claire. Ces deux situations sont représentées sur les Figures 5 et 6 ci-dessous.

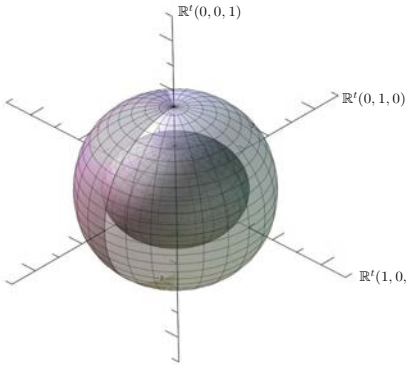

FIGURE 5.
Sphère ordinaire et extraordinaire
dans le domaine des hautes fréquences.

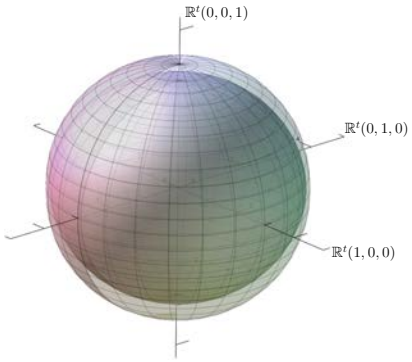

FIGURE 6.
Sphère ordinaire et extraordinaire
dans le domaine des très hautes fréquences.

1.2.3.2. *Excursion dans le régime des basses fréquences.* Lorsque la fréquence diminue et se rapproche de la valeur ε^{-1}, la distinction avec les situations étudiées aux paragraphes 1.2.1 et 1.2.2 devient très nette. Le régime n'est plus du tout perturbatif. En dessous de certaines fréquences de coupure, la sphères extraordinaire puis la sphère ordinaire disparaissent. On passe ensuite en dessous de certaines *fréquences de résonance*, et on voit surgir des objets topologiques nouveaux: les sphères laissent place à des cônes qui peuvent être de deux types, ordinaire ou extraordinaire. Ils sont représentés sur les Figures 7 et 8 ci-dessous.

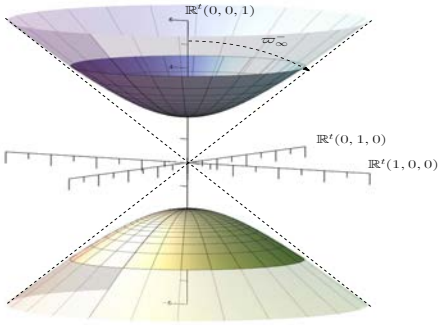

FIGURE 7.
Cône de résonance ordinaire.

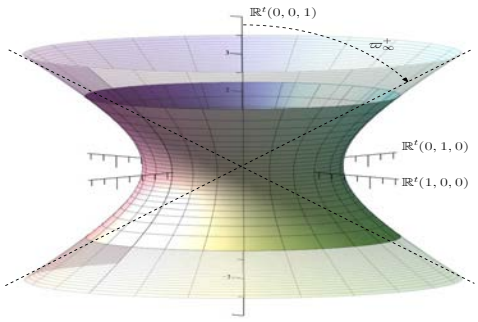

FIGURE 8.
Cône de résonance extraordinaire.

L'étude de ces objets et de leur géométrie est importante. Cela permet de classifier les ondes et de comprendre la manière dont elles se propagent dans un plasma froid magnétisé. C'est cet objectif qui est atteint dans le Chapitre 2.

La prise en compte de la géométrie permet d'établir que les ondes de sifflement (appelées *whistler waves* en anglais) ne peuvent pas se propager de manière purement parallèle aux lignes de champ magnétique dans la magnétosphère terrestre. De même, la compréhension précise de la manière dont s'opère la transition entre les différents objets géométriques, lorsque la fréquence évolue, apporte des renseignements. Entre autres choses, cela montre que le contact entre les nappes ordinaires et extraordinaires de la variété caractéristique, ne peut se faire qu'en un seul point et selon des modalités très précises, voir la Figure 9. Ce genre d'information est utile pour déterminer la façon dont les ondes se mélangent au voisinage de ce point.

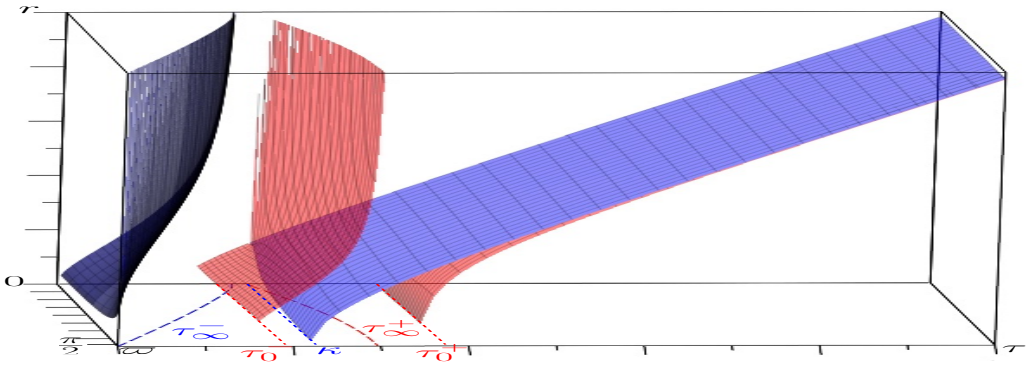

FIGURE 9.
La variété caractéristique dans le jeu de variables réduites de la Figure 11.

1.2.4. **Influence d'un champ magnétique extérieur sur un plasma chaud.** Dans le cas des plasmas froids magnétisés, il est possible de résoudre les relations de dispersion de manière algébrique et exacte. Cette propriété donne accès à une paramétrisation explicite de la variété caractéristique. Elle conduit à la description géométrique qui est évoquée dans les paragraphes précédents.

Au contraire, dans le cas des plasmas chauds magnétisés, les relations de dispersion ne peuvent pas être résolues explicitement. La propagation des ondes est toujours gouvernée par un tenseur diélectrique σ. Mais la définition et le sens de l'opérateur σ soulèvent problème. En effet, σ agit comme un multiplicateur de Fourier dont le symbole est obtenu via des intégrales singulières et une sommation dont le contenu demande à être clarifié. Ces difficultés d'analyse sont la conséquence de *résonances cinétiques*.

Notons $\mathbf{p} = r\ {}^t(\cos\omega \sin\varpi\,,\, \sin\omega \sin\varpi\,,\, \cos\varpi) \in \mathbb{R}^3$, les coordonnées sphériques de $\mathbf{p}$. Notons également $\mathbf{b}_e(\mathbf{x}) := |\mathbf{B}_e(\mathbf{x})|$ l'amplitude du champ magnétique, et $\xi_\parallel$ la composante de $\xi \in \mathbb{R}^3$ qui est parallèle à la direction $\mathbf{B}_e(\mathbf{x})$. Alors, une fréquence $\tau \in \mathbb{R}$ est résonante si et seulement si elle vérifie:

$$D(\mathbf{x},\mathbf{p},\tau,\xi) := \langle r\rangle\ \tau\ +\ r\ \xi_\parallel\ \cos\varpi\ +\ m\ \mathbf{b}_e(\mathbf{x})\ =\ 0\,, \qquad \langle r\rangle := \sqrt{1+r^2}\,.$$

La fonction $D(\cdot)$ est parfois appelée *fonction de dispersion gyrobalistique*. Elle intervient au dénominateur dans les expressions intégrales donnant $\sigma(\cdot)$, comme on peut le voir en combinant (3.3.20) et (3.3.28). Elle introduit par ce biais des singularités. Examinons maintenant le contenu de D. Le terme $\langle r\rangle\,\tau + r\,\xi_{\|}\,\cos\varpi$ peut être vu comme une fréquence décalée par effet Doppler. Le terme $m\,\mathbf{b}_e(\mathbf{x})$ correspond quant à lui à une harmonique de la gyrofréquence $\mathbf{b}_e(\mathbf{x})$. Du fait des non linéarités, les électrons peuvent en effet tournoyer autour des lignes de champ à la fréquence $m\,\mathbf{b}_e(\mathbf{x})$.

Si l'on s'en tient à (3.3.20) et (3.3.28), les positions $(\mathbf{x},\mathbf{p},\tau,\xi)$ en lesquelles la fonction D s'annule apportent (du moins en apparence) une grosse contribution au niveau de $\sigma(\cdot)$. Ainsi, l'interaction entre les ondes et les particules chargées devient forte, lorsque la fréquence de l'onde décalée par effet Doppler se rapproche d'une harmonique de la fréquence cyclotron. Cela correspond à des résonances qui, puisqu'elles impliquent $\mathbf{p}$ au niveau de leur définition, présentent un caractère cinétique. Comme expliqué ci-dessus, en accord avec les principes physiques de base exposés dans l'article [28], ces résonances proviennent d'un phénomène d'interaction onde-particule. *Le traitement rigoureux de ces résonances et de l'inhomogénéité (toujours présente) du champ magnétique est ce qui motive les développements du Chapitre 3.*

1.3. Structure et contenu du document, perspectives

1.3.1. **Relations de dispersion dans les plasmas froids magnétisés.** Le **Chapitre 2** commence avec la Section 2.2 par la modélisation des plasmas froids magnétisés. Comme indiqué précédemment, on s'appuie sur l'exemple de la magnétosphère terrestre et des ceintures de Van Allen. On considère que la plupart des particules sont dans un état d'équilibre thermodynamique local. La description d'un tel état stationnaire fait l'objet du paragraphe 2.2.2. Toutefois, les plasmas non collisionnels comportent une fraction qui se trouve hors équilibre (voir le paragraphe 2.2.3), que l'on gère dans le cadre d'une analyse perturbative. Il s'agit alors de fixer les différents paramètres en adéquation avec la situation physique étudiée (c'est le paragraphe 2.2.4). Le paragraphe 2.2.5 est consacré à la modélisation du champ magnétique terrestre, via un modèle de dipôle magnétique. On obtient alors après adimensionnement (paragraphe 2.2.6), un système d'équations aux dérivées partielles qui fait intervenir le petit paramètre $\varepsilon \ll 1$, inverse de la fréquence électron cyclotron. Ce paramètre sert alors d'unité de mesure à laquelle toutes les autres quantités sont comparées. Cela permet de définir ce qu'est le régime asymptotique froid (paragraphe 2.2.7).

On est de cette façon amené à étudier une version singulière du système de Vlasov-Maxwell relativiste, c'est à dire une version dans laquelle apparaissent des paramètres raides. On travaille alors dans le cadre de l'optique géométrique, en cherchant des solutions sous la forme de développements WKB impliquant une unique phase non-linéaire $\phi(\mathbf{t},\mathbf{x})$ (voir le paragraphe 2.2.8). A la fois la fonction de distribution $\mathrm{f}(\cdot)$ et l'onde $(\mathbf{E},\mathbf{B})(\cdot)$ oscillent à la fréquence ε^{-1} selon la phase $\phi(\mathbf{t},\mathbf{x})$. Autrement dit, les oscillations de l'onde $(\mathbf{E},\mathbf{B})(\cdot)$ sont associées à celles de $\mathrm{f}(\cdot)$ qui en retour influencent la propagation de $(\mathbf{E},\mathbf{B})(\cdot)$. C'est sur ce mélange qu'est basée notre analyse des relations de dispersion.

La Section 2.3 est dédiée à la détermination de $\mathscr{V}$, ainsi qu'à sa description précise. Dans le paragraphe 2.3.1, on extrait un système simplifié d'équations à partir du premier terme du développement WKB, ce qui mène à terme à la définition de la variété caractéristique $\mathscr{V}$ qui est associée aux plasmas froids magnétisés (paragraphe 2.3.2). Le paragraphe 2.3.3 est consacré à la preuve du Théorème 1.

Notre analyse permet notamment de voir que la propagation parallèle, souvent présentée comme étant représentative de la situation générale, est en fait un cas très particulier. Elle ne se produit pas en présence d'inhomogénéités. Plusieurs paramétrisations de $\mathscr{V}$ sont ensuite proposées (paragraphe 2.3.4), donnant accès aux différentes descriptions du paragraphe 1.2.3. En corollaire du Théorème 1, on obtient une justification rigoureuse des équations eikonales relatives à l'évolution en temps de la phase $\phi(\cdot)$. Enfin, dans le Paragraphe 2.3.4.5, on collecte un certain nombre de renseignements qualitatifs sur la structure des émissions naturelles électrostatiques et électromagnétiques (aussi appelées chorus waves ou *earthsongs*) qui sont captées dans la magnétosphère [8].

1.3.2. **Relations de dispersion dans les plasmas chauds magnétisés.** Le **Chapitre 3** commence (Section 3.2) par un travail de modélisation des plasmas chauds magnétisés, s'appuyant sur le cas concret des tokamaks. Le paragraphe 3.2.1 est consacré à l'étude des états d'équilibre toroïdaux des équations de Vlasov-Maxwell. Dans le paragraphe 3.2.1.1, on exhibe des champs magnétiques axisymétriques à divergence nulle, issus de considérations physiques. Puis, on discute la notion d'équilibre fluide, via les équations de Grad-Shafranov (paragraphe 3.2.1.2). Pour compléter cette approche préliminaire, on considère dans le paragraphe 3.2.1.3 des équilibres incorporant des aspects cinétiques. À partir de là, on extrait une nouvelle version adimensionnée des équations de Vlasov-Maxwell relativistes. C'est le paragraphe 3.2.2. Ensuite, après avoir défini dans le paragraphe 3.2.3 une notion de régime asymptotique chaud, on récupère un système comportant plus de termes singuliers que dans le chapitre 2.

La Section 3.3 contient l'essentiel de l'analyse mathématique. On commence par extraire, au niveau du paragraphe 3.3.1.1, dans le contexte de l'optique géométrique, un système simplifié d'équations. Ce système fait apparaître les résonances cinétiques qui ont été introduites en 1.2.4. On en discute l'interprétation physique au paragraphe 3.3.1.3. On extrait alors une définition formelle de la variété caractéristique (paragraphe 3.3.1.4) associée aux plasmas chauds magnétisés. Comme indiqué en 1.2.4, la définition de cette variété caractéristique fait encore intervenir un tenseur diélectrique $\sigma(\cdot)$. Dans le paragraphe 3.3.2, on justifie l'existence et le bien-fondé de ce tenseur diélectrique dans le cas où τ et ξ sont réels. L'analyse repose sur l'introduction de la transformée de Hilbert (paragraphe 3.3.2.2), dont on étudie l'action via des estimations en norme Lipschitz (paragraphe 3.3.2.3) et en norme L^1 (paragraphe 3.3.2.4). Enfin, les cas particuliers des propagations parallèles et perpendiculaires sont étudiés au paragraphe 3.3.3.

La procédure qui est adoptée pour parvenir à l'ensemble des résultats évoqués ci-dessus est à notre connaissance nouvelle.

1.3.3. **Objectifs, résultats et nouveautés.** Ce travail s'intéresse à la description des plasmas magnétisés, en l'absence de collisions. En lien avec les applications, deux situations concrètes et typiques sont examinées : les plasmas froids de la magnétosphère terrestre et les plasmas chauds des tokamaks. L'accent est mis sur la propagation des ondes électromagnétiques dans une gamme de fréquences comparables à la fréquence électron cyclotron. Les phénomènes hors équilibre observés dans ce régime sont en lien avec des questions fondamentales concernant les interactions onde-particule, le transport anormal, les propriétés de confinement, etc.

Un apport important de cette thèse est le suivant. On montre, données expérimentales à l'appui, que la modélisation dans ces plasmas des phénomènes hors équilibre relève d'une optique géométrique de type dispersive pour le système de Vlasov-Maxwell relativiste. On valide ainsi deux modèles (le froid et le chaud), permettant d'aborder mathématiquement sur des bases fiables les questions évoquées ci-dessus.

Les analyses asymptotiques qui en découlent sont intéressantes, et susceptibles de nombreux développements. Elles sont amorcées dans ce document via la justification d'équations eikonales. On arrive ainsi à déterminer de manière rigoureuse ce que sont les rayons suivis par les ondes électromagnétiques, et à en déduire quelques interprétations physiques. À titre d'exemple, dans le chapitre 2, on obtient un certain nombre de renseignements qualitatifs concernant l'émission des ondes en mode siffleur. De même, dans le chapitre 3, on explique comment les résonances électron cyclotron interviennent au niveau des propriétés diéléctriques du milieu.

Historiquement, plusieurs approches ont été proposées en vue d'obtenir les relations de dispersion associées aux plasmas magnétisés, voir [1, 13, 14, 15, 18, 22] pour le cas froid et [2, 9, 16, 23, 24, 27] pour le cas chaud. Les résultats connus sont valables lorsque le champ magnétique extérieur est constant et lorsque la fonction de distribution à l'équilibre dépend seulement de $\mathbf{p}$. Ils ne s'appliquent pas tel quel en présence d'inhomogénéités. Or l'étude des magnétosphères et des tokamaks met en jeu de telles inhomogénéités, avec des effets impactants.

Pour prendre en compte les variations de $\tilde{\mathbf{B}}_e(\cdot)$ et de $\tilde{\mathrm{f}}^{\mathrm{d}}_\alpha(\cdot)$, telles qu'elles sont dictées par la physique, on adimensionne les équations, et on procède à un calcul BKW. Cela conduit à une description précise et rigoureuse des variétés caractéristiques. Appliqués en l'absence d'inhomogénéités, nos énoncés redonnent - et c'est heureux - les résultats déjà établis. Mais ils fournissent bien au delà des formules qui sont adaptées aux magnétosphères et aux tokamaks, et qui sont directement exploitables.

Le chapitre 2 qui traite le cas des plasmas froids, a donné lieu à un article publié en 2017 dans la revue *Kinetic and Related Models* [6]. Les résultats principaux sont résumés au travers du Théorème 1. Par ailleurs, on montre (Théorème 2) l'absence de propagation purement parallèle aux lignes du champ magnétique. Dans la pratique, les ondes se dispersent dans le cône (de type ordinaire ou extraordinaire selon les cas) qui entoure la direction du champ magnétique. Ce sont là deux conséquences originales de cette analyse.

Le chapitre 3 qui porte sur les plasmas chauds de tokamaks montre que les ondes électromagnétiques sont gouvernées par un tenseur diéléctrique $\sigma(\cdot)$. Le contenu de la matrice $\sigma(\cdot)$ est détaillé dans le théorème 3. L'analyse des coefficients de $\sigma(\cdot)$ dans le domaine des fréquences réelles est difficile d'accès. Elle est pertinente du point de vue de la physique. Elle est un passage obligé en vue de décrire mathématiquement la propagation des singularités oscillantes. Cette dernière étude repose sur l'analyse d'intégrales singulières impliquant la transformée de Hilbert.

1.3.4. **Quelques perspectives.** Que ce soit dans le cas des plasmas froids ou chauds, l'analyse des termes d'ordre supérieur dans la hiérarchie WKB est une direction de recherche intéressante. La construction de solutions approchées pour les systèmes de Vlasov-Maxwell qui ont été exhibés dans les Chapitres 2 et 3 serait à poursuivre. En particulier, l'étude des équations de transport (qui correspondent aux termes d'ordre ε^0) permettrait sans doute de mieux appréhender les mécanismes de transfert d'énergie entre les ondes et les particules. Se pose aussi la question de la justification des développements WKB.

Les descriptions précises des variétés caractéristiques obtenues aux Chapitres 2 et 3 peuvent être exploitées pour mettre en place des méthodes de traçage de rayons, voir par exemple les perspectives évoquées en Section 3.3.4. Elles ouvrent également la perspective de travaux d'analyse relatifs aux problèmes évoqués dans le paragraphe précédent.

References

[1] E. V. Appleton. Wireless studies of the ionosphere. *J. Inst. Electr. Eng*, 71:642–650, 1932.

[2] G. Bekefi. *Radiation processes in plasmas*. Wiley, 1966.

[3] S. Benzoni. *Cours de Master 2: EDP dispersives*. 2009.

[4] C. Cheverry. Can One Hear Whistler Waves? *Comm. Math. Phys.*, 338(2):641–703, 2015.

[5] C. Cheverry. Anomalous transport. *J. Differential Equations*, 262(3):2987–3033, 2017.

[6] C. Cheverry and A. Fontaine. Dispersion relations in cold magnetized plasmas. *Kinet. Relat. Models*, 10(2):373–421, 2017.

[7] C. Cremaschini and M. Tessarotto. Kinetic description of rotating tokamak plasmas with anisotropic temperatures in the collisionless regime. *Physics of Plasmas (1994-present)*, 18(11):112502, 2011.

[8] F. Darrouzet. *Etude de la magnétosphère terrestre par l'analyse multipoint des donnéees de la mission CLUSTER. Contributions à la caractérisation des frontières et de la magnétosphère interne*. PhD thesis, Université d'Orléans, 2006.

[9] R. C. Davidson. *Handbook of plasma physics*. North-Holland, 1983.

[10] Bruno Després, Lise-Marie Imbert-Gérard, and Ricardo Weder. Hybrid resonance of Maxwell's equations in slab geometry. *J. Math. Pures Appl. (9)*, 101(5):623–659, 2014.

[11] C. Gillmor. Wilhelm Altar, Edward Appleton, and the magneto-ionic theory. *Proceedings of the American Philosophical Society*, 126(5):395–440, 1982.

[12] R. T. Glassey and J. W. Schaeffer. Global existence for the relativistic Vlasov-Maxwell system with nearly neutral initial data. *Comm. Math. Phys.*, 119(3):353–384, 1988.

[13] D. R. Hartree. The propagation of electromagnetic waves in a stratified medium. *Mathematical Proceedings of the Cambridge Philosophical Society*, 25:97–120, 1929.

[14] R. A. Helliwell. *Whistlers and Related Ionospheric Phenomena*. Stanford University Press. 1965.

[15] C.F. Kennel. Low frequency whistler mode. *Journal of Plasma Physics*, 71:1– 28, 1966.

[16] N. A. Krall and A. W. Trivelpiece. *Principles of plasma physics*. McGray-Hill, 1973.

[17] R. A. Lopez, P. S. Moya, V. Munoz, A. F. Vinas, and J. A. Valdivia. Kinetic transverse dispersion relation for relativistic magnetized electron-positron plasmas with maxwell-juttner velocity distribution functions. *Physics of Plasmas*, 21, 2014.

[18] D. C. Montgomery and D. A. Tidman. *Plasma kinetic theory*. McGraw-Hill Book Company, 1964.

[19] V. Munoz, F. A. Asenjo, R. A. Dominguez, J. A. Lopez, A. Valdivia, A. Vinas, and T. Hada. Large-amplitude electromagnetic waves in magnetized relativistic plasmas with temperature. *Nonlin. Processes Geophys.*, 21:217–236, 2014.

[20] T. Passot, C. Sulem, and P.-L. Sulem, editors. *Topics in kinetic theory*, volume 46 of *Fields Institute Communications*. American Mathematical Society, Providence, RI, 2005. Lectures from the workshop held in Toronto, ON, March 29–April 2, 2004.

[21] R. Schlickeiser. General properties of small-amplitude fluctuations in magnetized and unmagnetized collision poor plasmas. i. the dielectric tensor. *Physics of Plasmas*, 17, 2010.

[22] D. Sidhu and H. Unz. The magneto-ionic theory for drifting plasma: The whistler mode. *Transactions of the Kansas Academy of Science*, 70(4):432–450, 1967.

[23] T. H. Stix. *Waves in plasma*. American Institute of Physics, 1992.

[24] D. G. Swanson. *Plasma waves*. Academic, 1989.

[25] A. Tomori. Numerical plasma dispersion relation solver. *WDS'15 Proceedings of Contributed Papers - Physics*, pages 206–211, 2015.

[26] E. R. Tracy, A. J. Brizard, A. S. Richardson, and A. N. Kaufman. *Ray Tracing and Beyond: Phase Space Methods in Plasma Wave Theory*. Cambridge University Press, 2014.

[27] B. A. Trubnikov. *Plasma Physics and the Problem of Controlled Thermonuclear Reactions*, volume 3. Pergamon, 1959.

[28] B. T. Tsurutani and Lakhina G. S. Some basic concepts of wave-particle interactions in collisionless plasmas. *Reviews of Geophysics*, 35:491–502, 1997.

[29] A. A. Vlasov. The vibrational properties of an electron gas. *Soviet Physics Uspekhi*, 10(6):721, 1968.

[30] H. Xie and Y. Xiao. Pdrk: a general kinetic dispersion relation solver for magnetized plasma. *Plasma Science and Technology*, 18(2), 2016.

[31] K. Yamaguchi, T. Matsumuro, Y. Omura, and D. Nunn. Ray tracing of whistler-mode chorus elements. *Ann. Geophys.*, 31:665–673, 2013.

CHAPTER 2

Dispersion relations in cold magnetized plasmas

This chapter is the subject of the following publication :
C. Cheverry and A. Fontaine, *Dispersion relation in cold magnetized plasmas*,
Kinetic and Related Models, Vol 10, Issue 2, June 2017, 373–421.

Résumé. En partant de modèles cinétiques adaptés aux plasmas froids non collisionnels, on fournit une description complète de la variété caractéristique sur laquelle repose la propagation d'ondes éléctromagnétiques. Tout comme dans [4, 13, 17], l'analyse est basée sur un calcul asymptotique, exploitant la présence au niveau des équations de Vlasov-Maxwell relativistes d'un paramètre grand : la gyrofréquence éléctronique. La méthode est inspirée de l'optique géométrique [29, 33]. Elle permet d'unifier tous les précédents résultats [8, 12, 31, 37, 38, 40], tout en incorporant de nouveaux aspects. En particulier, l'influence non triviale [5, 9, 10, 24] des variations en espace de la densité, de la température et du champ magnétique sont mises en évidence. De cette manière, une vision globale des relations de dispersion est fournise, avec d'importantes applications en physique des plasmas.

Mots clés. Équations de Vlasov-Maxwell relativistes ; Plasmas froids magnétisés ; Phénomènes plasma hors équilibre ; Propagation d'ondes éléctromagnétiques ; Relations de dispersion ; Variété caractéristique ; Équations de Appleton-Hartree ; Équation eikonal.

Abstract. Starting from kinetic models of cold magnetized collisionless plasmas, we provide a complete description of the characteristic variety sustaining electromagnetic wave propagation. As in [4, 13, 17], the analysis is based on some asymptotic calculus exploiting the presence at the level of dimensionless relativistic Vlasov-Maxwell equations of a large parameter: the electron gyrofrequency. The method is inspired from geometric optics [29, 33]. It allows to unify all the preceding results [8, 12, 31, 37, 38, 40], while incorporating new aspects. Specifically, the non trivial effects [5, 9, 10, 24] of the spatial variations of the background density, temperature and magnetic field are exhibited. In this way, a comprehensive overview of the dispersion relations becomes available, with important possible applications in plasma physics [7, 28, 30].

Keywords. Relativistic Vlasov-Maxwell equations; Cold magnetized plasmas; Plasma phenomena out of equilibrium; Electromagnetic wave propagation; Dispersion relations; characteristic variety; Appleton-Hartree equations; eikonal equations.

2.1. Introduction

The Appleton-Hartree equation, sometimes referred to as the Appleton-Lassen equation, is a mathematical expression that describes the refractive index for electromagnetic wave propagation in a *cold magnetized* plasma. Historically [15], it was developed in the context of the magneto-ionic theory. The form that is still widely exploited in plasma physics [12, 30, 37] is valid in the case of a *uniform* magnetic field. It resulted from the works of E. Appleton [1] and D. Hartree [20] between 1929 and 1932. It was definitely established during the 1960s, in a series of articles [22, 36], technical notes [39] and books [21, 30].

Despite the abundance of literature on the subject, more refined models are still the focus of ongoing research. It is because numerous factors may be considered: the framework may be relativistic [8, 40]; it may look at the oblique propagation [31, 38]; it can select a special frequency range (to point out for instance whistler waves [7, 36]); it may incorporate the influence of boundaries [2, 10]; and, last but not least, it can take into account the presence of spatial inhomogeneities. The aim of the present article is to discuss this issue through a new comprehensive approach that encompasses all the foregoing elements, while adding significant additional information concerning the last one.

A complete mathematical formulation of the problem is available by coming back to the original relativistic Vlasov-Maxwell (RVM) system. The general setting is as in [16], or see directly at (2.2.7)-(2.2.8). It allows to take a principle-based approach. One challenge is to fix adequately the physical framework. This must be done with a close link to concrete situations and in accordance with the basic concepts of plasma physics. As a prototype of a cold magnetized plasma, we will consider the earth's magnetosphere. This choice allows access to exhaustive, reliable and verifiable data. Simplifications come from three basic requirements. As stated in Assumption 2.2.1, the temperatures and the densities of the species are supposed to undergo only slight variations. As prescribed in Assumption 2.2.2, partially or fully ionized space plasmas have almost the same number of positive (ions) and negative (electrons) charges, and therefore behave *quasineutral* [18, 19]. Moreover, as indicated in Assumption 2.2.3, most particles are in a state of local *cold* thermodynamic equilibrium [8, 31]. There remains, however, a limited but very significant fraction of the plasma which is out of equilibrium. The related nonthermal facets play a central role in many applications. They are usually tackled through some stability analysis [26].

Another key aspect of astrophysical plasmas is the decisive intervention of some exterior magnetic field $\tilde{\mathbf{B}}_e$. From this point of view, the situation is very similar to that of magnetic confinement fusion [4, 13, 14]. The charged particles are deflected by $\tilde{\mathbf{B}}_e$ through the Lorentz force. The strong influence of $\tilde{\mathbf{B}}_e$ leads to the introduction of a small dimensionless parameter ε, with $0 < \varepsilon \ll 1$, defined at the level of (2.2.48), and coming from the inverse of the electron cyclotron frequency. In addition, the geomagnetic field $\tilde{\mathbf{B}}_e$ is inhomogeneous. More precisely, it can be approximated by a dipole model. With position $\mathbf{x}$ in some open set $\Omega \subset \mathbb{R}^3$, it takes the form $\tilde{\mathbf{B}}_e \equiv \varepsilon^{-1}\,\mathbf{B}_e(\mathbf{x})$, where the function $\mathbf{B}_e(\cdot)$ is subjected to Assumptions 2.2.4 and 2.2.5. As shown in (2.2.40), it follows that the Vlasov equation contains the penalization term $\varepsilon^{-1}\,(\mathbf{p} \times \mathbf{B}_e(\mathbf{x})) \cdot \nabla_{\mathbf{p}}$, where $\mathbf{p} \in \mathbb{R}^3$ is a momentum.

A work of preparation allows to extract the dimensionless version of the RVM equations. Then, the parameter ε can serve as a unit of measurement to which all the dimensionless quantities can be compared. By this way, we are led to a singular version of the RVM system. The corresponding asymptotic analysis is part of a long tradition of mathematical works in gyrokinetics [4, 13], fast rotating fluids [6] and geometric optics [29, 33]. The uniform case, that is when the function $\mathbf{B}_e(\cdot)$ is constant, has been extensively studied. However, the realistic frameworks [5, 7] imply non-constant functions $\mathbf{B}_e(\cdot)$. Now, the variations of $\mathbf{B}_e(\cdot)$ raise numerous difficulties. Their effects have not been investigated so far; they remain poorly understood; and they do not fall under the scope of classical results. The complications stem from the penalization term $\varepsilon^{-1}\,(\mathbf{p}\times\mathbf{B}_e(\mathbf{x}))\cdot\nabla_{\mathbf{p}}$ that involves a large skew-adjoint differential operator with *variable coefficients*.

The present article is starting to address this problem. It shows that the variations of $\mathbf{B}_e(\cdot)$, both in amplitude and directions, play a crucial role in electromagnetic wave propagation. In a logical order, they impact the dispersion relations, the eikonal equations, and finally the ray tracing methods [25, 41]. They have therefore important practical implications. To make our main results readable and usable, some notation is needed.

A propagating wave located at the position $(\mathbf{t},\mathbf{x})\in M:=[0,1]\times\Omega$ may be characterized by its temporal frequency $\tau\in\mathbb{R}$ and its wave vector $\xi\in\mathbb{R}^3$, with $(\tau,\xi)\in\mathbb{R}^4\setminus\{0\}$. The position $(\mathbf{t},\mathbf{x},\tau,\xi)\in T^*M$ must satisfy restrictions. It must belong to a subset $\mathscr{V}$ of T^*M called the *characteristic variety*, and specified in Paragraph 2.3.2.1 (see Definition 2.3.1). In practice, $(\mathbf{t},\mathbf{x},\tau,\xi)\in\mathscr{V}$ if and only if τ and ξ are linked by dispersion relations. These relations appear to depend on $\mathbf{x}\in\Omega$, on $|\tau|\in\mathbb{R}_+$, on $r:=|\xi|\in\mathbb{R}_+$ and on the angle $\varpi\in[0,\pi]$ between ξ and $\mathbf{B}_e(\mathbf{x})$. On the other hand, they do not involve the time $\mathbf{t}\in[0,1]$ and the polar angle $\omega\in[0,2\,\pi]$. In other words, the relation $(\mathbf{t},\mathbf{x},\tau,\xi)\in\mathscr{V}$ is equivalent to impose $(|\tau|,r)\in\mathrm{V}(\mathbf{x},\varpi)$ for some subset $\mathrm{V}(\mathbf{x},\varpi)$ of the quadrant $\mathbb{R}_+\times\mathbb{R}_+$.

In the magnetosphere, signals split up into two characteristic components. In the case of *oblique* propagation ($\varpi\neq 0$), this translates into a partition $\mathrm{V}(\mathbf{x},\varpi)=\mathrm{V}_o(\mathbf{x},\varpi)\sqcup\mathrm{V}_x(\mathbf{x},\varpi)$. The part $\mathrm{V}_o(\mathbf{x},\varpi)$ is associated to *ordinary* waves (o-waves), whereas the subset $\mathrm{V}_x(\mathbf{x},\varpi)$ is related to *extraordinary* waves (x-waves). O-waves and x-waves are commonly observed. A precise mathematical definition of $\mathrm{V}_o(\mathbf{x},\varpi)$ and $\mathrm{V}_x(\mathbf{x},\varpi)$ is given in the statement below.

Theorem 1. *[oblique dispersion relations, when $\varpi\neq 0(\pi)$] Introduce as in Definition 2.3.3 the resonance frequencies $\tau_\infty^\pm(\cdot)$ with $\tau_\infty^-(\mathbf{x},\varpi)<\tau_\infty^+(\mathbf{x},\varpi)$, and as in Definition 2.3.2 the cutoff frequencies $\tau_0^\pm(\cdot)$ with $\tau_0^-(\mathbf{x})<\tau_0^+(\mathbf{x})$. With the functions $g_\pm(\cdot)$ of Definition 2.3.4, both sets $\mathrm{V}_o(\mathbf{x},\varpi)$ and $\mathrm{V}_x(\mathbf{x},\varpi)$ consist of two connected components, namely:*

$$\mathrm{V}_o(\mathbf{x},\varpi)=\mathrm{V}_o^+(\mathbf{x},\varpi)\sqcup\mathrm{V}_o^-(\mathbf{x},\varpi)\,,\qquad \mathrm{V}_x(\mathbf{x},\varpi)=\mathrm{V}_x^+(\mathbf{x},\varpi)\sqcup\mathrm{V}_x^-(\mathbf{x},\varpi)\,,$$

with the explicit formulas:

$$\mathrm{V}_o^-(\mathbf{x},\varpi):=\{(\tau,r)\in\mathbb{R}_+\times\mathbb{R}_+\,;\,\tau\leq\tau_\infty^-(\mathbf{x},\varpi)\,,\,r^2=g_+(\mathbf{x},\varpi,\tau)\}\,, \tag{2.1.1a}$$

$$\mathrm{V}_o^+(\mathbf{x},\varpi):=\{(\tau,r)\in\mathbb{R}_+\times\mathbb{R}_+\,;\,\kappa\leq\tau\,,\,r^2=g_+(\mathbf{x},\varpi,\tau)\}\,, \tag{2.1.1b}$$

$$\mathrm{V}_x^-(\mathbf{x},\varpi):=\{(\tau,r)\in\mathbb{R}_+\times\mathbb{R}_+\,;\,\tau_0^-(\mathbf{x})<\tau<\tau_\infty^+(\mathbf{x},\varpi)\,,\,r^2=g_-(\mathbf{x},\varpi,\tau)\}\,, \tag{2.1.1c}$$

$$\mathrm{V}_x^+(\mathbf{x},\varpi):=\{(\tau,r)\in\mathbb{R}_+\times\mathbb{R}_+\,;\,\tau_0^+(\mathbf{x})\leq\tau\,,\,r^2=g_-(\mathbf{x},\varpi,\tau)\}\,. \tag{2.1.1d}$$

The description of the characteristic variety $\mathscr{V}$ through (2.1.1) is directly applicable in a large number of situations. That is why it is highlighted in this introduction. However, this representation implies a special choice of parameterization, which is not appropriate in the case $\varpi = 0$. Precisely, one important contribution of the present article is also to provide a global and intrinsic view of $\mathscr{V}$ (Definition 2.3.1) that allows to study $\mathscr{V}$ in its different facets (Section 2.3.4). In particular, in Paragraph 2.3.4.2, we investigate what happens if we fix $\tau \in \mathbb{R}_+^*$, that is if we consider sets given by $\{\xi \in \mathbb{R}^3\,;\, (\mathbf{t}, \mathbf{x}, \tau, \xi) \in \mathscr{V}\}$. By this way, according to the values of τ, we can recover various pictures. This could include one or two (more or less) nested spheres (Figures 36 and 22). This can also result in one or two connected unbounded sets with conic shape (Figures 19 and 20).

Another significant aspect of our study is the topological decomposition (valid only in the oblique case $\varpi \neq 0$) of $\mathscr{V}$ into connected components. From this perspective, the case of *parallel* propagation ($\varpi = 0$), which is often presented as being indicative of the general situation, appears rather to be a very singular situation. As revealed in Paragraph 2.3.3.3, as can be seen by comparing Figure 16 ($\varpi = 0$) and Figure 17 ($\varpi \to 0$), and as you can guess by looking at Figure 18, it is a composite of ordinary and extraordinary waves. The classical physical nomenclature (in terms of *Alfvèn*, *whistler*, ... and *electrostatic* waves) which is recalled in Paragraph 2.3.3.1 does not take into account this mixture. As a matter of fact, it is based on other considerations.

Theorem 1 gives access to rigorously justified eikonal equations (Lemmas 2.3.18 and 2.3.20) governing the propagation of the phases ϕ. To this end, it suffices to replace in (2.3.40) the variables τ and ξ respectively by $\partial_{\mathbf{t}}\phi(\mathbf{t}, \mathbf{x})$ and $\nabla_{\mathbf{x}}\phi(\mathbf{t}, \mathbf{x})$. The variations of $\mathbf{B}_e(\cdot)$ come into play through the dependence of ϖ and $g_\pm(\cdot)$ on $\mathbf{B}_e(\cdot)$, see (2.3.38) and Definition 2.3.4. As a by product, as shown in Section 2.3.4, purely parallel propagation cannot occur.

In the following text, special emphasis will be placed on frequencies which are in a range around or below, but comparable to the electron cyclotron frequency ε^{-1}. The reasons for this are the following. First, this range is where the exterior magnetic field $\mathbf{B}_e(\cdot)$ has the most influence by a clear separation between ordinary waves and extraordinary waves, and by the appearance of exactly two *cutoff* frequencies and two *resonance* frequencies. Secondly, as is well-known [22, 28, 40], this is where the propagation can be responsible for the energisation of confined plasmas and particle loss [38] through a mechanism of wave-particle interaction [7].

Now, when dealing with the plasmasphere, looking at such frequencies means to focus on Very Low Frequency waves (VLF radio frequencies in the range of 100 Hz to 10 kHz). Experimentally (Figure 26), there are a lower band and a upper band (corresponding to the two resonance frequencies) where VLF emissions arise. The monochromatic elements forming the fine structure of chorus have been mathematically interpreted in [7] as coming from a mesoscopic caustic effect. It was done on the basis of the classical toy model of [12, 30, 37], which is derived from *parallel* propagation ($\varpi = 0$) in the presence of a *uniform* magnetic field. Beyond this preliminary approach, to fully understand the morphological properties of chorus emissions, Theorem 1 is required. As outlined in Paragraph 2.3.4.5, a lot of information about chorus emissions [27, 28, 35, 41] can be extracted from it.

2.2. Kinetic descriptions issued from plasma physics

To model the behavior of a real plasma, we may simplify its characteristics. This is what is done in this Section 2.2. The basic equations are the Relativistic Vlasov-Maxwell equations (RVM equations) recalled in Paragraph 2.2.1. Exact solutions can be produced by looking at local thermodynamic equilibria (Paragraph 2.2.2). However, there are many situations where complex plasma phenomena (Paragraph 2.2.3) play a decisive part.

In Paragraph 2.2.4, we present such a framework issued from near-Earth space plasmas. This application involves a strong external magnetic field, satisfying special assumptions (Paragraph 2.2.5). In Paragraph 2.2.6, we derive the dimensionless form of RVM equations. By this way, we get a basic model (Paragraph 2.2.7) which can serve for the description of electromagnetic waves (Paragraph 2.2.8). This model corresponds to a linear perturbative regime. It is built with the system of equation (2.2.52)-(2.2.53)-(2.2.54) involving the small parameter $\varepsilon \equiv |\varepsilon_1| \ll 1$.

2.2.1. **Relativistic Vlasov-Maxwell equations.** The topic of RVM equations has been widely discussed [4, 7, 13, 16, 26]. The corresponding framework is recalled hereafter. The speed of light is $c_0 \simeq 2,99 \times 10^8\, m\, s^{-1}$. Let $L \in \mathbb{R}_+^*$ be a characteristic spatial length. The original spatial variable is $\tilde{\mathbf{x}} \in \tilde{\Omega}$, where $\tilde{\Omega}$ is some non-empty open set of $\mathbb{R}^3$. We fix the observation time $T \in \mathbb{R}_+^*$ as $T := L/c_0$. The original time variable is $\tilde{\mathbf{t}} \in [0, T]$. There are corresponding rescaled versions:

$$\mathbf{t} := \frac{\tilde{\mathbf{t}}}{T} \in [0,1]\,, \qquad \mathbf{x} = (\mathbf{x}^1, \mathbf{x}^2, \mathbf{x}^3) := \frac{\tilde{\mathbf{x}}}{L} \in \Omega := \left\{ \frac{\tilde{\mathbf{x}}}{L}\,;\, \tilde{\mathbf{x}} \in \tilde{\Omega} \right\}. \tag{2.2.1}$$

The original space and momentum variables are $(\tilde{\mathbf{x}}, \tilde{\mathbf{p}})$ with:

$$\tilde{\mathbf{x}} = (\tilde{\mathbf{x}}^1, \tilde{\mathbf{x}}^2, \tilde{\mathbf{x}}^3) \in \tilde{\Omega} \subset \mathbb{R}^3\,, \qquad \tilde{\mathbf{p}} = (\tilde{\mathbf{p}}^1, \tilde{\mathbf{p}}^2, \tilde{\mathbf{p}}^3) \in \mathbb{R}^3\,.$$

We consider a plasma which is confined inside $\tilde{\Omega}$, and which consists of N distinct species labelled by $\alpha \in \{1, \cdots, N\}$. The particles of the α^{th} species have charge e_α and rest mass m_α. The number $\alpha = 1$ will be associated with electrons. Thus, the elementary charge is $e \equiv -e_1 \simeq 1,6 \times 10^{-19}\, C$ and the electron rest mass is $m_e \equiv m_1 \simeq 9,1 \times 10^{-31}\, kg$. Recall that the proton-to-electron mass ratio $\beta \simeq 1836$ is a dimensionless quantity, so that:

$$\iota_1 := \frac{m_1}{m_e} = 1\,, \qquad \iota_\alpha := \frac{m_1}{m_\alpha} \lesssim \beta^{-1} \simeq 10^{-3}\,, \qquad \forall\, \alpha \in \{2, \cdots, N\}\,. \tag{2.2.2}$$

On the other hand, the charge e_α is an integer multiple of e. More precisely:

$$\forall\, \alpha \in \{2, \cdots, N\}\,, \qquad \exists\, k_\alpha \in \mathbb{N}^*\,; \qquad k_\alpha \simeq 1\,, \qquad e_\alpha = k_\alpha\, e\,. \tag{2.2.3}$$

The velocity $\tilde{\mathbf{v}}_\alpha$ of a particle of type α is limited by $|\tilde{\mathbf{v}}_\alpha| \leq c_0$, and it is linked to the momentum $\tilde{\mathbf{p}} \in \mathbb{R}^3$ through:

$$\frac{\tilde{\mathbf{v}}_\alpha(\tilde{\mathbf{p}})}{c_0} = \frac{\tilde{\mathbf{p}}}{m_\alpha\, c_0} \left(1 + \frac{|\tilde{\mathbf{p}}|^2}{m_\alpha^2\, c_0^2} \right)^{-1/2}, \qquad \frac{\tilde{\mathbf{p}}(\tilde{\mathbf{v}}_\alpha)}{m_\alpha\, c_0} = \frac{\tilde{\mathbf{v}}_\alpha}{c_0} \left(1 - \frac{|\tilde{\mathbf{v}}_\alpha|^2}{c_0^2} \right)^{-1/2}. \tag{2.2.4}$$

The kinetic distribution function (KDF) of the α^{th} species is denoted by $\tilde{\mathrm{f}}^{\mathrm{k}}_\alpha(\tilde{\mathrm{t}},\tilde{\mathbf{x}},\tilde{\mathbf{p}})$. It is composed of:

- A *dominant stationary* part $\tilde{\mathrm{f}}^{\mathrm{d}}_\alpha(\tilde{\mathbf{x}},\tilde{\mathbf{p}})$; - A *smaller moving* part $\tilde{\mathrm{f}}^{\mathrm{s}}_\alpha(\tilde{\mathrm{t}},\tilde{\mathbf{x}},\tilde{\mathbf{p}})$.

The density ratio $\nu \in \mathbb{R}^*_+$ between these two populations is assumed to be small and independant of α:

$$\tilde{\mathrm{f}}^{\mathrm{k}}_\alpha(\tilde{\mathrm{t}},\tilde{\mathbf{x}},\tilde{\mathbf{p}}) = \tilde{\mathrm{f}}^{\mathrm{d}}_\alpha(\tilde{\mathbf{x}},\tilde{\mathbf{p}}) + \nu\ \tilde{\mathrm{f}}^{\mathrm{s}}_\alpha(\tilde{\mathrm{t}},\tilde{\mathbf{x}},\tilde{\mathbf{p}})\,, \quad (\tilde{\mathrm{t}},\tilde{\mathbf{x}},\tilde{\mathbf{p}}) \in \mathbb{R}_+ \times \tilde{\Omega} \times \mathbb{R}^3\,, \quad \nu \ll 1\,. \tag{2.2.5}$$

The charge density $\tilde{\rho}$ and the current density $\tilde{\jmath}$ are given by:

$$\tilde{\rho} \equiv \tilde{\rho}(\tilde{\mathrm{f}}^{\mathrm{k}}_1,\cdots,\tilde{\mathrm{f}}^{\mathrm{k}}_N)(\tilde{\mathrm{t}},\tilde{\mathbf{x}}) \equiv \tilde{\rho}(\tilde{\mathrm{f}}^{\mathrm{k}}_\alpha)(\tilde{\mathrm{t}},\tilde{\mathbf{x}}) := \sum_{\alpha=1}^{N} \int_{\mathbb{R}^3} e_\alpha\ \tilde{\mathrm{f}}^{\mathrm{k}}_\alpha(\tilde{\mathrm{t}},\tilde{\mathbf{x}},\tilde{\mathbf{p}})\ d\tilde{\mathbf{p}}\,, \tag{2.2.6a}$$

$$\tilde{\jmath} \equiv \tilde{\jmath}(\tilde{\mathrm{f}}^{\mathrm{k}}_1,\cdots,\tilde{\mathrm{f}}^{\mathrm{k}}_N)(\tilde{\mathrm{t}},\tilde{\mathbf{x}}) \equiv \tilde{\jmath}(\tilde{\mathrm{f}}^{\mathrm{k}}_\alpha)(\tilde{\mathrm{t}},\tilde{\mathbf{x}}) := \sum_{\alpha=1}^{N} \int_{\mathbb{R}^3} e_\alpha\ \tilde{\mathbf{v}}_\alpha(\tilde{\mathbf{p}})\ \tilde{\mathrm{f}}^{\mathrm{k}}_\alpha(\tilde{\mathrm{t}},\tilde{\mathbf{x}},\tilde{\mathbf{p}})\ d\tilde{\mathbf{p}}\,. \tag{2.2.6b}$$

We impose a (stationary, divergence and curl-free) external magnetic field $\tilde{\mathbf{B}}_e : \tilde{\Omega} \longrightarrow \mathbb{R}^3$. We also take into account some collective self-consistent electromagnetic field $(\tilde{\mathbf{E}},\tilde{\mathbf{B}})(\tilde{\mathrm{t}},\tilde{\mathbf{x}})$, which is created by all plasma particles. Then, neglecting the collisional effects, the time evolution of the KDF can be modelled through the Vlasov equation:

$$\partial_{\tilde{\mathrm{t}}}\tilde{\mathrm{f}}^{\mathrm{k}}_\alpha + \tilde{\mathbf{v}}_\alpha(\tilde{\mathbf{p}})\cdot\nabla_{\tilde{\mathbf{x}}}\tilde{\mathrm{f}}^{\mathrm{k}}_\alpha + e_\alpha\left[\tilde{\mathbf{E}}(\tilde{\mathrm{t}},\tilde{\mathbf{x}}) + \tilde{\mathbf{v}}_\alpha(\tilde{\mathbf{p}})\times\left(\tilde{\mathbf{B}}(\tilde{\mathrm{t}},\tilde{\mathbf{x}}) + \tilde{\mathbf{B}}_e(\tilde{\mathbf{x}})\right)\right]\cdot\nabla_{\tilde{\mathbf{p}}}\tilde{\mathrm{f}}^{\mathrm{k}}_\alpha = 0\,. \tag{2.2.7}$$

On the other hand, the self-consistent electromagnetic field $(\tilde{\mathbf{E}},\tilde{\mathbf{B}})(\tilde{\mathrm{t}},\tilde{\mathbf{x}})$ is subjected to the Maxwell equations:

$$\partial_{\tilde{\mathrm{t}}}\tilde{\mathbf{E}} - c_0^2\ \nabla_{\tilde{\mathbf{x}}}\times\tilde{\mathbf{B}} = -\,\epsilon_0^{-1}\ \tilde{\jmath}(\tilde{\mathrm{f}}^{\mathrm{k}}_\alpha)\,, \qquad \nabla_{\tilde{\mathbf{x}}}\cdot\tilde{\mathbf{E}} = \epsilon_0^{-1}\ \tilde{\rho}(\tilde{\mathrm{f}}^{\mathrm{k}}_\alpha)\,, \tag{2.2.8a}$$

$$\partial_{\tilde{\mathrm{t}}}\tilde{\mathbf{B}} + \nabla_{\tilde{\mathbf{x}}}\times\tilde{\mathbf{E}} = 0\,, \qquad \nabla_{\tilde{\mathbf{x}}}\cdot\tilde{\mathbf{B}} = 0\,. \tag{2.2.8b}$$

In (2.2.8), the physical constant $\epsilon_0 \simeq 8,8\times10^{-12}\,F\,m^{-1}$ stands for the vacuum permitivity.

2.2.2. **Dominant stationary part in a state of local thermodynamic equilibrium.** The unknowns in (2.2.7)-(2.2.8) are the $\tilde{\mathrm{f}}^{\mathrm{k}}_\alpha(\cdot)$ and $(\tilde{\mathbf{E}},\tilde{\mathbf{B}})(\cdot)$. For $\nu = 0$ and $(\tilde{\mathbf{E}},\tilde{\mathbf{B}}) = (0,0)$, we simply find:

$$(\tilde{\mathrm{f}}^{\mathrm{k}}_1(\tilde{\mathrm{t}},\tilde{\mathbf{x}},\tilde{\mathbf{p}}),\cdots,\tilde{\mathrm{f}}^{\mathrm{k}}_N(\tilde{\mathrm{t}},\tilde{\mathbf{x}},\tilde{\mathbf{p}}),\tilde{\mathbf{E}}(\tilde{\mathrm{t}},\tilde{\mathbf{x}}),\tilde{\mathbf{B}}(\tilde{\mathrm{t}},\tilde{\mathbf{x}})) = (\tilde{\mathrm{f}}^{\mathrm{d}}_1(\tilde{\mathbf{x}},\tilde{\mathbf{p}}),\cdots,\tilde{\mathrm{f}}^{\mathrm{d}}_N(\tilde{\mathbf{x}},\tilde{\mathbf{p}}),0,0)\,. \tag{2.2.9}$$

This expression is assumed to satisfy (2.2.7) modulo some small term (to be specified later):

$$\tilde{\mathbf{v}}_\alpha(\tilde{\mathbf{p}})\cdot\nabla_{\tilde{\mathbf{x}}}\tilde{\mathrm{f}}^{\mathrm{d}}_\alpha + e_\alpha\ \left[\tilde{\mathbf{v}}_\alpha(\tilde{\mathbf{p}})\times\tilde{\mathbf{B}}_e(\tilde{\mathbf{x}})\right]\cdot\nabla_{\tilde{\mathbf{p}}}\tilde{\mathrm{f}}^{\mathrm{d}}_\alpha \simeq 0\,, \qquad \forall\,\alpha\in\{1,\cdots,N\}\,. \tag{2.2.10}$$

It is also an equilibrium from the viewpoint of waves, meaning that:

$$\epsilon_0^{-1}\ \tilde{\jmath}(\tilde{\mathrm{f}}^{\mathrm{d}}_\alpha)(\tilde{\mathbf{x}}) = 0\,, \tag{2.2.11a}$$

$$\tilde{\rho}(\tilde{\mathrm{f}}^{\mathrm{d}}_\alpha)(\tilde{\mathbf{x}}) = 0\,. \tag{2.2.11b}$$

The aim of this subsection 2.2.2 is to give a detailed description of special functions $\tilde{\mathrm{f}}^{\mathrm{d}}_\alpha(\cdot)$ satisfying (2.2.10) and (2.2.11), together with a number of other relevant physical constraints. As a matter of fact, the two paragraphs 2.2.2.1 and 2.2.2.2 will consider (2.2.11b). On the

other hand, the paragraph 2.2.2.3 will give a precise description of $\tilde{\mathrm{f}}^{\mathrm{d}}_{\alpha}(\cdot)$, complemented by the examination of (2.2.10) and the verification of (2.2.11a).

2.2.2.1. *Cold, warm and hot plasma temperatures.* A plasma which turns to be spatially in Local Thermodynamic Equilibrium (LTE) can be characterized at the position $\tilde{\mathbf{x}}$ with a few parameters, like the temperatures $\tilde{\theta}^{\mathrm{d}}_{\alpha}(\tilde{\mathbf{x}})$ and the densities $\tilde{\mathbf{n}}^{\mathrm{d}}_{\alpha}(\tilde{\mathbf{x}})$ of the α^{th} species. Both $\tilde{\theta}^{\mathrm{d}}_{\alpha}(\cdot)$ and $\tilde{\mathbf{n}}^{\mathrm{d}}_{\alpha}(\cdot)$ are building blocks in the construction of $\tilde{\mathrm{f}}^{\mathrm{d}}_{\alpha}(\cdot)$. Retain for instance that $\tilde{\mathbf{n}}^{\mathrm{d}}_{\alpha}(\cdot)$ can be recovered from $\tilde{\mathrm{f}}^{\mathrm{d}}_{\alpha}(\cdot)$ through the integral formula:

$$\tilde{\mathbf{n}}^{\mathrm{d}}_{\alpha}(\tilde{\mathbf{x}}) := \int_{\mathbb{R}^3} \tilde{\mathrm{f}}^{\mathrm{d}}_{\alpha}(\tilde{\mathbf{x}},\tilde{\mathbf{p}})\, d\tilde{\mathbf{p}}\,, \qquad \tilde{\mathbf{x}} \in \tilde{\Omega}\,, \qquad \alpha \in \{1,\cdots,N\}\,. \tag{2.2.12}$$

Denote simply by $\theta^{\mathrm{d}}_{\alpha} \in \mathbb{R}^*_+$ and $n^{\mathrm{d}}_{\alpha} \in \mathbb{R}^*_+$ typical sizes of $\tilde{\theta}^{\mathrm{d}}_{\alpha}(\cdot)$ and $\tilde{\mathbf{n}}^{\mathrm{d}}_{\alpha}(\cdot)$. We require that the two quantities $\tilde{\theta}^{\mathrm{d}}_{\alpha}(\tilde{\mathbf{x}})$ and $\tilde{\mathbf{n}}^{\mathrm{d}}_{\alpha}(\tilde{\mathbf{x}})$ do not deviate too far from $\theta^{\mathrm{d}}_{\alpha}$ and n^{d}_{α}. In other words:

Assumption 2.2.1. *[possible but slight variations in temperatures and densities] There is a constant $c \in]0,1[$ such that:*

$$0 < c\,\theta^{\mathrm{d}}_{\alpha} \le \tilde{\theta}^{\mathrm{d}}_{\alpha}(\tilde{\mathbf{x}}) \le c^{-1}\,\theta^{\mathrm{d}}_{\alpha}\,, \quad 0 < c\,n^{\mathrm{d}}_{\alpha} \le \tilde{\mathbf{n}}^{\mathrm{d}}_{\alpha}(\tilde{\mathbf{x}}) \le c^{-1}\,n^{\mathrm{d}}_{\alpha}\,, \quad \forall\,\tilde{\mathbf{x}} \in \tilde{\Omega}\,. \tag{2.2.13}$$

Recall that $k_B \simeq 1,38 \times 10^{-23}\, m^2\, kg\, s^{-2}\, K^{-1}$ stands for the Boltzmann constant, and also retain the relationship $1\, eV \simeq 1,16 \times 10^4\, k_B\, K$. The electron temperature ($T_e \equiv T_1$) and the ion temperatures (denoted by T_α for $\alpha > 1$) can be expressed either in kelvin (K) or in electronvolt (eV). Because of the large difference in mass, the electrons will come to thermodynamic equilibrium amongst themselves much faster than they will come into equilibrium with the ions or neutral atoms. For this reason, the ion temperatures may be very different from (usually much lower than) the electron temperature:

$$T_\alpha \le T_e \equiv T_1\,, \qquad \forall\,\alpha \in \{1,\cdots,N\}\,. \tag{2.2.14}$$

Based on the relative temperatures of the electrons, ions and neutrals, plasmas are classified as thermal or non-thermal. Introduce the thermal speed:

$$v^{th}_{\alpha} := \Big(\frac{k_B\, T_\alpha}{m_\alpha}\Big)^{1/2} \in \mathbb{R}^*_+\,. \tag{2.2.15}$$

It is linked to the dimensionless parameter $\theta^{\mathrm{d}}_{\alpha}$ through:

$$\theta^{\mathrm{d}}_{\alpha} := \frac{v^{th}_{\alpha}}{c_0} \in \mathbb{R}^*_+\,. \tag{2.2.16}$$

These two quantities v^{th}_{α} and $\theta^{\mathrm{d}}_{\alpha}$ can also be viewed as measures of temperature. Combining (2.2.2) and (2.2.14), we get:

$$\frac{v^{th}_{\alpha}}{v^{th}_{1}} = \frac{\theta^{\mathrm{d}}_{\alpha}}{\theta^{\mathrm{d}}_{1}} = \Big(\frac{T_\alpha}{T_1}\Big)^{1/2} \times \Big(\frac{m_1}{m_\alpha}\Big)^{1/2} \lesssim \Big(\frac{T_\alpha}{T_1}\Big)^{1/2} \times \Big(\frac{1}{\beta}\Big)^{1/2} \ll 1\,. \tag{2.2.17}$$

As a rule of thumb, temperatures T_α well below $100\, eV$ are said *cold*; those which are about $100\, eV$ ($\theta^{\mathrm{d}}_{\alpha} \simeq 10^{-2}$) are considered *warm*; those with T_α ranging from $100\, eV$ to $10\, keV$ ($10^{-2} \lesssim \theta^{\mathrm{d}}_{\alpha} \lesssim 1$) become progressively *hot*; particles with higher energies ($1 \lesssim \theta^{\mathrm{d}}_{\alpha}$) are termed *energetic* or *relativistic*.

2.2.2.2. *Quasi-neutrality.* A plasma consists of approximately equal numbers of positively charged ions and negatively charged electrons. This property is expressed by (2.2.11b). In view of (2.2.6a) and (2.2.12), this can also take the following equivalent form.

Assumption 2.2.2. *The plasma is quasi-neutral in the sense that:*

$$e\ \tilde{\mathbf{n}}_1^{\mathrm{d}}(\tilde{\mathbf{x}}) \ = \ \sum_{\alpha=2}^{N} e_\alpha\ \tilde{\mathbf{n}}_\alpha^{\mathrm{d}}(\tilde{\mathbf{x}})\,, \qquad \forall\, \tilde{\mathbf{x}} \in \tilde{\Omega}\,. \tag{2.2.18}$$

The interpretation of (2.2.18) is the existence of a background neutralizing ion population. In view of (2.2.3), (2.2.13) and (2.2.18), we can infer that:

$$e\ n_1^{\mathrm{d}} \ \simeq \ \sum_{\alpha=2}^{N} e_\alpha\ n_\alpha^{\mathrm{d}}\,, \qquad n_\alpha^{\mathrm{d}} \simeq n_1^{\mathrm{d}}\,, \qquad \forall\, \alpha \in \{2, \cdots, N\}\,. \tag{2.2.19}$$

2.2.2.3. *Velocity distribution function.* Several existing models can be used to describe $\tilde{\mathrm{f}}_\alpha^{\mathrm{d}}(\cdot)$. The basic descriptions rely on the following choice.

Definition 2.2.1. *The Maxwell-Boltzmann distribution is given by:*

$$\tilde{\mathrm{f}}_\alpha^{\mathrm{d}}(\tilde{\mathbf{x}}, \tilde{\mathbf{p}}) = \frac{\tilde{\mathbf{n}}_\alpha^{\mathrm{d}}(\tilde{\mathbf{x}})}{m_\alpha^3\, c_0^3}\ \mathcal{M}^b_{\tilde{\theta}_\alpha^{\mathrm{d}}(\tilde{\mathbf{x}})}\Big(\frac{|\tilde{\mathbf{p}}|}{m_\alpha\, c_0}\Big)\,, \qquad \mathcal{M}^b_\theta(r) := \frac{1}{\pi^{3/2}}\ \frac{1}{\theta^3}\ \exp\Big(-\frac{r^2}{\theta^2}\Big)\,. \tag{2.2.20}$$

Retain that:

$$\partial_\theta \mathcal{M}^b_\theta(r) = \frac{1}{\theta}\ \mathfrak{m}^b_\theta(r)\ \mathcal{M}^b_\theta(r)\,, \qquad \mathfrak{m}^b_\theta(r) := -\,3 + 2\,\Big(\frac{r}{\theta}\Big)^2\,. \tag{2.2.21}$$

Moreover, $\mathcal{M}^b_\theta(\cdot)$ is a smooth probability density function (for the measure $4\,\pi\, r^2\, dr$):

$$\int_{\mathbb{R}^3} \mathcal{M}^b_\theta(|\mathbf{p}|)\ d\mathbf{p} \ = \ 4\ \pi \int_0^{+\infty} \mathcal{M}^b_\theta(r)\ r^2\ dr \ = \ 1\,, \qquad \forall\, \theta \in \mathbb{R}_+^*\,. \tag{2.2.22}$$

Assumption 2.2.3. *[the dominant stationnary parts of all species are in a state of local cold thermodynamic equilibrium] For all $\alpha \in \{1, \cdots, N\}$, we have (2.2.20) and the relation (2.2.13) is satisfied for some $\theta_\alpha^{\mathrm{d}} \lesssim 10^{-2}$.*

In the scientific literature [23, 40], the term *cold plasma* is sometimes associated with a Dirac mass in the momentum $\tilde{\mathbf{p}}$, in which case $\theta = 0$ or equivalently $\mathcal{M}(r) \equiv (4\,\pi)^{-1}\, r^{-2}\, \delta_{|r=0}$. However, the temperatures are not zero. The use of (2.2.20) is therefore more refined, while keeping track of concentration effects through the (possible) smallness of θ.

Electrons are lighter than ions and neutral atoms. This is why they can easier reach higher energies. This is especially true in the case of the outer Van Allen belt as it will be explained in Paragraph 2.2.4. It follows that the dominant populations can inherit more complex structures than (2.2.20). As long as $\theta_\alpha^{\mathrm{d}} \lesssim 10^{-2}$, we can keep (2.2.20) to describe $\tilde{\mathrm{f}}_\alpha^{\mathrm{d}}(\cdot)$. But beyond, that is for hot plasmas ($10^{-2} \lesssim \theta_\alpha^{\mathrm{d}} \lesssim 1$) and all the more so for relativistic beams ($1 \lesssim \theta_\alpha^{\mathrm{d}}$), it might be preferable to select a Maxwell-Jüttner distribution function. Such relativistic aspects will be examined in a forthcoming publication. Here, we will stay in the context of (2.2.20). Assuming (2.2.20), we find that:

$$\begin{aligned} \big[\tilde{\mathbf{v}}_\alpha \cdot \nabla_{\tilde{\mathbf{x}}} + \ e_\alpha\ (\tilde{\mathbf{v}}_\alpha \times \tilde{\mathbf{B}}_e) \cdot \nabla_{\tilde{\mathbf{p}}}\big](\ln \tilde{\mathrm{f}}_\alpha^{\mathrm{d}}) &= \tilde{\mathbf{v}}_\alpha \cdot \nabla_{\tilde{\mathbf{x}}}(\ln \tilde{\mathrm{f}}_\alpha^{\mathrm{d}}) \\ &= \ \tilde{\mathbf{v}}_\alpha \cdot \nabla_{\tilde{\mathbf{x}}}(\ln \tilde{\mathbf{n}}_\alpha^{\mathrm{d}}) + \tilde{\mathbf{v}}_\alpha \cdot \nabla_{\tilde{\mathbf{x}}}(\ln \tilde{\theta}_\alpha^{\mathrm{d}})\ \mathfrak{m}^b_{\tilde{\theta}_\alpha^{\mathrm{d}}}\Big(\frac{|\tilde{\mathbf{p}}|}{m_\alpha\, c_0}\Big)\,. \end{aligned} \tag{2.2.23}$$

If the temperature and the density are constant, that is if $\tilde{\theta}^{\rm d}_\alpha(\cdot) \equiv \theta^{\rm d}_\alpha$ and $\tilde{\mathbf{n}}^{\rm d}_\alpha(\cdot) \equiv n^{\rm d}_\alpha$, the right-hand term of (2.2.23) disappears. Then, the expression (2.2.20) yields exact solutions to the equation (2.2.10). On the contrary, when $\nabla_{\tilde{\mathbf{x}}}(\ln \tilde{\theta}^{\rm d}_\alpha) \not\equiv 0$ or when $\nabla_{\tilde{\mathbf{x}}}(\ln \tilde{\mathbf{n}}^{\rm d}_\alpha) \not\equiv 0$, this term is sure to contribute (more or less strongly). As revealed by the dimensionless version of the equations (see Paragraph 2.2.6), the induced effect depends on the variations of $\tilde{\theta}^{\rm d}_\alpha(\cdot)$ and $\tilde{\mathbf{n}}^{\rm d}_\alpha(\cdot)$ in $\tilde{\mathbf{x}}$, but also on the size of the temperature $\theta^{\rm d}_\alpha$.
The expression $\tilde{\rm f}^{\rm d}_\alpha(\cdot)$ issued from (2.2.20) involves even functions. It makes no contribution to the current density in (2.2.6b). When dealing with (2.2.20), the constraint (2.2.11a) is sure to be satisfied.

2.2.3. **Plasma phenomena out of equilibrium.** *Collisionless* plasmas are characterized by a Knudsen number K_n larger than one. It follows that the possible discrepencies from the Maxwell-Boltzmann distributions are not immediately relaxed. Expressions like (2.2.9), where the $\tilde{\rm f}^{\rm d}_\alpha(\cdot)$ are adjusted as in (2.2.20), are therefore not sufficiently exhaustive to fully describe realistic plasmas. In particular, in connection with observed phenomena, the following aspect may need to be incorporated:

- *Spatial variations in the position* $\tilde{\mathbf{x}}$**:** As already taken into account, most concrete situations involve non constant functions $\tilde{\mathbf{n}}^{\rm d}_\alpha(\cdot) - n^{\rm d}_\alpha$ and $\tilde{\theta}^{\rm d}_\alpha(\cdot) - \theta^{\rm d}_\alpha$. A perturbative approach is required to absorb the remainders obtained when computing (2.2.7), see the right-hand term of (2.2.23).
- *Anisotropic effects in the momentum* $\tilde{\mathbf{p}}$**:** There is a plethora of factors that produce inhomogeneities according to the different directions $|\tilde{\mathbf{p}}|^{-1}\,\tilde{\mathbf{p}} \in \mathbb{S}^2$ of $\tilde{\mathbf{p}}$. Examples include lighting strikes, solar flares, ohming heating, neutral beam injections, high-frequency and radio-frequency waves. Obviously, such features cannot be included inside (2.2.20), because this expression depends only on $|\tilde{\mathbf{p}}|$.
- *Dynamical aspects***:** The anisotropy in $\tilde{\mathbf{p}}$ can be enhanced by the external magnetic field $\tilde{\mathbf{B}}_e(\cdot)$ through the Lorentz force. This results in microscopic time-dependent instabilities, known as anomalous transport.
- *Electromagnetic perturbations***:** In practice, fluctuations of the electric field and of the magnetic field (near $\tilde{\mathbf{B}}_e$) are recorded. In contrast with (2.2.9), the self-consistent field $(\tilde{\mathbf{E}}, \tilde{\mathbf{B}})(\cdot)$ is in general non-trivial.

To grasp plasma instabilities or plasma processes which are not in thermal equilibrium, we can perform a stability analysis in the vicinity of (2.2.9). This amounts to take $\nu \in \mathbb{R}^*_+$ with $\nu \ll 1$ in (2.2.5). From now on, the focus will be on (2.2.7)-(2.2.8) in the context of the perturbative regime (2.2.5). With a dominant stationary part adjusted as in (2.2.20), we look at the extra part $\tilde{\rm f}^{\rm s}_\alpha(\cdot)$, which is governed by:

$$\left\{\begin{array}{l} \partial_{\tilde{\mathbf{t}}}\tilde{\rm f}^{\rm s}_\alpha + \tilde{\mathbf{v}}_\alpha(\tilde{\mathbf{p}})\cdot\nabla_{\tilde{\mathbf{x}}}\tilde{\rm f}^{\rm s}_\alpha + e_\alpha\,\big[\,\tilde{\mathbf{E}} + \tilde{\mathbf{v}}_\alpha(\tilde{\mathbf{p}})\times(\tilde{\mathbf{B}}+\tilde{\mathbf{B}}_e)\,\big]\cdot\nabla_{\tilde{\mathbf{p}}}\tilde{\rm f}^{\rm s}_\alpha \\ \qquad\qquad = -\,\nu^{-1}\,\tilde{\mathbf{v}}_\alpha(\tilde{\mathbf{p}})\cdot\nabla_{\tilde{\mathbf{x}}}\tilde{\rm f}^{\rm d}_\alpha - \nu^{-1}e_\alpha\,\tilde{\mathbf{E}}\cdot\nabla_{\tilde{\mathbf{p}}}\tilde{\rm f}^{\rm d}_\alpha\,, \\ \partial_{\tilde{\mathbf{t}}}\tilde{\mathbf{B}} + \nabla_{\tilde{\mathbf{x}}}\times\tilde{\mathbf{E}} = 0\,, \\ \partial_{\tilde{\mathbf{t}}}\tilde{\mathbf{E}} - c_0^2\,\nabla_{\tilde{\mathbf{x}}}\times\tilde{\mathbf{B}} = -\,\epsilon_0^{-1}\nu\,\tilde{\jmath}(\tilde{\rm f}^{\rm s}_1,\cdots,\tilde{\rm f}^{\rm s}_N)\,, \end{array}\right. \tag{2.2.24}$$

together with:

$$\nabla_{\tilde{\mathbf{x}}}\cdot\tilde{\mathbf{E}} = \epsilon_0^{-1}\nu\,\tilde{\rho}(\tilde{\rm f}^{\rm s}_1,\cdots,\tilde{\rm f}^{\rm s}_N)\,, \qquad \nabla_{\tilde{\mathbf{x}}}\cdot\tilde{\mathbf{B}} = 0\,. \tag{2.2.25}$$

2.2.4. **Some concrete situation.** The description through (2.2.20) of the underlying medium can be further specified with regard to the applications in physics. We will consider the case of Near-Earth space plasmas [24], inside the exosphere (where $K_n > 1$). In the inner magnetosphere, we can distinguish two types of particle structures, which can involve special values of temperatures and densities, falling into the context of the description of cold plasmas from Paragraph 2.2.2.

• **C1**. The plasmasphere is a doughnut-shaped region which rotates with the Earth. It is a cold plasma ($\simeq 1\,\mathrm{eV}$) made of H^+ (nominally about 80%), He^+ (10 − 20%) and O^+ (a few percent). As noted in [9], the average electronic temperature is $T_e \simeq 6 \times 10^3\, K$, so that $\theta_1^{\mathrm{d}} \simeq 10^{-3}$. As a result, the selection of (2.2.20) for all $\alpha \in \{1, \cdots, N\}$ is adequate. The plasmaspheric concentration is around a mean value which is close to $n_1^{\mathrm{d}} = 10^8\, electrons/m^3$. The functions $\tilde{\mathbf{n}}_\alpha^{\mathrm{d}}(\cdot)$ may vary slightly from place to place, especially when crossing the slot region. Global realistic profiles for $\tilde{\mathbf{n}}_\alpha^{\mathrm{d}}(\cdot)$ are suggested in [9, 24]. ◦

• **C2**. The outer Van Allen belt partly overlaps with the plasmasphere. It is a concentric, tyre-shaped belt containing ionic and neutral species which may be globally cold, warm, or possibly hot (but certainly not beyond). This belt can also implicate *highly energetic* ($\simeq 1\,\mathrm{MeV}$) electron fluxes which may be trapped [5, 7] by the geomagnetic field. These fast charged parcticles travel along the field lines. They stay approximately at a fixed L-shell, where the density is almost constant. We can therefore take $\tilde{\mathbf{n}}_\alpha^{\mathrm{d}}(\cdot) \equiv n_\alpha^{\mathrm{d}}$ for all $\alpha \in \{1, \cdots, N\}$. In particular, as in **C1.**, we can fix $n_1^{\mathrm{d}} = 10^8\, electrons/m^3$. Moreover, as long as the fraction of hot and energetic particles remains small, even for $\alpha = 1$, we can still select (2.2.20) and incorporate the relativistic aspects inside $\tilde{\mathrm{f}}_1^{\mathrm{s}}$. ◦

In what follows, the two above contexts will be systematically tested. This will appear throughout the text inside paragraphs that will be preceded by the title **Discussion**.

2.2.5. **Inhomogeneous magnetized plasmas.** Most cold plasmas [4, 7, 13, 18] are under the influence of a strong external magnetic field which can be prescribed through some adequate function $\tilde{\mathbf{B}}_e : \tilde{\Omega} \longrightarrow \mathbb{R}^3$, with amplitude $\tilde{\mathbf{b}}_e(\tilde{\mathbf{x}}) := |\tilde{\mathbf{B}}_e(\tilde{\mathbf{x}})|$. The function $\tilde{\mathbf{b}}_e(\cdot)$ is assumed to be of the order $b_e \in \mathbb{R}_+^*$. More precisely, we can find $c \in]0, 1[$ such that:

$$0 < c\, b_e \leq \tilde{\mathbf{b}}_e(\tilde{\mathbf{x}}) \leq c^{-1}\, b_e\,, \qquad \forall\, \tilde{\mathbf{x}} \in \tilde{\Omega}\,. \tag{2.2.26}$$

In view of (2.2.1), we can consider the following rescaled version of $\tilde{\mathbf{B}}_e(\cdot)$:

$$\mathbf{B}_e(\mathbf{x}) := \frac{\tilde{\mathbf{B}}_e(L\,\mathbf{x})}{b_e}\,, \qquad \mathbf{b}_e(\mathbf{x}) := |\mathbf{B}_e(\mathbf{x})|\,. \tag{2.2.27}$$

Then, the condition (2.2.26) becomes:

Assumption 2.2.4. *[nowhere-vanishing external magnetic field] There is $c \in]0, 1[$ such that:*

$$0 < c \leq \mathbf{b}_e(\mathbf{x}) \leq c^{-1}\,, \qquad \forall\, \mathbf{x} \in \Omega\,. \tag{2.2.28}$$

The function $\mathbf{B}_e(\cdot)$ generates a unit vector field:

$$e_3(\mathbf{x}) := \mathbf{b}_e(\mathbf{x})^{-1}\, \mathbf{B}_e(\mathbf{x}) \in \mathbb{S}^2 := \{\mathbf{x} \in \mathbb{R}^3\,;\, |\mathbf{x}| = 1\}\,. \tag{2.2.29}$$

Complete $e_3(\mathbf{x})$ into some right-handed orthonormal basis $(e_1, e_2, e_3)(\mathbf{x})$, with:

$$e_j(\cdot) = {}^t(e_j^1, e_j^2, e_j^3)(\cdot) \in \mathcal{C}^\infty(\Omega; \mathbb{S}^2)\,, \qquad \forall\, j \in \{1,2,3\}\,. \tag{2.2.30}$$

With the preceding ingredients, we can define some orthogonal matrix $O(\mathbf{x})$ and some constant skew-symmetric matrix Λ according to:

$$O := \begin{pmatrix} e_1^1 & e_2^1 & e_3^1 \\ e_1^2 & e_2^2 & e_3^2 \\ e_1^3 & e_2^3 & e_3^3 \end{pmatrix} = {}^tO^{-1}\,, \qquad \Lambda := \begin{pmatrix} 0 & 1 & 0 \\ -1 & 0 & 0 \\ 0 & 0 & 0 \end{pmatrix} = -\,{}^t\Lambda\,. \tag{2.2.31}$$

Assumption 2.2.5. *[divergence and curl-free external magnetic field] The function $\mathbf{B}_e(\cdot)$ is smooth, with $\mathbf{B}_e \in \mathcal{C}^\infty(\Omega; \mathbb{R}^3)$. It is such that:*

$$\nabla_{\mathbf{x}} \cdot \mathbf{B}_e(\mathbf{x}) = 0\,, \qquad \forall\, \mathbf{x} \in \Omega\,, \tag{2.2.32a}$$

$$\nabla_{\mathbf{x}} \times \mathbf{B}_e(\mathbf{x}) = 0\,, \qquad \forall\, \mathbf{x} \in \Omega\,. \tag{2.2.32b}$$

Generally, magnetic field lines are curved. In most concrete situations, the function $\mathbf{B}_e(\cdot)$ is a well-known non constant function of $\mathbf{x} \in \mathbb{R}^3$. As depicted below, cylindrical coordinates $(\rho, \varphi, z) \in \mathbb{R}_+^* \times \mathbb{R}^2$ can be used to mark the position of $\mathbf{x}$. Recall that, for any vector field $\mathbf{A} = A_\rho\, e_\rho + A_\varphi\, e_\varphi + A_z\, e_z$, the divergence and the curl are given by the dipole model:

$$\nabla \cdot \mathbf{A} = \frac{1}{\rho}\frac{\partial}{\partial \rho}(\rho A_\rho) + \frac{1}{\rho}\frac{\partial A_\varphi}{\partial \varphi} + \frac{\partial A_z}{\partial z}\,, \tag{2.2.33a}$$

$$\nabla \times \mathbf{A} = \left(\frac{1}{\rho}\frac{\partial A_z}{\partial \varphi} - \frac{\partial A_\varphi}{\partial z}\right) e_\rho + \left(\frac{\partial A_\rho}{\partial z} - \frac{\partial A_z}{\partial \rho}\right) e_\varphi + \frac{1}{\rho}\left(\frac{\partial}{\partial \rho}(\rho A_\rho) - \frac{\partial A_\rho}{\partial \varphi}\right) e_z\,. \tag{2.2.33b}$$

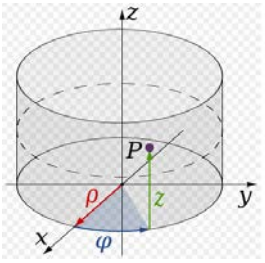

Discussion 2.2.1. *[external magnetic field] In the case of Near-Earth plasmas, just take $L = R^e$, where $R^e \simeq 6,3 \times 10^6\, m$ is the Earth radius. The plasmasphere and the two Van Allen belts occupy some area between altitudes of $2\,R^e$ and $8\,R^e$. We can work with:*

$$\Omega^e := \{\, (\rho, \varphi, z) \in \mathbb{R}_+^* \times \mathbb{R}^2\,;\, 2 < \rho^2 + z^2 < 8\,\}\,.$$

The magnitude of the geomagnetic field, as it can be measured at the surface of the earth, is about $b_e \simeq 10^{-5}\, T$. The Earth's magnetic field $\mathbf{B}_e \equiv \mathbf{B}_e^e$ does not depend on the angle φ. As mentioned for instance in [5, 7], it can be approximated by:

$$\mathbf{B}_e^e(\rho, z) := \frac{1}{(\rho^2 + z^2)^{5/2}} \begin{pmatrix} -\,3\,\rho\, z \\ 0 \\ \rho^2 - 2\, z^2 \end{pmatrix}, \qquad \mathbf{b}_e^e \equiv |\mathbf{B}_e^e| = \frac{(\rho^2 + 4\, z^2)^{1/2}}{(\rho^2 + z^2)^2}\,. \tag{2.2.34}$$

Observe that the two functions $\mathbf{B}_e^e(\cdot)$ and $\mathbf{b}_e^e(\cdot)$ are homogeneous in (ρ, z) of degree -3. We can recover (2.2.28) with $c = 8^{-3}$. Applying (2.2.33a) and (2.2.33b), we see easily that both conditions (2.2.32a) and (2.2.32b) are met. ∘

2.2.6. **Dimensionless equations.** The aim here is to write the system (2.2.24)-(2.2.25) in dimensionless form (Paragraph 2.2.6.1). By doing so, we have to take into account the effects induced by the spatial variations of $\tilde{\mathbf{n}}^{\mathrm{d}}_\alpha(\tilde{\mathbf{x}})$, $\tilde{\theta}^{\mathrm{d}}_\alpha(\tilde{\mathbf{x}})$ and $\tilde{\mathbf{B}}_e(\tilde{\mathbf{x}})$. Then, it is useful to straighten the field lines (Paragraph 2.2.6.2). Moreover, in connection with the application to the earth's context, it is important to give (Paragraph 2.2.6.3) a precise description of (the relative sizes of) the various physical parameters.

2.2.6.1. *Rescalings.* Let us recall (2.2.27), and define rescaled versions of $\tilde{\mathbf{n}}^{\mathrm{d}}_\alpha(\cdot)$ and $\tilde{\theta}^{\mathrm{d}}_\alpha(\cdot)$:

$$\mathbf{n}^{\mathrm{d}}_\alpha(\mathbf{x}) := (n^{\mathrm{d}}_\alpha)^{-1}\tilde{\mathbf{n}}^{\mathrm{d}}_\alpha(L\,\mathbf{x}) \simeq 1\,, \qquad \theta^{\mathrm{d}}_\alpha(\mathbf{x}) := (\theta^{\mathrm{d}}_\alpha)^{-1}\tilde{\theta}^{\mathrm{d}}_\alpha(L\,\mathbf{x}) \simeq 1\,. \tag{2.2.35}$$

This says nothing about the comparison of the selfconsistent magnetic field $\tilde{\mathbf{B}}$ to the typical size b_e of $\tilde{\mathbf{b}}_e(\cdot)$. From the Ampère's law in (2.2.24), we can infer that $\tilde{\mathbf{B}} \simeq \nu\,\theta^{\mathrm{d}}_\alpha\,b_e$. With this in mind, we can further define new unknowns by the relations:

$$\mathbf{v}_\alpha(\mathbf{p}) := (c_0)^{-1}\tilde{\mathbf{v}}_\alpha(\tilde{\mathbf{p}})\,, \qquad \mathbf{p}_\alpha := (m_\alpha\; c_0\,\theta^{\mathrm{d}}_\alpha)^{-1}\tilde{\mathbf{p}}_\alpha\,, \qquad \forall\,\alpha\in\{1,\cdots,N\}\,, \tag{2.2.36a}$$

$$\mathrm{f}_\alpha(\mathbf{t},\mathbf{x},\mathbf{p}_\alpha) := (n^{\mathrm{d}}_\alpha)^{-1}m^3_\alpha\; c^3_0\;(\theta^{\mathrm{d}}_\alpha)^3\;\tilde{\mathrm{f}}^{\mathrm{s}}_\alpha(\tilde{\mathrm{t}},\tilde{\mathbf{x}},\tilde{\mathbf{p}})\,, \qquad \forall\,\alpha\in\{1,\cdots,N\}\,, \tag{2.2.36b}$$

$$\mathbf{E}(\mathbf{t},\mathbf{x}) := (\nu\;\theta^{\mathrm{d}}_1\;c_0\;b_e)^{-1}\;\tilde{\mathbf{E}}(\tilde{\mathrm{t}},\tilde{\mathbf{x}})\,, \qquad \mathbf{B}(\mathbf{t},\mathbf{x}) := (\nu\;\theta^{\mathrm{d}}_1\;b_e)^{-1}\;\tilde{\mathbf{B}}(\tilde{\mathrm{t}},\tilde{\mathbf{x}})\,. \tag{2.2.36c}$$

From now on, the time-spatial position is $(\mathbf{t},\mathbf{x})$, with $(\mathbf{t},\mathbf{x})\in M := [0,1]\times\Omega$. Let T^*M be the cotangent bundle associated with M. With (2.2.36a), the vectors $\mathbf{v}_\alpha$ and $\mathbf{p}_\alpha$ are linked by the relations issued from (2.2.4), that is:

$$\mathbf{p}_\alpha(\mathbf{v}_\alpha) := \frac{\mathbf{v}_\alpha}{\theta^{\mathrm{d}}_\alpha\;(1-|\mathbf{v}_\alpha|^2)^{1/2}}\,, \qquad \mathbf{v}_\alpha(\mathbf{p}_\alpha) := \frac{\theta^{\mathrm{d}}_\alpha\;\mathbf{p}_\alpha}{\langle\theta^{\mathrm{d}}_\alpha\,|\mathbf{p}_\alpha|\rangle}\,, \qquad \langle r\rangle := \sqrt{1+r^2}\,. \tag{2.2.37}$$

Among the fundamental plasma parameters, we can mention (for $\alpha=1$) the electron gyrofrequency (or cyclotron frequency) $\omega_{ce}\equiv\omega_{c1}$ and the electron plasma frequency (or plasma oscillation) $\omega_{pe}\equiv\omega_{p1}$. For $\alpha\in\{2,\cdots,N\}$, we could cite the ion gyrofrequencies $\omega_{c\alpha}$ and the ion plasma frequencies $\omega_{p\alpha}$. For simplicity of presentation, we define below these quantities with an algebraic sign:

$$\omega_{c\alpha} := \frac{e_\alpha\;b_e}{m_\alpha}\,, \qquad \omega_{p\alpha} := \sqrt{\frac{n^{\mathrm{d}}_\alpha\;e^2_\alpha}{m_\alpha\;\epsilon_0}}\,, \qquad \forall\,\alpha\in\{1,\cdots,N\}\,. \tag{2.2.38}$$

There are corresponding dimensionless coefficients ε_α and μ_α, given by:

$$\varepsilon_\alpha := (L\,\omega_{c\alpha})^{-1}c_0\,, \qquad \mu_\alpha := (\omega_{c\alpha})^{-1}\omega_{p\alpha}\,, \qquad \forall\,\alpha\in\{1,\cdots,N\}\,. \tag{2.2.39}$$

Then, the new Vlasov equation is:

$$\begin{aligned}
&\partial_{\mathbf{t}}\mathrm{f}_\alpha + \frac{\theta^{\mathrm{d}}_\alpha}{\langle\theta^{\mathrm{d}}_\alpha\,|\mathbf{p}_\alpha|\rangle}\;\mathbf{p}_\alpha\cdot\nabla_{\mathbf{x}}\mathrm{f}_\alpha + \frac{\theta^{\mathrm{d}}_1}{\theta^{\mathrm{d}}_\alpha}\;\frac{\nu}{\varepsilon_\alpha}\;\Big[\mathbf{E}+\frac{\theta^{\mathrm{d}}_\alpha}{\langle\theta^{\mathrm{d}}_\alpha\,|\mathbf{p}_\alpha|\rangle}\;\mathbf{p}_\alpha\times\mathbf{B}\Big]\cdot\nabla_{\mathbf{p}_\alpha}\mathrm{f}_\alpha \\
&\quad + \frac{1}{\varepsilon_\alpha}\;\frac{1}{\langle\theta^{\mathrm{d}}_\alpha\,|\mathbf{p}_\alpha|\rangle}\;(\mathbf{p}_\alpha\times\mathbf{B}_e(\mathbf{x}))\cdot\nabla_{\mathbf{p}_\alpha}\mathrm{f}_\alpha + \frac{\theta^{\mathrm{d}}_1}{\theta^{\mathrm{d}}_\alpha}\;\frac{\mathbf{n}^{\mathrm{d}}_\alpha}{\varepsilon_\alpha}\;\partial_r\mathcal{M}^b_{\theta^{\mathrm{d}}_\alpha(\mathbf{x})}\Big(|\mathbf{p}_\alpha|\Big)\;\frac{\mathbf{p}_\alpha\cdot\mathbf{E}}{|\mathbf{p}_\alpha|} \\
&\quad + \frac{1}{\nu}\;\frac{\theta^{\mathrm{d}}_\alpha}{\langle\theta^{\mathrm{d}}_\alpha\,|\mathbf{p}_\alpha|\rangle}\;\mathbf{p}_\alpha\cdot\nabla_{\mathbf{x}}\mathbf{n}^{\mathrm{d}}_\alpha\;\mathcal{M}^b_{\theta^{\mathrm{d}}_\alpha(\mathbf{x})}(|\mathbf{p}_\alpha|) \\
&\quad + \frac{1}{\nu}\;\mathbf{n}^{\mathrm{d}}_\alpha\;\frac{\theta^{\mathrm{d}}_\alpha}{\langle\theta^{\mathrm{d}}_\alpha\,|\mathbf{p}_\alpha|\rangle}\;\mathbf{p}_\alpha\cdot\nabla_{\mathbf{x}}(\ln\,\theta^{\mathrm{d}}_\alpha)\;(\mathfrak{m}^b_{\theta^{\mathrm{d}}_\alpha(\mathbf{x})}\,\mathcal{M}^b_{\theta^{\mathrm{d}}_\alpha(\mathbf{x})})(|\mathbf{p}_\alpha|) \;=\; 0\,.
\end{aligned} \tag{2.2.40}$$

On the other hand, the Maxwell's equations become:

$$\partial_{\mathbf{t}}\mathbf{B} + \nabla_{\mathbf{x}} \times \mathbf{E} = 0\,, \qquad \partial_{\mathbf{t}}\mathbf{E} - \nabla_{\mathbf{x}} \times \mathbf{B} = -\jmath(\mathrm{f}_\alpha)\,, \tag{2.2.41a}$$

$$\nabla_{\mathbf{x}} \cdot \mathbf{B} = 0\,, \qquad \nabla_{\mathbf{x}} \cdot \mathbf{E} = \rho(\mathrm{f}_\alpha)\,, \tag{2.2.41b}$$

where we have introduced:

$$\rho(\mathrm{f}_1, \cdots, \mathrm{f}_N)(\mathbf{t}, \mathbf{x}) \equiv \rho(\mathrm{f}_\alpha)(\mathbf{t}, \mathbf{x}) := \sum_{\alpha=1}^{N} \frac{1}{\theta_1^{\mathrm{d}}} \frac{\mu_\alpha^2}{\varepsilon_\alpha} \int_{\mathbb{R}^3} \mathrm{f}_\alpha(\mathbf{t}, \mathbf{x}, \mathbf{p}_\alpha)\, d\mathbf{p}_\alpha\,, \tag{2.2.42a}$$

$$\jmath(\mathrm{f}_1, \cdots, \mathrm{f}_N)(\mathbf{t}, \mathbf{x}) \equiv \jmath(\mathrm{f}_\alpha)(\mathbf{t}, \mathbf{x}) := \sum_{\alpha=1}^{N} \frac{\theta_\alpha^{\mathrm{d}}}{\theta_1^{\mathrm{d}}} \frac{\mu_\alpha^2}{\varepsilon_\alpha} \int_{\mathbb{R}^3} \frac{\mathbf{p}_\alpha}{\langle \theta_\alpha^{\mathrm{d}} |\mathbf{p}_\alpha| \rangle}\, \mathrm{f}_\alpha(\mathbf{t}, \mathbf{x}, \mathbf{p}_\alpha)\, d\mathbf{p}_\alpha\,. \tag{2.2.42b}$$

A quick calculation indicates that the two relations of (2.2.41b) are propagated by the evolution equation (2.2.40)-(2.2.41a). Therefore, it suffices to check (2.2.41b) at the time $t = 0$, and then to focuss on (2.2.41a).

2.2.6.2. *Straightening the field lines.* Equation (2.2.40) is not yet in a suitable form. Still, we need to straighten out the field lines. Recall (2.2.29)-(2.2.31) so that:

$$\mathbf{B}_e(\mathbf{x}) = \mathbf{b}_e(\mathbf{x})\; e_3(\mathbf{x}) = \mathbf{b}_e(\mathbf{x})\; O(\mathbf{x})\; {}^t(0,0,1)\,, \qquad \forall\, \mathbf{x} \in \Omega\,. \tag{2.2.43}$$

In view of Discussion 2.2.1, the directions of the unit vector field $e_3(\cdot)$, and therefore of $\mathbf{B}_e(\cdot)$, can vary with changes in $\mathbf{x} \in \Omega$. To remedy this situation, we replace simultaneously $\mathbf{B}_e$, $\mathbf{B}$, $\mathbf{E}$ and $\mathbf{p}_\alpha$ according to:

$$\mathbf{b}_e\, {}^t(0,0,1) = {}^tO\, \mathbf{B}_e\,, \qquad B := {}^tO\, \mathbf{B}\,, \qquad E := {}^tO\, \mathbf{E}\,, \qquad p_\alpha := {}^tO\, \mathbf{p}_\alpha\,. \tag{2.2.44}$$

For the sake of simplicity, the subscript α that identifies the different momentum variables p_α will be omitted. Concerning $p \equiv p_\alpha \in \mathbb{R}^3$, we can pass from cartesian to spherical coordinates, with orthonormal basis $(e_r, e_\varpi, e_\omega)$. This gives rise to:

$$p = r\; {}^t(\cos\omega\, \sin\varpi, \sin\omega\, \sin\varpi, \cos\varpi)\,, \qquad (\varpi, \omega, r) \in \mathbb{T}^2 \times \mathbb{R}_+\,, \qquad r = |p| = |\mathbf{p}|\,. \tag{2.2.45}$$

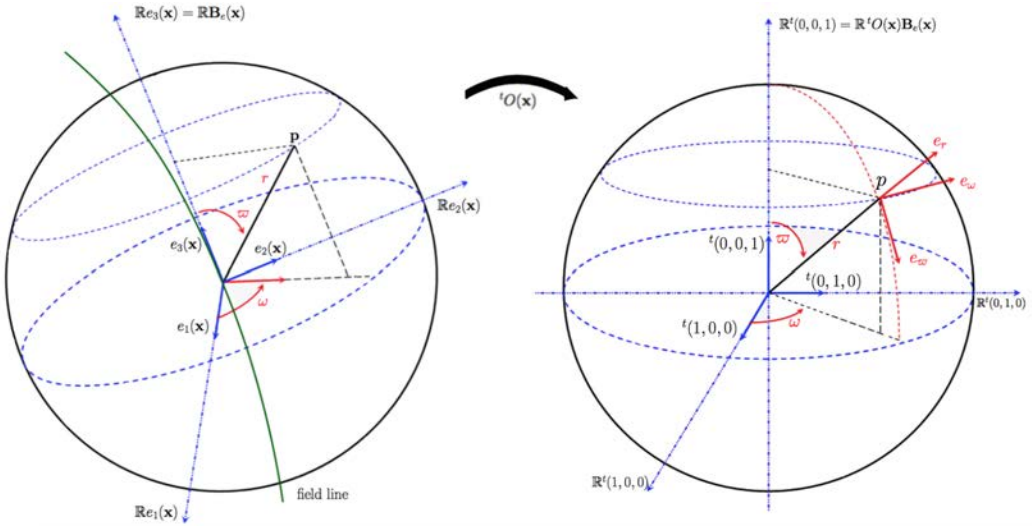

FIGURE 10. Spherical coordinates of $p \in \mathbb{R}^3$ after straigntening.

From now on, the spatial-velocity position is marked by $\mathbf{y} := (\mathbf{x}, \varpi, \omega, r) \in \Omega \times \mathbb{T}^2 \times \mathbb{R}_+$. We modify $\mathrm{f}_\alpha(\cdot)$ to fit with the preceding adjustements:

$$f_\alpha(\mathbf{t}, \mathbf{y}) \equiv f(\mathbf{t}, \mathbf{x}, \varpi, \omega, r) := \mathrm{f}_\alpha\big(\mathbf{t}, \mathbf{x}, r\, O(\mathbf{x})\, (\cos\omega\, \sin\varpi, \sin\omega\, \sin\varpi, \cos\varpi)\big)\,.$$

As usual, the symbol $\mathcal{S}$ refers to the Schwartz space. We consider functions $f(\cdot)$ satisfying uniformly in $(\mathbf{t}, \mathbf{x}, \varpi, \omega) \in M \times \mathbb{T}^2$ the conditions:

$$f \in \mathcal{C}^\infty(M \times \mathbb{T}^2 \times \mathbb{R}_+; \mathbb{R})\,, \qquad f(\mathbf{t}, \mathbf{x}, \varpi, \omega, \cdot) \in \mathcal{S}(\mathbb{R}_+; \mathbb{R})\,. \tag{2.2.46}$$

The gradient $\nabla_{\mathbf{p}}$ is converted into the spherical gradient ∇_p, with:

$$\nabla_p f := \frac{\partial f}{\partial r}\, e_r + \frac{1}{r}\, \frac{\partial f}{\partial \varpi}\, e_\varpi + \frac{1}{r\, \sin\varpi}\, \frac{\partial f}{\partial \omega}\, e_\omega\,.$$

The change of variables $(\mathbf{x}, \mathbf{p}) \to (\mathbf{x}, p)$ on the right of (2.2.44) induces some extra term when transforming $(\mathbf{v} \cdot \nabla_{\mathbf{x}})\mathrm{f}$ accordingly. Some application $Q(\cdot)$ does appear. This is a vector valued quadratic form in p, namely:

$$Q(\mathbf{x}, p) := \begin{pmatrix} O(\mathbf{x})\, p \cdot \partial_{\mathbf{x}^1} e_1 & O(\mathbf{x})\, p \cdot \partial_{\mathbf{x}^2} e_1 & O(\mathbf{x})\, p \cdot \partial_{\mathbf{x}^3} e_1 \\ O(\mathbf{x})\, p \cdot \partial_{\mathbf{x}^1} e_2 & O(\mathbf{x})\, p \cdot \partial_{\mathbf{x}^2} e_2 & O(\mathbf{x})\, p \cdot \partial_{\mathbf{x}^3} e_2 \\ O(\mathbf{x})\, p \cdot \partial_{\mathbf{x}^1} e_3 & O(\mathbf{x})\, p \cdot \partial_{\mathbf{x}^2} e_3 & O(\mathbf{x})\, p \cdot \partial_{\mathbf{x}^3} e_3 \end{pmatrix} O(\mathbf{x})\, p \in \mathbb{R}^3\,.$$

Put aside the integral operators:

$$\rho(f) := \int_0^{+\infty} \int_0^\pi \int_{-\pi}^\pi f(\varpi, \omega, r)\; r^2\, \sin\varpi\; dr\, d\varpi\, d\omega\,, \tag{2.2.47a}$$

$$\mathcal{J}(\theta; f) := \int_0^{+\infty} \int_0^\pi \int_{-\pi}^\pi \frac{r^3}{\langle \theta\, r\rangle} \begin{pmatrix} \cos\omega\, \sin\varpi \\ \sin\omega\, \sin\varpi \\ \cos\varpi \end{pmatrix} f(\varpi, \omega, r)\; \sin\varpi\; dr\, d\varpi\, d\omega\,. \tag{2.2.47b}$$

2.2.6.3. *The hierarchy between dimensionless parameters.* For further analysis, it is crucial to produce values for the parameters ε_α, $\theta_\alpha^{\mathrm{d}}$ and μ_α which could be meaningful from a physical point of view. It is also important to compare these quantities to one another. To this end, the following dimensionless number (which comes from the inverse of the electron cyclotron frequency):

$$\varepsilon \equiv |\varepsilon_1| := \frac{c_0}{L\, |\omega_{c1}|} = \frac{c_0\, m_e}{L\, e\, b_e} \simeq \frac{10^{-3}}{L\, b_e}\,, \tag{2.2.48}$$

will serve as a unit of measure.

Discussion 2.2.2. *[about the size of ε] As indicated in (2.2.39), the number ε appears to be the ratio beween the reference frequency $1/T = c_0/L$ and the gyrofrequency ω_{ce}. This appears to be a small parameter. The plasmasphere begins above the upper ionosphere and extends outwards. It contains the inner Van Allen belt, which is located between $1R^e$ and $2R^e$. Its outer boundary, known as the plasmapause, can vary with geomagnetic activity. During quiet period, it can expand outward to $7R^e$ or beyond. On the contrary, during magnetic storms, it moves at around $5R^e$. The outer Van Allen belt covers altitudes of approximately 4 to $8R^e$. In short, we can take the mean value $L \simeq 5R^e$, so that $\varepsilon \simeq 10^{-4}$.* ∘

From now on, we take $\varepsilon := 10^{-4} \ll 1$ as the small reference parameter to which all other quantities will be compared. For instance, with (2.2.2), keep in mind that:

$$|\varepsilon_\alpha| \,=\, \frac{e}{|e_\alpha|}\,\frac{m_\alpha}{m_e}\,\varepsilon \simeq \frac{\varepsilon}{\iota_\alpha} \gtrsim \beta\,\varepsilon \simeq 1\,, \qquad \forall\,\alpha \in \{2,\cdots,N\}\,. \tag{2.2.49}$$

Discussion 2.2.3. *[about the size of the coefficients $\theta_\alpha^{\rm d}$] The measurements recorded in the plasmasphere indicate that $\theta_1^{\rm d} \simeq \varepsilon$. The ratio $\theta_\alpha^{\rm d}/\theta_1^{\rm d}$ is given by (2.2.17). In view of (2.2.2) and (2.2.14), it is very small. The model (2.2.20) is therefore suitable for all α. In the limit ε goes to zero, we can even say that the kinetic distribution functions are given by Dirac masses. This explains the cold plasma approximation, which is sometimes applied in geophysical research [23, 40]. As regards the outer Van Allen belt, the situation is more problematic. It may still be considered that $\theta_\alpha^{\rm d} \lesssim \varepsilon$ and that $\mathrm{f}_\alpha^{\rm d}(\cdot)$ is as in (2.2.20) for all $\alpha \in \{2,\cdots,N\}$. However, the presence sometimes of a large amount of hot electrons might also point in favour of a Maxwell-Jüttner distribution.* ∘

Discussion 2.2.4. *[about the size of the coefficients μ_α] In view of (2.2.39), the access to μ_1 requires to evaluate b_e, m_e and $n_1^{\rm d}$. How to fix these quantities has already been explained. We find that $\mu := |\mu_1|$ can vary from 1 to about 300 in the magnetosphere. We remark that:*

$$|\mu_\alpha| \,=\, \Big(\frac{n_\alpha^{\rm d}\,m_\alpha}{\epsilon_0}\Big)^{1/2}\,\frac{1}{b_e} \,=\, \Big(\frac{n_\alpha^{\rm d}\,m_\alpha}{n_1^{\rm d}\,m_1}\Big)^{1/2}\,|\mu_1| \geq \mu\,, \qquad \forall\,\alpha \in \{1,\cdots,N\}\,. \tag{2.2.50}$$

We can also find that:

$$\frac{\mu_\alpha^2}{\varepsilon_\alpha} \,=\, \frac{e_\alpha\,n_\alpha^{\rm d}}{e_1\,n_1^{\rm d}}\,\frac{\mu^2}{\varepsilon} \simeq \frac{\mu^2}{\varepsilon}\,, \qquad \forall\,\alpha \in \{1,\cdots,N\}\,. \tag{2.2.51}$$

∘

In practice, the value of $\mu := |\mu_1|$ can vary. As indicated in Definition 2.3.8, it can be locally compared to $\mathbf{b}_e(\mathbf{x}) \simeq 1$. The plasma is termed underdense when $\mu < \mathbf{b}_e(\mathbf{x})$ and overdense when $\mathbf{b}_e(\mathbf{x}) < \mu$. To track the influence of μ, this parameter will not be normalized in what follows. At all events, retain that the size of ε is always small, and far below μ.

Discussion 2.2.5. *[about the size of ν] We will adjust ν in such a way that $\nu \lesssim \varepsilon$. By this way, we can stay in a perturbative regime, even if $\theta_1^{\rm d} \simeq 1$. Indeed:*

- *Smallness of $\tilde{\mathbf{B}}$ in comparison with $\tilde{\mathbf{B}}_e$:* In view of (2.2.36c), the condition $\mathbf{B} \simeq 1$ *implies $\tilde{\mathbf{B}} \simeq \nu\,\theta_1^{\rm d}\,b_e \lesssim \varepsilon\,b_e$. With (2.2.26), we can be sure that $|\tilde{\mathbf{B}}| \lesssim \varepsilon\,|\tilde{\mathbf{B}}_e|$.*
- *Smallness of $\nu\,\tilde{\mathrm{f}}_\alpha^{\rm s}$ in comparison with $\tilde{\mathrm{f}}_\alpha^{\rm d}$:* When computing $\tilde{\mathrm{f}}_\alpha^{\rm k}(\cdot)$ *through (2.2.5), the part $\nu\,\tilde{\mathrm{f}}_\alpha^{\rm s}(\cdot)$ appears as a small modification of $\tilde{\mathrm{f}}_\alpha^{\rm d}(\cdot)$. This makes sense whatever the parameter $\theta_\alpha^{\rm d}$ is, small or large. Indeed, the amplitude of $\tilde{\mathrm{f}}_\alpha^{\rm s}(\cdot)$ as prescribed by (2.2.36b) with $\mathrm{f}_\alpha \simeq 1$ is equivalent to the amplitude of $\tilde{\mathrm{f}}_\alpha^{\rm d}(\cdot)$ given by (2.2.20).*

In concrete terms, we will impose $\nu \sim \varepsilon$.

2.2.7. **The cold asymptotic regime.** The discussion can be put in the context of some asymptotic analysis (when ε goes to 0). To this end, the coefficients ε_α, $\theta^{\rm d}_\alpha$ and μ_α must be viewed as functions of $\varepsilon \in]0,1]$. In view of the preceding study, when dealing with the plasmasphere, the three following assumptions can be retained:

- *(Cp1)*: For all $\alpha \in \{1,\cdots,N\}$, we have $\theta^{\rm d}_\alpha(\varepsilon) \sim \varepsilon$ with $\varepsilon \ll 1$.
- *(Cp2)*: For all $\alpha \in \{1,\cdots,N\}$, the dominant stationary part $\tilde{\rm f}^{\rm d}_\alpha(\cdot)$ is given by the Maxwell-Boltzmann KDF (2.2.20).
- *(Cp3)*: The perturbation is such that $\nu \sim \varepsilon$.

As already explained, the hypotheses *(Cp1)* and *(Cp2)* correspond to a cold thermal plasma. On the other hand, the hypothesis *(Cp3)* means that only a small fraction of the plasma is out of equilibrium. By combining information from Section 2.2.6 with *(Cp1)*, *(Cp2)* and *(Cp3)*, we can simplify (2.2.40)-(2.2.41a)-(2.2.41b) as indicated below. First, due to *(Cp2)*, there is almost no distinction between the cases $\alpha = 1$ and $\alpha \in \{2,\cdots,N\}$. The only difference is that $|\varepsilon_\alpha| \simeq 1$ for all $\alpha \in \{2,\cdots,N\}$, whereas $|\varepsilon_1| = \varepsilon \ll 1$. Thus, for all $\alpha \in \{1,\cdots,N\}$, we can impose:

$$
\begin{aligned}
&\partial_{\mathbf{t}} f_\alpha + \frac{\varepsilon}{\langle \varepsilon\, r\rangle}\, O(\mathbf{x})\, p\cdot\nabla_{\mathbf{x}} f_\alpha + \frac{\varepsilon}{\langle \varepsilon\, r\rangle}\, Q(\mathbf{x},p)\cdot\nabla_p f_\alpha \\
&\quad + \frac{\varepsilon}{\varepsilon_\alpha}\,\Big[E + \frac{\varepsilon}{\langle \varepsilon\, r\rangle}\, p\times B\Big]\cdot\nabla_p f_\alpha \,-\, \frac{1}{\varepsilon_\alpha}\,\frac{\mathbf{b}_e(\mathbf{x})}{\langle \varepsilon\, r\rangle}\,\partial_\omega f_\alpha \\
&\quad + \frac{\mathbf{n}^{\rm d}_\alpha(\mathbf{x})}{\varepsilon_\alpha}\,\partial_r \mathcal{M}^b_{\theta^{\rm d}_\alpha(\mathbf{x})}(r)\,\frac{p\cdot E}{r} + \frac{1}{\langle \varepsilon\, r\rangle}\, O(\mathbf{x})\, p\cdot\nabla_{\mathbf{x}}\mathbf{n}^{\rm d}_\alpha(\mathbf{x})\,\mathcal{M}^b_{\theta^{\rm d}_\alpha(\mathbf{x})}(r) \\
&\quad + \frac{1}{\langle \varepsilon\, r\rangle}\,\mathbf{n}^{\rm d}_\alpha(\mathbf{x})\, O(\mathbf{x})\, p\cdot\nabla_{\mathbf{x}}(\ln\,\theta^{\rm d}_\alpha)(\mathbf{x})\,(\mathfrak{m}^b_{\theta^{\rm d}_\alpha(\mathbf{x})}\,\mathcal{M}^b_{\theta^{\rm d}_\alpha(\mathbf{x})})(r) \,=\, 0\,.
\end{aligned}
\tag{2.2.52}
$$

For $\alpha \in \{2,\cdots,N\}$, this equation (2.2.52) contains no singular term (of the order ε^{-1}), and it is weakly nonlinear. On the contrary, for $\alpha = 1$, we can note the presence of a fast rotating term (of the order ε^{-1}), of a large source term (of size ε^{-1}), and of some $O(1)$ nonlinear contribution (of the form $E\cdot\nabla_p f_\alpha$).

The equation (2.2.41) does not need to be changed, except that the compatibility conditions contained in (2.2.41b) must be conveniently weighted:

$$
\partial_{\mathbf{t}}\mathbf{B} + \nabla_{\mathbf{x}}\times\mathbf{E} = 0\,, \qquad \nabla_{\mathbf{x}}\cdot\mathbf{B} = 0\,, \tag{2.2.53a}
$$

$$
\partial_{\mathbf{t}}\mathbf{E} - \nabla_{\mathbf{x}}\times\mathbf{B} = -\,\jmath(\mathrm{f}_\alpha)\,, \qquad \varepsilon\,\nabla_{\mathbf{x}}\cdot\mathbf{E} = \varepsilon\,\rho(\mathrm{f}_\alpha)\,, \tag{2.2.53b}
$$

and except that the two expressions $\rho(\mathrm{f}_\alpha)$ and $\jmath(\mathrm{f}_\alpha)$ can be further specified by using *(Cp1)* and (2.2.51) in order to find:

$$
\rho(\mathrm{f}_\alpha)(\mathbf{t},\mathbf{x}) \equiv \rho^{\rm c}(f_\alpha)(\mathbf{t},\mathbf{x}) := -\,\frac{\mu^2}{\varepsilon^2}\int_{\mathbb{R}^3} f_1\, dp + \sum_{\alpha=2}^N \frac{\mu^2}{\varepsilon^2}\int_{\mathbb{R}^3} f_\alpha\, dp\,, \tag{2.2.54a}
$$

$$
\jmath(\mathrm{f}_\alpha)(\mathbf{t},\mathbf{x}) \equiv \jmath^{\rm c}(f_\alpha)(\mathbf{t},\mathbf{x}) := -\,\frac{\mu^2}{\varepsilon}\int_{\mathbb{R}^3} \frac{p}{\langle \varepsilon\, r\rangle}\, f_1\, dp + \sum_{\alpha=2}^N \frac{\mu^2}{\varepsilon}\int_{\mathbb{R}^3} \frac{p}{\langle \varepsilon\, r\rangle}\, f_\alpha\, dp\,. \tag{2.2.54b}
$$

2.2.8. **Within the framework of geometrical optics.** The plasmas can support a wide variety of wave phenomena. We refer to [10, 12, 28] for an overview. In most cases, these phenomena appear to be interconnected sets of particles and fields which can evolve in a periodically repeating fashion [7]. In order to capture the precise features underlying the propagation of such plasma waves, a good strategy is to start from the dimensionless version of the RVM system which has just been exhibited in Paragraph 2.2.7, made up of (2.2.52)-(2.2.53) together with (2.2.54). This allows to set the discussion within the coherent framework of geometric optics [29, 33]. The corresponding asymptotic analysis is new for two main reasons. The first, which is well detailed in Sections 2.1 and 2.2.5, comes from the spatial variations of the magnetic field; the second is due to the *mesoscopic* precision of our model. It is important here to discuss this second aspect more thoroughly. Being interested in the propagation of *electromagnetic waves* means to focus on oscillations of the self-consistent field $(E,B)(\cdot)$. Since the function $(E,B)(\cdot)$ depends only on $(\mathbf{t},\mathbf{x})$, a key point is that only *time-space oscillations* can be involved at this level. With this in mind, we can introduce some smooth phase function $\phi \in \mathcal{C}^\infty(M;\mathbb{R})$, which depends on the *macroscopic* variable $(\mathbf{t},\mathbf{x}) \in M$ but certainly not on the *kinetic* variable $p \in \mathbb{R}^3$.

Assumption 2.2.6. *[non-stationary phase] The function ϕ is such that:*

$$\forall\,(\mathbf{t},\mathbf{x}) \in M\,, \qquad (\partial_{\mathbf{t}}\phi, \nabla_{\mathbf{x}}\phi)(\mathbf{t},\mathbf{x}) \neq 0\,. \tag{2.2.55}$$

The oscillating behaviour of $(E,B)(\cdot)$ may be viewed as a sum of monophase pieces which can be modelled by:

$$(E,B)(\mathbf{t},\mathbf{x}) \equiv (E^\varepsilon,B^\varepsilon)(\mathbf{t},\mathbf{x}) = (\mathscr{E},\mathscr{B})\Big(\mathbf{t},\mathbf{x},\frac{\phi(\mathbf{t},\mathbf{x})}{\varepsilon}\Big)\,, \qquad \varepsilon \in]0,1]\,.$$

Usually, the time evolution of $(E,B)(\cdot)$ is considered in the framework of MHD descriptions, through *fluid* models based on Maxwell's equations, involving the variables $(\mathbf{t},\mathbf{x})$. This has the advantage of simplicity. But this also means various simplifying assumptions which are debatable when dealing with plasma phenomena out of equilibrium. To understand all subtleties induced by the underlying presence of $p \in \mathbb{R}^3$, it is necessary to come back to the original RVM system. To this end, we seek the complete solution u of (2.2.52)-(2.2.53) in the form of a basic *monophase* representation implying ϕ through:

$$u(\mathbf{t},\mathbf{y}) = \begin{pmatrix} f_1(\mathbf{t},\mathbf{y}) \\ \vdots \\ f_N(\mathbf{t},\mathbf{y}) \\ B(\mathbf{t},\mathbf{x}) \\ E(\mathbf{t},\mathbf{x}) \end{pmatrix} = u^\varepsilon(\mathbf{t},\mathbf{y}) = \mathscr{U}\Big(\mathbf{t},\mathbf{y},\frac{\phi(\mathbf{t},\mathbf{x})}{\varepsilon}\Big)\,, \qquad \mathbf{y} = (\mathbf{x},\varpi,\omega,r)\,. \tag{2.2.56}$$

In (2.2.56), the profile $\mathscr{U}$ is assumed to be periodic in the *fast* variable $\theta \in \mathbb{T} := \mathbb{R}/(2\,\pi\,\mathbb{Z})$. The coordinates inside $(\mathbf{t},\mathbf{y})$ are considered as *slow* variables. When dealing with capital letters like U, the different font styles $\mathscr{U}$, $\mathcal{U}$ and U will be used for expressions depending respectively on the variables $(\mathbf{t},\mathbf{y},\theta)$, $(\mathbf{t},\mathbf{y})$ and $(\mathbf{t},\mathbf{x},\varpi,\omega)$. When studying (2.2.52)-(2.2.53), a first stage is to exhibit approximate solutions.

Given $N \in \mathbb{N}^*$, we aim at a precision of the order $O(\varepsilon^{N-1})$ through expansions like:

$$
\begin{aligned}
u_a^\varepsilon(\mathbf{t},\mathbf{y},\mathbf{r}) \,&=\, \begin{pmatrix} f_{a,1}^\varepsilon(\mathbf{t},\mathbf{y}) \\ \vdots \\ f_{a,N}^\varepsilon(\mathbf{t},\mathbf{y}) \\ B_a^\varepsilon(\mathbf{t},\mathbf{x}) \\ E_a^\varepsilon(\mathbf{t},\mathbf{x}) \end{pmatrix} \,=\, \mathscr{U}_a^\varepsilon\Big(\mathbf{t},\mathbf{y},\tfrac{\phi(\mathbf{t},\mathbf{x})}{\varepsilon}\Big) \\
&=\sum_{j=0}^{N} \varepsilon^j\ \mathscr{U}_j\Big(\mathbf{t},\mathbf{y},\frac{\phi(\mathbf{t},\mathbf{x})}{\varepsilon}\Big) \,=\sum_{j=0}^{N} \varepsilon^j \begin{pmatrix} \mathscr{F}_{j,1}(\mathbf{t},\mathbf{y},\phi(\mathbf{t},\mathbf{x})/\varepsilon) \\ \vdots \\ \mathscr{F}_{j,N}(\mathbf{t},\mathbf{y},\phi(\mathbf{t},\mathbf{x})/\varepsilon) \\ \mathscr{B}_j(\mathbf{t},\mathbf{x},\phi(\mathbf{t},\mathbf{x})/\varepsilon) \\ \mathscr{E}_j(\mathbf{t},\mathbf{x},\phi(\mathbf{t},\mathbf{x})/\varepsilon) \end{pmatrix}.
\end{aligned}
\tag{2.2.57}
$$

In (2.2.57), the profiles $\mathscr{U}_j(\mathbf{t},\mathbf{y},\theta)$ are assumed to be smooth bounded real valued functions:

$$
\mathscr{U}_j = {}^t(\mathscr{F}_{j,1},\cdots,\mathscr{F}_{j,N},\mathscr{B}_j,\mathscr{E}_j) \in \mathcal{C}_b^\infty(M\times\mathbb{T}^2\times\mathbb{R}_+\times\mathbb{T};\mathbb{R}^{N+6})\,, \qquad \forall\, j\in\{0,\cdots,N\}\,,
$$

with Fourier series:

$$
\mathscr{U}_j(\mathbf{t},\mathbf{y},\theta) = \sum_{l\in\mathbb{Z}} \mathcal{U}_j^l(\mathbf{t},\mathbf{y})\ e^{i\,l\,\theta}\,, \qquad \mathcal{U}_j^l = {}^t(\mathcal{F}_{j,1}^l,\cdots,\mathcal{F}_{j,N}^l,B_j^l,E_j^l) \equiv \bar{\mathcal{U}}_j^{-l}\,. \tag{2.2.58}
$$

It is understood that the function $\mathcal{F}_{j,\alpha}^l(\cdot)$ and its derivatives at all orders satisfy (2.2.46). Plugg the real valued function $u_a^\varepsilon(\cdot)$ of (2.2.57) into (2.2.52)-(2.2.53) and into (2.2.54). Collect the contributions having the same power of ε in factor, sorted in increasing order. By this way, we get the condition:

$$
\sum_{j=-1}^{+\infty} \varepsilon^j\ \mathscr{G}_j\Big(\mathbf{t},\mathbf{y},\frac{\phi(t,\mathbf{x})}{\varepsilon}\Big) = 0\,, \qquad \mathscr{G}_j(\mathbf{t},\mathbf{y},\theta) = \sum_{l\in\mathbb{Z}} \mathcal{G}_j^l(\mathbf{t},\mathbf{y})\ e^{i\,l\,\theta}\,, \qquad \mathcal{G}_j^l \equiv \bar{\mathcal{G}}_j^{-l}\,. \tag{2.2.59}
$$

It turns out that the expressions $\mathscr{G}_j(\cdot)$ depend only on terms $\mathscr{U}_i$ with $i \le j+1$. In particular, for $j=-1$, we get the preliminary constraint:

$$
\mathscr{G}_{-1}(\mathbf{t},\mathbf{y},\theta,\mathscr{U}_0) = 0\,. \tag{2.2.60}
$$

The equation (2.2.60) is interesting and difficult to solve. It contains polarization conditions on $\mathscr{U}_0$. Above all, it includes the so-called *eikonal equation* which allows to determine ϕ and which therefore governs the geometry of the propagation.

An approximate solution $u_a^\varepsilon(\cdot)$ can be derived by solving successively the conditions $\mathscr{G}_j \equiv 0$ for $j=-1$, $j=0$, and so on $\cdots$ up to $j=N-1$. The corresponding WKB analysis would be meaningful, but it is postponed to other articles.

From now on, we focus on the initialization procedure, based on (2.2.60), which already requires a substantial amount of work.

2.3. Cold plasma dispersion relations

From now on, the matter is to solve the condition (2.2.60), which is inherited from the cold plasma model exposed in Paragraph 2.2.7, that is from (2.2.52)-(2.2.53)-(2.2.54). Given $\ell\in\mathbb{N}$, the Fourier coefficient $\mathcal{G}_{-1}^\ell$ depends only on $\mathcal{U}_0^\ell$. There remains:

$$
\mathcal{G}_{-1}^\ell(\mathcal{U}_0^\ell) \equiv 0\,, \qquad \forall\,\ell\in\mathbb{Z}\,. \tag{2.3.1}
$$

The expressions $\mathcal{G}_{-1}^{\ell}(\cdot)$ are linear with respect to $\mathcal{U}_0^l$ with coefficients depending on the choice of ϕ. With (2.2.58) and (2.2.59), it follows that:

$$\mathcal{G}_{-1}^{\ell}(\mathcal{U}_0^{\ell}) = \bar{\mathcal{G}}_{-1}^{-\ell}(\bar{\mathcal{U}}_0^{-\ell}) = \overline{\mathcal{G}_{-1}^{-\ell}(\mathcal{U}_0^{-\ell})}\,, \qquad \mathcal{G}_{-1}^{\ell}(0) = 0\,, \qquad \forall\, \ell \in \mathbb{Z}\,. \tag{2.3.2}$$

The situation under study is very dispersive. After adjusting ϕ in order to obtain $\mathcal{G}_{-1}^{l} \equiv 0$ (and therefore $\bar{\mathcal{G}}_{-1}^{-l} \equiv 0$) for some $l \in \mathbb{Z}^*$, the other conditions $\mathcal{G}_{-1}^{\ell} \equiv 0$ (with $\ell \neq |l|$) are in general not verified (except for the trivial choice $\mathcal{U}_0^{\ell} \equiv 0$). This is why, at leading order, only one Fourier coefficient will be switched on.

Assumption 2.3.1. *[presence of a non-trivial monochromatic electromagnetic oscillation] There is some non-zero integer $l \in \mathbb{Z}^*$ such that:*

$$(E_0^l, B_0^l) \equiv (\bar{E}_0^{-l}, \bar{B}_0^{-l}) \not\equiv 0\,, \qquad \mathcal{U}_0^{\ell} \equiv 0\,, \qquad \forall\, \ell \in \mathbb{Z} \setminus \{-l, l\}\,. \tag{2.3.3}$$

Due to (2.3.2) and (3.3.7), the conditions inside (2.3.1) reduce to:

$$\mathcal{G}_{-1}^{l}(\mathcal{U}_0^l) \equiv 0\,, \qquad \mathcal{U}_0^l = {}^t(\mathcal{F}_{0,1}^l, \cdots, \mathcal{F}_{0,N}^l, B_0^l, E_0^l)\,. \tag{2.3.4}$$

This Section 2.3 is devoted to the analysis of (2.3.4).

2.3.1. **The first step of the WKB calculus.** With $l \in \mathbb{Z}^*$ as in Assumption 3.3.1, introduce:

$$\tau := l\, \partial_{\mathbf{t}}\phi(\mathbf{t}, \mathbf{x}) \in \mathbb{R}\,, \qquad \xi := l\, {}^t O(\mathbf{x})\, \nabla_{\mathbf{x}}\phi(\mathbf{t}, \mathbf{x}) \in \mathbb{R}^3\,. \tag{2.3.5}$$

Recall that, due to (2.2.55), we have $(\tau, \xi) \neq (0, 0)$. From (2.2.52), knowing that $\varepsilon_1 = -\varepsilon$ and $\varepsilon_\alpha \lesssim 1$ for $\alpha \neq 1$, we can extract:

$$\big[i\,\tau + \mathbf{b}_e\, \partial_\omega\big]\, \mathcal{F}_{0,1}^l = \mathbf{n}_1^{\mathrm{d}}\; \partial_r \mathcal{M}_{\theta_1^{\mathrm{d}}}^b(r)\; r^{-1}\; p \cdot E_0^l\,, \tag{2.3.6}$$

together with:

$$\forall\, \alpha \in \{2, \cdots, N\}, \qquad i\,\tau\, \mathcal{F}_{0,\alpha}^l = 0\,. \tag{2.3.7}$$

In view of (2.3.6), an electric oscillation ($E_0^l \not\equiv 0$) is correlated with an oscillation of the electron density distribution ($\mathcal{F}_{0,1}^l \not\equiv 0$). On the contrary, the density distributions of ions contain no oscillations (at leading order). In order to satisfy (2.3.7), we must impose:

$$\forall\, \alpha \in \{2, \cdots, N\}, \qquad \mathcal{F}_{0,\alpha}^l = 0\,. \tag{2.3.8}$$

With the $f_{a,\alpha}^{\varepsilon}$ as in (2.2.57), exploiting (2.3.8), the charge density ρ and the electric current $\jmath$ which are given by (2.2.54) can be expanded in powers of $\varepsilon \in\,]0, 1]$ according to:

$$\rho(f_{a,\alpha}^{\varepsilon})(\mathbf{t}, \mathbf{x}) \;=\; -\,\frac{\mu^2}{\varepsilon^2}\,\Big(\int_{\mathbb{R}^3} \mathcal{F}_{0,1}^l(\mathbf{t}, \mathbf{y})\; dp\Big)\; e^{i\, l\, \phi(\mathbf{t},\mathbf{x})/\varepsilon} \;+\; O\Big(\frac{1}{\varepsilon}\Big)\,, \tag{2.3.9a}$$

$$\jmath(f_{a,\alpha}^{\varepsilon})(\mathbf{t}, \mathbf{x}) \;=\; -\,\frac{\mu^2}{\varepsilon}\,\Big(\int_{\mathbb{R}^3} p\; \mathcal{F}_{0,1}^l(\mathbf{t}, \mathbf{y})\; dp\Big)\; e^{i\, l\, \phi(\mathbf{t},\mathbf{x})/\varepsilon} \;+\; O(1)\,. \tag{2.3.9b}$$

Coming back to (2.2.52)-(2.2.53), with the definitions of (2.2.47), we have to consider:

$$\xi \times E_0^l + \tau\ B_0^l = 0\,. \tag{2.3.10a}$$

$$\xi \times B_0^l - \tau\ E_0^l = i\ \mu^2\ \mathcal{J}\big(0; \mathcal{F}_{0,1}^l(\mathbf{t},\mathbf{x},\cdot)\big)\,, \tag{2.3.10b}$$

$$\rho(\mathcal{F}_{0,1}^l(\mathbf{t},\mathbf{x},\cdot)) = 0\,, \qquad \xi \cdot B_0^l = 0\,. \tag{2.3.10c}$$

The rest of the article is devoted to the study of the system (2.3.6)-(2.3.10) on $(\mathcal{F}_{0,1}^l, B_0^l, E_0^l)$. The subscript α is not present at the level of (2.3.6)-(2.3.10). Thus, without any possibility of confusion, we can drop the subscript 1 at the level of $\theta_1^{\rm d}$, $\mathbf{n}_1^{\rm d}$ and $\mathcal{F}_{0,1}^l$. From now on, $\theta^{\rm d}$, $\mathbf{n}^{\rm d}$ and $\mathcal{F}_0^l$ stand for $\theta_1^{\rm d}$, $\mathbf{n}_1^{\rm d}$ and $\mathcal{F}_{0,1}^l$.

2.3.1.1. *Looking for reduced-form equations on the electric part.* The aim here is to extract from (2.3.6)-(2.3.10) necessary conditions involving only E_0^l. Let us go step-by-step.

∘ 2.3.1.1.a) Eliminating the presence of the variable r. The expression $\mathcal{F}_0^l \equiv \mathcal{F}_{0,1}^l$ can always be factored into:

$$\mathcal{F}_0^l(\mathbf{t},\mathbf{y}) = F_0^l(\mathbf{t},\mathbf{x},\varpi,\omega)\ \partial_r \mathcal{M}^b_{\theta^{\rm d}}(r)\,, \qquad F_0^l \in \mathcal{C}^\infty(M\times\mathbb{T}^2;\mathbb{C})\,.$$

This allows to convert (2.3.6) into:

$$\big[i\,\tau + \mathbf{b}_e\,\partial_\omega\big]\,F_0^l = \mathbf{n}^{\rm d}\ (\cos\omega\,\sin\varpi, \sin\omega\,\sin\varpi, \cos\varpi)\cdot E_0^l\,. \tag{2.3.11}$$

On the other hand, we have:

$$\begin{aligned}\int_0^{+\infty} r^3\,\partial_r \mathcal{M}^b_{\theta^{\rm d}}(r)\,dr &= -\frac{1}{\pi^{3/2}}\int_0^{+\infty}\Big(\frac{r^2}{(\theta^{\rm d})^2}\Big)^{3/2}\exp\Big(-\frac{r^2}{(\theta^{\rm d})^2}\Big)\,d\Big(\frac{r^2}{(\theta^{\rm d})^2}\Big)\\ &= -\frac{1}{\pi^{3/2}}\,\Gamma\Big(\frac{5}{2}\Big) = -\frac{3}{4\,\pi}\,.\end{aligned}$$

Coming back to (2.2.47b), it follows that:

$$\mathcal{J}(0;\mathcal{F}_0^l) \equiv \mathcal{J}_0(F_0^l) := -\frac{3}{4\,\pi}\int_0^\pi\!\!\int_{-\pi}^\pi \begin{pmatrix}\cos\omega\,\sin\varpi\\ \sin\omega\,\sin\varpi\\ \cos\varpi\end{pmatrix} F_0^l(\mathbf{t},\mathbf{x},\varpi,\omega)\ \sin\varpi\ d\varpi\,d\omega\,. \tag{2.3.12}$$

In the same way, we can compute:

$$\rho(\mathcal{F}_0^l(\mathbf{t},\mathbf{x},\cdot)) \equiv \rho_0(F_0^l) := -\frac{1}{\pi^{3/2}\,\theta^{\rm d}(\mathbf{x})}\int_0^\pi\!\!\int_{-\pi}^\pi F_0^l(\mathbf{t},\mathbf{x},\varpi,\omega)\ \sin\varpi\ d\varpi\,d\omega\,. \tag{2.3.13}$$

∘ 2.3.1.1.b) Eliminating the presence of the variable ω. This can be done by a Fourier analysis:

$$F_0^l(\mathbf{t},\mathbf{x},\varpi,\omega) = \sum_{m\in\mathbb{Z}} F_0^{l,m}(\mathbf{t},\mathbf{x},\varpi)\ e^{i\,m\,\omega}\,.$$

Then, the condition (2.3.11) can be declined into:

$$i\ \big[\tau - \mathbf{b}_e(\mathbf{x})\big]\,F_0^{l,-1} = 2^{-1}\,\mathbf{n}^{\rm d}\ (E_0^{l1} + i\,E_0^{l2})\ \sin\varpi\,, \tag{2.3.14a}$$

$$i\ \tau\ F_0^{l,0} = \mathbf{n}^{\rm d}\ E_0^{l3}\ \cos\varpi\,, \tag{2.3.14b}$$

$$i\ \big[\tau + \mathbf{b}_e(\mathbf{x})\big]\,F_0^{l,+1} = 2^{-1}\,\mathbf{n}^{\rm d}\ (E_0^{l1} - i\,E_0^{l2})\ \sin\varpi\,, \tag{2.3.14c}$$

$$i\ \big[\tau + m\,\mathbf{b}_e(\mathbf{x})\big]\,F_0^{l,m} = 0\,, \qquad \forall\, m\in\mathbb{Z}\setminus\{-1,0,1\}\,. \tag{2.3.14d}$$

On the other hand, we are left with:

$$\mathcal{J}_0(F_0^l) \equiv \mathcal{J}_0(F_0^{l,-1}, F_0^{l,0}, F_0^{l,1}) = -\frac{3}{4}\int_0^\pi \begin{pmatrix} F_0^{l,1} + F_0^{l,-1} \\ i\,(F_0^{l,1} - F_0^{l,-1}) \\ 2\,\mathrm{cotan}\,\varpi\; F_0^{l,0} \end{pmatrix}(\mathbf{t},\mathbf{x},\varpi)\;(\sin\varpi)^2\;d\varpi\,, \tag{2.3.15}$$

together with:

$$\rho_0(F_0^l) \equiv \rho_0(F_0^{l,0}) = -\frac{2}{\pi^{1/2}\,\theta^{\mathrm{d}}(\mathbf{x})}\int_0^\pi F_0^{l,0}(\mathbf{t},\mathbf{x},\varpi)\;\sin\varpi\;d\varpi\,. \tag{2.3.16}$$

Now, from (2.3.14b), we can deduce that:

$$i\;\tau\;\pi^{1/2}\;\theta^{\mathrm{d}}\;\rho_0(F_0^l) \;=\; -2\;\mathbf{n}^{\mathrm{d}}\;E_0^{l3}\int_0^\pi \cos\varpi\;\sin\varpi\;d\varpi \;=\; 0\,. \tag{2.3.17}$$

Remark 2.3.1. *For $\tau \neq 0$, the first condition and the second condition inside (2.3.10c) are obvious consequences of respectively (2.3.17) and (2.3.10a). Thus, when $\tau \neq 0$, we can forget the compatibility condition (2.3.10c).*

∘ 2.3.1.1.c) Eliminating the presence of the magnetic component B_0^l. Multiply the line (2.3.10b) by τ. In the expression thus obtained, use (2.3.10a) to replace $\tau\,B_0^l$. This yields:

$$\xi \times (\xi \times E_0^l) + \tau^2\,E_0^l \;=\; -\,i\;\mu^2\;\tau\;\mathcal{J}_0(F_0^l)\,. \tag{2.3.18}$$

∘ 2.3.1.1.d) Eliminating the presence of the density component F_0^l. The idea here is to exploit the equations of (2.3.14) in order to exhibit a relation between $\mathcal{J}_0(\mathcal{F}_0^l)$ and E_0^l. To begin with, from (2.3.14), we can extract:

$$\Sigma(\mathbf{x},\tau)\begin{pmatrix} F_0^{l,1} + F_0^{l,-1} \\ i\,(F_0^{l,1} - F_0^{l,-1}) \\ 2\,\mathrm{cotan}\,\varpi\; F_0^{l,0} \end{pmatrix} = \mathbf{n}^{\mathrm{d}}\begin{pmatrix} E_0^{l,1}\,\sin\varpi \\ E_0^{l,2}\,\sin\varpi \\ E_0^{l,3}\,\cos\varpi \end{pmatrix},$$

where we have introduced the skew-Hermitian matrix:

$$\Sigma(\mathbf{x},\tau) := \begin{pmatrix} i\,\tau & +\mathbf{b}_e(\mathbf{x}) & 0 \\ -\mathbf{b}_e(\mathbf{x}) & i\,\tau & 0 \\ 0 & 0 & i\,\tau \end{pmatrix}. \tag{2.3.19}$$

Multiply this identity by $(\sin\varpi)^2$ and integrate with respect to $d\varpi$. There remains:

$$\Sigma(\mathbf{x},\tau)\;\mathcal{J}_0(F_0^l) = -\,\mathbf{n}^{\mathrm{d}}\,E_0^l\,. \tag{2.3.20}$$

Then, by applying Σ to (2.3.18), we get:

$$\mathfrak{N}\,E_0^l = 0\,, \qquad \mathfrak{N}(\mathbf{x},\tau,\xi) := \Sigma(\mathbf{x},\tau)\left(\xi\,{}^t\xi + (\tau^2 - |\xi|^2)\,Id\right) - \;i\;\mu^2\,\mathbf{n}^{\mathrm{d}}\,\tau\,Id\,. \tag{2.3.21}$$

At this stage, we can state that a *necessary condition* to obtain non-trivial solutions $\mathcal{U}_0^l \not\equiv 0$ of the system (2.3.4), satisfying $E_0^l \not\equiv 0$, is to impose $det\,\mathfrak{N}(\mathbf{x},\tau,\xi) = 0$. The discussion about a *sufficient condition* requires to distinguish between the values of τ.

2.3.1.2. *The stationary case ($\tau = 0$).* When $\tau = 0$, we simply find $det\, \mathfrak{N}(\mathbf{x}, 0, \xi) = 0$. In fact, the step 2.3.1.1.c) makes no sense since it removes the information contained in (2.3.10b). The same applies for the step 2.3.1.1.d) since the matrix $\Sigma(\mathbf{x}, 0)$ is not invertible. The situation $\tau = 0$ must therefore be handled separately.

Lemma 2.3.1 (trace of the dispersion relations in the stationary case)**.** *For $\tau = 0$, the system (2.3.6)-(2.3.10) has a solution $(\mathcal{F}_0^l, B_0^l, E_0^l)$ satisfying Assumption 3.3.1 if and only if the position $(\mathbf{x}, \xi) \in T^*(\Omega)$ is such that $\xi^3 = 0$.*

Proof. The matter here is to deal with:

$$\mathbf{b}_e\, \partial_\omega F_0^l = \mathbf{n}^{\mathrm{d}}\ (\cos\omega\, \sin\varpi, \sin\omega\, \sin\varpi, \cos\varpi) \cdot E_0^l\,, \tag{2.3.22a}$$

$$\xi \times E_0^l = 0\,, \tag{2.3.22b}$$

$$\xi \times B_0^l = i\ \mu^2\ \mathcal{J}_0(F_0^l)\,, \tag{2.3.22c}$$

$$\rho_0(F_0^l) = 0\,, \qquad \xi \cdot B_0^l = 0\,. \tag{2.3.22d}$$

The condition (2.3.22a) - or the condition (2.3.14) for $\tau = 0$ - is equivalent to:

$$F_0^{l,-1} \ = \ +\, i\ (2\,\mathbf{b}_e)^{-1}\, \mathbf{n}^{\mathrm{d}}\ (E_0^{l1} + i\, E_0^{l2})\ \sin\varpi\,, \tag{2.3.23a}$$

$$F_0^{l,+1} \ = \ -\, i\ (2\,\mathbf{b}_e)^{-1}\, \mathbf{n}^{\mathrm{d}}\ (E_0^{l1} - i\, E_0^{l2})\ \sin\varpi\,, \tag{2.3.23b}$$

together with $F_0^{l,m} = 0$ for all $m \in \mathbb{Z} \setminus \{-1, 0, 1\}$ and $E_0^{l3} = 0$. In the preceding lines, there is no condition on $F_0^{l,0}$. We can always adjust the component $F_0^{l,0}$ so that the first condition of (2.3.22d) is satisfied, which amounts to impose:

$$\int_0^\pi F_0^{l,0}(\mathbf{t}, \mathbf{x}, \varpi)\ \sin\varpi\ d\varpi \ = \ 0\,.$$

The part (2.3.22b) says that the direction E_0^l is parallel to ξ. In particular, we have $\xi^3 = 0$. Using (2.3.15) together with (2.3.23), we get $\xi \cdot \mathcal{J}_0(F_0^l) = 0$. This is all we need to adjust B_0^l through (2.3.22c) and the second relation in (2.3.22d). □

2.3.1.3. *The electron cyclotron resonance frequencies ($\tau = \pm \mathbf{b}_e(\mathbf{x})$).* The position $\mathbf{x} \in \Omega$ being fixed, the electron cyclotron resonance frequency is given by the value $|\tau| = \mathbf{b}_e(\mathbf{x})$. It plays a crucial role in plasma physics (and also in condensed matter and accelerator physics). When $|\tau| = \mathbf{b}_e(\mathbf{x})$, the difficulty comes from the step 2.3.1.1.d). The matrix $\Sigma(\mathbf{x}, \mathbf{b}_e(\mathbf{x}))$ is not invertible. This is why this situation must be tackled separately. We will deal here with the case $\tau = +\mathbf{b}_e$ (the other case $\tau = -\mathbf{b}_e$ being very similar).

Lemma 2.3.2 (trace of the dispersion relations at the resonance frequencies)**.** *For $\tau = \mathbf{b}_e(\mathbf{x})$, the system (2.3.6)-(2.3.10) has a solution $(\mathcal{F}_0^l, B_0^l, E_0^l)$ satisfying Assumption 3.3.1 if and only if the position $(\mathbf{x}, \xi) \in T^*(\Omega)$ is such that $det\, \mathfrak{N}(\mathbf{x}, \mathbf{b}_e(\mathbf{x}), \xi) = 0$.*

Proof. From Paragraph 2.3.1.1, we know already that the condition $det\, \mathfrak{N}(\mathbf{x}, \mathbf{b}_e(\mathbf{x}), \xi) = 0$ is necessary. To show that it is also sufficient, assume that $det\, \mathfrak{N}(\mathbf{x}, \mathbf{b}_e(\mathbf{x}), \xi) = 0$. Then, there is some $E_0^l \not\equiv 0$ such that:

$$\mathfrak{N}(\mathbf{x}, \mathbf{b}_e(\mathbf{x}), \xi)\, E_0^l \ = \ 0\,. \tag{2.3.24}$$

From (2.3.19), we can see that $(1,i,0)\cdot\Sigma(\mathbf{x},\mathbf{b}_e(\mathbf{x}))=0$. Then, looking at $(1,i,0)\cdot\mathfrak{N}\,E_0^l=0$, we can extract $E_0^{l1}+i\,E_0^{l2}=0$. Therefore, the condition (2.3.14a) with $\tau=\mathbf{b}_e(\mathbf{x})$ is met. On the other hand, the relations (2.3.14b) and (2.3.14c) impose:

$$F_0^{l,0} \;=\; -\,i\;\mathbf{b}_e^{-1}\,\mathbf{n}^{\mathrm{d}}\;E_0^{l3}\;\cos\varpi\,, \tag{2.3.25a}$$

$$F_0^{l,1} \;=\; -\,i\;(2\,\mathbf{b}_e)^{-1}\,\mathbf{n}^{\mathrm{d}}\;E_0^{l1}\;\sin\varpi\,. \tag{2.3.25b}$$

The constraint (2.3.14d) implies $F_0^{l,m}=0$ for all $m\in\mathbb{Z}\setminus\{-1,0,1\}$. Adjust B_0^l as indicated in (2.3.10a), that is in such a way that $B_0^l=-\mathbf{b}_e^{-1}\,\xi\times E_0^l$. In view of Remark 2.3.1, there remains to look at (2.3.10b), or equivalently at (2.3.18). First, with (2.3.25), we get:

$$-\,\frac{3}{4}\int_0^\pi F_0^{l,1}(\mathbf{t},\mathbf{x},\varpi)\;(\sin\varpi)^2\;d\varpi \;=\; i\,(2\,\mathbf{b}_e)^{-1}\,\mathbf{n}^{\mathrm{d}}\;E_0^{l1}\,, \tag{2.3.26a}$$

$$-\,\frac{3}{4}\int_0^\pi 2\;F_0^{l,0}(\mathbf{t},\mathbf{x},\varpi)\;\cos\varpi\;\sin\varpi\;d\varpi \;=\; i\;\mathbf{b}_e^{-1}\,\mathbf{n}^{\mathrm{d}}\;E_0^{l3}\,. \tag{2.3.26b}$$

Recalling (2.3.15), we can define:

$$\mathcal{J}_0^1(F_0^{l,-1}) := \mathcal{J}_0(F_0^{l,-1},0,0)^1 = -\,\frac{3}{4}\int_0^\pi F_0^{l,-1}(\mathbf{t},\mathbf{x},\varpi)\;(\sin\varpi)^2\;d\varpi\,.$$

By developing the content of the equation (2.3.18) with $\tau=\mathbf{b}_e(\mathbf{x})$, and by eliminating E_0^{l2} through the relation $E_0^{l2}=i\,E_0^{l1}$, we get:

$$\Big(|\xi^1|^2+\mathbf{b}_e^2-|\xi|^2+i\,\xi^1\,\xi^2-\frac{\mu^2\,\mathbf{n}^{\mathrm{d}}}{2}\Big)\,E_0^{l1}+\xi^1\,\xi^3\,E_0^{l3} \;=-\,i\,\mu^2\,\mathbf{b}_e\,\mathcal{J}_0^1(F_0^{l,-1})\,, \tag{2.3.27a}$$

$$\Big(\xi^1\,\xi^2+i\,(|\xi^2\,|^2+\mathbf{b}_e^2-|\xi|^2)-i\,\frac{\mu^2\,\mathbf{n}^{\mathrm{d}}}{2}\Big)\,E_0^{l1}+\xi^2\,\xi^3\,E_0^{l3} \;=-\,\mu^2\,\mathbf{b}_e\,\mathcal{J}_0^1(F_0^{l,-1})\,, \tag{2.3.27b}$$

$$(\xi^1+i\xi^2)\,\xi^3\,E_0^{l1}+(|\xi^3|^2+\mathbf{b}_e^2-|\xi|^2-\mu^2\,\mathbf{n}^{\mathrm{d}})\,E_0^{l3} \;=\; 0\,. \tag{2.3.27c}$$

The subsystem (2.3.27a)-(2.3.27b) is overdetermined. It implies a compatibility condition, which can be exhibited by looking at the combination $i\,$(2.3.27a) $+$(2.3.27b) $=0$, which is:

$$i\,\Big(2\,\mathbf{b}_e^2-|\xi|^2-|\xi^3|^2-\mu^2\,\mathbf{n}^{\mathrm{d}}\Big)\;E_0^{l1}+(\xi^2+i\,\xi^1)\,\xi^3\,E_0^{l3}=0\,. \tag{2.3.28}$$

Assuming (2.3.28), the equations (2.3.27a)-(2.3.27b) can be solved by adjusting $\mathcal{J}_0^1(F_0^{l,-1})$ accordingly. It suffices to select adequately some $F_0^{l,-1}(\mathbf{t},\mathbf{x})$ not depending on ϖ. This can be done because no condition on $F_0^{l,-1}(\cdot)$ has been imposed so far.

To conclude, it suffices to observe that the system (2.3.24) and (2.3.27c)-(2.3.28) are equivalent. Indeed, the two first components of (2.3.24) correspond to the conditions $(1,i,0)\cdot\mathfrak{N}\,E_0^l=0$ and $(i,1,0)\cdot\mathfrak{N}\,E_0^l=0$, and they turn to be $E_0^{l1}+i\,E_0^{l2}=0$ together with (2.3.28). Furthermore, the equation (2.3.27c) is the same as the third component of (2.3.24). □

Remark 2.3.2. *The part (E_0^{l1},E_0^{l3}) extracted from the vector $E_0^l\not\equiv 0$ of (2.3.24) is necessarily such that $(E_0^{l1},E_0^{l3})\not\equiv(0,0)$, and it satisfies (2.3.27c)-(2.3.28). This can be achieved if and only if we have:*

$$(|\xi^1|^2+|\xi^2|^2)\;|\xi^3|^2-(2\,\mathbf{b}_e^2-|\xi|^2-|\xi^3|^2-\mu^2\,\mathbf{n}^{\mathrm{d}})\;(\mathbf{b}_e^2-|\xi|^2+|\xi^3|^2-\mu^2\,\mathbf{n}^{\mathrm{d}})=0\,. \tag{2.3.29}$$

This condition is equivalent to $det\,\mathfrak{N}(\mathbf{x},\mathbf{b}_e(\mathbf{x}),\xi)=0$. *In fact, the left-hand side of (2.3.29) is exactly* $-i\,\mathbf{b}_e(\mathbf{x})^{-2}\,det\,\mathfrak{N}(\mathbf{x},\mathbf{b}_e(\mathbf{x}),\xi)$.

2.3.1.4. *The non-singular case* $(\tau\neq 0$ *and* $\tau\neq\pm\mathbf{b}_e(\mathbf{x}))$. This situation is simpler.

Lemma 2.3.3 (dispersion relations in the non-singular case)**.** *For* $\tau\in\mathbb{R}\setminus\{0,\pm\mathbf{b}_e(\mathbf{x})\}$, *the system (2.3.6)-(2.3.10) has a solution* $(\mathcal{F}_0^l,B_0^l,E_0^l)$ *satisfying Assumption 3.3.1 if and only if the position* $(\mathbf{x},\xi)\in T^*(\Omega)$ *is such that* $det\,\mathfrak{N}(\mathbf{x},\tau,\xi)=0$.

Proof. Remark that:

$$det\;\Sigma(\mathbf{x},\tau)\;=\;i\;\tau\;\left[-\tau^2+\mathbf{b}_e(\mathbf{x})^2\right]. \tag{2.3.30}$$

Looking at (2.3.10) and at the steps 2.3.1.1⋆) indicates that the condition $det\,\mathfrak{N}(\mathbf{x},\tau,\xi)=0$ is also sufficient to find a solution of (2.3.4) satisfying Assumption 3.3.1. □

In the next Paragraph 2.3.2, we examine more carefully the content of this restriction.

2.3.2. **The characteristic variety of cold magnetized plasmas.** Readers should refer to the Paragraph 2.3.2.1 if there is doubt about notations or definitions. This information will be used repeatedly in what follows. It is also needed when applying Theorem 1.

2.3.2.1. *Notations and definitions.* With the rescaled version (2.2.35) of the electron density $\mathbf{n}^d\equiv\mathbf{n}_1^d$ and with $\mu\equiv|\mu_1|$ as in (2.2.50), introduce:

$$\kappa\equiv\kappa(\mathbf{x}):=\mathbf{n}^{\mathrm{d}}(\mathbf{x})^{1/2}\,\mu\in\mathbb{R}_+^*. \tag{2.3.31}$$

With $\mathbf{b}_e$ and τ as in (2.2.27) and (2.3.5), look at the skew-Hermitian matrix:

$$\Sigma(\mathbf{x},\tau)\;:=\;\begin{pmatrix} i\,\tau & +\mathbf{b}_e(\mathbf{x}) & 0\\ -\mathbf{b}_e(\mathbf{x}) & i\,\tau & 0\\ 0 & 0 & i\,\tau\end{pmatrix},\qquad(\mathbf{x},\tau)\in\Omega\times\mathbb{R}^*. \tag{2.3.32}$$

With the preceding ingredients, consider the matrix:

$$\mathfrak{N}(\mathbf{x},\tau,\xi):=\Sigma(\mathbf{x},\tau)\,(\,\xi\,{}^t\xi+(\tau^2-|\xi|^2)\,Id\,)-i\,\kappa(\mathbf{x})^2\,\tau\,Id. \tag{2.3.33}$$

As will be seen later, all the values of $(\tau,\xi)\in\mathbb{R}^4\setminus\{0\}$, including the singular cases 2.3.1.2 and 2.3.1.3, can be treated together. To this end, the variable τ must be factorized from the characteristic polynomial $det\,\mathfrak{N}$. As will be shown in Lemma 2.3.5, see the definitions (2.3.50)-(2.3.51), there exists an explicit function $\chi\in\mathcal{C}^\infty(\Omega\times(\mathbb{R}^4\setminus\{0\}))$ such that:

$$\forall\,(\mathbf{x},\tau,\xi)\in\Omega\times(\mathbb{R}^4\setminus\{0\}),\qquad det\,\mathfrak{N}(\mathbf{x},\tau,{}^tO(\mathbf{x})\,\xi)=\;-i\;\tau\;\chi(\mathbf{x},\tau,\xi). \tag{2.3.34}$$

The matrix O has been defined at the level of (2.2.31), while the matrix $\mathfrak{N}$ is given by (2.3.33) with κ and Σ as in (2.3.31) and (2.3.32). For all $\mathbf{x}\in\Omega$, the function $\chi(\mathbf{x},\cdot)$ is polynomial with respect to the dual variables $(\tau,\xi)\in\mathbb{R}^4$. Thus, given $\mathbf{x}\in\Omega$, the zeros of $\chi(\mathbf{x},\cdot)$ define some algebraic variety in $T^*_{(\mathbf{t},\mathbf{x})}M$.

Definition 2.3.1. *[characteristic variety] The characteristic variety which can be associated with cold magnetized plasmas is the subset* $\mathscr{V}$ *of* T^*M *composed of:*

$$\mathscr{V}:=\{(\mathbf{t},\mathbf{x},\tau,\xi)\in[0,1]\times\Omega\times(\mathbb{R}^4\setminus\{0\})\,;\,\chi(\mathbf{x},\tau,\xi)=0\}. \tag{2.3.35}$$

The representation (2.3.35) of $\mathscr{V}$ offers a complete intrinsic vision of the characteristic variety. Now, we can decompose the direction $\xi = {}^tO(\mathbf{x})\,\xi \in \mathbb{R}^3$ of (2.3.5) in spherical coordinates, as we did for $p \in \mathbb{R}^3$ in Paragraph 2.2.6.2. With the convention:

$$S_{ph}(r,\omega,\varpi) := {}^t(r\cos\omega\,\sin\varpi\,,\, r\sin\omega\,\sin\varpi\,,\, r\cos\varpi\,)\,, \tag{2.3.36}$$

we have:

$$\xi = S_{ph}(r,\omega,\varpi)\,, \qquad (r,\omega,\varpi) \in \mathbb{R}_+ \times [0,2\,\pi[\times[0,\pi]\,. \tag{2.3.37}$$

Note that the couple (ω,ϖ) inside (2.3.37) differs from the the one of Figure 10. There will be no possible confusion since the decomposition (2.2.45) of $p \in \mathbb{R}^3$ will no longer be used.

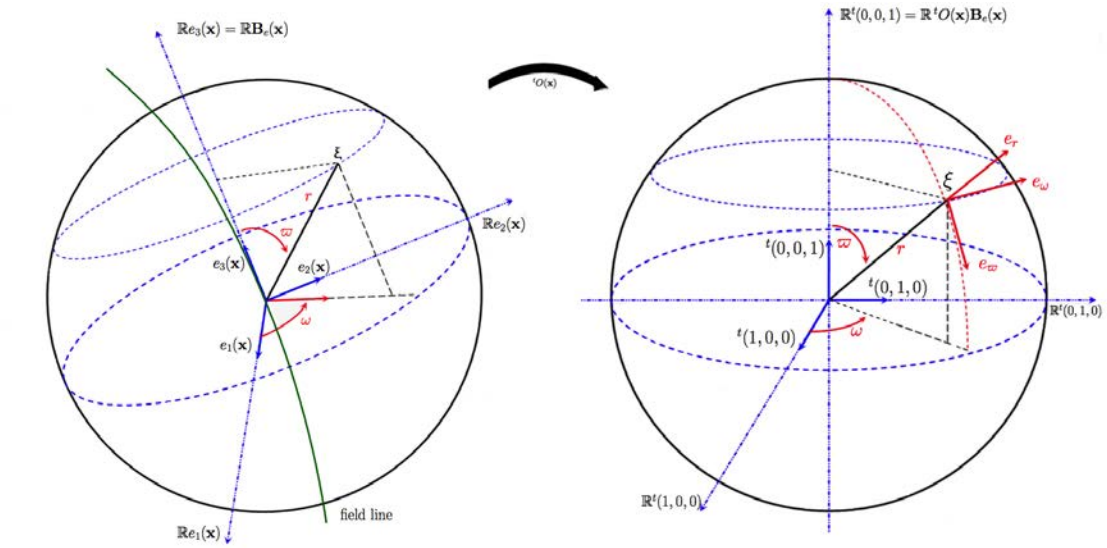

FIGURE 11. Spherical coordinates of $\xi \in \mathbb{R}^3$ after straigntening.

Below, we fix $(\mathbf{t},\mathbf{x}) \in M$ and we introduce useful objects when investigating what happens in the cotangent space $T^*_{(\mathbf{t},\mathbf{x})}M$. According to the forthcoming presentation, the discussion will not directly involve the direction ξ but instead the variable $\xi = {}^tO(\mathbf{x})\,\xi$ through the spherical representation (r,ω,ϖ) of ξ, see the definition (2.3.36)-(2.3.37) and Figure 11. In fact, due to some gyrotropic invariance, the angle ω will be almost absent. In particular, the function $\chi(\cdot)$ of Lemma 2.3.5 does not depend on ω. It remains to deal with (r,ϖ). Now, since the matrix $O(\mathbf{x})$ is orthogonal, there is an obvious link between (r,ϖ) and ξ, namely:

$$r = |\xi| = |\xi|\,, \qquad \varpi = \arctan\Big(\frac{|\xi \times \mathbf{B}_e(\mathbf{x})|}{\xi \cdot \mathbf{B}_e(\mathbf{x})}\Big) = \arctan\Big(\frac{|\xi \times \mathbf{B}_e(\mathbf{x})|}{\xi \cdot \mathbf{B}_e(\mathbf{x})}\Big)\,. \tag{2.3.38}$$

With (r,ϖ) as in (2.3.38) and $\chi_{\mathbf{x},\varpi}(\cdot)$ as in (2.3.50)-(2.3.51), retain that:

$$\forall\,(\mathbf{x},\tau,\xi) \in \Omega \times (\mathbb{R}^4 \setminus \{0\})\,, \qquad \chi(\mathbf{x},\tau,\xi) = \chi(\mathbf{x},\tau,\xi) = \chi_{\mathbf{x},\varpi}(\tau,r)\,. \tag{2.3.39}$$

As explained in the introduction, the *characteristic variety* $\mathscr{V}$ can be written:

$$\mathscr{V} := \Big\{ (\mathbf{t},\mathbf{x},\tau,\xi) \in T^*M \,;\, (|\tau|,|\xi|) \in \mathrm{V}(\mathbf{x},\varpi) = \mathrm{V}_o(\mathbf{x},\varpi) \sqcup \mathrm{V}_x(\mathbf{x},\varpi) \Big\} . \tag{2.3.40}$$

As indicated in (2.3.40), the subset $\mathrm{V}_o(\mathbf{x},\varpi)$ (for *ordinary* waves) and the subset $\mathrm{V}_x(\mathbf{x},\varpi)$ (for *extraordinary* waves) form some non-trivial partition:

$$\emptyset \subsetneq \mathrm{V}_o(\mathbf{x},\varpi) \subsetneq \mathrm{V}(\mathbf{x},\varpi) , \qquad \emptyset \subsetneq \mathrm{V}_x(\mathbf{x},\varpi) \subsetneq \mathrm{V}(\mathbf{x},\varpi) , \qquad \mathrm{V}_o(\mathbf{x},\varpi) \cap \mathrm{V}_x(\mathbf{x},\varpi) = \emptyset .$$

They can be recovered from Theorem 1 through ingredients $\tau_0^\pm(\cdot)$, $\tau_\infty^\pm(\cdot)$ and $g_\pm(\cdot)$ that are clearly specified in the definitions below.

Definition 2.3.2. *[cutoff frequencies] The left handed cutoff frequency $\tau_0^-(\cdot)$ and the right handed cutoff frequency $\tau_0^+(\cdot)$ are the two functions $\tau_0^\pm : \Omega \longrightarrow \mathbb{R}_+$ given by:*

$$\tau_0^\pm(\mathbf{x}) := \frac{1}{2} \Big(\pm \mathbf{b}_e(\mathbf{x}) + \sqrt{\mathbf{b}_e(\mathbf{x})^2 + 4\,\kappa(\mathbf{x})^2} \Big) , \qquad 0 < \tau_0^- < \tau_0^+ . \tag{2.3.41}$$

Definition 2.3.3. *[resonance frequencies] The lower resonance frequency $\tau_\infty^-(\cdot)$ and the upper resonance frequency $\tau_\infty^+(\cdot)$ are the two functions $\tau_\infty^\pm : \Omega \times [0,\pi] \longrightarrow \mathbb{R}_+$, with $0 \leq \tau_\infty^- \leq \tau_\infty^+$, defined by:*

$$\tau_\infty^\pm(\mathbf{x},\varpi)^2 := \frac{1}{2} \Big(\mathbf{b}_e(\mathbf{x})^2 + \kappa(\mathbf{x})^2 \pm \sqrt{(\mathbf{b}_e(\mathbf{x})^2 + \kappa(\mathbf{x})^2)^2 - 4\,\mathbf{b}_e(\mathbf{x})^2\,\kappa(\mathbf{x})^2\,\cos^2\varpi} \Big) . \tag{2.3.42}$$

Definition 2.3.4. *[dispersion relations for ordinary waves and extraordinary waves] The links $r^2 = g_\pm(\mathbf{x},\varpi,\tau)$ inside (2.1.1) involve the (generalized) Appleton-Hartree functions:*

$$g_\pm \,:\, (\Omega \times [0,\pi] \times \mathbb{R}_+) \setminus \{ (\mathbf{x},\varpi,\tau) \,;\, \tau = \tau_\infty^\pm(\mathbf{x},\varpi) \} \longrightarrow \mathbb{R}$$

given by:

$$g_\pm(\mathbf{x},\varpi,\tau) := \frac{\tau^2\ \mathcal{P}(\mathbf{x},\varpi,\tau) \pm \mathbf{b}_e(\mathbf{x})\ \kappa(\mathbf{x})^2\ \sqrt{\mathcal{Q}(\mathbf{x},\varpi,\tau)}}{2\ (\tau^2 - \tau_\infty^+(\mathbf{x},\varpi)^2)\ (\tau^2 - \tau_\infty^-(\mathbf{x},\varpi)^2)} , \tag{2.3.43}$$

where:

$$\mathcal{P} := ((\tau^2-\kappa^2)^2 - \mathbf{b}_e^2\,\tau^2)\,\sin^2\varpi + (\tau^2-\kappa^2)\,(\tau^2 - \mathbf{b}_e^2 - \kappa^2)\,(1+\cos^2\varpi) \tag{2.3.44a}$$

$$= 2\ (\tau^2-\kappa^2)\ (\tau^2 - \kappa^2 - \mathbf{b}_e^2) - \mathbf{b}_e^2\,\kappa^2\ \sin^2\varpi ,$$

$$\mathcal{Q} := \mathbf{b}_e^2\ \sin^4\varpi\ \tau^4 + 4\,\tau^2\,(\tau^2-\kappa^2)^2\ \cos^2\varpi . \tag{2.3.44b}$$

Retain that all the expressions inside Definitions 2.3.3 and 2.3.4 can be interpreted as depending on ξ or ξ. It suffices to exploit (2.3.38).

2.3.2.2. *The characteristic variety from the physical viewpoint.* In what follows, we will work in the non-singular case, with $\tau \neq 0$ and with $|\tau| \neq \mathbf{b}_e(\mathbf{x})$. Introduce:

$$\mathfrak{n} := \frac{\xi}{\tau} \in \mathbb{R}^3 , \qquad \varsigma := \frac{\kappa(\mathbf{x})^2}{\tau^2 - \mathbf{b}_e(\mathbf{x})^2} \in \mathbb{R} , \qquad \gamma := \frac{\mathbf{b}_e(\mathbf{x})}{\tau} \in \mathbb{R}^* . \tag{2.3.45}$$

In optics, the following basic notions often come into play.

Definition 2.3.5. *The refractive index is the vector $\mathfrak{n} \in \mathbb{R}^3$ given by (2.3.45).*

Definition 2.3.6. *With ς and γ as in (2.3.45), the conductivity tensor $\sigma(\cdot)$ is the skew-Hermitian invertible matrix:*

$$\sigma(\mathbf{x},\tau) := -\,\kappa(\mathbf{x})^2\,\Sigma(\mathbf{x},\tau)^{-1} = \begin{pmatrix} i\,\varsigma\,\tau & -\gamma\,\varsigma\,\tau & 0 \\ +\gamma\,\varsigma\,\tau & i\,\varsigma\,\tau & 0 \\ 0 & 0 & i\,\kappa^2\,\tau^{-1} \end{pmatrix},\ (\mathbf{x},\tau) \in \Omega\times\big(\mathbb{R}\backslash\{0,\pm\mathbf{b}_e(\mathbf{x})\}\big).$$

Convections currents resulting from the plasma electrons and ions are usually accounted for the derivation of some *dielectric tensor*.

Definition 2.3.7. *The relative permittivity $D(\mathbf{x},\tau)$, called sometimes the dielectric tensor, is the Hermitian matrix:*

$$D(\mathbf{x},\tau)\ :=\ Id + i\,\tau^{-1}\,\sigma(\mathbf{x},\tau)\,.$$

In most plasma physics books [12, 30, 37], the presentation of $\mathscr{V}$ is achieved in a way that differs from (2.3.35). There, the construction of $\mathscr{V}$ is based on the Definitions 2.3.5, 2.3.6 and 2.3.7. Now, to recover (2.3.35) from $\mathfrak{n}$, σ and D, we can proceed as follows.

Lemma 2.3.4. *For $\tau \in \mathbb{R} \setminus \{0,\pm\mathbf{b}_e(\mathbf{x})\}$, the condition $(\mathbf{t},\mathbf{x},\tau,\xi) \in \mathscr{V}$ is equivalent to the restriction $det\,\mathfrak{M}(\mathbf{x},\tau,{}^tO(\mathbf{x})\,\xi) = 0$ where:*

$$\mathfrak{M}(\mathbf{x},\tau,\xi) := \mathfrak{n}\,{}^t\mathfrak{n} + (1-|\mathfrak{n}|^2)\,Id + i\,\tau^{-1}\,\sigma(\mathbf{x},\tau) = \mathfrak{n}\,{}^t\mathfrak{n} - |\mathfrak{n}|^2\,Id + D(\mathbf{x},\tau)\,. \tag{2.3.46}$$

Proof. Let us start by computing the determinant:

$$det\,\Sigma(\mathbf{x},\tau)\ =\ i\ \tau\ \big[-\tau^2 + \mathbf{b}_e(\mathbf{x})^2\big]\,. \tag{2.3.47}$$

Thus, for $\tau \in \mathbb{R} \setminus \{0,\pm\mathbf{b}_e(\mathbf{x})\}$, the matrix $\Sigma(\mathbf{x},\tau)$ is invertible. By construction, we have:

$$\mathfrak{N}(\mathbf{x},\tau,\xi) = \tau^2\ \Sigma(\mathbf{x},\tau)\ \mathfrak{M}(\mathbf{x},\tau,\xi)\,. \tag{2.3.48}$$

Combining (2.3.34), (2.3.35) and (2.3.47), this explains the result. □

The function $\mathfrak{M}(\cdot)$ of physicists is clearly not defined for the values $\tau = 0$ and $\tau = \pm\mathbf{b}_e(\mathbf{x})$. By contrast, the function $\chi(\cdot)$ is defined and smooth everywhere, while containing as much information. That is why the use of $\chi(\cdot)$ is mathematically more suitable.

Lemma 2.3.5. *There exists a function $\chi(\cdot) \in \mathcal{C}^\infty(\Omega \times (\mathbb{R}^4 \setminus \{0\}))$ such that:*

$$det\,\mathfrak{M}(\mathbf{x},\tau,\xi) = \frac{\chi(\mathbf{x},\tau,\xi)}{\tau^6\,(\tau^2 - \mathbf{b}_e(\mathbf{x})^2)}\,. \tag{2.3.49}$$

The function $\chi(\cdot)$ does not depend on the angle $\omega \in [0, 2\,\pi[$. Given $(\mathbf{x},\varpi) \in \Omega \times [0,\pi]$, it can be put in the form $\chi(\mathbf{x},\tau,\xi) = \chi_{\mathbf{x},\varpi}(\tau,|\xi|)$, where $\chi(\mathbf{x},\cdot)$ is polynomial in (τ,ξ) whereas $\chi_{\mathbf{x},\varpi}(\cdot)$ is a bivariate polynomial in $(\tau,|\xi|)$. More precisely, written as a polynomial in $|\xi|$, the function $\chi_{\mathbf{x},\varpi}(\tau,\cdot)$ is biquadratic:

$$\chi_{\mathbf{x},\varpi}(\tau,|\xi|) = \mathcal{A}_{\mathbf{x},\varpi}(\tau)\ |\xi|^4 - \mathcal{B}_{\mathbf{x},\varpi}(\tau)\ |\xi|^2 + \mathcal{C}_{\mathbf{x}}(\tau)\,. \tag{2.3.50}$$

The coefficients $\mathcal{A}_{\mathbf{x},\varpi}(\cdot)$, $\mathcal{B}_{\mathbf{x},\varpi}(\cdot)$ and $\mathcal{C}_{\mathbf{x}}(\cdot)$ are in $\mathbb{R}[\tau]$, given by the explicit formulas:

$$\text{(2.3.51a)}\quad \mathcal{A}_{\mathbf{x},\varpi}(\tau) := \tau^4 - \tau^2\ \big(\mathbf{b}_e(\mathbf{x})^2 + \kappa(\mathbf{x})^2\big) + \mathbf{b}_e(\mathbf{x})^2\ \kappa(\mathbf{x})^2\ \cos^2\varpi$$
$$= (\tau^2 - \kappa(\mathbf{x})^2)\ (\tau^2 - \mathbf{b}_e(\mathbf{x})^2) - \mathbf{b}_e(\mathbf{x})^2\ \kappa(\mathbf{x})^2\ \sin^2\varpi\,,$$

$$\text{(2.3.51b)}\quad \mathcal{B}_{\mathbf{x},\varpi}(\tau) := \tau^2\ \Big[((\tau^2 - \kappa(\mathbf{x})^2)^2 - \mathbf{b}_e(\mathbf{x})^2\ \tau^2)\ \sin^2\varpi$$
$$+ (\tau^2 - \kappa(\mathbf{x})^2)\ (\tau^2 - \mathbf{b}_e(\mathbf{x})^2 - \kappa(\mathbf{x})^2)(1 + \cos^2\varpi)\Big] = \tau^2\,\mathcal{P}\,,$$

$$\text{(2.3.51c)}\quad \mathcal{C}_{\mathbf{x}}(\tau) := \tau^2\ (\tau^2 - \kappa(\mathbf{x})^2)\,((\tau^2 - \kappa(\mathbf{x})^2)^2 - \mathbf{b}_e(\mathbf{x})^2\ \tau^2)\,.$$

Proof. First, note that:

$$\text{(2.3.52)}\qquad \gamma^2\,\varsigma + 1 - \varsigma = \frac{\tau^2 - \kappa^2}{\tau^2}\,,\qquad (1-\varsigma)^2 - \gamma^2\,\varsigma^2 = \frac{(\tau^2 - \kappa^2)^2 - \mathbf{b}_e^2\ \tau^2}{\tau^2\,(\tau^2 - \mathbf{b}_e^2)}\,.$$

The computation of $det\,\mathfrak{M}(\mathbf{x},\tau,\xi)$ is completely similar to the calculus of R. Fitzpatrick, see the line (4.43) at page 94 of [12]:

$$\text{(2.3.53)}\qquad det\,\mathfrak{M}(\mathbf{x},\tau,\xi) = \mathfrak{a}_{\mathbf{x},\varpi}(\tau)\ |\mathfrak{n}|^4 - \mathfrak{b}_{\mathbf{x},\varpi}(\tau)\ |\mathfrak{n}|^2 + \mathfrak{c}_{\mathbf{x}}(\tau)\,,$$

where:

$$\text{(2.3.54a)}\qquad \mathfrak{a}_{\mathbf{x},\varpi} := (1-\varsigma)\,\sin^2\varpi + (\gamma^2\,\varsigma + 1 - \varsigma)\,\cos^2\varpi\,,$$
$$\text{(2.3.54b)}\qquad \mathfrak{b}_{\mathbf{x},\varpi} := \big((1-\varsigma)^2 - \gamma^2\,\varsigma^2\big)\,\sin^2\varpi + (1-\varsigma)\ (\gamma^2\,\varsigma + 1 - \varsigma)\,(1 + \cos^2\varpi)\,,$$
$$\text{(2.3.54c)}\qquad \mathfrak{c}_{\mathbf{x}} := (\gamma^2\,\varsigma + 1 - \varsigma)\,\big((1-\varsigma)^2 - \gamma^2\,\varsigma^2\big)\,.$$

Then, with (2.3.52) and the definitions of $\mathfrak{n}$, γ and ς from (2.3.45), it suffices to write (2.3.53) as a rational fraction in powers of τ to get the result from Lemma 2.3.5. □

The restriction $\chi_{\mathbf{x},\varpi}(\tau,|\xi|) = 0$ inside (2.3.35) can be handled as a quadratic equation to be solved for $|\xi|^2$, with discriminant $\Delta := \mathcal{B}^2 - 4\,\mathcal{A}\,\mathcal{C}$. As a consequence of Lemma 2.3.6 below, the corresponding roots prove to be (positive, negative or zero) *real* numbers.

Lemma 2.3.6. *The discriminant*

$$\text{(2.3.55)}\qquad \Delta(\mathbf{x},\varpi,\tau) := \mathcal{B}_{\mathbf{x},\varpi}(\tau)^2 - 4\,\mathcal{A}_{\mathbf{x},\varpi}(\tau)\,\mathcal{C}_{\mathbf{x}}(\tau)\,,$$

can be put in the form:

$$\text{(2.3.56)}\qquad \Delta = \mathbf{b}_e^2\ \kappa^4\ \mathcal{Q}\,,\qquad \mathcal{Q} := \tau^2\ \big[\,4\,(\tau^2 - \kappa^2)^2\ \cos^2\varpi + \tau^2\ \mathbf{b}_e^2\ \sin^4\varpi\,\big]\,.$$

The function $\mathcal{Q}(\cdot)$ is defined as in (2.3.44b). It is clearly non-negative. It vanishes if and only if $\tau = 0$ or if $(\tau,\varpi) = (\kappa, 0)$.

Proof. It follows from the second formulas listed in (2.3.51). When computing Δ, it suffices to identify the terms which are in factor of the different powers of $\sin^2\varpi$. □

2.3.2.3. *The physical motivations behind the study of the characteristic variety.* Looking at the set $\mathscr{V} \subset T^*M$ is interesting because we can send or receive information only by using points (τ, ξ) in the phase space T^*M which are microlocalized inside $\mathscr{V}$.

Lemma 2.3.7. *A necessary and sufficient condition to find solutions $\mathcal{U}_0^l$ to the system (2.3.4), with some non-trivial electromagnetic part $(E_0^l, B_0^l) \not\equiv 0$ satisfying Assumption 3.3.1, is to impose the eikonal equation:*

$$(\mathbf{t}, \mathbf{x}, l\,\partial_{\mathbf{t}}\phi(\mathbf{t}, \mathbf{x}), l\,\nabla_{\mathbf{x}}\phi(\mathbf{t}, \mathbf{x})) \in \mathscr{V}, \qquad \forall\,(\mathbf{t}, \mathbf{x}) \in M\,. \tag{2.3.57}$$

Proof. When $\tau \in \mathbb{R}^*$, in view of (2.3.34), the condition (2.3.57) is equivalent to:

$$det\,\mathfrak{N}(\mathbf{x}, l\,\partial_{\mathbf{t}}\phi(\mathbf{t}, \mathbf{x}), l\,{}^tO(\mathbf{x})\,\nabla_{\mathbf{x}}\phi(\mathbf{t}, \mathbf{x})) = 0\,. \tag{2.3.58}$$

Now, from Paragraphs 2.3.1.4 and 2.3.1.3, we know that (2.3.58) is a necessary and sufficient condition.

In the stationary case, when $\tau = 0$, Paragraph 2.3.1.2 says that $\xi^3 = 0$ or equivalently that $\varpi = \pi/2$ is a NSC. Thus, it suffices to show that the restriction (2.3.35), that is:

$$\chi(\mathbf{x}, 0, \xi) = \chi(\mathbf{x}, 0, l\,\nabla_{\mathbf{x}}\phi(\mathbf{t}, \mathbf{x})) = \chi_{\mathbf{x},\varpi}(0, |\xi|) = 0 \tag{2.3.59}$$

can be realized if and only if $\varpi = \pi/2$. With (2.3.51), just remark that:

$$\mathcal{A}_{\mathbf{x},\varpi}(0) = \mathbf{b}_e(\mathbf{x})^2\ \kappa(\mathbf{x})^2\ \cos^2\varpi\,, \qquad \mathcal{B}_{\mathbf{x},\varpi}(0) = 0\,, \qquad \mathcal{C}_{\mathbf{x}}(0) = 0\,,$$

so that:

$$\chi_{\mathbf{x},\varpi}(0, |\xi|) = \mathbf{b}_e(\mathbf{x})^2\ \kappa(\mathbf{x})^2\ \cos^2\varpi\ |\xi|^4\,.$$

Since $|\xi| \neq 0$, we must have $\cos\varpi = 0$, that is $\varpi = \pi/2$ as required.

□

2.3.2.4. *Some geometrical interpretation of the characteristic variety.* Consider the cone:

$$\mathscr{C}(\varpi) := \{\, r\ {}^t(\cos\omega\,\sin\varpi, \sin\omega\,\sin\varpi, \cos\varpi)\,;\,(r, \omega) \in \mathbb{R}_+ \times [0, 2\,\pi]\,\}\,.$$

The set $\mathscr{V}$ can be viewed as the union of disjoint subsets:

$$\mathscr{V} = \cup\{(\mathbf{t}, \mathbf{x}, \mathscr{V}_{\mathbf{x}}^*)\,;\,(\mathbf{t}, \mathbf{x}) \in M\}\,, \qquad \mathscr{V}_{\mathbf{x}}^* := \cup\{\mathscr{V}^*(\mathbf{x}, \varpi)\,;\,\varpi \in [0, \pi]\} \subset T^*_{(\mathbf{t},\mathbf{x})}M\,.$$

Thereby, the set $\mathscr{V}_{\mathbf{x}}^*$ is the section above the position $(\mathbf{t}, \mathbf{x}) \in M$ of the characteristic variety $\mathscr{V}$. It is contained in the four dimensional cotangent fiber $T^*_{(\mathbf{t},\mathbf{x})}M \equiv \mathbb{R}^4$. Its form does not depend on $\mathbf{t} \in [0, 1]$. Now, the refined subset $\mathscr{V}^*(\mathbf{x}, \varpi)$ is obtained by further fixing ϖ, namely:

$$\mathscr{V}^*(\mathbf{x}, \varpi) := \{(\tau, \xi) \in \mathbb{R}^4 \setminus \{0\}\,;\,(\tau, \xi) \in \mathscr{V}_{\mathbf{x}}^*\,,\,\xi \in \mathscr{C}(\varpi)\} \subset T^*_{(\mathbf{t},\mathbf{x})}M\,.$$

With S_{ph} as in (2.3.36), we can fix $(\mathbf{x}, \varpi) \in \Omega \times [0, \pi]$, and define(we will not mark the star $*$ at the level of V):

$$\mathrm{V}(\mathbf{x}, \varpi) := \{(\tau, r) \in \mathbb{R}_+ \times \mathbb{R}_+\,;\,(\tau, S_p(r, 0, \varpi)) \in \mathscr{V}^*(\mathbf{x}, \varpi)\}\,. \tag{2.3.60}$$

With ξ as in (2.3.37), the coefficients $\mathcal{A}$, $\mathcal{B}$ and $\mathcal{C}$ depend only on $\mathbf{x}$, τ^2 and ϖ. Thus, starting from $\mathrm{V}(\mathbf{x}, \varpi)$, we can recover the whole section $\mathscr{V}^*(\mathbf{x}, \varpi)$ by rotations:

$$\mathscr{V}^*(\mathbf{x}, \varpi) = \{(\tau, S_p(r, \omega, \varpi))\,;\,(|\tau|, r) \in \mathrm{V}(\mathbf{x}, \varpi)\,,\ \omega \in [0, 2\,\pi[\,\}\,. \tag{2.3.61}$$

This rotational invariance can be clearly seen in Figures 19, 20, 36 and 22. By this way, the issue reduces to the study of $\mathrm{V}(\mathbf{x},\varpi)$, which is generically a one-dimensional subset of the quadrant $\mathbb{R}_+\times\mathbb{R}_+$. Note also that the coefficients $\mathcal{A}$ and $\mathcal{B}$ satisfy:

$$\mathcal{A}_{\mathbf{x},\varpi}(\tau)=\mathcal{A}_{\mathbf{x},\pi-\varpi}(\tau)\,,\qquad \mathcal{B}_{\mathbf{x},\varpi}(\tau)=\mathcal{B}_{\mathbf{x},\pi-\varpi}(\tau)\,,\qquad \forall\,(\mathbf{x},\tau,\varpi)\in\Omega\times\mathbb{R}\times[0,\pi[\,.$$

This brief discussion can be summarized in a remark.

Remark 2.3.3. *All the geometrical information is provided by the intersection of $\mathscr{V}^*_{\mathbf{x}}$ with the quadrant of an hyperplane. More precisely, we can focus on:*

$$\mathscr{V}^*_{\mathbf{x}}\cap\left\{\,(\tau,\xi)\in\mathbb{R}^4\,;\,0<\tau\,,\,\xi^1=0\,,\,0<\xi^3\,\right\}\subset T^*_{(\mathbf{t},\mathbf{x})}M\,,$$

and then recover the whole set $\mathscr{V}^*_{\mathbf{x}}$ by changing $\tau\in\mathbb{R}_+$ into $-\tau$, by replacing $\xi^3\in\mathbb{R}_+$ by $-\xi^3$, and by applying rotations with axis $\mathbb{R}\,^t(0,0,1)$ and angles $\omega\in[0,2\,\pi[$. This means also that, in practice, we can restrict our attention to the case $(\tau,\varpi)\in\mathbb{R}_+\times[0,\pi/2]$.

Lemma 2.3.6 indicates that the situation $\varpi=0$ (existence of a double root when $\tau=\kappa$) and the other cases $\varpi\in]0,\frac{\pi}{2}]$ must be distinguished. In plasma physics books, the two values $\varpi=0$ and $\varpi=\frac{\pi}{2}$ are usually studied separately, and they are exploited to obtain a classification of waves. However, this viewpoint does not give access to a complete vision of the characteristic variety $\mathscr{V}$. In what follows, we will rather consider that the generic situation is when $\varpi\in]0,\frac{\pi}{2}[$, while the two cases $\varpi=0$ and $\varpi=\frac{\pi}{2}$ can be recovered as (very special) endpoints.

2.3.3. **Parallel, oblique and perpendicular propagation.** In the Paragraph 2.3.3.1, we recall what happens when dealing with the case of *parallel* $(\varpi=0(\pi))$ *non-resonant* $(|\tau|\neq\mathbf{b}_e(\mathbf{x}))$ propagation. The general situation of *oblique* $(\varpi\neq0(\pi))$ propagation is detailed after, in Paragraph 2.3.3.2. Then, we will come back to the parallel case $\varpi=0$ (in Paragraph 2.3.3.3) and to the *perpendicular* case $\varpi=\frac{\pi}{2}$ (in Paragraph 2.3.3.4). Finally, there are different ways to describe $\mathscr{V}^*_{\mathbf{x}}$. We can either study what occurs for a fixed value of $\varpi\in[0,\frac{\pi}{2}]$, as above when involving $\mathscr{V}^*(\mathbf{x},\varpi)$,. Or we can set the value of $\xi\in\mathbb{R}^3$ (see Paragraph 2.3.4.3) or of $\tau\in\mathbb{R}$ (see Paragraph 2.3.4.2).

2.3.3.1. *Parallel* $(\varpi=0(\pi))$ *non-singular* $(\tau\in\mathbb{R}^*_+\setminus\{\mathbf{b}_e(\mathbf{x})\})$ *propagation.* The matter here is to study the equation $\chi_{\mathbf{x},0}(\tau,|\xi|)=0$, which is simply:

$$\begin{aligned}(\tau^2-\kappa^2)\,\Big[(\tau^2-\mathbf{b}_e^2)\,|\xi|^4-2\,\tau^2\,(\tau^2-\mathbf{b}_e^2-\kappa^2)\,|\xi|^2\\ +\tau^2\,\left((\tau^2-\kappa^2)^2-\mathbf{b}_e^2\,\tau^2\right)\Big]\;=\;0\,.\end{aligned}\tag{2.3.62}$$

Either we have $\tau^2-\kappa^2=0$ or $Z=|\xi|^2$ must be subjected to:

$$(\tau^2-\mathbf{b}_e^2)\;Z^2-2\;\tau^2\;(\tau^2-\mathbf{b}_e^2-\kappa^2)\;Z+\tau^2\;\left((\tau^2-\kappa^2)^2-\mathbf{b}_e^2\,\tau^2\right)=0\,.$$

Since $|\tau|\neq\mathbf{b}_e(\mathbf{x})$, this quadratic equation has two roots $Z_1(\mathbf{x},\tau)$ and $Z_2(\mathbf{x},\tau)$ given by:

$$Z_1(\mathbf{x},\tau):=\frac{\tau^2\,(\tau^2-\mathbf{b}_e^2-\kappa^2)+\mathbf{b}_e\,\kappa^2\,\tau}{\tau^2-\mathbf{b}_e^2}\,,\qquad Z_2(\mathbf{x},\tau):=\frac{\tau^2\,(\tau^2-\mathbf{b}_e^2-\kappa^2)-\mathbf{b}_e\,\kappa^2\,\tau}{\tau^2-\mathbf{b}_e^2}\,.$$

The set $\mathrm{V}(\mathbf{x},0)$ is usually (see for instance [12]-chapter 4) separated into connected parts, corresponding to the different possibilities marked above.

a) Parallel *left-handed* circularly polarized wave ($|\xi|^2 = Z_1(\mathbf{x},\tau)$). Knowing that $\tau \in \mathbb{R}_+^*$, this can be achieved for some $|\xi| \in \mathbb{R}_+$ if and only if:

$$0 \le Z_1(\mathbf{x},\tau) = \frac{\tau\,(\tau^2 + \mathbf{b}_e\,\tau - \kappa^2)}{\tau + \mathbf{b}_e} \quad \Longleftrightarrow \quad \tau_0^-(\mathbf{x}) \le \tau\,. \tag{2.3.63}$$

We find only one connected component:

$$\mathrm{V}_l(\mathbf{x},0) \;=\; \Big\{\,(\tau,r) \in \mathbb{R}_+\times\mathbb{R}_+\,;\,\tau_0^- \le \tau\,,\; r^2 = \tau^2 - \kappa(\mathbf{x})^2\,\tau/(\tau+\mathbf{b}_e(\mathbf{x}))\,\Big\}\,. \tag{2.3.64}$$

b) Parallel *right-handed* circularly polarized wave ($|\xi|^2 = Z_2(\mathbf{x},\tau)$). Knowing that $\tau \in \mathbb{R}_+^*$, this can be achieved for some $|\xi| \in \mathbb{R}_+$ if and only if:

$$0 \le Z_2(\mathbf{x},\tau) = \frac{\tau\,(\tau^2 - \mathbf{b}_e\,\tau - \kappa^2)}{\tau - \mathbf{b}_e} \quad \Longleftrightarrow \quad 0 < \tau < \mathbf{b}_e \;\text{ or }\; \tau_0^+(\mathbf{x}) \le \tau\,. \tag{2.3.65}$$

Accordingly, the set $\mathrm{V}_r(\mathbf{x},0)$ can be split into two connected parts $\mathrm{V}_r^-(\mathbf{x},0)$ and $\mathrm{V}_r^+(\mathbf{x},0)$ which are distinguished below.

b.1) The first part $\mathrm{V}_r^-(\mathbf{x},0)$ contains both the dispersion relation for *Alfvèn* waves (values of τ such that $0 \lesssim \tau$) and the dispersion relation for *whistler* (or *electron cyclotron*) waves (values of τ such that $\tau \lesssim \mathbf{b}_e$):

$$\mathrm{V}_r^-(\mathbf{x},0) := \Big\{(\tau,r)\,;\,0<\tau<\mathbf{b}_e(\mathbf{x})\,,\,0<r\,,\,r^2 = \tau^2 - \kappa(\mathbf{x})^2\,\tau/(\tau-\mathbf{b}_e(\mathbf{x}))\,\Big\}\,. \tag{2.3.66}$$

b.2) The second is the standard right-handed circularly polarized wave:

$$\mathrm{V}_r^+(\mathbf{x},0) := \Big\{(\tau,r)\,;\,\tau_0^+(\mathbf{x}) \le \tau\,,\,0<r\,,\,r^2 = \tau^2 - \kappa(\mathbf{x})^2\,\tau/(\tau-\mathbf{b}_e(\mathbf{x}))\,\Big\}\,. \tag{2.3.67}$$

c) Parallel longitudinal wave or *electrostatic* plasma wave ($\tau = \kappa$). With κ as in (2.3.31), this means a link between τ and $\mathbf{x}$, whereas no condition is imposed on $|\xi|$. We find the vertical half-line $\mathrm{V}_0(\mathbf{x},0) := \{(\kappa,r)\,;\,r \in \mathbb{R}_+\}$.

Briefly, retain that:

$$\mathrm{V}(\mathbf{x},0) = \mathrm{V}_l(\mathbf{x},0) \cup \mathrm{V}_r^-(\mathbf{x},0) \cup \mathrm{V}_r^+(\mathbf{x},0) \cup \mathrm{V}_0(\mathbf{x},0)\,. \tag{2.3.68}$$

The corresponding curves are represented on Figure 12 below:

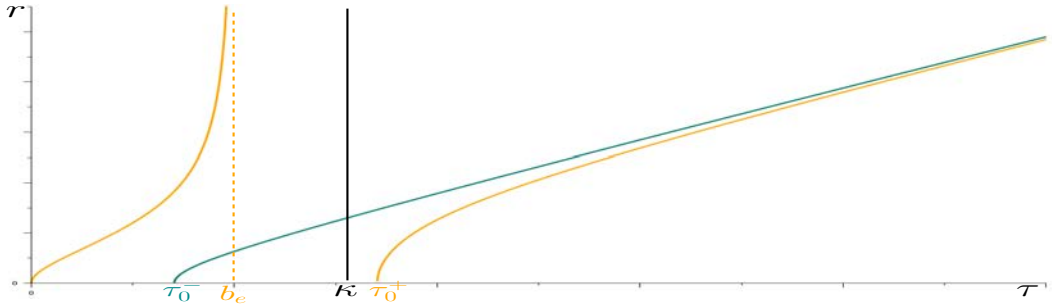

FIGURE 12. Parallel propagation ($\varpi = 0$). Standard nomenclature. $\mathrm{V}_r(\mathbf{x},0)$ (in orange), $\mathrm{V}_l(\mathbf{x},0)$ (in blue-green) and $\mathrm{V}_0(\mathbf{x},0)$ (in black).

2.3.3.2. *Oblique ($\varpi \in]0, \frac{\pi}{2}]$) non-singular ($\tau \in \mathbb{R}_+^* \setminus \{\mathbf{b}_e(\mathbf{x})\}$) propagation.* We first study the coefficient $\mathcal{A}$ which is in factor of $|\xi|^4$ in the equation $\chi_{\mathbf{x},\varpi}(\tau, |\xi|) = 0$.

Lemma 2.3.8. *With $\tau_\infty^\pm(\cdot)$ as in (2.3.42), we have:*

$$\mathcal{A}_{\mathbf{x},\varpi}(\tau) = (\tau^2 - \tau_\infty^-(\mathbf{x},\varpi)^2)\ (\tau^2 - \tau_\infty^+(\mathbf{x},\varpi)^2)\,. \tag{2.3.69}$$

Proof. This follows from direct calculations. □

For $\tau \neq \tau_\infty^\pm$, as a consequence of Lemma 2.3.6, the equation $\chi_{\mathbf{x},\varpi}(\tau, |\xi|) = 0$ has two distinct real solutions which can be described by:

$$|\xi|^2 = g_\pm(\mathbf{x},\varpi,\tau) = \frac{\mathcal{B} \pm \mathbf{b}_e\, \kappa^2\, \sqrt{\mathcal{Q}}}{2\ \mathcal{A}} = \frac{2\ \mathcal{C}}{\mathcal{B} \mp \mathbf{b}_e\, \kappa^2\, \sqrt{\mathcal{Q}}}\,. \tag{2.3.70}$$

When $g_\pm(\mathbf{x},\varpi,\tau) < 0$, there is no mathematical solution. The associated waves are usually considered to be evanescent. On the contrary, when $0 \leq g_\pm(\mathbf{x},\varpi,\tau)$, the condition (2.3.70) is achieved for some $|\xi| \in \mathbb{R}_+$. This means that a wave can be propagated. To distinguish between these two situations, we have to study the functions $g_\pm(\mathbf{x},\varpi,\cdot)$. To illustrate the following discussion, we can directly plot the graphs of the functions $g_\pm(\mathbf{x},\varpi,\cdot)$. The content of Figures 13 and 14 is justified below.

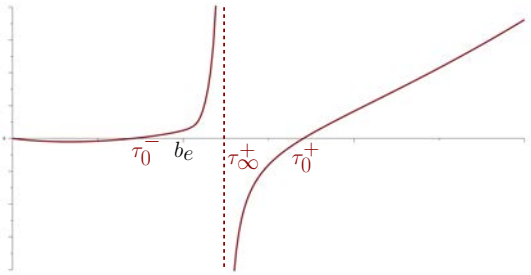

FIGURE 13. Graph of $g_-(\mathbf{x},\varpi,\cdot)$.

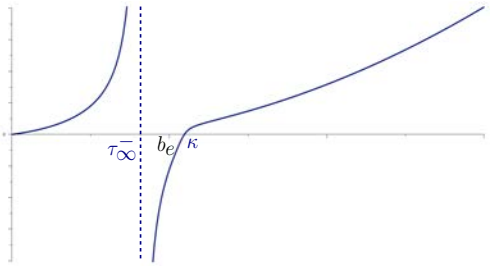

FIGURE 14. Graph of $g_+(\mathbf{x},\varpi,\cdot)$.

Lemma 2.3.9. *[properties of the functions $\tau_\infty^\pm(\mathbf{x},\cdot)$] For all $\mathbf{x} \in \Omega$, the function $\tau_\infty^+(\mathbf{x},\cdot)$ is strictly increasing on the interval $[0,\pi/2]$, and it satisfies:*

$$\tau_\infty^+(\mathbf{x},0) = \max\left(\mathbf{b}_e(\mathbf{x})\,;\,\kappa(\mathbf{x})\right), \qquad \tau_\infty^+(\mathbf{x},\pi/2) = \sqrt{\mathbf{b}_e(\mathbf{x})^2 + \kappa(\mathbf{x})^2}\,. \tag{2.3.71}$$

For all $\mathbf{x} \in \Omega$, the function $\tau_\infty^-(\mathbf{x},\cdot)$ is strictly decreasing on $[0,\pi/2]$, with:

$$\tau_\infty^-(\mathbf{x},0) = \min\left(\mathbf{b}_e(\mathbf{x})\,;\,\kappa(\mathbf{x})\right), \qquad \tau_\infty^-(\mathbf{x},\pi/2) = 0\,. \tag{2.3.72}$$

Proof. By direct calculation. □

Lemma 2.3.10. *[comparison of resonance and cutoff frequencies] If $\sqrt{2}\ \mathbf{b}_e(\mathbf{x}) < \kappa(\mathbf{x})$, we have:*

$$\tau_\infty^-(\mathbf{x},\varpi) < \tau_0^-(\mathbf{x})\,, \qquad \forall\,(\mathbf{x},\varpi) \in \Omega \times [0,\pi]\,. \tag{2.3.73}$$

If $\kappa(\mathbf{x}) < \sqrt{2}\ \mathbf{b}_e(\mathbf{x})$, we have $\tau_0^-(\mathbf{x}) < \mathbf{b}_e(\mathbf{x})$ and $\tau_0^-(\mathbf{x}) < \tau_\infty^-(\mathbf{x},0)$. Moreover:

$$\tau_0^-(\mathbf{x}) < \tau_\infty^+(\mathbf{x},\varpi) < \tau_0^+(\mathbf{x})\,, \qquad \forall\,(\mathbf{x},\varpi) \in \Omega \times [0,\pi]\,. \tag{2.3.74}$$

Proof. Assume that $\sqrt{2}\ \mathbf{b}_e(\mathbf{x}) < \kappa(\mathbf{x})$. In view of (2.3.72), to get (2.3.73), it suffices to note that:

$$\tau_\infty^-(\mathbf{x},0) = \frac{1}{2}\Big(-\mathbf{b}_e + \sqrt{\mathbf{b}_e^2 + 8\,\mathbf{b}_e^2}\Big) < \frac{1}{2}\Big(-\mathbf{b}_e + \sqrt{\mathbf{b}_e^2 + 4\,\kappa^2}\Big) = \tau_0^-(\mathbf{x})\,.$$

The other comparisons follow from straightforward computations. □

Lemma 2.3.11. *Fix $(\mathbf{x},\varpi) \in \Omega \times [0,\frac{\pi}{2}]$. The functions $g_+(\mathbf{x},\varpi,\cdot)$ and $g_-(\mathbf{x},\varpi,\cdot)$ of (2.3.43) are of class C^∞ respectively on the domains $\mathbb{R}_+ \setminus \{\tau_\infty^-(\mathbf{x},\varpi)\}$ and $\mathbb{R}_+ \setminus \{\tau_\infty^+(\mathbf{x},\varpi)\}$.*

Proof. With the expressions given in Definition 2.3.4, the functions $g_\pm(\mathbf{x},\varpi,\cdot)$ are clearly of class C^∞ on $\mathbb{R}_+ \setminus \{\tau_\infty^+(\mathbf{x},\varpi), \tau_\infty^-(\mathbf{x},\varpi)\}$. Moreover, using the right part of (2.3.70), they can be written in the form:

$$g_\pm(\mathbf{x},\varpi,\tau) = \frac{2\ \tau^2\ (\tau^2-\kappa^2)\ ((\tau^2-\kappa^2)^2 - \mathbf{b}_e^2\,\tau^2)}{\tau^2\,\mathcal{P}(\varpi,\tau) \mp \sqrt{\mathbf{b}_e^2\,\kappa^4\,\mathcal{Q}(\varpi,\tau)}}\,. \tag{2.3.75}$$

The difficulty is to show that $g_\pm(\mathbf{x},\varpi,\cdot)$ is well defined and smooth near $\tau_\infty^\pm(\mathbf{x},\varpi)$. To this end, we have to examine more precisely the denominator in (2.3.75). First, combining (2.3.51b)-(2.3.51c) and (2.3.69), the term $\Delta = \mathbf{b}_e^2\kappa^4\mathcal{Q}$ of (2.3.56) can be written:

$$\Delta = \tau^4\ \mathcal{P}^2 - 4\ \tau^2\ (\tau^2-(\tau_\infty^+)^2)\ (\tau^2-(\tau_\infty^-)^2)\ (\tau^2-\kappa^2)\ ((\tau^2-\kappa^2)^2 - \mathbf{b}_e^2\,\tau^2)\,.$$

For $\tau = \tau_\infty^\pm$, it follows that:

$$(\tau_\infty^\pm)^2\ \mathcal{P}(\mathbf{x},\varpi,\tau_\infty^\pm) \mp \sqrt{\mathbf{b}_e^2\,\kappa^4\,\mathcal{Q}(\mathbf{x},\varpi,\tau_\infty^\pm)} = (\tau_\infty^\pm)^2\,(\mathcal{P}(\mathbf{x},\varpi,\tau_\infty^\pm) \mp |\mathcal{P}(\mathbf{x},\varpi,\tau_\infty^\pm)|)\,.$$

In view of the second formulas in (2.3.44a) and (2.3.51a), we have:

$$\begin{aligned}\mathcal{P}(\mathbf{x},\varpi,\tau) &= \mathcal{A} + (\tau^2-\kappa^2)\,(\tau^2 - \mathbf{b}_e^2 - 2\,\kappa^2)\\ &= (\tau^2-(\tau_\infty^+)^2)\,(\tau^2-(\tau_\infty^-)^2) + (\tau^2-\kappa^2)\,(\tau^2-\mathbf{b}_e^2-2\,\kappa^2)\,.\end{aligned} \tag{2.3.76}$$

From (2.3.76) and Lemma 2.3.9, we can easily deduce that:

$$\mathcal{P}(\mathbf{x},\varpi,\tau_\infty^+) = ((\tau_\infty^+)^2-\kappa^2)\,((\tau_\infty^+)^2 - (\mathbf{b}_e^2+2\,\kappa^2)) < 0\,, \tag{2.3.77a}$$

$$\mathcal{P}(\mathbf{x},\varpi,\tau_\infty^-) = ((\tau_\infty^-)^2-\kappa^2)\,((\tau_\infty^-)^2 - (\mathbf{b}_e^2+2\kappa^2)) > 0\,. \tag{2.3.77b}$$

And therefore:

$$(\tau_\infty^+)^2\ \mathcal{P}(\mathbf{x},\varpi,\tau_\infty^+) - \sqrt{\mathbf{b}_e^2\,\kappa^4\,\mathcal{Q}(\mathbf{x},\varpi,\tau_\infty^+)} = 2\ (\tau_\infty^+)^2\ \mathcal{P}(\mathbf{x},\varpi,\tau_\infty^+) < 0\,, \tag{2.3.78a}$$

$$(\tau_\infty^-)^2\ \mathcal{P}(\mathbf{x},\varpi,\tau_\infty^-) + \sqrt{\mathbf{b}_e^2\,\kappa^4\,\mathcal{Q}(\mathbf{x},\varpi,\tau_\infty^-)} = 2\ (\tau_\infty^-)^2\ \mathcal{P}(\mathbf{x},\varpi,\tau_\infty^-) > 0\,. \tag{2.3.78b}$$

This means that the denominator of (2.3.75) does not vanish. This gives the conclusion. □

Lemma 2.3.12. *[zeros of the functions $g_\pm(\mathbf{x},\varpi,\cdot) : \mathbb{R}_+ \setminus \{\tau_\infty^\mp(\mathbf{x},\varpi)\} \longrightarrow \mathbb{R}$]*

$$\{\tau \in \mathbb{R}_+ \setminus \{\tau_\infty^-(\mathbf{x},\varpi)\}\,;\ g_+(\mathbf{x},\varpi,\tau) = 0\} \ = \ \{0, \kappa(\mathbf{x})\}\,, \tag{2.3.79a}$$

$$\{\tau \in \mathbb{R}_+ \setminus \{\tau_\infty^+(\mathbf{x},\varpi)\}\,;\ g_-(\mathbf{x},\varpi,\tau) = 0\} \ = \ \{0, \tau_0^-(\mathbf{x}), \tau_0^+(\mathbf{x})\}\,. \tag{2.3.79b}$$

Proof. From (2.3.43)-(2.3.44b), we get easily $g_\pm(\mathbf{x},\varpi,0) = 0$. Now, when $g_\pm(\mathbf{x},\varpi,\tau) = 0$, by definition, the value $|\xi| = 0$ must be a solution to the equation $\chi_{\mathbf{x},\varpi}(\tau,|\xi|) = 0$. In view of (2.3.50), this implies $\mathcal{C}(\tau) = 0$. Recalling the discussion in Paragraph 2.3.3.1, we find:

$$\{\tau \in \mathbb{R}_+^*\,;\ \mathcal{C}_{\mathbf{x}}(\tau) = 0\} = \{\kappa(\mathbf{x}), \tau_0^-(\mathbf{x}), \tau_0^+(\mathbf{x})\}\,.$$

Now, using (2.3.43) and (2.3.44), we can directly check that:

$$g_+(\mathbf{x},\varpi,\kappa(\mathbf{x}))=0\,,\qquad g_-(\mathbf{x},\varpi,\kappa(\mathbf{x}))\neq 0\,. \tag{2.3.80}$$

On the other hand, the choice $\tau=\tau_0^\pm$ corresponds to $\tau^2-\kappa^2=\mp\mathbf{b}_e\,\tau$. With (2.3.51b), this gives rise to:

$$\mathcal{B}(\tau_0^\pm)=(\tau_0^\pm)^2((\tau_0^\pm)^2-\kappa^2)((\tau_0^\pm)^2-\mathbf{b}_e^2-\kappa^2)(1+\cos^2\varpi)\,,\ \ \mathcal{C}(\tau_0^\pm)=0\,,\ \ \Delta(\tau_0^\pm)=\mathcal{B}(\tau_0^\pm)^2\,.$$

Coming back to (2.3.70), we see that $g_\pm(\mathbf{x},\varpi,\tau_0^\pm)=0$ if and only if $(\mathcal{B}\pm|\mathcal{B}|)(\tau_0^\pm)=0$. From (2.3.41), we can infer that:

$$\kappa^2<\kappa^2+\mathbf{b}_e^2<(\tau_0^+)^2=\kappa^2+\frac{1}{2}\,\mathbf{b}_e\,\big[\mathbf{b}_e+\sqrt{\mathbf{b}_e^2+4\,\kappa^2}\big]\quad\Longrightarrow\quad 0<\mathcal{B}(\tau_0^+)\,, \tag{2.3.81}$$

so that:

$$g_+\big(\mathbf{x},\varpi,\tau_0^+(\mathbf{x})\big)\neq 0\,,\qquad g_-\big(\mathbf{x},\varpi,\tau_0^+(\mathbf{x})\big)=0\,. \tag{2.3.82}$$

Similarly, from (2.3.41), we can obtain:

$$(\tau_0^-)^2=\kappa^2+\frac{1}{2}\,\mathbf{b}_e\,\big[\mathbf{b}_e-\sqrt{\mathbf{b}_e^2+4\,\kappa^2}\big]<\kappa^2<\kappa^2+\mathbf{b}_e^2\quad\Longrightarrow\quad 0<\mathcal{B}(\tau_0^-)\,. \tag{2.3.83}$$

It follows that:

$$g_+\big(\mathbf{x},\varpi,\tau_0^-(\mathbf{x})\big)\neq 0\,,\qquad g_-\big(\mathbf{x},\varpi,\tau_0^-(\mathbf{x})\big)=0\,. \tag{2.3.84}$$

Combining (2.3.80), (2.3.82) and (2.3.84), we can deduce (2.3.79a) and (2.3.79b). □

Lemma 2.3.13. *[asymptotic behaviors near the resonance frequencies]*

$$\lim_{\tau\to(\tau_\infty^-)^-} g_+(\mathbf{x},\varpi,\tau)=+\infty\,,\qquad \lim_{\tau\to(\tau_\infty^-)^+} g_+(\mathbf{x},\varpi,\tau)=-\infty\,, \tag{2.3.85a}$$

$$\lim_{\tau\to(\tau_\infty^+)-} g_-(\mathbf{x},\varpi,\tau)=+\infty\,,\qquad \lim_{\tau\to(\tau_\infty^+)^+} g_-(\mathbf{x},\varpi,\tau)=-\infty\,. \tag{2.3.85b}$$

Proof. In view of (2.3.69)-(2.3.70), to obtain (2.3.85a)-(2.3.85b), it suffices to show that:

$$\frac{(\tau_\infty^-)^2\ \mathcal{P}(\varpi,\tau_\infty^-)+\mathbf{b}_e\,\kappa^2\,\sqrt{\mathcal{Q}(\varpi,\tau_\infty^-)}}{2\ ((\tau_\infty^-)^2-(\tau_\infty^+)^2)}<0\,, \tag{2.3.86a}$$

$$\frac{(\tau_\infty^+)^2\ \mathcal{P}(\varpi,\tau_\infty^+)-\mathbf{b}_e\,\kappa^2\,\sqrt{\mathcal{Q}(\varpi,\tau_\infty^+)}}{2\ ((\tau_\infty^+)^2-(\tau_\infty^-)^2)}<0\,. \tag{2.3.86b}$$

Taking into account Lemma 2.3.9, we have $\tau_\infty^-\leq\kappa\leq\tau_\infty^+$, as well as $\tau_\infty^-<\tau_\infty^+$. Applying (2.3.77b), we find (2.3.86a). Similarly, (2.3.86b) comes from (2.3.77a). □

We are now able to distinguish between the different regions of wave propagation. This can be done by selecting the connected parts of $\mathrm{V}(\mathbf{x},\varpi)$. This means to isolate where the functions $g_-(\mathbf{x},\varpi,\cdot)$ and $g_+(\mathbf{x},\varpi,\cdot)$ are positive. We will adopt the following classification.

a) Oblique <u>*ordinary*</u> wave ($|\xi|^2=g_+(\mathbf{x},\varpi,\tau)\geq 0$). With Lemmas 2.3.11 and 2.3.12, together with the intermediate value theorem, we get:

$$g_+(\mathbf{x},\varpi,\tau)\geq 0\iff\tau\in[0,\tau_\infty^-(\mathbf{x},\varpi)[\,\cup[\kappa(\mathbf{x}),+\infty[\,. \tag{2.3.87}$$

The set $\mathrm{V}_o(\mathbf{x},\varpi)$ consists of two connnected parts $\mathrm{V}_o^-(\mathbf{x},\varpi)$ and $\mathrm{V}_o^+(\mathbf{x},\varpi)$ which are defined by:

$$\mathrm{V}_o^-(\mathbf{x},\varpi) := \{(\tau,r)\,;\, 0<\tau<\tau_\infty^-(\mathbf{x},\varpi)\,,\, 0\le r\,,\, r^2=g_+(\mathbf{x},\varpi,\tau)\}\,, \tag{2.3.88a}$$

$$\mathrm{V}_o^+(\mathbf{x},\varpi) := \{(\tau,r)\,;\, \kappa(\mathbf{x})\le\tau\,,\, 0\le r\,,\, r^2=g_+(\mathbf{x},\varpi,\tau)\}\,. \tag{2.3.88b}$$

The part of $\mathrm{V}_o^-(\mathbf{x},\varpi)$ with $0\lesssim\tau$ gives the dispersion relation for *Alfvèn* waves. The part of $\mathrm{V}_o^-(\mathbf{x},\varpi)$ with $\tau\lesssim\tau_\infty^-(\mathbf{x},\varpi)$ determines the dispersion relation for *whistler* waves.

b) Oblique <u>*extraordinary*</u> wave ($|\xi|^2=g_-(\mathbf{x},\varpi,\tau)\ge 0$). The set $\mathrm{V}_x(\mathbf{x},\varpi)$ is also composed of two connected parts $\mathrm{V}_x^-(\mathbf{x},\varpi)$ and $\mathrm{V}_x^+(\mathbf{x},\varpi)$ which are defined by:

$$\mathrm{V}_x^-(\mathbf{x},\varpi) := \{(\tau,r)\,;\, \tau_0^-(\mathbf{x})\le\tau<\tau_\infty^+(\mathbf{x},\varpi)\,,\, 0\le r\,,\, r^2=g_-(\mathbf{x},\varpi,\tau)\}\,, \tag{2.3.89a}$$

$$\mathrm{V}_x^+(\mathbf{x},\varpi) := \{(\tau,r)\,;\, \tau_0^+(\mathbf{x})\le\tau\,,\, 0\le r\,,\, r^2=g_-(\mathbf{x},\varpi,\tau)\}\,. \tag{2.3.89b}$$

Retain that:

$$\mathrm{V}(\mathbf{x},\varpi)=\mathrm{V}_o^-(\mathbf{x},\varpi)\sqcup\mathrm{V}_o^+(\mathbf{x},\varpi)\sqcup\mathrm{V}_x^-(\mathbf{x},\varpi)\sqcup\mathrm{V}_x^+(\mathbf{x},\varpi)\,. \tag{2.3.90}$$

The case of perpendicular propagation ($\varpi=\pi/2$) can be incorporated within the general framework of oblique propagation. However, using (2.3.42), we get $\tau_\infty^-(\mathbf{x},\pi/2)=0$. It follows that $\mathrm{V}_o^-(\mathbf{x},\pi/2)=\{(0,r)\,;\,r\in\mathbb{R}_+\}$. Thus, the set $\mathrm{V}_o(\mathbf{x},\pi/2)$ reduces to the vertical half-line $\{\tau=0\}$ together with the connected component $\mathrm{V}_o^+(\mathbf{x},\pi/2)$ which is associated to what physicists call *ordinary* waves. On the other hand, the set $\mathrm{V}_x(\mathbf{x},\pi/2)$ is still composed of two disjoint connected parts $\mathrm{V}_x^-(\mathbf{x},\pi/2)$ and $\mathrm{V}_x^+(\mathbf{x},\pi/2)$ which correspond to *extraordinary* waves. Some sets $\mathrm{V}_o(\mathbf{x},\varpi)$ and $\mathrm{V}_x(\mathbf{x},\varpi)$ are represented on Figure 15 below.

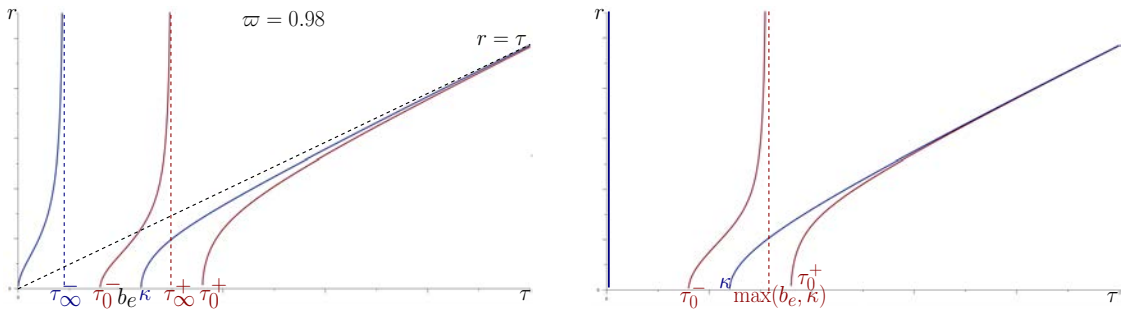

(a) General case ($\varpi=0.98$). (b) Perpendicular case ($\varpi=\pi/2$).

FIGURE 15. Oblique propagation for angles $\varpi\in]0,\pi/2]$:
- Ordinary waves $\mathrm{V}_o(\mathbf{x},\varpi)=\mathrm{V}_o^-(\mathbf{x},\varpi)\sqcup\mathrm{V}_o^+(\mathbf{x},\varpi)$ in blue;
- Extraordinary waves $\mathrm{V}_x(\mathbf{x},\varpi)=\mathrm{V}_x^-(\mathbf{x},\varpi)\sqcup\mathrm{V}_x^+(\mathbf{x},\varpi)$ in red.

2.3.3.3. *Come back to parallel propagation.* In this Paragraph 2.3.3.3, we examine again the case of parallel propagation. But, to this end, we follow the approach of (2.3.88) and (2.3.89). This allows to provide a fresh perspective on what happens when $\varpi = 0$. When $\varpi = 0$, the formula (2.3.43) yields:

$$g_\pm(\mathbf{x}, 0, \tau) = \tau^2 - \frac{\kappa(\mathbf{x})^2\,\tau}{\tau \pm sgn(\tau - \kappa(\mathbf{x}))\ \mathbf{b}_e(\mathbf{x})}\,. \tag{2.3.91}$$

Recall (2.3.81) which guarantees that $\kappa < \tau_0^+$. As a consequence of (2.3.91), the definitions (2.3.67) of $\mathrm{V}_r^+(\mathbf{x}, 0)$ and (2.3.89b) of $\mathrm{V}_x^+(\mathbf{x}, 0)$ coincide. The function $g_\pm(\mathbf{x}, 0, \cdot)$ is not suitable for the description of the other components of $\mathrm{V}(\mathbf{x}, 0)$. This is because $g_\pm(\mathbf{x}, 0, \cdot)$ is not continuous at the point $\tau = \kappa$.

Definition 2.3.8. *[overdense and underdense plasmas] The plasma is said <u>overdense</u> at the spatial position* $\mathbf{x}$ *if* $\mathbf{b}_e(\mathbf{x}) < \kappa$. *Otherwise, it is said <u>underdense</u>.*

For $\varpi = 0$, the identity (2.3.42) gives rise to:

$$\tau_\infty^-(\mathbf{x}, 0) = \begin{cases} \kappa(\mathbf{x}) & \text{if} \quad \kappa(\mathbf{x}) < \mathbf{b}_e(\mathbf{x})\,, \\ \mathbf{b}_e(\mathbf{x}) & \text{if} \quad \mathbf{b}_e(\mathbf{x}) < \kappa(\mathbf{x})\,, \end{cases} \qquad \tau_\infty^+(\mathbf{x}, 0) = \begin{cases} \kappa(\mathbf{x}) & \text{if} \quad \mathbf{b}_e(\mathbf{x}) < \kappa(\mathbf{x})\,, \\ \mathbf{b}_e(\mathbf{x}) & \text{if} \quad \kappa(\mathbf{x}) < \mathbf{b}_e(\mathbf{x})\,. \end{cases}$$

Under the overdense condition, we find:

$$\mathrm{V}_o^-(\mathbf{x}, 0) \equiv \mathrm{V}_r^-(\mathbf{x}, 0)\,, \qquad \mathrm{V}_x^-(\mathbf{x}, 0) \cup \mathrm{V}_o^+(\mathbf{x}, 0) \equiv \mathrm{V}_l(\mathbf{x}, 0)\,.$$

Under the underdense condition, we can further decompose $\mathrm{V}_x^-(\mathbf{x}, 0)$ into the disjoint union of $\mathrm{V}_x^{--}(\mathbf{x}, 0)$ and $\mathrm{V}_x^{-+}(\mathbf{x}, 0)$, with:

$$\mathrm{V}_x^{--}(\mathbf{x}, 0) := \{\tau_0^- < \tau < \kappa(\mathbf{x})\,;\ 0 \le r\,,\ r^2 = \tau^2 - \kappa(\mathbf{x})^2\,\tau\,(\tau + \mathbf{b}_e(\mathbf{x}))^{-1}\}\,,$$

$$\mathrm{V}_x^{-+}(\mathbf{x}, 0) := \{\kappa(\mathbf{x}) \le \tau < \mathbf{b}_e(\mathbf{x})\,;\ 0 \le r\,,\ r^2 = \tau^2 - \kappa(\mathbf{x})^2\,\tau\,(\tau - \mathbf{b}_e(\mathbf{x}))^{-1}\}\,.$$

Then, we can recover:

$$\mathrm{V}_o^-(\mathbf{x}, 0) \cup \mathrm{V}_x^{-+}(\mathbf{x}, 0) \equiv \mathrm{V}_r^-(\mathbf{x}, 0)\,, \qquad \mathrm{V}_x^{--}(\mathbf{x}, 0) \cup \mathrm{V}_o^+(\mathbf{x}, 0) \equiv \mathrm{V}_l(\mathbf{x}, 0)\,.$$

Finally, due to the disontinuity of the functions $g_\pm(\mathbf{x}, 0, \cdot)$, the case $\tau = \kappa$ has to be treated separetely. In fact, the corresponding study is exactly the same as in Paragraph 2.3.3.1*c)*. We recover the case of parallel longitudinal waves. These considerations together with Figures 12, 16 and 17 clarify the connections between the physical approach of Paragraph 2.3.3.1 and the mathematical presentation of the actual Paragraph 2.3.3.3.

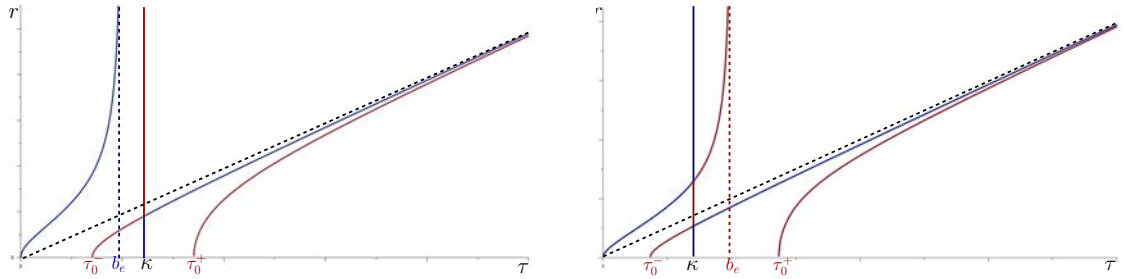

(a) Overdense case. (b) Underdense case.

FIGURE 16. Parallel propagation ($\varpi = 0$). Mixing of $\mathrm{V}_x(\mathbf{x}, 0)$ and $\mathrm{V}_o(\mathbf{x}, 0)$.

2.3.3.4. *Parallel and perpendicular propagation viewed as limited cases.* When $\varpi \in]0, \pi/2[$, the set $\mathrm{V}(\mathbf{x}, \varpi)$ has two resonances which are located at $\tau = \tau_\infty^-(\mathbf{x}, \varpi)$ and at $\tau = \tau_\infty^+(\mathbf{x}, \varpi)$. On the contrary, the two extreme cases $\varpi = 0$ and $\varpi = \pi/2$ are often presented as having only one resonance each. This would suggest a change in the type of representation. But this is illusive. Indeed, one of the two oblique resonances degenerates into a vertical half-line when ϖ goes to 0 or $\pi/2$. More precisely, the resonance $\tau_\infty^+(\mathbf{x}, \varpi)$ gives rise to the electrostatic plasma waves when $\varpi \to 0$, while $\tau_\infty^-(\mathbf{x}, \varpi)$ evolves into the vertical half-line $\{\tau = 0\}$ when $\varpi \to \pi/2$. This behaviour is illustrated on Figure 17.

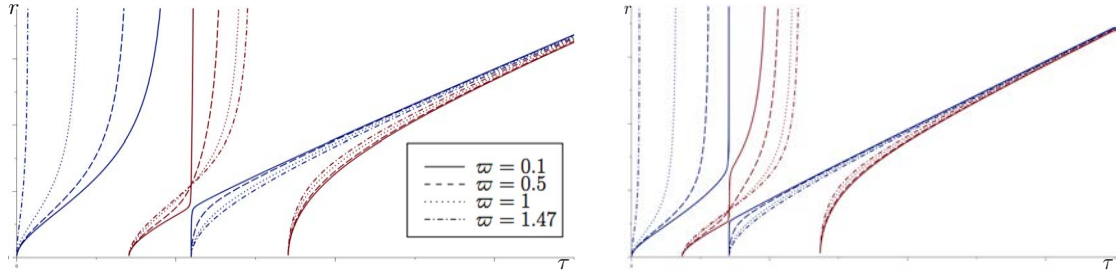

(a) Overdense case. (b) Underdense case.

FIGURE 17. Evolution of $\mathrm{V}_x(\mathbf{x}, \varpi)$ and $\mathrm{V}_o(\mathbf{x}, \varpi)$ in function of ϖ.
Asymptotic behaviour when $\varpi \to 0$ (see $\varpi = 0.1 \sim 0$) and $\varpi \to \pi/2$ (see $\varpi = 1.47 \sim \pi/2$).

2.3.4. **Other parametrizations of the characteristic variety.** Until now, to describe the set $\mathscr{V}$, we have looked at the direction $\xi \in \mathbb{R}^3$ (in fact at $|\xi| \in \mathbb{R}_+^*$ for a given $\varpi \in [0, \pi]$) as a function of the frequency $\tau \in \mathbb{R}_+^*$, with τ selected in convenient subdomains. The aim of this Section 2.3.4 is to investigate the other ways to proceed.

2.3.4.1. *The characteristic variety at a fixed value of ω.* The description of $\mathscr{V}_{\mathbf{x}}^*$ through the functions $g_\pm(\cdot)$ does not involve ω and the sign of τ. As observed in Paragraph 2.3.2.4, this means that $\mathscr{V}_{\mathbf{x}}^*$ is invariant under rotations with axis $\mathbb{R}\,^t(0, 0, 1)$ and angles $\omega \in [0, 2\,\pi[$. Since we can recover the case $\omega \neq 0$ from the case $\omega = 0$ by such rotations, it suffices to consider the case $\omega = 0$. To this end, as pointed in Remark 2.3.3, we can cut $\mathscr{V}_{\mathbf{x}}^*$ with a well-chosen quadrant of an hyperplane. Moreover, we can consider $\varpi \in [0, \pi]$ as a variable rather than as a parameter (like we did before in Paragraph 2.3.3.2). By doing so, we get a three dimensional representation of $\mathscr{V}_{\mathbf{x}}^*$, which could be materialized through:

$$\mathcal{V}_{\mathbf{x}}^* := \{(\varpi, \tau, r) \in [0, \pi] \times \mathbb{R}_+^2 \,;\, (\tau, S_p(r, 0, \varpi)) \in \mathscr{V}_{\mathbf{x}}^*\}\,.$$

In accordance with the classification of Paragraph 2.3.3.2 into the categories *a)* and *b)*, the set $\mathcal{V}_{\mathbf{x}}^*$ can be separated into connected parts:

$$\mathcal{V}_{\mathbf{x}}^* = \mathcal{V}_o^-(\mathbf{x}) \cup \mathcal{V}_o^+(\mathbf{x}) \cup \mathcal{V}_x^-(\mathbf{x}) \cup \mathcal{V}_x^+(\mathbf{x}) \subset [0, \pi] \times \mathbb{R}_+^2\,.$$

With $(\varpi, r) \in [0, \pi] \times \mathbb{R}_+$, these components are defined by:

$$\mathcal{V}_o^-(\mathbf{x}) := \{(\varpi, \tau, r)\,;\, 0 \leq \tau < \tau_\infty^-(\mathbf{x}, \varpi)\,,\, r^2 = g_+(\mathbf{x}, \varpi, \tau)\}\,, \tag{2.3.92a}$$

$$\mathcal{V}_o^+(\mathbf{x}) := \{(\varpi, \tau, r)\,;\, \kappa(\mathbf{x}) \leq \tau\,,\, r^2 = g_+(\mathbf{x}, \varpi, \tau)\}\,, \tag{2.3.92b}$$

$$\mathcal{V}_x^-(\mathbf{x}) := \{(\varpi, \tau, r)\,;\, \tau_0^-(\mathbf{x}) \leq \tau < \tau_\infty^+(\mathbf{x}, \varpi)\,,\, r^2 = g_-(\mathbf{x}, \varpi, \tau)\}\,, \tag{2.3.92c}$$

$$\mathcal{V}_x^+(\mathbf{x}) := \{(\varpi, \tau, r)\,;\, \tau_0^+(\mathbf{x}) \leq \tau\,,\, r^2 = g_-(\mathbf{x}, \varpi, \tau)\}\,. \tag{2.3.92d}$$

The sets $\mathcal{V}_o^{\pm}(\mathbf{x})$ and $\mathcal{V}_x^{\pm}(\mathbf{x})$ are drawn on Figure 18. We also include (in the plane $r = 0$) the graphs of the functions $\tau_\infty^{\pm}(\mathbf{x}, \cdot) : [0, \pi/2] \longrightarrow \mathbb{R}_+$.

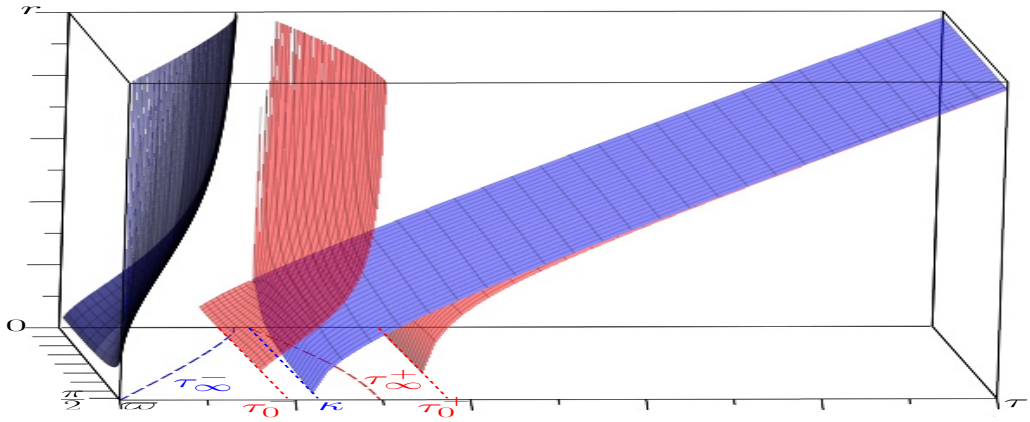

FIGURE 18. The characteristic variety in the variables (τ, ϖ, r).
From left to right: $\mathcal{V}_o^-(\mathbf{x})$, $\mathcal{V}_x^-(\mathbf{x})$, $\mathcal{V}_o^+(\mathbf{x})$ and $\mathcal{V}_x^+(\mathbf{x})$.

2.3.4.2. *The characteristic variety at a fixed value of τ.* Our purpose here is to give a detailed description of the following set:

$$\boldsymbol{\mathcal{V}}(\mathbf{x}, \tau) := \{\, \xi \in \mathbb{R}^3 \,;\, (\tau, \xi) \in \mathscr{V}_{\mathbf{x}}^* \,\}\,.$$

For a given $\xi \in \mathbb{R}^3$, we use the notation $\xi = S_{ph}(|\xi|, \omega_\xi, \varpi_\xi)$ which comes from the convention of Figure 11 to represent ξ. In connection with what has been done in Paragraph 2.3.3.2, the set $\boldsymbol{\mathcal{V}}(\mathbf{x}, \tau)$ can be decomposed into $\boldsymbol{\mathcal{V}}(\mathbf{x}, \tau) = \boldsymbol{\mathcal{V}}_o(\mathbf{x}, \tau) \cup \boldsymbol{\mathcal{V}}_x(\mathbf{x}, \tau)$ with:

$$\boldsymbol{\mathcal{V}}_o(\mathbf{x}, \tau) := \{\, \xi \in \mathbb{R}^3 \,;\, (\tau, |\xi|) \in \ \mathrm{V}_o(\mathbf{x}, \varpi_\xi)\}\,, \tag{2.3.93a}$$

$$\boldsymbol{\mathcal{V}}_x(\mathbf{x}, \tau) := \{\, \xi \in \mathbb{R}^3 \,;\, (\tau, |\xi|) \in \ \mathrm{V}_x(\mathbf{x}, \varpi_\xi)\}\,. \tag{2.3.93b}$$

The access to $\boldsymbol{\mathcal{V}}$ is achieved through the functions $g_\pm(\cdot)$. Now, given $(\mathbf{x}, \tau) \in \Omega \times \mathbb{R}_+$, the domain of definition, the sign, the regularity and the behaviour of $g_\pm(\mathbf{x}, \cdot, \tau) : [0, \pi/2] \longrightarrow \mathbb{R}$ depend strongly on the choice of τ. Recall that we have to deal with the additional condition $|\xi|^2 = g_\pm(\mathbf{x}, \varpi, \tau) \geq 0$. Thus, of particular interest are the intervals where $g_\pm(\mathbf{x}, \cdot, \tau)$ is non-negative. We can first deal with the case of $g_+(\cdot)$.

Lemma 2.3.14. *[study of the function $g_+(\mathbf{x}, \cdot, \tau)$] Two situations must be distinguished.*
i) Case $\tau \in \tau_\infty^-(\mathbf{x}, [0, \pi/2]) = [0, \min(\mathbf{b}_e(\mathbf{x}), \kappa(\mathbf{x}))]$. There exists a unique $\varpi_\infty^-(\mathbf{x}, \tau) \in [0, \pi/2]$ such that the function $g_+(\mathbf{x}, \cdot, \tau)$ is defined and continuous on the domain $[0, \pi/2] \setminus \{\varpi_\infty^-(\mathbf{x}, \tau)\}$. It is non-negative if and only if $\varpi \in [0, \varpi_\infty^-(\mathbf{x}, \tau)[$. Moreover, we have:

$$\lim_{\varpi \to (\varpi_\infty^-(\mathbf{x}, \tau))^-} g_+(\mathbf{x}, \varpi, \tau) = +\infty\,. \tag{2.3.94}$$

ii) Case $\tau \in \mathbb{R}_+ \setminus \tau_\infty^-(\mathbf{x}, [0, \pi/2]) =]\min(\mathbf{b}_e(\mathbf{x}), \kappa(\mathbf{x})), +\infty[$. The function $g_+(\mathbf{x}, \cdot, \tau)$ is defined and continuous on the whole interval $[0, \pi/2]$. It is non-negative if and only if $\tau \geq \kappa(\mathbf{x})$.

Proof. From the proof of Lemma 2.3.11, we know that $g_+(\mathbf{x},\cdot,\tau)$ is defined and continuous except if $\tau=\tau_\infty^-(\mathbf{x},\varpi)$. Given $\tau\in\mathbb{R}_+$, from Lemma 2.3.9, this can happen for some angle $\varpi_\infty^-(\mathbf{x},\tau)\in[0,\pi/2]$ if and only if we are in case *i)*. Now, assuming *i)*, we have:

$$\tau<\tau_\infty^-(\mathbf{x},\varpi)\le\tau_\infty^+(\mathbf{x},\varpi)\quad\Longleftrightarrow\quad\varpi\in\big[0,\varpi_\infty^-(\mathbf{x},\tau)\big[\,. \tag{2.3.95}$$

Then, coming back to the expression (2.3.43) and using the information (2.3.95), we can identify as in *i)* the interval where $g_+(\mathbf{x},\cdot,\tau)$ is non-negative, as well as the asymptotic behaviour (2.3.94). In fact, to get both *i)* and *ii)*, it suffices to look at Figure 14. □

Similarly, we can consider $g_-(\mathbf{x},\cdot,\tau)$.

Lemma 2.3.15. *[study of the function $g_-(\mathbf{x},\cdot,\tau)$] Two situations must be distinguished.*

i) Case $\tau\in\tau_\infty^+(\mathbf{x},[0,\pi/2])=\big[\max(\mathbf{b}_e(\mathbf{x}),\kappa(\mathbf{x})),\sqrt{\mathbf{b}_e(\mathbf{x})^2+\kappa(\mathbf{x})^2}\big]$. *There exists some (unique) angle $\varpi_\infty^+(\mathbf{x},\tau)\in[0,\pi/2]$ such that the function $g_-(\mathbf{x},\cdot,\tau)$ is defined and continuous on the domain $[0,\pi/2]\setminus\{\varpi_\infty^+(\mathbf{x},\tau)\}$. It is non-negative if and only if $\varpi\in\big[\varpi_\infty^+(\mathbf{x},\tau),\pi/2\big]$. Moreover, we have:*

$$\lim_{\varpi\to(\varpi_\infty^+(\mathbf{x},\tau))^+} g_-(\mathbf{x},\varpi,\tau)\;=\;+\infty\,. \tag{2.3.96}$$

ii) Case $\tau\in\mathbb{R}_+\setminus\tau_\infty^+(\mathbf{x},[0,\pi/2])$. *The function $g_-(\mathbf{x},\cdot,\tau)$ is defined and continuous on the whole interval $[0,\pi/2]$. It is non-negative if and only if we have either $\tau\in\big[\tau_0^+(\mathbf{x}),+\infty\big[$ or $\tau\in\big[\tau_0^-(\mathbf{x}),\max\big(\,\mathbf{b}_e(\mathbf{x})\,;\,\kappa(\mathbf{x})\,\big)\big]$.*

Proof. From the proof of Lemma 2.3.11, we know that $g_-(\mathbf{x},\cdot,\tau)$ is defined and continuous except if $\tau=\tau_\infty^+(\mathbf{x},\varpi)$. Given $\tau\in\mathbb{R}_+$, from Lemma 2.3.9, this can happen for some angle $\varpi_\infty^+(\mathbf{x},\tau)\in[0,\pi/2]$ if and only if we are in case *i)*. Now, assuming *i)*, we have:

$$\tau\in\big]\tau_\infty^+(\mathbf{x},\varpi),\sqrt{\mathbf{b}_e(\mathbf{x})^2+\kappa(\mathbf{x})^2}\big]\quad\Longleftrightarrow\quad\varpi\in\big[0,\varpi_\infty^+(\mathbf{x},\tau)\big[\,. \tag{2.3.97}$$

Then, using (2.3.43), (2.3.78a) and (2.3.97), we can deduce (2.3.96). To see where $g_-(\mathbf{x},\cdot,\tau)$ is non-negative, simply exploit Figure 13. □

The wave equation describes the propagation of electromagnetic waves in a *vacuum*. In its dimensionless version, it takes the form:

$$\partial_{\mathbf{tt}}^2E-\Delta_{\mathbf{xx}}E=0\,,\qquad\partial_{\mathbf{tt}}^2B-\Delta_{\mathbf{xx}}B=0\,.$$

The characteristic varieties associated with these two equations (on E and B) are the same. They are simply given by the light cone:

$$\mathscr{V}_l:=\big\{\,(\mathbf{t},\mathbf{x},\tau,\xi)\in T^*M\,;\;\tau^2-|\xi|^2=0\,\big\}\,. \tag{2.3.98}$$

Then, given $\tau\in\mathbb{R}_+^*$, we recover the *sphere* of radius τ:

$$\boldsymbol{\mathcal{V}}_l(\mathbf{x},\tau)\equiv\boldsymbol{\mathcal{V}}_l(\tau):=\big\{\,\xi\in\mathbb{R}^3\,;\;|\xi|=\tau\,\big\}\,. \tag{2.3.99}$$

Now, in the presence of an exterior magnetic field, the picture (2.3.99) is strongly affected. The first effect, already encoded within (2.3.93), is the well-known separation of $\boldsymbol{\mathcal{V}}$ into the two parts $\boldsymbol{\mathcal{V}}_o$ and $\boldsymbol{\mathcal{V}}_x$ corresponding to *ordinary* and *extraordinary* waves. The second impact is a disappearance of $\boldsymbol{\mathcal{V}}_o(\mathbf{x},\tau)$ and $\boldsymbol{\mathcal{V}}_x(\mathbf{x},\tau)$ when τ falls into the gap between resonance and cutoff frequencies, and their resurgence in the form of *cones* below resonance frequencies. With this in mind, we can highlight the following distinctions.

Definition 2.3.9. *[related to Figure 19] For* $(\mathbf{x},\tau) \in \Omega \times \big[0, \min\big(\mathbf{b}_e(\mathbf{x}), \kappa(\mathbf{x})\big)\big]$*, the set* $\boldsymbol{\mathcal{V}}_o(\mathbf{x},\tau)$ *is referred as an ordinary resonance cone.*

Proposition 2.3.1. *[* $\tau \in \big[0, \min\big(\mathbf{b}_e(\mathbf{x}), \kappa(\mathbf{x})\big)\big]$ *] The ordinary resonance cones* $\boldsymbol{\mathcal{V}}_o(\mathbf{x},\tau)$ *are comprised of exactly two unbounded connected components, say* $\boldsymbol{\mathcal{V}}_o^a(\mathbf{x},\tau)$ *and* $\boldsymbol{\mathcal{V}}_o^b(\mathbf{x},\tau)$*, which are respectively above and below the plane* $\{\xi; \xi^3 = 0\}$ *and given by:*

$$\boldsymbol{\mathcal{V}}_o^a(\mathbf{x},\tau) := \big\{\, \xi = S_{ph}(r,\omega_\xi,\varpi_\xi)\,;\ 0 \le r\,,\ -\pi \le \omega_\xi \le \pi\,, \\ 0 \le \varpi_\xi \le \varpi_\infty^-(\mathbf{x},\tau)\,,\ r^2 = g_+(\mathbf{x},\varpi,\tau) \,\big\}\,, \tag{2.3.100a}$$

$$\boldsymbol{\mathcal{V}}_o^b(\mathbf{x},\tau) := \big\{\, \xi = S_{ph}(r,\omega_\xi,\varpi_\xi)\,;\ 0 \le r\,,\ -\pi \le \omega_\xi \le \pi\,, \\ \pi - \varpi_\infty^-(\mathbf{x},\tau) \le \varpi_\xi \le \pi\,,\ r^2 = g_+(\mathbf{x},\varpi,\tau) \,\big\}\,. \tag{2.3.100b}$$

Proof. This statement is a direct consequence of Lemma 2.3.14, case *i)*. In particular, the asymptotic behaviour (2.3.94) implies that neither $\boldsymbol{\mathcal{V}}_o^a(\mathbf{x},\tau)$ nor $\boldsymbol{\mathcal{V}}_o^b(\mathbf{x},\tau)$ are bounded. On the contrary, for large values of r, these two sets become close to the two cones:

$$\mathcal{C}_o^a(\mathbf{x},\tau) := \big\{\, \xi\,;\ \varpi_\xi = \varpi_\infty^-(\mathbf{x},\tau) \,\big\}\,, \qquad \mathcal{C}_o^b(\mathbf{x},\tau) := \big\{\, \xi\,;\ \varpi_\xi = \pi - \varpi_\infty^-(\mathbf{x},\tau) \,\big\}\,. \qquad \square$$

The distortion from $\boldsymbol{\mathcal{V}}_l$ is here obvious. As long as τ remains sufficiently small, which means in practice that we deal with Very Low Frequency waves (at approximately 1 kHz), there is no similarity between $\boldsymbol{\mathcal{V}}_o(\mathbf{x},\tau)$ and $\boldsymbol{\mathcal{V}}_l(\tau)$. The same applies to $\boldsymbol{\mathcal{V}}_x(\mathbf{x},\tau)$.

Definition 2.3.10. *[related to Figure 20] For* $(\mathbf{x},\tau) \in \Omega \times \big[\max(\mathbf{b}_e,\kappa), \sqrt{\mathbf{b}_e^2 + \kappa^2}\,\big]$*, the set* $\boldsymbol{\mathcal{V}}_x(\mathbf{x},\tau)$ *is referred as an extraordinary resonance cone.*

Proposition 2.3.2. *[* $\tau \in \big[\max(\mathbf{b}_e,\kappa), \sqrt{\mathbf{b}_e^2 + \kappa^2}\,\big]$ *] The extraordinary resonance cones* $\boldsymbol{\mathcal{V}}_x(\mathbf{x},\tau)$ *are unbounded connected sets given by:*

$$\boldsymbol{\mathcal{V}}_x(\mathbf{x},\tau) := \big\{\ \xi = S_{ph}(r,\omega_\xi,\varpi_\xi)\,;\ 0 \le r\,,\ -\pi \le \omega_\xi \le \pi\,, \\ \varpi_\infty^+(\mathbf{x},\tau) \le \varpi_\xi \le \pi - \varpi_\infty^+(\mathbf{x},\tau)\,,\ r^2 = g_-(\mathbf{x},\varpi_\xi,\tau) \,\big\}\,, \tag{2.3.101}$$

Proof. This statement is a direct consequence of Lemma 2.3.15, case *i)*. In particular, the asymptotic behaviour (2.3.96) implies that the set $\boldsymbol{\mathcal{V}}_x(\mathbf{x},\tau)$ is not bounded. Indeed, for large values of r, it becomes close to the cone:

$$\mathcal{C}_x(\mathbf{x},\tau) := \big\{\, \xi\,;\ \varpi_\xi = \varpi_\infty^+(\mathbf{x},\tau) \,\big\} \cup \big\{\, \xi\,;\ \varpi_\xi = \pi - \varpi_\infty^+(\mathbf{x},\tau) \,\big\}\,. \qquad \square$$

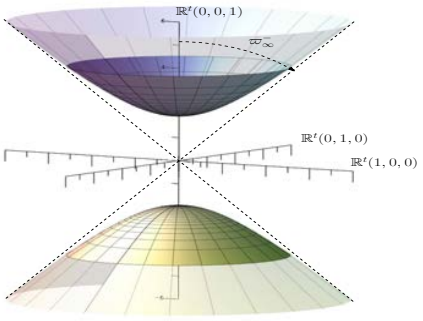

FIGURE 19. Ordinary resonance cone. $\boldsymbol{\mathcal{V}}_o(\mathbf{x},\tau)$ for $\tau \in [0, \min(\mathbf{b}_e(\mathbf{x}), \kappa(\mathbf{x}))]$.

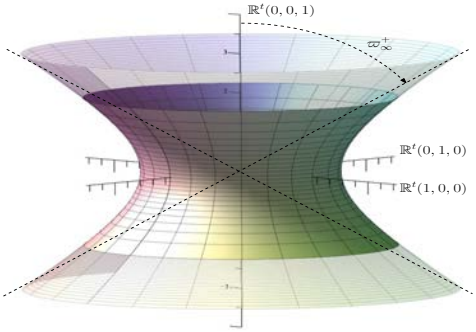

FIGURE 20. Extraordinary resonance cone. $\boldsymbol{\mathcal{V}}_x(\mathbf{x},\tau)$ for $\tau \in [\max(\mathbf{b}_e(\mathbf{x}), \kappa(\mathbf{x})), \sqrt{\mathbf{b}_e(\mathbf{x})^2 + \kappa(\mathbf{x})^2}]$.

Above their corresponding cutoff frequencies, the sets $\boldsymbol{\mathcal{V}}_o(\mathbf{x},\tau)$ and $\boldsymbol{\mathcal{V}}_x(\mathbf{x},\tau)$ are restored in the form of bounded sets which are homeomorphic to spheres.

Definition 2.3.11. *[related to Figure 36] For $(\mathbf{x},\tau)\in\Omega\times[\kappa(\mathbf{x}),+\infty[$, the set $\boldsymbol{\mathcal{V}}_o(\mathbf{x},\tau)$ is referred as an ordinary sphere.*

Proposition 2.3.3. *[$\tau\in[\kappa(\mathbf{x}),+\infty[$] The ordinary spheres $\boldsymbol{\mathcal{V}}_o(\mathbf{x},\tau)$ are bounded connected sets given by:*

$$\boldsymbol{\mathcal{V}}_o(\mathbf{x},\tau):=\{\,\xi=S_{ph}(r,\omega_\xi,\varpi_\xi)\,;\;0\leq r\,,\;-\pi\leq\omega_\xi\leq\pi\,,\;0\leq\varpi_\xi\leq\pi\,,\;r^2=g_+(\mathbf{x},\varpi_\xi,\tau)\,\}\,. \tag{2.3.102}$$

Proof. This statement is a direct consequence of Lemma 2.3.14, case *ii)*. □

Definition 2.3.12. *[related to Figure 22] For $(\mathbf{x},\tau)\in\Omega\times[\tau_0^+(\mathbf{x}),+\infty[$, the set $\boldsymbol{\mathcal{V}}_x(\mathbf{x},\tau)$ is referred as an extraordinary sphere.*

Proposition 2.3.4. *[$\tau\in[\tau_0^+(\mathbf{x}),+\infty[$] The extraordinary spheres $\boldsymbol{\mathcal{V}}_x(\mathbf{x},\tau)$ are bounded connected sets given by:*

$$\boldsymbol{\mathcal{V}}_x(\mathbf{x},\tau):=\{\,\xi=S_{ph}(r,\omega_\xi,\varpi_\xi)\,;\;0\leq r\,,\;-\pi\leq\omega_\xi\leq\pi\,,\;0\leq\varpi_\xi\leq\pi\,,\;r^2=g_-(\mathbf{x},\varpi_\xi,\tau)\,\}\,. \tag{2.3.103}$$

Proof. This statement is a direct consequence of Lemma 2.3.15, case *ii)*. □

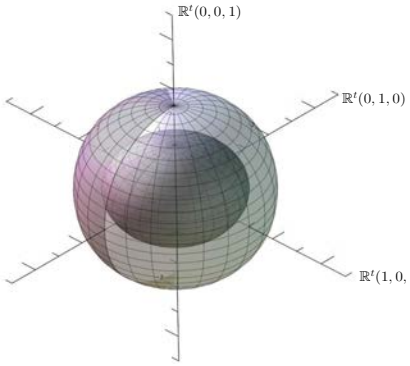

FIGURE 21. The extraordinary sphere nested into the ordinary sphere, for $\tau\gtrsim\tau_0^+(\mathbf{x})$.

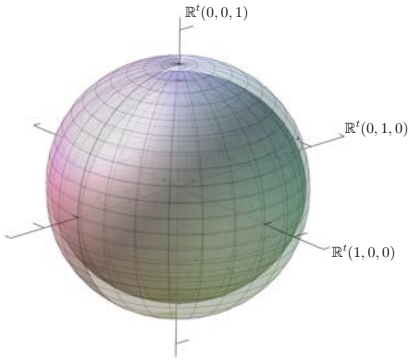

FIGURE 22. Asymptotic merge of the ordinary and extraordinary spheres, for $\tau\gg\tau_0^+(\mathbf{x})$.

The ordinary resonance cone can appear with an ordinary sphere if $\kappa(\mathbf{x})<\sqrt{2}\mathbf{b}_e(\mathbf{x})$ (see Lemma 2.3.10). An extraordinary resonance cone can occur with an ordinary sphere which, in this case, is located inside. For the sake of clarity such configurations are not made apparent in Figure 19 and 20). For $\tau>\tau_0^+(\mathbf{x})$, the extraordinary sphere and the ordinary sphere coexist (see Figures 36 and 22), the first being included in the second. At higher frequencies, that is concretely above 1 MHz, the distinction between $\boldsymbol{\mathcal{V}}_o(\mathbf{x},\tau)$ and $\boldsymbol{\mathcal{V}}_x(\mathbf{x},\tau)$ becomes almost invisible. For $\tau\gg\tau_0^+(\mathbf{x})$, these both sets just look like $\mathscr{V}_l$. Indeed, from (2.3.43)-(2.3.44), we can easily infer that:

$$\lim_{\tau\longrightarrow+\infty}\tau^{-2}\,g_\pm(\mathbf{x},\varpi,\tau)=1\,.$$

2.3.4.3. *The characteristic variety as a graph of functions depending on τ.* The purpose of this Paragraph 2.3.4.3 is to convert the condition $(\mathbf{t},\mathbf{x},\tau,\xi)\in\mathscr{V}$ by expressing τ as a function of ξ (in fact of r at fixed angle ϖ). From Definition 2.3.1, Lemma 2.3.5 and (2.3.60), recalling the convention (2.3.37), we can assert that:

$$(\mathbf{t},\mathbf{x},\tau,\xi)\in\mathscr{V}\iff(|\tau|,r)\in\mathrm{V}(\mathbf{x},\varpi)\cap\mathbb{R}_+^2\iff\chi_{\mathbf{x},\varpi}(|\tau|,r)=0\,. \tag{2.3.104}$$

As noted in the article [31], interpreted as a polynomial in the variable τ instead of $|\mathfrak{n}|$, the characteristic equation $\chi_{\mathbf{x},\varpi}(\tau,|\xi|)=0$ turns to be of fourth order in τ^2. More precisely, we have $\chi_{\mathbf{x},\varpi}(\tau,r)=P_{\mathbf{x},\varpi,r}(\tau^2)$ with:

$$\begin{aligned}P_{\mathbf{x},\varpi,r}(X):=\;&X^4-(\mathbf{b}_e^2+3\,\kappa^2+2\,r^2)\;X^3\\&+\big(r^4+2\,r^2\,(\mathbf{b}_e^2+2\,\kappa^2)+\mathbf{b}_e^2\,\kappa^2+3\,\kappa^4\big)\;X^2\\&-\big(r^4\,(\mathbf{b}_e^2+\kappa^2)+r^2\,(2\,\kappa^4+\mathbf{b}_e^2\,\kappa^2\,(1+\cos^2\varpi))+\kappa^6\big)\;X\\&+r^4\,\mathbf{b}_e^2\,\kappa^2\,\cos^2(\varpi)\,.\end{aligned} \tag{2.3.105}$$

Explicit algebraic expressions $\tau(\mathbf{x},|\xi|,\varpi)$ are of course available, but they are not so easy to implement. We will proceed differently. Another way to extract information is to study the properties of the function $g_\pm(\mathbf{x},\varpi,\cdot)$. We start by looking at the two extreme situations ($\varpi=0$ and $\varpi=\pi/2$). Then, we consider the oblique case $\varpi\in\,]0,\pi/2[$.

∘ 2.3.4.3.a) Parallel case ($\varpi=0$). To describe the set $\mathrm{V}(\mathbf{x},0)$ as a graph of functions depending on τ, we can come back to Paragraph 2.3.3.1. With the formulas inside (2.3.64), (2.3.66) and (2.3.67) in mind, we can define:

$$L(\mathbf{x},\tau):=\tau^2-\frac{\kappa(\mathbf{x})^2\,\tau}{\tau+\mathbf{b}_e(\mathbf{x})}\,,\qquad\forall\,(\mathbf{x},\tau)\in\Omega\times\mathbb{R}_+\,, \tag{2.3.106a}$$

$$R(\mathbf{x},\tau):=\tau^2-\frac{\kappa(\mathbf{x})^2\,\tau}{\tau-\mathbf{b}_e(\mathbf{x})}\,,\qquad\forall\,(\mathbf{x},\tau)\in\Omega\times\big(\mathbb{R}_+\setminus\{\mathbf{b}_e(\mathbf{x})\}\big)\,. \tag{2.3.106b}$$

Lemma 2.3.16. *Fix $\mathbf{x}\in\Omega$. The application $L(\mathbf{x},\cdot):[\tau_0^-(\mathbf{x}),+\infty[\longrightarrow\mathbb{R}_+$ as well as the two applications:*

$$R(\mathbf{x},\cdot):[0,\mathbf{b}_e(\mathbf{x})[\longrightarrow\mathbb{R}_+\,,\qquad R(\mathbf{x},\cdot):[\tau_0^+(\mathbf{x}),+\infty[\longrightarrow\mathbb{R}_+\,,$$

are $\mathcal{C}^\infty$-diffeomorphisms.

Proof. For L, remark that:

$$\partial_\tau L(\mathbf{x},\tau)=2\,\tau-\frac{\kappa^2\,\mathbf{b}_e}{(\tau+\mathbf{b}_e)^2}=\frac{2\,\tau\,(\tau^2+\mathbf{b}_e\,\tau)+2\,\mathbf{b}_e\,(\tau^2+\mathbf{b}_e\,\tau)-\kappa^2\,\mathbf{b}_e}{(\tau+\mathbf{b}_e)^2}\,. \tag{2.3.107}$$

From (2.3.63), we know that $\tau^2+\mathbf{b}_e\,\tau\geq\kappa^2$ if $\tau\geq\tau_0^-(\mathbf{x})$. Then, looking at the right-hand term of (2.3.107), we get the first result. Otherwise, just compute $\partial_\tau R(\mathbf{x},\tau)$. □

When $\varpi=0$, there is a mix between ordinary and extraordinary waves. This effect is enhanced under the underdense assumption, see Figure 23. It follows that the independent use of $L(\mathbf{x},\cdot)$ or $R(\mathbf{x},\cdot)$ is not suitable to get inversion formulas that are globally defined in ϖ. The reason is that the expressions $L(\mathbf{x},\cdot)$ or $R(\mathbf{x},\cdot)$ (taken separately) do not allow a continuous connection to $g_\pm(\mathbf{x},\cdot)$ when ϖ goes to 0. To remedy this, we have to blend

the functions $L(\mathbf{x},\cdot)$ and $R(\mathbf{x},\cdot)$ accordingly. This induces the technicalities reproduced below. We start with the overdense case (Definition 2.3.8) which is simpler. For ordinary waves below the resonance frequency, just take:

$$F^1_{+,ov}(\mathbf{x},r) := \big(\sqrt{R(\mathbf{x},\cdot)}\big|_{[0,\mathbf{b}_e(\mathbf{x})[}\big)^{-1}(r)\,, \tag{2.3.108}$$

to recover:

$$\mathrm{V}^-_o(\mathbf{x},0) = \{\,(\tau,r)\,;\,0\le r\,,\,\tau = F^1_{+,ov}(\mathbf{x},r)\,\}\,.$$

For extraordinary waves located below the resonance frequency, we have to follow the red curve in Figure 23-(a). This means introducing:

$$F^1_{-,ov}(\mathbf{x},r) := \begin{cases} \big(\sqrt{L(\mathbf{x},\cdot)}\big|_{[\tau_0^-(\mathbf{x}),\kappa(\mathbf{x})[}\big)^{-1}(r) & \text{if} \quad r\le\sqrt{L(\mathbf{x},\kappa(\mathbf{x}))}\,,\\ \kappa(\mathbf{x}) & \text{if} \quad r\ge\sqrt{L(\mathbf{x},\kappa(\mathbf{x}))}\,,\end{cases}$$

in order to obtain:

$$\mathrm{V}^-_x(\mathbf{x},0) = \{\,(\tau,r)\,;\,0\le r\,,\,\tau = F^1_{-,ov}(\mathbf{x},r)\,\}\,.$$

For ordinary waves above the cutoff frequency, we have to reconstruct the blue curve in Figure 23-(a). Just define:

$$F^2_{+,ov}(\mathbf{x},r) := \begin{cases} \kappa(\mathbf{x}) & \text{if} \quad r\le\sqrt{L(\mathbf{x},\kappa(\mathbf{x}))}\,,\\ \big(\sqrt{L(\mathbf{x},\cdot)}\big|_{[\kappa(\mathbf{x}),+\infty[}\big)^{-1}(r) & \text{if} \quad r\ge\sqrt{L(\mathbf{x},\kappa(\mathbf{x}))}\,,\end{cases}$$

that gives access to:

$$\mathrm{V}^+_o(\mathbf{x},0) = \{\,(\tau,r)\,;\,0\le r\,,\,\tau = F^2_{+,ov}(\mathbf{x},r)\,\}\,.$$

We now move to the underdense case. As already noted in Paragraph 2.3.3.3, the situation is more intricated when $\mathbf{b}_e(\mathbf{x}) > \kappa$. However, the logic is the same. We have to follow the coloured lines (blue and red) at the level of Figure 23-(b). Briefly define:

$$F^1_{+,un}(\mathbf{x},r) := \begin{cases} \big(\sqrt{R(\mathbf{x},\cdot)}\big|_{[0,\kappa(\mathbf{x})[}\big)^{-1}(r) & \text{if} \quad r\le\sqrt{R(\mathbf{x},\kappa(\mathbf{x}))}\,,\\ \kappa(\mathbf{x}) & \text{if} \quad r\ge\sqrt{R(\mathbf{x},\kappa(\mathbf{x}))}\,,\end{cases}$$

$$F^1_{-,un}(\mathbf{x},r) := \begin{cases} \big(\sqrt{L(\mathbf{x},\cdot)}\big|_{[\tau_0^-(\mathbf{x}),\kappa(\mathbf{x})[}\big)^{-1}(r) & \text{if} \quad r\le\sqrt{L(\mathbf{x},\kappa(\mathbf{x}))}\,,\\ \kappa(\mathbf{x}) & \text{if} \quad \sqrt{L(\mathbf{x},\kappa(\mathbf{x}))}\le r\le\sqrt{R(\mathbf{x},\kappa(\mathbf{x}))}\,,\\ \big(\sqrt{R(\mathbf{x},\cdot)}\big|_{[\kappa(\mathbf{x}),+\infty[}\big)^{-1}(r) & \text{if} \quad r\ge\sqrt{R(\mathbf{x},\kappa(\mathbf{x}))}\end{cases}$$

$$F^2_{+,un}(\mathbf{x},r) := \begin{cases} \kappa(\mathbf{x}) & \text{if} \quad r\le\sqrt{L(\mathbf{x},\kappa(\mathbf{x}))}\,,\\ \big(\sqrt{L(\mathbf{x},\cdot)}\big|_{[\kappa(\mathbf{x}),+\infty[}\big)^{-1}(r) & \text{if} \quad r\ge\sqrt{L(\mathbf{x},\kappa(\mathbf{x}))}\,.\end{cases}$$

The sets $\mathrm{V}^\pm_o(\mathbf{x},0)$ and $\mathrm{V}^-_x(\mathbf{x},0)$ are then given by:

$$\mathrm{V}^-_o(\mathbf{x},0) = \{\,(\tau,r)\,;\,0\le r\,,\,\tau = F^1_{+,un}(\mathbf{x},r)\,\}\,,$$
$$\mathrm{V}^-_x(\mathbf{x},0) = \{\,(\tau,r)\,;\,0\le r\,,\,\tau = F^1_{-,un}(\mathbf{x},r)\,\}\,,$$
$$\mathrm{V}^+_o(\mathbf{x},0) = \{\,(\tau,r)\,;\,0\le r\,,\,\tau = F^2_{+,un}(\mathbf{x},r)\,\}\,.$$

The situation of $\mathrm{V}^+_x(\mathbf{x},0)$ is simpler because $\mathrm{V}^+_x(\mathbf{x},0)$ just coincides with $\mathrm{V}^+_r(\mathbf{x},0)$. It suffices to define:

$$F^2_-(\mathbf{x},r) := \big(\sqrt{R(\mathbf{x},\cdot)}\big|_{[\tau_0^+(\mathbf{x}),+\infty[}\big)^{-1}(r)\,,$$

to recover $\mathrm{V}_x^+(\mathbf{x},0)$ through:

$$\mathrm{V}_x^+(\mathbf{x},0) = \{(\tau,r)\,;\,0\le r\,,\,\tau = F_-^2(\mathbf{x},r)\}\,.$$

The sets $\mathrm{V}_o^\pm(\mathbf{x},0)$ and $\mathrm{V}_x^\pm(\mathbf{x},0)$ are represented on Figure 23 below.

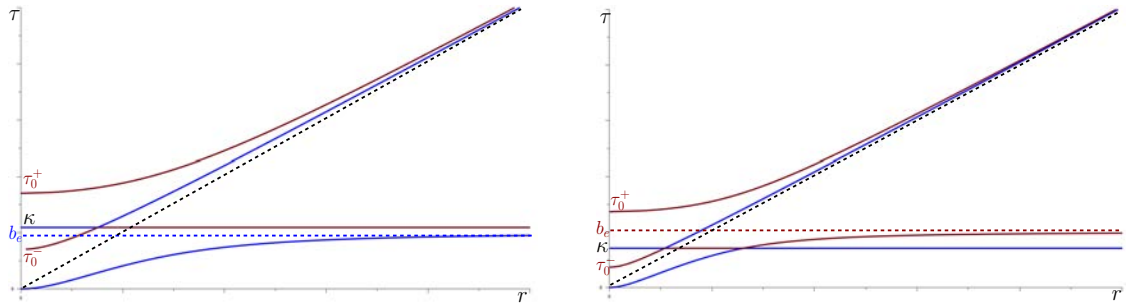

(a) Overdense case. (b) Underdense case.

FIGURE 23. Parallel propagation ($\varpi = 0$) with τ written as a function of r. Mixing of $\mathrm{V}_x(\mathbf{x},0)$ and $\mathrm{V}_o(\mathbf{x},0)$.

∘ 2.3.4.3.b) Perpendicular case ($\varpi = \pi/2$). We simply find:

$$g_+(\mathbf{x},\pi/2,\tau) = \tau^2 - \kappa(\mathbf{x})^2\,,\qquad g_-(\mathbf{x},\pi/2,\tau) = \frac{(\tau^2-\kappa(\mathbf{x})^2)^2 - \mathbf{b}_e(\mathbf{x})^2\,\tau^2}{\tau^2 - \mathbf{b}_e(\mathbf{x})^2 - \kappa(\mathbf{x})^2}\,.$$

Lemma 2.3.17. *Fix $\mathbf{x}\in\Omega$. The application $g_+(\mathbf{x},\pi/2,\cdot) : [\kappa(\mathbf{x}),+\infty[\longrightarrow \mathbb{R}_+$ as well as the two applications:*

$$g_-(\mathbf{x},\pi/2,\cdot) : [\tau_0^-(\mathbf{x}),\sqrt{\mathbf{b}_e(\mathbf{x})^2+\kappa(\mathbf{x})^2}[\ \longrightarrow \mathbb{R}_+\,,\quad g_-(\mathbf{x},\pi/2,\cdot) : [\tau_0^+(\mathbf{x}),+\infty[\longrightarrow \mathbb{R}_+\,.$$

are $\mathcal{C}^\infty$-diffeomorphisms.

Proof. This is obvious for $g_+(\mathbf{x},\pi/2,\cdot)$. For $\tau \neq \sqrt{\mathbf{b}_e(\mathbf{x})^2+\kappa^2}$, this follows from:

$$\partial_\tau g_-(\mathbf{x},\pi/2,\tau) \;=\; 2\,\tau\,\frac{(\tau^2-\mathbf{b}_e^2-\kappa^2)^2+\mathbf{b}_e^2\,\kappa^2}{(\tau^2-\mathbf{b}_e^2-\kappa^2)^2} > 0\,.$$ □

∘ 2.3.4.3.c) Oblique case ($\varpi\in]0,\pi/2[$). The analog of Lemmas 2.3.16 and 2.3.17 would be to show that $\partial_\tau g_\pm(\mathbf{x},\varpi,\cdot)$ has a specific sign. The corresponding calculation seems rather complicated. We use a weaker (more accessible) result, which is sufficient for our purpose.

Lemma 2.3.18. *Fix $\mathbf{x}\in\Omega$. Select any angle $\varpi\in]0,\pi/2[$. The four applications:*

$$g_+(\mathbf{x},\varpi,\cdot) : [0,\tau_\infty^-(\mathbf{x},\varpi)[\longrightarrow \mathbb{R}_+\,,\qquad g_+(\mathbf{x},\varpi,\cdot) : [\kappa(\mathbf{x}),+\infty[\longrightarrow \mathbb{R}_+\,,$$
$$g_-(\mathbf{x},\varpi,\cdot) : [\tau_0^-(\mathbf{x}),\tau_\infty^+(\mathbf{x},\varpi)[\longrightarrow \mathbb{R}_+\,,\qquad g_-(\mathbf{x},\varpi,\cdot) : [\tau_0^+(\mathbf{x}),+\infty[\longrightarrow \mathbb{R}_+\,,$$

are homeomorphisms.

Proof. Fix $r\in\mathbb{R}_+$. From (2.3.104) and (2.3.105), we can easily infer that:

$$\#\{\tau\in\mathbb{R}_+\,;\,(\tau,r)\in \mathrm{V}(\mathbf{x},\varpi)\}\le 4\,. \tag{2.3.109}$$

On the other hand, from Paragraph 2.3.3.2, we have (2.3.90). As recorded in Lemmas 2.3.11 and 2.3.12, the function $g_+(\mathbf{x},\varpi,\cdot)$ is continuous on $[0,\tau_\infty^-(\mathbf{x},\varpi)[$, and it satisfies:

$$g_+(\mathbf{x},\varpi,0)=0\,,\qquad \lim_{\tau\to(\tau_\infty^-)-} g_+(\mathbf{x},\varpi,\tau)=+\infty\,.$$

In this context, given $r\in\mathbb{R}_+$, the intermediate value theorem states that $r^2=g_+(\mathbf{x},\varpi,\tau)$ for some $\tau\in[0,\tau_\infty^-(\mathbf{x},\varpi)[$. In other words, we have $(\tau,r)\in \mathrm{V}_o^-(\mathbf{x},\varpi)$. Similarly, applying again Lemmas 2.3.11 and 2.3.12 but arguing this time with $g_-(\mathbf{x},\varpi,\cdot)$ and $g_+(\mathbf{x},\varpi,\cdot)$ on well-chosen intervals, we get:

$$\#\left\{\tau\in\mathbb{R}_+\,;\,(\tau,r)\in\mathrm{V}_*^\sigma(\mathbf{x},\varpi)\right\}\geq 1\,,\qquad \forall\,(*,\sigma)\in\{o,x\}\times\{\pm\}\,. \tag{2.3.110}$$

Combining (2.3.109) and (2.3.110), we can assert that:

$$\#\left\{\tau\in\mathbb{R}_+\,;\,(\tau,r)\in\mathrm{V}(\mathbf{x},\varpi)\right\}=4\,,\qquad \#\left\{\tau\in\mathbb{R}_+\,;\,(\tau,r)\in\mathrm{V}_*^\sigma(\mathbf{x},\varpi)\right\}=1\,. \tag{2.3.111}$$

This means that the function $g_+(\mathbf{x},\varpi,\cdot)$ is a bijection from $[0,\tau_\infty^-(\mathbf{x},\varpi)[$ to $[0,+\infty[$, and from $[\kappa,+\infty[$ to $[0,+\infty[$. This implies also that the function $g_-(\mathbf{x},\varpi,\cdot)$ is a bijection from the interval $[\tau_0^-(\mathbf{x}),\tau_\infty^+(\mathbf{x},\varpi)[$ to $[0,+\infty[$, and from $[\tau_0^+(\mathbf{x}),+\infty[$ to $[0,+\infty[$. Since both $g_+(\mathbf{x},\varpi,\cdot)$ and $g_-(\mathbf{x},\varpi,\cdot)$ are continuous and injective on their respective intervals of definition, the corresponding inverse functions are continuous. □

∘ 2.3.4.3.d) Synthesis of the results ($\varpi\in[0,\pi/2]$). By combining the results of the preceding paragraphs, a *global* description of the parts $\mathrm{V}_*^\sigma(\mathbf{x},\varpi)$ inside $\mathrm{V}(\mathbf{x},\varpi)$ becomes available. To this end, for all position $\mathbf{x}\in\Omega$, for all angle $\varpi\in[0,\pi]$, for all symbol $*\in\{ov,un\}$, and for all $r\in\mathbb{R}_+$, define:

$$f^1_{+,\star}(\mathbf{x},\varpi,r):=\begin{cases}\left(\sqrt{g_+(\mathbf{x},\varpi,\cdot)}\big|_{[0,\tau_\infty^-(\mathbf{x},\varpi)[}\right)^{-1}(r) & \text{if}\quad \varpi\in\,]0,\pi[\,,\\ F^1_{+,\star}(\mathbf{x},r) & \text{if}\quad \varpi=0(\pi)\,,\end{cases} \tag{2.3.112a}$$

$$f^2_{+,\star}(\mathbf{x},\varpi,r):=\begin{cases}\left(\sqrt{g_+(\mathbf{x},\varpi,\cdot)}\big|_{[\kappa(\mathbf{x}),+\infty[}\right)^{-1}(r) & \text{if}\quad \varpi\in\,]0,\pi[\,,\\ F^2_{+,\star}(\mathbf{x},r) & \text{if}\quad \varpi=0(\pi)\,,\end{cases} \tag{2.3.112b}$$

$$f^1_{-,\star}(\mathbf{x},\varpi,r):=\begin{cases}\left(\sqrt{g_-(\mathbf{x},\varpi,\cdot)}\big|_{[\tau_0^-(\mathbf{x}),\tau_\infty^+(\mathbf{x},\varpi)[}\right)^{-1}(r) & \text{if}\quad \varpi\in\,]0,\pi[\,,\\ F^1_{-,\star}(\mathbf{x},r) & \text{if}\quad \varpi=0(\pi)\,,\end{cases} \tag{2.3.112c}$$

$$f^2_{-}(\mathbf{x},\varpi,r):=\begin{cases}\left(\sqrt{g_-(\mathbf{x},\varpi,\cdot)}\big|_{[\tau_0^+(\mathbf{x}),+\infty[}\right)^{-1}(r) & \text{if}\quad \varpi\in\,]0,\pi[\,,\\ F^2_{-}(\mathbf{x},r) & \text{if}\quad \varpi=0(\pi)\,.\end{cases} \tag{2.3.112d}$$

Then, the components of the characteristic variety $\mathscr{V}$ can be viewed as the graphs of continuous functions on $\Omega\times[0,\pi]\times\mathbb{R}_+$. As a matter of fact, for all $(\mathbf{x},\varpi)\in\Omega\times[0,\pi]$, the sets $\mathrm{V}_o^\pm(\mathbf{x},\varpi)$ and $\mathrm{V}_x^\pm(\mathbf{x},\varpi)$ are given by:

$$\mathrm{V}_o^-(\mathbf{x},\varpi):=\left\{\,(\tau,r)\,;\,0\leq r\,,\,\tau=f^1_{+,\star}(\mathbf{x},\varpi,r)\,\right\}, \tag{2.3.113a}$$

$$\mathrm{V}_o^+(\mathbf{x},\varpi):=\left\{\,(\tau,r)\,;\,0\leq r\,,\,\tau=f^2_{+,\star}(\mathbf{x},\varpi,r)\,\right\}. \tag{2.3.113b}$$

$$\mathrm{V}_x^-(\mathbf{x},\varpi):=\left\{\,(\tau,r)\,;\,0\leq r\,,\,\tau=f^1_{-,\star}(\mathbf{x},\varpi,r)\,\right\}, \tag{2.3.113c}$$

$$\mathrm{V}_x^+(\mathbf{x},\varpi):=\left\{\,(\tau,r)\,;\,0\leq r\,,\,\tau=f^2_{-}(\mathbf{x},\varpi,r)\,\right\}. \tag{2.3.113d}$$

2.3.4.4. *The eikonal equation.* In Paragraph 2.3.1, we have approximated the RVM equations by using the WKB theory. The first outcome of this procedure is an eikonal equation which provides a simplified but pertinent representation of electromagnetic wave propagation in terms of geometric optics.

◦ 2.3.4.4.a) The concrete form of the eikonal equation. Paragraph 2.3.4.3 allows to formulate *globally in space* the Cauchy problem *in time* satisfied by ϕ. To produce the eikonal equation, introduce the angle $\varpi(\mathbf{x},\xi) \in [0,\pi]$ between the directions ξ and $\mathbf{B}_e(\mathbf{x})$. When ξ and $\mathbf{B}_e(\mathbf{x})$ are not parallel vectors, this angle is accessible through:

$$\varpi(\mathbf{x},\xi) := arccotan\left(\frac{\xi\cdot\mathbf{B}_e(\mathbf{x})/|\xi|\,\mathbf{b}_e(\mathbf{x})}{\sqrt{1-\left(\xi\cdot\mathbf{B}_e(\mathbf{x})/|\xi|\,\mathbf{b}_e(\mathbf{x})\right)^2}}\right), \qquad (\mathbf{x},\xi)\in\Omega\times\mathbb{R}^3\,. \tag{2.3.114}$$

When ξ and $\mathbf{B}_e(\mathbf{x})$ are parallel vectors, just adopt the conventions:

$$\varpi(\mathbf{x},\xi) := \left\{\begin{array}{lllll} \pi & \text{if} & \xi = s\,\mathbf{B}_e(\mathbf{x}) & \text{with} & s<0\,,\\ 0 & \text{if} & \xi = s\,\mathbf{B}_e(\mathbf{x}) & \text{with} & s>0 \end{array}\right., \qquad (\mathbf{x},\xi)\in\Omega\times\mathbb{R}^3\,. \tag{2.3.115}$$

For all $(\mathbf{x},\xi)\in\Omega\times\mathbb{R}^3$, we can also define:

$$\lambda^i_{+,*}(\mathbf{x},\xi) := -f^i_{+,*}\left(\mathbf{x},\varpi(\mathbf{x},\xi),|\xi|\right), \qquad (i,*)\in\{1,2\}\times\{ov,un\}\,, \tag{2.3.116a}$$

$$\lambda^1_{-,*}(\mathbf{x},\xi) := -f^1_{-,*}\left(\mathbf{x},\varpi(\mathbf{x},\xi),|\xi|\right), \qquad *\in\{ov,un\}\,, \tag{2.3.116b}$$

$$\lambda^2_{-}(\mathbf{x},\xi) := -f^2_{-}\left(\mathbf{x},\varpi(\mathbf{x},\xi),|\xi|\right). \tag{2.3.116c}$$

Lemma 2.3.19. *Let $\phi\in\mathcal{C}^\infty(M;\mathbb{R})$ be a function subjected to (2.3.57) with $l=1$. The choice of the value $l=1$ is to simplify the presentation. Then, the condition:*

$$\left(\varpi(\mathbf{x},\nabla_{\mathbf{x}}\phi(\mathbf{t},\mathbf{x})),\,\partial_{\mathbf{t}}\phi(\mathbf{t},\mathbf{x}),\,|\nabla_{\mathbf{x}}\phi(\mathbf{t},\mathbf{x})|\right)\in\mathcal{V}^\dagger_\ell(\mathbf{x}), \qquad (\dagger,\ell)\in\{+,-\}\times\{o,x\}$$

amounts to the same thing as:

$$\partial_{\mathbf{t}}\phi(\mathbf{t},\mathbf{x}) + \lambda^i_{\pm,*}(\mathbf{x},\nabla_{\mathbf{x}}\phi(\mathbf{t},\mathbf{x})) = 0\,, \qquad (i,*)\in\{1,2\}\times\{ov,un\} \tag{2.3.117}$$

with the following correspondences:

$$(\dagger,\ell)=(-,o)\implies(i,\pm)=(1,+)\,, \qquad (\dagger,\ell)=(+,o)\implies(i,\pm)=(2,+)\,,$$
$$(\dagger,\ell)=(-,x)\implies(i,\pm)=(1,-)\,, \qquad (\dagger,\ell)=(+,x)\implies(i,\pm)=(2,-)\,,$$

and $*$ is given by ov (resp. un) if $\mathbf{b}_e(\mathbf{x})<\kappa(\mathbf{x})$ (resp. $\mathbf{b}_e(\mathbf{x})>\kappa(\mathbf{x})$).

Proof. This follows directly from (2.3.113). □

Lemma 2.3.18, together with the definitions (2.3.113) and (2.3.116), only yields the continuity of the functions $\lambda^i_{\pm,*}(\cdot)$. This is not enough to ensure the existence and the uniqueness of smooth ($\mathcal{C}^1$) solutions to the Hamilton-Jacobi equation (2.3.117). However, when dealing in the overdense case with the so-called whistler dispersion relation $\lambda^1_{+,ov}(\cdot)$, the local in time ($\mathcal{C}^1$) well-posedness of the Cauchy problem (2.3.117)-(2.3.121) can be obtained by selecting large values of $|\nabla_{\mathbf{x}}\phi(\mathbf{t},\mathbf{x})|$.

Lemma 2.3.20. *For all relatively compact open set $O\subset\Omega$, there exists a constant C such that $\lambda^1_{+,ov}(\cdot)$ is of class $\mathcal{C}^1$ on $O\times B(0,C)^c$.*

Proof. The expression $\lambda^1_{+,ov}(\cdot)$ can be accessed via (2.3.116a) and (2.3.112a). Thus, the aim is to study the regularity of the functions $g_+(\cdot)$ and $F^1_{+,ov}(\cdot)$. The first difficulty is to examine what happens when $\varpi = 0$ and $\varpi = \pi$.

On the one hand, the function $\varpi(\cdot)$ of (2.3.114) is not differentiable when ξ and $\mathbf{B}_e(\mathbf{x})$ have parallel directions. Note however that this singularity is artificial. Indeed, the definition of $g_+(\cdot)$ only involves terms in $\sin^2\varpi(\cdot)$ and $\cos^2\varpi(\cdot)$ which both are of class $\mathcal{C}^1$. On the other hand, the two extreme situations $\varpi = 0$ (i.e. study of $F^1_{+,ov}$) and $\varpi = \pi/2$ have already been treated in Lemmas 2.3.16 and 2.3.17. It follows that the discussion may be limited to the case $\varpi \in]\delta, \pi - \delta[$ with $\delta \in \mathbb{R}^*_+$ small enough. From now on, the matter is to show that, for some well chosen $\delta > 0$, we have:

$$\forall\, (\varpi,\tau) \in]\delta, \pi-\delta[\times]\tau^-_\infty(\mathbf{x},\varpi) - \delta, \tau^-_\infty(\mathbf{x},\varpi)[\,, \qquad \partial_\tau g_+(\mathbf{x},\varpi,\tau) > 0\,. \tag{2.3.118}$$

For $\varpi \in]0,\pi/2[$ and $\tau < \tau^-_\infty(\mathbf{x},\varpi)$, we can compute:

$$\partial_\tau g_+(\mathbf{x},\varpi,\tau) \,=\, \frac{1}{(\tau^2-(\tau^+_\infty)^2)(\tau^2-(\tau^-_\infty)^2)}\left(P(\varpi,\tau) - \frac{Q(\varpi,\tau)}{(\tau^2-(\tau^+_\infty)^2)} - \frac{Q(\varpi,\tau)}{(\tau^2-(\tau^-_\infty)^2)}\right),$$

where:

$$P(\mathbf{x},\varpi,\tau) := 2\,\tau\,\mathcal{P}(\mathbf{x},\varpi,\tau) + \tau^2\,\partial_\tau\mathcal{P}(\mathbf{x},\varpi,\tau) + \frac{\mathbf{b}_e\,\kappa^2\,\partial_\tau\mathcal{Q}(\mathbf{x},\varpi,\tau)}{2\,\sqrt{\mathcal{Q}(\mathbf{x},\varpi,\tau)}}\,, \tag{2.3.119a}$$

$$Q(\mathbf{x},\varpi,\tau) := 2\,\tau^3\left[\mathcal{P}(\mathbf{x},\varpi,\tau) + \mathbf{b}_e\,\kappa^2\,\sqrt{\tau^{-4}\,\mathcal{Q}(\mathbf{x},\varpi,\tau)}\right]. \tag{2.3.119b}$$

Combining (2.3.77) and (2.3.78), we easily get that:

$$Q\big(\mathbf{x},\varpi,\tau^-_\infty(\mathbf{x},\varpi)\big) := 4\,\tau^-_\infty(\mathbf{x},\varpi)^3\;\mathcal{P}\big(\mathbf{x},\varpi,\tau^-_\infty(\mathbf{x},\varpi)\big) > 0\,. \tag{2.3.120}$$

It follows that:

$$\lim_{\tau\,\to\,\tau^-_\infty(\mathbf{x},\varpi)^-} \partial_\tau g_+(\mathbf{x},\varpi,\tau) = +\infty\,.$$

This is sufficient to deduce (2.3.118). □

∘ 2.3.4.4.b) Deviation from parallel propagation. In the constant coefficient case, if $\xi\wedge\mathbf{B}_e = 0$ at time $t = 0$, this remains true along the characteristics at all times $t \in \mathbb{R}^*_+$. Now, in the presence of spatial inhomogeneities, parallel propagation would mean that the well prepared rays of geometrical optics, i.e. the rays associated to (2.3.117) and started from positions $(\mathbf{x},\xi) \in T^*M$ such that $\xi \wedge \mathbf{B}_e(\mathbf{x}) = 0$, would follow the field lines. The aim of this Paragraph is precisely to dismiss this possibility.

To simplify, we focus on the whistler dispersion relation $\lambda^1_{+,ov}(\cdot)$. Recall that κ is given by $\kappa(\mathbf{x}) := \mathbf{n}^{\mathrm{d}}(\mathbf{x})^{1/2}\,\mu$. To detect only the effects of the variations of $\mathbf{B}_e(\cdot)$, we assume that κ does not depend on $\mathbf{x}$. This amounts to suppose that there are no variations in density. Let $O \Subset \Omega$. With C as in Lemma 2.3.20, consider a function $\phi_0 \in \mathcal{C}^\infty(O;\mathbb{R})$ satisfying:

$$\forall\,\mathbf{x}\in O\,, \qquad \varpi\big(\mathbf{x},\nabla_{\mathbf{x}}\phi_0(\mathbf{x})\big) = 0\,, \qquad C < |\nabla_{\mathbf{x}}\phi_0(\mathbf{x})|\,.$$

Complete the Hamilton-Jacobi equation (2.3.117) with the initial data:

$$\forall\,\mathbf{x}\in O\,, \qquad \phi(0,\mathbf{x}) = \phi_0(\mathbf{x})\,. \tag{2.3.121}$$

The smoothness of $\lambda^1_{+,ov}(\cdot)$ guarantees the local in time well-posedness of the Cauchy problem (2.3.117)-(2.3.121), see [11]. Thus, restricting a little the size of O if necessary, we can find $T \in]0,1]$ small enough and a unique function ϕ of class $\mathcal{C}^1$ satisfying:

(2.3.122)
$$\forall\, (\mathbf{t},\mathbf{x}) \in [0,T]\times O\,, \quad \partial_{\mathbf{t}}\phi(\mathbf{t},\mathbf{x}) + \lambda^1_{+,ov}\big(\mathbf{x}, \nabla_{\mathbf{x}}\phi(\mathbf{t},\mathbf{x})\big) = 0\,, \quad \phi(0,\mathbf{x}) = \phi_0(\mathbf{x})\,.$$

To show that purely parallel propagation does not occur for whistler waves, it suffices to exhibit some $(\mathbf{t},\mathbf{x}) \in [0,T]\times O$ such that $\varpi\big(\mathbf{x}, \nabla_{\mathbf{x}}\phi(\mathbf{t},\mathbf{x})\big) > 0$. To this end, it is more convenient to work in the straightened coordinates of [7]. With the notations from Discussion 2.2.1 in mind, introduce the diffeomorphism $\mathrm{Y}_e : \Omega \longrightarrow \mathrm{Y}_e(\Omega)$ which is defined through the curvilinear coordinates:

$$\mathrm{Y}^1_e := z\,(\rho^2+z^2)^{-3/2} \in \mathbb{R}\,, \qquad \mathrm{Y}^2_e := -\,\rho^4\,(\rho^2+z^2)^{-3} \in \mathbb{R}^*_-\,, \qquad \mathrm{Y}^3_e := \phi \in \mathbb{R}\,.$$

This gives rise to a triply orthogonal system $(\nabla_{\mathbf{x}}\mathrm{Y}^j_e)_{1\leq j\leq 3}$ satisfying $\nabla_{\mathbf{x}}\mathrm{Y}^1_e = \mathbf{B}_e$. Adopt the conventions:

$$d^j_e := |\nabla_{\mathbf{x}}\mathrm{Y}^j_e \circ \mathrm{Y}_e^{-1}|\,, \qquad \forall\, j \in \{1,2,3\}\,. \tag{2.3.123}$$

In particular, we have $d^1_e \equiv \mathbf{b}_e \circ \mathrm{Y}_e^{-1}$. From now on, we will note $\mathbf{y}$ the current variable in the domain $\mathrm{Y}_e(\Omega)$. With these conventions, the coordinates $\mathbf{y}^1$, $\mathbf{y}^2$ and $\mathbf{y}^3$ can be interpreted respectively as a sort of latitude, (negative) altitude and longitude. Define:

$$\boldsymbol{\phi}(\mathbf{t},\mathbf{y}) := \phi(\mathbf{t}, \mathrm{Y}_e^{-1}(\mathbf{y}))\,, \qquad \boldsymbol{\phi}_0(\mathbf{y}) := \phi_0(\mathrm{Y}_e^{-1}(\mathbf{y}))\,.$$

The new expression $\boldsymbol{\phi}$ is subjected to:

$$\partial_{\mathbf{t}}\boldsymbol{\phi}(\mathbf{t},\mathbf{y}) + \Lambda^1_{+,ov}\big(\mathbf{y}, \nabla_{\mathbf{y}}\boldsymbol{\phi}(\mathbf{t},\mathbf{y})\big) = 0\,, \qquad \boldsymbol{\phi}(0,\mathbf{y}) = \boldsymbol{\phi}_0(\mathbf{y})\,, \tag{2.3.124}$$

where, for $\xi = {}^t(\xi^1,\xi^2,\xi^3) \in \mathbb{R}^3$, we have introduced:

$$\Lambda^1_{+,ov}(\mathbf{y},\xi) := -f^1_{+,ov}(\mathrm{Y}_e^{-1}(\mathbf{y}), \varpi(\mathbf{y},\xi), N(\mathbf{y},\xi))\,, \tag{2.3.125}$$

with:

$$N(\mathbf{y},\xi) := \sqrt{\sum_{1\leq j\leq 3} (\xi^j)^2\; d^j_e(\mathbf{y})^2}\,, \tag{2.3.126a}$$

$$\varpi(\mathbf{y},\xi) := \mathrm{arccotan}\left(\frac{d^1_e\;\xi^1}{\sqrt{(d^2_e)^2\,(\xi^2)^2 + (d^3_e)^2\,(\xi^3)^2}}\right)\,. \tag{2.3.126b}$$

Lemma 2.3.21. *[characterization of purely parallel propagation] The following assertions are equivalent:*
(i) For all $(\mathbf{t},\mathbf{x}) \in [0,T]\times O$, we have $\varpi\big(\mathbf{x}, \nabla_{\mathbf{x}}\phi(\mathbf{t},\mathbf{x})\big) = 0$.
(ii) For all $(\mathbf{t},\mathbf{y}) \in [0,T]\times \mathrm{Y}_e(O)$, we have $\partial_{\mathbf{y}^2}\boldsymbol{\phi}(\mathbf{t},\mathbf{y}) = \partial_{\mathbf{y}^3}\boldsymbol{\phi}(\mathbf{t},\mathbf{y}) = 0$.

Proof. With $\mathbf{x} = \mathrm{Y}_e^{-1}(\mathbf{y})$, the condition $\varpi\big(\mathbf{x}, \nabla_{\mathbf{x}}\phi(\mathbf{t},\mathbf{x})\big) = 0$ is equivalent to:

$$0 = \mathbf{B}_e(\mathbf{x}) \wedge \nabla_{\mathbf{x}}\phi(\mathbf{t},\mathbf{x}) = \partial_{\mathbf{y}^2}\boldsymbol{\phi}(\mathbf{t},\mathbf{y})\; \mathbf{B}_e(\mathbf{x}) \wedge \nabla_{\mathbf{x}}\mathrm{Y}^2_e(\mathbf{x}) + \partial_{\mathbf{y}^3}\boldsymbol{\phi}(\mathbf{t},\mathbf{y})\; \mathbf{B}_e(\mathbf{x}) \wedge \nabla_{\mathbf{x}}\mathrm{Y}^3_e(\mathbf{x})\,.$$

Since the three vectors $\mathbf{B}_e(\mathbf{x})$, $\nabla_{\mathbf{x}}\mathrm{Y}^2_e(\mathbf{x})$ and $\nabla_{\mathbf{x}}\mathrm{Y}^3_e(\mathbf{x})$ are orthogonal two by two, this can be achieved if and only if $\partial_{\mathbf{y}^2}\boldsymbol{\phi}(\mathbf{t},\mathbf{y}) = \partial_{\mathbf{y}^3}\boldsymbol{\phi}(\mathbf{t},\mathbf{y}) = 0$. □

We are now able to prove that purely paralel propagation does not exist:

Theorem 2. *Assume that κ is constant on Ω. Then, there exists some $(\mathbf{t},\mathbf{x}) \in [0,T]\times O$ such that $\varpi(\mathbf{x},\nabla_{\mathbf{x}}\phi(\mathbf{t},\mathbf{x})) > 0$.*

Proof. The function $\Lambda^1_{+,ov}(\cdot)$ introduced at the level of (2.3.124) cannot depend on $\mathbf{y}^3$ since we have $\partial_{\mathbf{y}^3} d^j \equiv 0$ for all $j \in \{1,2,3\}$ (see [7], Lemma 2.1). As a consequence, we have:

$$\forall\,(\mathbf{t},\mathbf{y}) \in [0,T]\times \mathrm{Y}_e(O)\,, \qquad \partial_{\mathbf{y}^3}\phi(\mathbf{t},\mathbf{y}) = 0\,.$$

Taking into account Lemma 2.3.21, the matter is to obtain $\partial_{\mathbf{y}^2}\phi(\mathbf{t},\mathbf{y}) \neq 0$ for some $(\mathbf{t},\mathbf{y})$. By contradiction, let us assume that we have $\partial_{\mathbf{y}^2}\phi(\cdot) \equiv 0$. Then, the equation (2.3.124) reduces to:

$$\partial_{\mathbf{t}}\phi(\mathbf{t},\mathbf{y}) + f^1_{+,ov}(\mathrm{Y}_e^{-1}(\mathbf{y}), 0, d^1_e(\mathbf{y})\,|\partial_{\mathbf{y}^1}\phi(\mathbf{t},\mathbf{y})|) = 0\,. \tag{2.3.127}$$

Moreover, looking at the derivative of (2.3.124) with respect to $\mathbf{y}^2$, we get:

$$\forall\,(\mathbf{t},\mathbf{y}) \in [0,T]\times \mathrm{Y}_e(O)\,, \qquad \partial_{\mathbf{y}^2}\Lambda^1_{+,ov}(\mathbf{y}, {}^t(\partial_{\mathbf{y}^1}\phi(\mathbf{t},\mathbf{y}),0,0)) = 0\,. \tag{2.3.128}$$

From (2.3.125), we can deduce:

$$\partial_{\mathbf{y}^2}\Lambda^1_{+,ov} = \nabla_{\mathbf{x}} f^1_{+,ov}\cdot\partial_{\mathbf{y}^2}\mathrm{Y}_e^{-1} + \partial_{\varpi} f^1_{+,ov}\times\partial_{\mathbf{y}^2}\boldsymbol{\varpi} + \partial_r f^1_{+,ov}\times\partial_{\mathbf{y}^2} N\,.$$

On the one hand, we have the relations:

$$\nabla_{\mathbf{x}} f^1_{+,ov} = -\frac{\nabla_{\mathbf{x}}\sqrt{g_+}}{\partial_\tau\sqrt{g_+}}\,, \qquad \partial_{\varpi} f^1_{+,ov} = -\frac{\partial_{\varpi}\sqrt{g_+}}{\partial_\tau\sqrt{g_+}}\,, \qquad \partial_r f^1_{+,ov} = \frac{1}{\partial_\tau\sqrt{g_+}}\,.$$

On the other hand, the dependence of $g_+(\cdot)$ on $\mathbf{x}$ and ϖ is achieved through $b_e(\mathbf{x})$ and $\cos^2\varpi$. It follows that:

$$\nabla_{\mathbf{x}}\sqrt{g_+}\cdot\partial_{\mathbf{y}^2}\mathrm{Y}_e^{-1}(\mathbf{y}) = \partial_{b_e}\sqrt{g_+}\times\partial_{\mathbf{y}^2} d^1_e\,, \qquad \partial_{\varpi}\sqrt{g_+}\times\partial_{\mathbf{y}^2}\boldsymbol{\varpi} = \partial_{\cos^2\varpi}\sqrt{g_+}\times\partial_{\mathbf{y}^2}\cos^2\boldsymbol{\varpi}\,.$$

Remark also that $\boldsymbol{\varpi}(\mathbf{y},\xi^1,0,0) = 0(\pi)$ so that $\sin\boldsymbol{\varpi}(\mathbf{y},\xi^1,0,0) = 0$. By combining the preceding information, we can assert that:

$$(\partial_{\mathbf{y}^2}\Lambda^1_{+,ov})(\mathbf{y}, {}^t(\xi^1,0,0)) = \frac{\partial_{\mathbf{y}^2} d^1_e(\mathbf{y})}{\partial_\tau\sqrt{g_+}}\left(|\xi^1| - \partial_{\mathbf{b}_e}\sqrt{g_+}\right)\,, \tag{2.3.129}$$

where $\partial_{\mathbf{b}_e}\sqrt{g_+}$ and $\partial_\tau\sqrt{g_+}$ are evaluated at the position:

$$(\mathbf{x},\varpi,\tau) = (\,\mathrm{Y}_e^{-1}(\mathbf{y})\,,\,0\,,\,f^1_{+,ov}(\mathrm{Y}_e^{-1}(\mathbf{y}),0,|\xi^1 d^1_e|)\,)\,.$$

Knowing that $\partial_{\mathbf{y}^2} d^1_e < 0$ - see [7], Lemma 2.1 - and that $\sqrt{g_+} \equiv F^1_{+,ov} \equiv \sqrt{R}$ when $\varpi = 0$ - see (2.3.108) and (2.3.112a)-, the condition (2.3.128) amounts to the same thing as:

$$\forall\,(\mathbf{t},\mathbf{y})\,, \qquad |\partial_{\mathbf{y}^1}\phi(\mathbf{t},\mathbf{y})| - \partial_{\mathbf{b}_e}\sqrt{R}(\mathrm{Y}_e^{-1}(\mathbf{y}),\partial_{\mathbf{t}}\phi(\mathbf{t},\mathbf{y})) = 0\,. \tag{2.3.130}$$

Another way to express (2.3.127) is to write:

$$|\partial_{\mathbf{y}^1}\phi(\mathbf{t},\mathbf{y})| = d^1_e(\mathbf{y})^{-1}\ \sqrt{R}(\mathrm{Y}_e^{-1}(\mathbf{y}),\partial_{\mathbf{t}}\phi(\mathbf{t},\mathbf{y}))\,.$$

With (2.3.106b), the left hand side of (2.3.130) is therefore:

$$\frac{1}{d^1_e}\ \sqrt{R}(\mathrm{Y}_e^{-1}(\mathbf{y}),\tau) + \frac{\kappa^2\,\tau}{2\,(\tau-b_e)^2\,\sqrt{R}(\mathrm{Y}_e^{-1}(\mathbf{y}),\tau)}\,, \qquad \tau := \partial_{\mathbf{t}}\phi(\mathbf{t},\mathbf{y})\,. \tag{2.3.131}$$

Since $\tau > 0$, this expression cannot be zero as required at the level of (2.3.130). This is the expected contradiction. □

2.3.4.5. *Physical interpretations.* Chorus emissions are the most common and most intense electromagnetic plasma waves that are observed in the radiation belts of the Earth. They must be related to radio science phenomena. They have long stimulated both experimental and theoretical research [20, 21, 39], see especially the fairly old review [35]. During the last years [3, 32, 41], with the advent of satellite-based investigation systems, they have received renewed interest. Today, they are studied even more intensively, especially because of their role as a viable mechanism for accelerating electrons [27, 38].

There is a general agreement that the mechanisms underlying the generation of very low frequency waves does rely on the cyclotron resonance interactions between the waves and the particles. The current discussions rather relate to the modalities of these interactions. In the recent contribution [7], the origin of the monochromatic elements forming the fine structure of chorus (see Figure 24) is mathematically interpreted as a mesoscopic caustic effect.

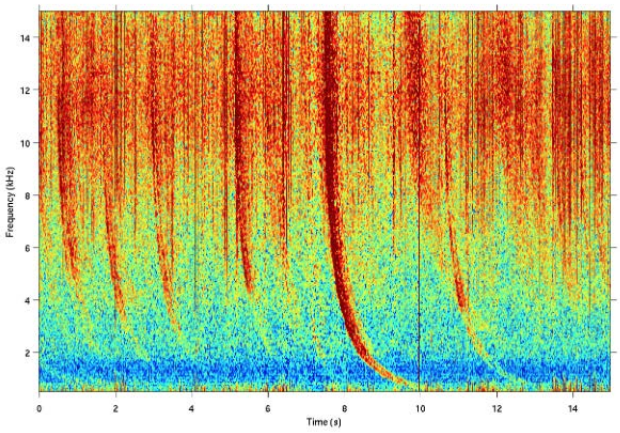

FIGURE 24. Spectrogram of chorus emission.

As a matter of fact, the deviation from parallel propagation which has been fully justified in Paragraph 2.3.4.4 comes to reinforce this principle. Indeed, this confirms that the waves (unlike the particles) do not travel along the field lines. Thus, instead of coming from the propagation along the field lines of some original wave packet, most electromagnetic signals would be the result of the procedure of creation of light detailed in [7]. The analysis of [7] was based on the classical whistler dispersion relation, as found in [12, 30, 37]. Below, by combining the refined model exhibited in Theorem 1 with the information from [7], we can get a better understanding of what happens.

According to [7], the wave packets are emitted inside the characteristic variety $\mathscr{V}$, all along the resonance cones (drawn at the level of Figures 19 and 20). Moreover, a signal which is generated at the time $\mathbf{t}$ from the position $(\mathbf{t}, \mathbf{x}, \tau, \xi) \in \mathscr{V}$ starts to travel at the velocity $|\nabla_\xi \lambda^i_{-,\star}(\mathbf{x}, \xi)|$. In view of the dispersion relations, the size of $|\nabla_\xi \lambda^i_{-,\star}(\mathbf{x}, \xi)|$ may be significant when ξ is located away from the resonance frequencies $\tau^\pm_\infty(\mathbf{x}, \varpi)$ with ϖ given by (2.3.38). Then, as described in Theorem 2 of [7], the electromagnetic signals should appear again and again over consecutive periods of almost equal length. They are marked by light-coloured vertical lines in the spectrograms, see Figure 26. On the contrary, the size of $|\nabla_\xi \lambda^i_{-,\star}(\mathbf{x}, \xi)|$ becomes small when ξ approaches $\tau^\pm_\infty(\mathbf{x}, \varpi)$. Then, there is almost no propagation. This could account for the creation of quasi-electrostatic waves. This difference in behaviour could explain why chorus emissions are usually composed of discrete narrowband wave elements accompanied by banded incoherent waves [27].

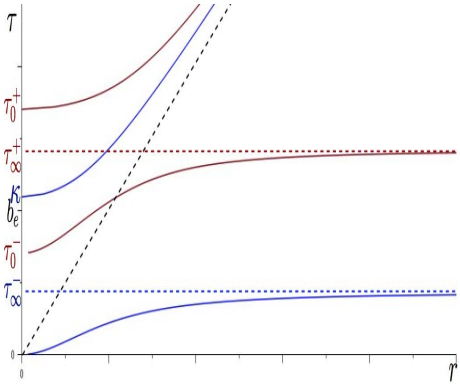

FIGURE 25. The characteristic variety as a graph of functions depending on τ.

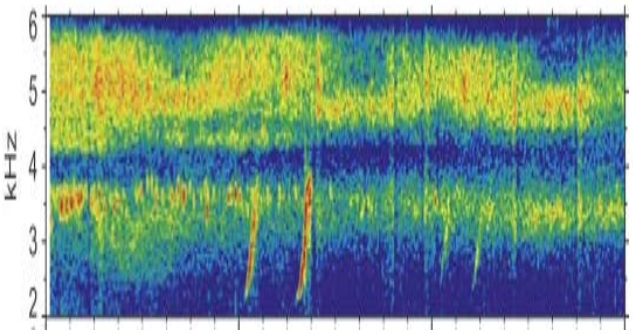

FIGURE 26. Whistler-mode chorus: Spectrogram of the electromagnetic field [34].

Moreover, chorus emissions usually occur in two frequency ranges, a *lower* band and some *upper* band, which are separated by a gap [27, 32, 35]. The high part of the lower band might correspond to the resonance frequency τ_∞^-. On the other hand, the upper band could be demimited from below by the cutoff frequency τ_0^- and at the top by the resonance frequency τ_∞^+. To well illustrate these correspondences, the comparison between Figures 25 and 26 is facilitated above. Note also that the lower and upper bands would be associated with respectively the ordinary and extraordinary modes of propagation,

The fact [32] that lower-band waves tend to be field-aligned ($\varpi \simeq 0$) whereas upper-band waves seem to be highly oblique ($\varpi \simeq \pi/2$) is another aspect that can be interpreted as a consequence of our analysis. Indeed, away from the emission points, the (non propagating) electrostatic waves should not be detected. Such waves are generated from the vertical lines in Figures 15 and 16. This yields the line $\tau \equiv \tau_\infty^+ = \kappa$ in the perpendicular case $\varpi = 0$, and $\tau \equiv \tau_\infty^- = 0$ in the parallel case $\varpi = \pi/2$. As a result, away from the emitting regions, one would expect to observe principally a lower-band (related to τ_∞^-) when $\varpi \simeq 0$, and a upper band (related to τ_∞^+) when $\varpi \simeq \pi/2$.

In conclusion, the refined structures of the characteristic variety $\mathscr{V}$ help to improve our understanding of the morphological properties of chorus emissions.

References

[1] E. V. Appleton. Wireless studies of the ionosphere. *J. Inst. Electr. Eng*, 71:642–650, 1932.

[2] A. Back, T. Hattori, S. Labrunie, J.-R. Roche, and P. Bertrand. Electromagnetic wave propagation and absorption in magnetised plasmas: variational formulations and domain decomposition, 2014.

[3] J. Bortnik, R. M. Thorne, and N. P. Meredith. The unexpected origin of plasmaspheric hiss from discrete chorus emissions. *Nature*, 452:62–66, 2008.

[4] M. Bostan and C. Negulescu. Mathematical models for strongly magnetized plasmas with mass disparate particles. *Discrete Contin. Dyn. Syst. Ser. B*, 15(3):513–544, 2011.

[5] M. Braun. Mathematical remarks on the Van Allen radiation belt: a survey of old and new results. *SIAM Rev.*, 23(1):61–93, 1981.

[6] J.-Y. Chemin, B. Desjardins, I. Gallagher, and E. Grenier. *Mathematical geophysics*, volume 32 of *Oxford Lecture Series in Mathematics and its Applications*. The Clarendon Press Oxford University Press, Oxford, 2006. An introduction to rotating fluids and the Navier-Stokes equations.

[7] C. Cheverry. Can One Hear Whistler Waves? *Comm. Math. Phys.*, 338(2):641–703, 2015.

[8] R. Ciurea-Borcia, G. Matthieussent, E. Le Bel, F. Simonet, and J. Solomon. Oblique whistler waves generated in cold plasma by relativistic electron beams. *Physics of plasmas*, 7(1):359–370, 2000.

[9] M.H. Denton, J.E. Borovsky, and T.E. Cayton. A density temperature description of the outer electron radiation belt during geomagnetic storms. *Journal of Geophysical Research: Space Physics*, 115, 2010.

[10] Bruno Després, Lise-Marie Imbert-Gérard, and Ricardo Weder. Hybrid resonance of Maxwell's equations in slab geometry. *J. Math. Pures Appl. (9)*, 101(5):623–659, 2014.

[11] L.C. Evans. *Partial Differential Equations*. Graduate Studies in Mathematics. American Mathematical Society, 2010.

[12] R. Fitzpatrick. *Plasma Physics: An Introduction*. Hardcover, 2014.

[13] E. Frénod and E. Sonnendrücker. Long time behavior of the two-dimensional Vlasov equation with a strong external magnetic field. *Math. Models Methods Appl. Sci.*, 10(4):539–553, 2000.

[14] P. Ghendrih, M. Hauray, and A. Nouri. Derivation of a gyrokinetic model. existence and uniqueness of specific stationary solution. *Kinetic and Related Models*, 2, Issue 4:707–725, 2009.

[15] C. Gillmor. Wilhelm Altar, Edward Appleton, and the magneto-ionic theory. *Proceedings of the American Philosophical Society*, 126(5):395–440, 1982.

[16] R. T. Glassey and J. W. Schaeffer. Global existence for the relativistic Vlasov-Maxwell system with nearly neutral initial data. *Comm. Math. Phys.*, 119(3):353–384, 1988.

[17] F. Golse and L. Saint-Raymond. The Vlasov-Poisson system with strong magnetic field. *J. Math. Pures Appl. (9)*, 78(8):791–817, 1999.

[18] F. Golse and L. Saint-Raymond. The Vlasov-Poisson system with strong magnetic field in quasineutral regime. *Math. Models Methods Appl. Sci.*, 13(5):661–714, 2003.
[19] D. Han-Kwan and F. Rousset. Quasineutral limit for vlasov-poisson with penrose stable data. *Ann. Sci. Ecole Norm. Sup.*, to appear, 2015.
[20] D. R. Hartree. The propagation of electromagnetic waves in a stratified medium. *Mathematical Proceedings of the Cambridge Philosophical Society*, 25:97–120, 1929.
[21] R. A. Helliwell. *Whistlers and Related Ionospheric Phenomena.* Stanford University Press. 1965.
[22] C.F. Kennel. Low frequency whistler mode. *Journal of Plasma Physics*, 71:1– 28, 1966.
[23] C.F. Kennel and H.E. Petschek. Limit on stably trapped particles. *Journal of Geophysical Research*, 9:2190–2202, 1966.
[24] E. Le Bel. *Etude physique et numérique de la saturation des ceintures de Van Allen.* PhD thesis, Paris 11, Orsay, 2001.
[25] W. Li, J. Bortnik, R. M. Thorne, Y. Nishimura, V. Angelopoulos, and L. Chen. Modulation of whistler mode chorus waves: 2. role of density variations. *Journal of Geophysical Research*, 116, Issue A6, 2011.
[26] Z. Lin and W. A. Strauss. Linear stability and instability of relativistic Vlasov-Maxwell systems. *Comm. Pure Appl. Math.*, 60(5):724–787, 2007.
[27] K. Liu, S.P. Gary, and D. Winske. Excitation of banded whistler waves in the magnetosphere. *Geophysical Research Letters*, 38, 2011.
[28] J. D. Menietti, J. S. Pickett, D. A. Gurnett, and J. D. Scudder. Electrostatic electron cyclotron waves observed by the plasma wave instrument on board polar. *Journal of Geophysical Research*, 106, 2001.
[29] G. Métivier. *The Mathematics of Nonlinear Optics.* 2009.
[30] D. C. Montgomery and D. A. Tidman. *Plasma kinetic theory.* McGraw-Hill Book Company, 1964.
[31] M. E. Oakes, R. B. Michie, K. H. Tsui, and J. E. Copeland. Cold plasma dispersion surfaces. *Journal of Plasma Physics*, 21:205–224, 1979.
[32] Y. Omura, M. Hikishima, Y. Katoh, D. Summers, and S. Yagitani. Nonlinear mechanisms of lower-band and upper-band vlf chorus emissions in the magnetosphere. *Journal of Geophysical Research*, 114, 2009.
[33] J. Rauch. *Hyperbolic Partial Differential Equations and Geometric Optics.* Graduate Studies in Mathematics. American Mathematical Society, 2012.
[34] O. Santolik, D.A. Gurnett, J.S. Pickett, M. Parrot, and N. Cornilleau-Wehrlin. Spatio-temporal structure of storm-time chorus. *Journal of Geophysical Research*, 108, Issue A7:SMP 7–1, 2003.
[35] S.S. Sazhin and M. Hayakawa. Magnetospheric chorus emissions: A review. *Planetary and Space Science*, 40:681–697, 1992.
[36] D. Sidhu and H. Unz. The magneto-ionic theory for drifting plasma: The whistler mode. *Transactions of the Kansas Academy of Science*, 70(4):432–450, 1967.
[37] T. H. Stix. *Waves in plasma.* American Institute of Physics, 1992.

[38] Harid V. *Coherent interactions between whistler mode waves and energetic electrons in the earth's radiation belts*. PhD thesis, Stanford, 2015.

[39] R. Woollett. *Electromagnetic wave propagation in a cold, collisionless atomic hydrogen plasma*. Nasa technical note, Nasa TN D-2071, 1964.

[40] F. Xiao, Thorne R. M., and D. Summers. Intsability of electromagnetic r-mode waves in a relativistic plasma. *Physics of plasmas*, 5:2489–2497, 1998.

[41] K. Yamaguchi, T. Matsumuro, Y. Omura, and D. Nunn. Ray tracing of whistler-mode chorus elements. *Ann. Geophys.*, 31:665–673, 2013.

CHAPTER 3

Dispersion relations in hot magnetized plasmas

Résumé. Les relations de dispersion associées aux plasmas chauds non collisionnels ont été beaucoup étudiées par le passé [2, 9, 10, 18, 27, 28, 32]. Pour autant, ce sujet est toujours d'actualité en physique des plasmas, voir les articles récents [13, 21, 26, 30, 36] ou les livres [24, 31]. L'objectif de cette partie est de mettre en place une analyse asymptotique des équations de Vlasov-Maxwell relativistes en vue de donner un sens rigoureux à la variété caractéristique. La discussion se fait dans le cadre des Tokamaks ; elle prend en compte les variations en espace du champ magnétique et de la fonction de distribution à l'équilibre. Pour pouvoir incorporer ces inhomogénéités, le problème est formulé en terme d'optique géométrique [23, 25]. De cette manière, les résultats antérieurs peuvent être unifiés, justifiés et étendus. Certains aspects sont nouveaux. Par exemple, le tenseur de permittivité diélectrique est défini dans le domaine des fréquences réelles via des intégrales singulières impliquant la transformée de Hilbert.

Mots clés. Plasmas chauds avec fort champ magnétique ; équations de Vlasov-Maxwell relativistes ; tokamaks ; relations de dispersion ; variété caractéristique ; interaction onde-particule ; résonances cinétiques ; tenseur diélectrique ; transformée de Hilbert.

Abstract. In the framework of hot magnetized collisionless plasmas, dispersion relations have been extensively studied in the past [2, 9, 10, 18, 27, 28, 32]. This subject is still topical in plasma physics, see the articles [13, 21, 26, 30, 36] and the recent books [24, 31]. The aim of this article is to provide a rigorous derivation of the characteristic variety, based on some asymptotic analysis of the relativistic Vlasov-Maxwell system. Special emphasis is made on the modeling of Tokamaks, with spatial variations of the magnetic field and of the equilibrium distribution function. In order to take into account the inhomogeneities, the problem is formulated in terms of geometrical optics [23, 25]. This allows to unify, justify and extend the preceding results. New aspects are indeed included. For instance, the dielectric tensor is defined for real frequencies through singular integrals involving the Hilbert transform.

Keywords. Hot magnetized plasmas ; relativistic Vlasov-Maxwell equations ; tokamaks ; dispersion relations ; characteristic variety ; wave particle interaction ; kinetic resonances ; dielectric tensor ; Hilbert transform.

3.1. Introduction

Dispersion relations have been extensively studied in plasma physics. It is because they are involved in a wide range of astrophysical contexts and laboratory experiments through wave-particle interaction [17, 33], transfer of power between waves and particles, heating of plasmas, reflectometry techniques [15], and so on. The preparatory works from the 1960s, 1970s and 1980s [2, 9, 10, 18, 27, 28, 32] are the template for recent numerical studies [30, 36], for contemporary investigations in more complex situations [13, 21, 24, 26, 31] or, like in the present text which is about tokamaks, for developments up to the case of non-uniform magnetized plasmas.

In real fusion machines, the dominant distribution function and the external magnetic field are inhomogeneous. They undergo significant fluctuations in position. These variations have a major effect on the geometry of wave propagation. Their impact is important when performing ray tracing, with many practical consequences [31]. It becomes decisive when looking at the transport equations (to measure power transfers between waves and particles) or in the perspective of long time studies [4, 5].

However, the presence of inhomogeneities is complicated to simulate. This is probably why, despite some attempts [29] and substantial progress exposed in the reference book [31], this subject has not been completely studied. Another reason is, without a doubt, a general principle of physics according to which a dispersion relation can be obtained by analyzing a plane monochromatic wave in a homogeneous medium, and then letting the medium's properties (in the dielectric tensor) vary slowly in position.

After verification, this principle holds true, but it is not so easy to determine what should vary, why and how. There are questions that remain unanswered. The aim of this article is precisely to check what the situation really is. It is to rigorously define the characteristic variety by extracting the corresponding dielectric tensor through a comprehensive study. To this end, it is not enough to extend existing procedures, which give formal results, provide partial information or rely on specific hypotheses. A new approach is needed.

In a plasma, the presence of a strong magnetic field makes the charged particles oscillate at the electron cyclotron frequency ε^{-1} with $\varepsilon \ll 1$. Away from thermal equilibrium, the repartition of the charged particles is therefore described by oscillating kinetic distribution functions whose structures are exhibited in [5]. This produces oscillating currents. Then, by a mesoscopic caustic effect [4], self-consistent oscillating electromagnetic waves are emitted. They act like coherent sources. Roughly speaking, it is as if the rays emanate from a *smooth nonlinear phase* $\phi(\mathbf{t}, \mathbf{x})$. The same applies to waves launching by antennas, in view of the radio frequency heating of tokamak plasmas.

It turns out that the propagation of electromagnetic oscillations in a hot quasi-neutral background of ions and electrons can be described in the framework of some asymptotic analysis. To some extent, we can consider WKB expansions involving a single phase $\phi(\mathbf{t}, \mathbf{x})$, as in (3.3.1). From there, the matter is to construct for the relativistic Vlasov-Maxwell system an adequate geometrical optics.

In comparison with usual theories in hyperbolic equations [23, 25], new difficulties come from the kinetic resonances which are hidden in the self-consistent picture. The propagation of waves is still governed by a dielectric tensor $\sigma(\cdot)$. But now the dielectric property becomes a reactive aspect of the wave-particle interaction. The aim of this article is to derive $\sigma(\cdot)$ from basic principles. Then, it is to rigorously define the content of $\sigma(\cdot)$ in the domain of *real* frequencies. When doing this, complications arise for instance from the singular integrals that play a part in the construction of $\sigma(\cdot)$.

Theorem 3 (eikonal equation in axisymmetric configurations)**.** *There exists a well-defined explicit skew-symmetric matrix $\sigma(\cdot)$, playing the part of a conductivity tensor, such that the eikonal equation governing wave propagation in tokamaks can be determined through the following Hamilton-Jacobi equation:*

$$\det\Big(\nabla_{\mathbf{x}}\phi\,{}^t\nabla_{\mathbf{x}}\phi+(\partial_{\mathbf{t}}\phi)^2\;Id-|\nabla_{\mathbf{x}}\phi|^2\;Id+i\;\partial_{\mathbf{t}}\phi\;\sigma(\mathbf{x},\partial_{\mathbf{t}}\phi,\nabla_{\mathbf{x}}\phi)\Big)=0\,. \tag{3.1.1}$$

More precisely, the matrix $\sigma(\cdot)$ is given by:

$$\sigma(\mathbf{x},\tau,\xi):=-4\,\pi\,i\;G^{\rm d}\big(\Psi(\rho,z)\big)\sum_{n\in\mathbb{Z}}\int_0^{+\infty}\!\!\int_0^{\pi}\frac{r^4\;\partial_r F^{\rm d}(r^2)}{\langle r\rangle\,(\tau+\tau_n)}\;T_n\;dr\,d\varpi\,. \tag{3.1.2}$$

where $F^{\rm d}(\cdot)$ and $G^{\rm d}(\cdot)$ are constitutive elements of the tokamak transient distribution (see Definition 3.2.2 and [8, 19]) and $\Psi(\cdot)$ is the poloidal flux function. At the level of (3.1.2), the "T_n" symbol stands for the Hermitian matrix:

$$T_n:=\left(\begin{array}{ccc}\dfrac{n^2\,J_n^2(\zeta)}{\zeta^2}\,\sin^3\varpi & \dfrac{i\,n\,J_n(\zeta)\,J_n'(\zeta)}{\zeta}\,\sin^3\varpi & \dfrac{n\,J_n^2(\zeta)}{\zeta}\,\cos\varpi\,\sin^2\varpi\\ -\dfrac{i\,n\,J_n(\zeta)\,J_n'(\zeta)}{\zeta}\,\sin^3\varpi & (J_n'(\zeta))^2\,\sin^3\varpi & -i\,J_n(\zeta)\,J_n'(\zeta)\,\cos\varpi\,\sin^2\varpi\\ \dfrac{n\,J_n^2(\zeta)}{\zeta}\,\cos\varpi\,\sin^2\varpi & i\,J_n(\zeta)\,J_n'(\zeta)\,\cos\varpi\,\sin^2\varpi & J_n^2(\zeta)\,\cos^2\varpi\,\sin\varpi\end{array}\right),$$

where $J_n(\cdot)$ denotes the n-th Bessel function of the first kind. Moreover, ζ and τ_n are given by:

$$\tau_n(\mathbf{x},r,\varpi,\xi):=\langle r\rangle^{-1}\;(r\,\xi_{\parallel}\,\cos\varpi+n\,\mathbf{b}_e)\,,\qquad \zeta(\mathbf{x},r,\varpi,\xi_\perp):=r\;\xi_\perp\;\sin\varpi\;\mathbf{b}_e(\mathbf{x})^{-1}\,.$$

This text is divided into two main chapters, Section 3.2 and Section 3.3.

The discussion begins in Section 3.2 with the modeling of hot magnetized collisionless plasmas in axisymmetric configurations, through the textbook case of tokamaks. The starting point is the relativistic Vlasov-Maxwell (RVM) system. A first step (Part 3.2.1) is to describe the content of toroidal equilibria. This means (Paragraph 3.2.1.1) to determine realistic external magnetic fields $\tilde{\mathbf{B}}_e(\cdot)$ and (Paragraphs 3.2.1.2 and 3.2.1.3) to exhibit distribution functions $\tilde{\rm f}_\alpha^{\rm d}(\cdot)$ satisfying the stationnary RVM system (3.2.3)-(3.2.4). A second stage (Part 3.2.2) is to perform some dimensionless analysis of the RVM system. The purpose (Part 3.2.3) is to interpret the hot regime in terms of some asymptotic analysis, where the size of all physical quantities is expressed in function of the small parameter ε.

By this way, we are led to a version of the RVM equations which is much more singular than in the article [6], with a number of new aspects which must be taken into account.

Section 3.3 contains the core of the analysis. Part 3.3.1 is devoted to a precise description of the *characteristic variety*. The framework of geometrical optics allows in the preliminary Paragraph 3.3.1.1 to extract a simplified system of equations. Then, in Paragraph 3.3.1.2, we perform a Fourier analysis through the Jacobi-Anger identity. In Paragraph 3.3.1.3, this leads to some interesting kinetic interpretation of the electron cyclotron resonances. By this way, in Paragraph 3.3.1.4, we can get a formal definition of the dielectric tensor $\sigma(\cdot)$. Now, the aim of Part 3.3.2 is to clarify the meaning of $\sigma(\cdot)$. This is achieved in several stages. First, in Paragraph 3.3.2.1, we perform a change of variables. Secondly, in Paragraph 3.3.2.2, we introduce the *Hilbert transform* and we study its action through Lipschitz estimates (Paragraph 3.3.2.3) and through L^1-estimates (Paragraph 3.3.2.4). Finally, the particular cases of perpendicular and parallel propagation are adressed in Part 3.3.2.2.

The mathematical difficulties which are solved in Part 3.3.2 in order to rigorously define the dielectric tensor $\sigma(\cdot)$ are original. They are issued from an interpretation of wave-particle interactions, where the gyroballistic dispersion functions [7, 31] are constitutive elements of $\sigma(\cdot)$. As an extension of the present work, the mechanisms of power transfer between particles and waves could be further investigated.

3.2. Hot magnetized plasmas in axisymmetric configurations

This section is dedicated to the modelling of hot magnetized plasmas in axisymmetric configurations. We will consider the case of Tokamaks, which is one of the most-researched candidates for producing controlled thermonuclear fusion power. Keeping in mind the physical observations, the discussion will be systematically tested in the Tokamak context. As in Chapter 2, we consider a plasma which is confined inside some non-empty open set $\tilde{\Omega}$ of $\mathbb{R}^3$ and which is composed of N distinct species (electrons, ions, $\cdots$) which are labelled by $\alpha \in \{1, \cdots, N\}$. Assumptions 2.2.1 and 2.2.2 on slight variations in temperatures and densities, and on quasineutrality are still supposed to hold. Unless otherwise stated, we will keep the notations from Section 2.2. Then, the kinetic distribution function (KDF) of the α^{th} species $\tilde{\mathrm{f}}^{\mathrm{k}}_\alpha(\tilde{\mathrm{t}}, \tilde{\mathbf{x}}, \tilde{\mathbf{p}})$ is subjected to the Vlasov equation:

$$\partial_{\tilde{\mathrm{t}}} \tilde{\mathrm{f}}^{\mathrm{k}}_\alpha + \tilde{\mathbf{v}}_\alpha(\tilde{\mathbf{p}}) \cdot \nabla_{\tilde{\mathbf{x}}} \tilde{\mathrm{f}}^{\mathrm{k}}_\alpha + e_\alpha \left[\tilde{\mathbf{E}}(\tilde{\mathrm{t}}, \tilde{\mathbf{x}}) + \tilde{\mathbf{v}}_\alpha(\tilde{\mathbf{p}}) \times \left(\tilde{\mathbf{B}}(\tilde{\mathrm{t}}, \tilde{\mathbf{x}}) + \tilde{\mathbf{B}}_e(\tilde{\mathbf{x}}) \right) \right] \cdot \nabla_{\tilde{\mathbf{p}}} \tilde{\mathrm{f}}^{\mathrm{k}}_\alpha = 0 \,. \tag{3.2.1}$$

Recall (3.2.17) for the definition of the two functionals $\tilde{\rho}(\cdot)$ and $\tilde{\jmath}(\cdot)$. The self-consistent electromagnetic field $(\tilde{\mathbf{E}}, \tilde{\mathbf{B}})(\cdot)$ inside (3.2.1) must satisfy the Maxwell equations:

$$\partial_{\tilde{\mathrm{t}}} \tilde{\mathbf{E}} - c_0^2 \, \nabla_{\tilde{\mathbf{x}}} \times (\tilde{\mathbf{B}} + \tilde{\mathbf{B}}_e) = -\, \epsilon_0^{-1} \, \tilde{\jmath}(\tilde{\mathrm{f}}^{\mathrm{k}}_\alpha) \,, \qquad \nabla_{\tilde{\mathbf{x}}} \cdot \tilde{\mathbf{E}} = \epsilon_0^{-1} \, \tilde{\rho}(\tilde{\mathrm{f}}^{\mathrm{k}}_\alpha) \,, \tag{3.2.2a}$$

$$\partial_{\tilde{\mathrm{t}}} \tilde{\mathbf{B}} + \nabla_{\tilde{\mathbf{x}}} \times \tilde{\mathbf{E}} = 0 \,, \qquad \nabla_{\tilde{\mathbf{x}}} \cdot (\tilde{\mathbf{B}} + \tilde{\mathbf{B}}_e) = 0 \,. \tag{3.2.2b}$$

The strategy is to seek solutions of (3.2.1)-(3.2.2) as perturbations of a stationary equilibrium state given by $\tilde{\mathrm{f}}^{\mathrm{k}}_\alpha(\tilde{\mathrm{t}}, \tilde{\mathbf{x}}, \tilde{\mathbf{p}}) \equiv \tilde{\mathrm{f}}^{\mathrm{d}}_\alpha(\tilde{\mathbf{x}}, \tilde{\mathbf{p}})$ for all $\alpha \in \{1, \cdots, N\}$ and $(\tilde{\mathbf{E}}, \tilde{\mathbf{B}}) \equiv (0, 0)$. A first

stage in this direction is to find functions $\tilde{\mathrm{f}}^{\mathrm{d}}_\alpha(\cdot)$ and $\tilde{\mathbf{B}}_e(\cdot)$ satisfying:

$$\tilde{\mathbf{v}}_\alpha(\tilde{\mathbf{p}})\cdot\nabla_{\tilde{\mathbf{x}}}\tilde{\mathrm{f}}^{\mathrm{d}}_\alpha + e_\alpha\,\left[\tilde{\mathbf{v}}_\alpha(\tilde{\mathbf{p}})\times\tilde{\mathbf{B}}_e(\tilde{\mathbf{x}})\right]\cdot\nabla_{\tilde{\mathbf{p}}}\tilde{\mathrm{f}}^{\mathrm{d}}_\alpha = 0\,,\qquad \forall\,\alpha\in\{1,\cdots,N\}\,, \tag{3.2.3}$$

together with:

$$c_0^2\,\nabla_{\tilde{\mathbf{x}}}\times\tilde{\mathbf{B}}_e = \epsilon_0^{-1}\,\tilde{\jmath}(\tilde{\mathrm{f}}^{\mathrm{d}}_\alpha)\,,\qquad \tilde{\rho}(\tilde{\mathrm{f}}^{\mathrm{d}}_\alpha) = 0\,,\qquad \nabla_{\tilde{\mathbf{x}}}\cdot\tilde{\mathbf{B}}_e = 0\,. \tag{3.2.4}$$

Section 3.2.1 exhibits realistic solutions to the system (3.2.3)-(3.2.4). Section 3.2.2 highlights dimensionless equations which are issued from (3.2.1)-(3.2.2). This leads in Section 3.2.3 to the notion of what is a *hot asymptotic regime*.

3.2.1. **Toroidal equilibrium.** The discussion is devoted here to the study of (3.2.3)-(3.2.4), that is to the determination of $\tilde{\mathbf{B}}_e(\cdot)$ and $\tilde{\mathrm{f}}^{\mathrm{d}}_\alpha(\cdot)$. In Paragraph 3.2.1.1, we select axisymmetric divergence free external magnetic fields $\tilde{\mathbf{B}}_e(\cdot)$ that are issued from physical considerations. In Paragraph 3.2.1.2, we explain how (3.2.3)-(3.2.4) is usually replaced by the *Grad-Shafranov* equations, giving rise to a notion of a fluid equilibrium. Finally, in Paragraph 3.2.1.3, we investigate directly (3.2.3)-(3.2.4) to find special solutions incorporating kinetic aspects.

3.2.1.1. *Axisymmetric inhomogeneous external magnetic fields.* In Tokamaks, the charged particles are confined by a strong external inhomogeneous magnetic field $\tilde{\mathbf{B}}_e(\cdot)\in\mathcal{C}^\infty(\tilde{\Omega};\mathbb{R}^3)$. Assumption 2.2.4 on the amplitude $\tilde{\mathbf{b}}_e(\cdot)$ of $\tilde{\mathbf{B}}_e(\cdot)$ is still supposed to hold. The divergence free condition of (3.2.4) is verified when $\tilde{\mathbf{B}}_e(\cdot)$ is issued from a magnetic potential.

Assumption 3.2.1. *[magnetic potential] There is a vector field* $\tilde{\mathbf{A}}\in\mathcal{C}^\infty(\tilde{\Omega};\mathbb{R}^3)$ *such that:*

$$\tilde{\mathbf{B}}_e(\tilde{\mathbf{x}}) = \nabla_{\tilde{\mathbf{x}}}\times\tilde{\mathbf{A}}(\tilde{\mathbf{x}})\,. \tag{3.2.5}$$

Consider the cylindrical coordinate system $(\tilde{\rho},\tilde{\varphi},\tilde{z})\in\mathbb{R}_+\times\mathbb{T}\times\mathbb{R}$ with corresponding orthonormal basis $(e_{\tilde{\rho}},e_{\tilde{\varphi}},e_{\tilde{z}})$. The second direction $e_{\tilde{\varphi}}$ is called the *toroidal* direction. On the other hand, the plane generated by the directions $e_{\tilde{\rho}}$ and $e_{\tilde{z}}$ is called the *poloidal* plane. Select a and R_0 with $0<a<R_0$. Then, define:

$$\tilde{\Omega} := \{(\tilde{\rho},\tilde{\varphi},\tilde{z})\in\mathbb{R}_+\times\mathbb{T}\times\mathbb{R}\,;\\ (\tilde{\rho}-R_0)^2+\tilde{z}^2\le a^2\,\}\,.$$

The domain $\tilde{\Omega}$ is represented on Figure 27. The positive numbers a and R_0 respectively stand for the minor and the major radius of the tokamak. A vector field like $\tilde{\mathbf{A}}$ can be decomposed in the basis $(e_{\tilde{\rho}},e_{\tilde{\varphi}},e_{\tilde{z}})$. This yields three components $\tilde{\mathbf{A}}_{\tilde{\rho}}$, $\tilde{\mathbf{A}}_{\tilde{\varphi}}$ and $\tilde{\mathbf{A}}_{\tilde{z}}$. We consider axisymmetric plasmas.

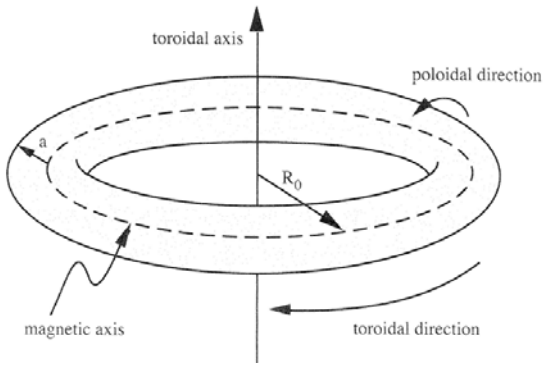

FIGURE 27. Axisymmetric configuration.

Assumption 3.2.2. *[axisymmetric toroidal equilibrium] The vector field* $\tilde{\mathbf{A}}(\cdot)$ *and the kinetic distribution functions* $\tilde{\mathrm{f}}_\alpha^{\mathrm{d}}(\cdot)$ *are exhibiting symmetry around the vertical axis* $\tilde{\rho}=0$.

In particular, all components $\tilde{\mathbf{A}}_{\tilde{\rho}}$, $\tilde{\mathbf{A}}_{\tilde{\varphi}}$ and $\tilde{\mathbf{A}}_{\tilde{z}}$ of $\tilde{\mathbf{A}}$ do not depend on $\tilde{\varphi}$. Then:

$$\tilde{\mathbf{B}}_e = \nabla_{\tilde{\mathbf{x}}} \times \tilde{\mathbf{A}} = -\partial_{\tilde{z}}\tilde{\mathbf{A}}_{\tilde{\varphi}}\, e_{\tilde{\rho}} + (\partial_{\tilde{z}}\tilde{\mathbf{A}}_{\tilde{\rho}} - \partial_{\tilde{\rho}}\tilde{\mathbf{A}}_{\tilde{z}})\, e_{\tilde{\varphi}} + \tilde{\rho}^{-1}\, \partial_{\tilde{\rho}}(\tilde{\rho}\ \tilde{\mathbf{A}}_{\tilde{\varphi}})\, e_{\tilde{z}}\,. \tag{3.2.6}$$

We have $\tilde{\mathbf{B}}_e := \tilde{\mathbf{B}}_e^t + \tilde{\mathbf{B}}_e^p$, where we have put apart the toroidal component $\tilde{\mathbf{B}}_e^t(\cdot)$ of $\tilde{\mathbf{B}}_e(\cdot)$:

$$\tilde{\mathbf{B}}_e^t := (\partial_{\tilde{z}}\tilde{\mathbf{A}}_{\tilde{\rho}} - \partial_{\tilde{\rho}}\tilde{\mathbf{A}}_{\tilde{z}})\, e_{\tilde{\varphi}}\,, \tag{3.2.7}$$

as well as the poloidal component $\tilde{\mathbf{B}}_e^p(\cdot)$ of $\tilde{\mathbf{B}}_e(\cdot)$, namely:

$$\tilde{\mathbf{B}}_e^p := -\partial_{\tilde{z}}\tilde{\mathbf{A}}_{\tilde{\varphi}}\, e_{\tilde{\rho}} + \tilde{\rho}^{-1}\, \partial_{\tilde{\rho}}(\tilde{\rho}\ \tilde{\mathbf{A}}_{\tilde{\varphi}})\, e_{\tilde{z}}\,. \tag{3.2.8}$$

Use *toroidal* coordinates $(r,\varphi,\theta)\in\mathbb{R}_+\times\mathbb{T}^2$ as indicated on Figure 28, with associated orthonormal basis $(e_r, e_\varphi, e_\theta)$. The domain of study becomes:

$$\tilde{\Omega} := \{\,(r,\varphi,\theta)\in\mathbb{R}_+\times\mathbb{T}^2\,;\, r\le a\,\}\,.$$

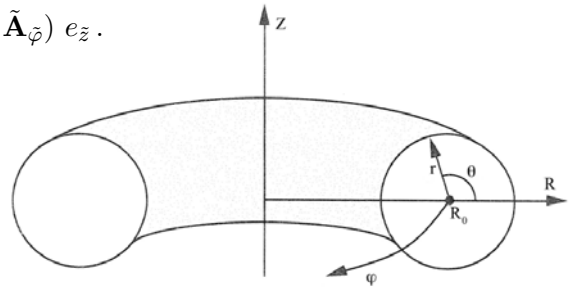

FIGURE 28. Toroidal coordinates.

Discussion 3.2.1. *[The case of Tore Supra] The amplitude of* b_e *is around* $b_e\simeq 4,5\,T$. *The major radius is* $\mathrm{R}_0\simeq 2,25\,m$, *whereas the minor radius is* $\mathrm{a}\simeq 0,7\,m$.

For axisymmetric systems, the field lines lie in nested magnetic flux surfaces. The cuts of these flux surfaces with the poloidal planes (which are the planes containing the $\tilde{z}-$axis) give rise to closed curves which can be viewed as the level sets $\mathscr{C}_\psi$ of a *poloidal flux function* $\tilde{\Psi}(\cdot)$. The family of poloidal cross sections $\{\mathscr{C}_\psi\}_\psi$ with $\psi\in\mathbb{R}_+$ is diffeomorphic to concentric circles. The function $\tilde{\Psi}(\cdot)$ can be viewed as depending on the variables $(\tilde{\rho},\tilde{z})$ or (r,θ). In the cylindrical coordinate system, the curve $\mathscr{C}_\psi$ takes the following form:

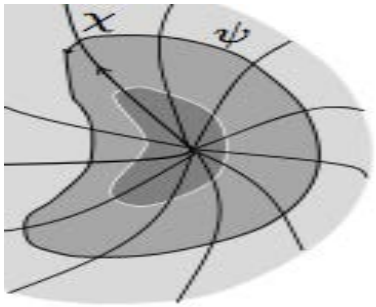

FIGURE 29. Cross sections.

$$\mathscr{C}_\psi = \{\,(\tilde{\rho},\tilde{z})\in\mathbb{R}_+\times\mathbb{R}\,;\,\tilde{\Psi}(\tilde{\rho},\tilde{z})=\psi\,\}\,. \tag{3.2.9}$$

In the toroidal coordinate system, it is:

$$\mathscr{C}_\psi = \{\,(r,\theta)\in\mathbb{R}_+\times\mathbb{T}\,;\,\tilde{\Psi}(r,\theta)=\psi\,\}\,. \tag{3.2.10}$$

By definition, we must have $\tilde{\mathbf{B}}_e^p\cdot\nabla\tilde{\Psi}\equiv 0$. It follows directly from (3.2.8) that $\tilde{\Psi}(\cdot)$ is a function of $\tilde{\rho}\,\tilde{A}_\varphi$. A possible choice for $\tilde{\Psi}(\cdot)$ is simply (see for instance [14], Section 1.3):

$$\tilde{\Psi}(\tilde{\rho},\tilde{z}) := \tilde{\rho}\ \tilde{A}_\varphi(\tilde{\rho},\tilde{z})\,. \tag{3.2.11}$$

The two components $\tilde{\mathbf{B}}_e^t(\cdot)$ and $\tilde{\mathbf{B}}_e^p(\cdot)$ can be written:

$$\tilde{\mathbf{B}}_e^t = \tilde{g}\ \nabla\tilde{\varphi}\,,\qquad \tilde{g}(\tilde{\rho},\tilde{z}) := \tilde{\rho}\ (\partial_{\tilde{z}}\tilde{\mathbf{A}}_{\tilde{\rho}} - \partial_{\tilde{\rho}}\tilde{\mathbf{A}}_{\tilde{z}})\,,\qquad \tilde{\mathbf{B}}_e^p = \nabla\tilde{\Psi}\times\nabla\tilde{\varphi}\,. \tag{3.2.12}$$

Let $(\tilde{\rho}_1, \tilde{z})$ and $(\tilde{\rho}_2, \tilde{z})$ be such that $\tilde{\Psi}(\tilde{\rho}_1, \tilde{z}) = \psi_1$ and $\tilde{\Psi}(\tilde{\rho}_2, \tilde{z}) = \psi_2$. The poloidal magnetic flux $\tilde{\Psi}_{pol}$ between the two magnetic surfaces $\mathscr{C}_{\psi_1}$ and $\mathscr{C}_{\psi_2}$ is the difference of $\tilde{\Psi}$ between the two positions $(\tilde{\rho}_1, \tilde{z})$ and $(\tilde{\rho}_2, \tilde{z})$. In other words [14]:

$$\tilde{\Psi}_{pol} := \int_{\tilde{\rho}_1}^{\tilde{\rho}_2} \tilde{\mathbf{B}}_e \cdot e_{\tilde{z}}\ 2\,\pi\,\tilde{\rho}\ d\tilde{\rho} = 2\,\pi\ \int_{\tilde{\rho}_1}^{\tilde{\rho}_2} \partial_{\tilde{\rho}}\tilde{\Psi}\ d\tilde{\rho} = 2\,\pi\ (\psi_2 - \psi_1)\,. \tag{3.2.13}$$

In [14], the function $\tilde{g}(\cdot)$ is called the *poloidal current function*. It can be freely adjusted. As a matter of fact, it suffices to integrate the second equation of (3.2.12) in order to recover the components $\tilde{\mathbf{A}}_{\tilde{\rho}}$ and $\tilde{\mathbf{A}}_{\tilde{z}}$ of $\tilde{\mathbf{A}}$. Now, a common assumption [5] is to consider that the function $\tilde{g}(\cdot)$ depends only on $\tilde{\Psi}$, say $\tilde{g} = \tilde{\mathrm{g}}(\tilde{\Psi})$ for some $\tilde{\mathrm{g}} \in \mathcal{C}^1(\mathbb{R};\mathbb{R})$. There is a similarity between the differential equations contained in (3.2.5)-(3.2.11) on the one hand and in (3.2.4)-(3.2.12) on the other hand. It follows that the poloidal current $\tilde{I}_{pol}$ enclosed by the two magnetic surfaces $\mathscr{C}_{\psi_1}$ and $\mathscr{C}_{\psi_2}$ is given by:

$$\tilde{I}_{pol} = 2\,\pi\ \varepsilon_0\ c_0^2\ [\tilde{\mathrm{g}}(\psi_2) - \tilde{\mathrm{g}}(\psi_1)]\,. \tag{3.2.14}$$

Sometimes the function $g(\cdot)$ is viewed as constant, see for example [35] (Section 3.1). This constant case is highlighted below.

Assumption 3.2.3. *[constant poloidal current density] The poloidal current function $\tilde{g}(\cdot)$ is constant. More precisely, the toroidal field $\tilde{\mathbf{B}}_e^t(\cdot)$ takes the form:*

$$\tilde{\mathbf{B}}_e^t(\tilde{\rho}, \tilde{z}) = b_e\,\mathrm{R}_0\,(\mathrm{R}_0 + r\,\cos\theta)^{-1}\ e_{\tilde{\varphi}} = b_e\,R_0\,\tilde{\rho}^{-1}\ e_{\tilde{\varphi}}\,, \qquad \tilde{g} \equiv b_e\,R_0\,. \tag{3.2.15}$$

The electric current that circulates in the primary coil of the tokamak is supposed to produce the poloidal magnetic field $\tilde{\mathbf{B}}_e^p(\cdot)$. In view of (3.2.12), the function $\tilde{\mathbf{B}}_e^p(\cdot)$ determines the choice of $\tilde{\Psi}(\cdot)$. When $\tilde{\Psi}(\cdot)$ does not depend on the angle θ, the poloidal cross sections form concentric circles. This special situation is described below.

Assumption 3.2.4. *[the cross sections $\mathscr{C}_\psi$ are concentric circles] The external magnetic field $\tilde{\mathbf{B}}_e^p(\cdot)$ takes the form:*

$$\tilde{\mathbf{B}}_e^p(r,\theta) = b_e\ r\ q(r)^{-1}\,(\mathrm{R}_0 + r\,\cos\theta)^{-1}\ e_\theta\,, \qquad \tilde{\Psi}(r) = b_e \int_0^r s\,\imath(s)\,ds\,, \tag{3.2.16}$$

where the function $\imath : [0,a] \longrightarrow \mathbb{R}_+^*$ is called the rotational transform, whereas the function $q : [0,a] \longrightarrow \mathbb{R}_+^*$ with $q(r) = \imath(r)^{-1}$ is called the safety factor.

The value $q(r)$ can be defined as the number of rotations a magnetic field line (located at a distance r from the magnetic axis) makes in the toroidal direction when it makes one loop on the poloidal plane. The term *safety factor* refers to the role it plays in determing the stability of a plasma. Values of $q(\cdot)$ larger than one lead to greater stability. In general (see [1]), the function $q(\cdot)$ is assumed to be increasing, and such that $q(0) \geq 1$.

In accordance with (2.2.6a) and (2.2.6b), at equilibrium, the *total charge density* $\tilde{\rho}^{\mathrm{d}}$ and the *total current density* $\tilde{\jmath}^{\mathrm{d}}$ can be defined as the sum of what the α^{th} species bring:

$$\tilde{\rho}^{\mathrm{d}} := \tilde{\rho}(\tilde{\mathrm{f}}^{\mathrm{d}}_{\alpha}) = \sum_{\alpha=1}^{N} \tilde{\rho}^{\mathrm{d}}_{\alpha}\,, \qquad \tilde{\rho}^{\mathrm{d}}_{\alpha} := \int_{\mathbb{R}^3} e_{\alpha}\ \tilde{\mathrm{f}}^{\mathrm{d}}_{\alpha}(\tilde{\mathrm{t}},\tilde{\mathbf{x}},\tilde{\mathbf{p}})\ d\tilde{\mathbf{p}}\,, \tag{3.2.17a}$$

$$\tilde{\jmath}^{\mathrm{d}} := \tilde{\jmath}(\tilde{\mathrm{f}}^{\mathrm{d}}_{\alpha}) = \sum_{\alpha=1}^{N} \tilde{\jmath}^{\mathrm{d}}_{\alpha}\,, \qquad \tilde{\jmath}^{\mathrm{d}}_{\alpha} := \int_{\mathbb{R}^3} e_{\alpha}\ \tilde{\mathbf{v}}_{\alpha}(\tilde{\mathbf{p}})\ \tilde{\mathrm{f}}^{\mathrm{d}}_{\alpha}(\tilde{\mathrm{t}},\tilde{\mathbf{x}},\tilde{\mathbf{p}})\ d\tilde{\mathbf{p}}\,. \tag{3.2.17b}$$

The first condition in (3.2.4) implies a link between $\tilde{\jmath}^{\mathrm{d}} := \tilde{\jmath}(\tilde{\mathrm{f}}^{\mathrm{d}}_{\alpha})$ and $\tilde{\mathbf{B}}_e$. Taking into account the relations inside (3.2.12), this furnishes:

$$\tilde{\jmath}^{\mathrm{d}} = \tilde{\jmath}^{\mathrm{d}t} + \tilde{\jmath}^{\mathrm{d}p}\,, \qquad \tilde{\jmath}^{\mathrm{d}t} := -\,\epsilon_0\ c_0^2\ \tilde{\rho}^{-1}\ \Delta^*\tilde{\Psi}\ e_{\tilde{\varphi}}\,, \qquad \tilde{\jmath}^{\mathrm{d}p} := \epsilon_0\ c_0^2\ \nabla\tilde{g}\times\nabla\tilde{\varphi}\,, \tag{3.2.18}$$

where the vector field $\tilde{\jmath}^{\mathrm{d}}$ is decomposed into a toroidal component $\tilde{\jmath}^{\mathrm{d}t}$ and a poloidal component $\tilde{\jmath}^{\mathrm{d}p}$, and where Δ^* is the differential operator:

$$\Delta^* := \tilde{\rho}\ \frac{\partial}{\partial\tilde{\rho}}\left(\frac{1}{\tilde{\rho}}\,\frac{\partial}{\partial\tilde{\rho}}\right) + \frac{\partial^2}{\partial\tilde{z}^2}\,. \tag{3.2.19}$$

At this stage, the axisymmetric magnetic field $\tilde{\mathbf{B}}_e(\cdot)$ is entirely determined by the two functions $\tilde{g}(\cdot)$ and $\tilde{\Psi}(\cdot)$. Additionnal requirements on $\tilde{g}(\cdot)$ and $\tilde{\Psi}(\cdot)$ are coming from (3.2.3) and (3.2.18) when specifying the kinetic distribution function $\tilde{\mathrm{f}}^{\mathrm{d}}_{\alpha}(\cdot)$. The determination of $\tilde{\mathrm{f}}^{\mathrm{d}}_{\alpha}(\cdot)$ is achieved in the two next Paragraphs 3.2.1.2 and 3.2.1.3.

3.2.1.2. *Fluid equilibria in magnetized plasmas.* Magnetohydrodynamics (MHD) or (in the presence of strong external electromagnetic fields) neoclassical models are what is meant by fluid theories. By virtue of their relative simplicity, these approaches constitute the most frequently used frameworks to deal with plasma equilibria. They are valid when the plasma is in a quiescent state. They require a minimum level of collisionality, that is an assumption of maxwellianity.

The fluid models involve macroscopic quantities such as the charge densities $\tilde{\rho}^{\mathrm{d}}$ and $\tilde{\rho}^{\mathrm{d}}_{\alpha}$, the current densities $\tilde{\jmath}^{\mathrm{d}}$ and $\tilde{\jmath}^{\mathrm{d}}_{\alpha}$, as well as the *density* $\tilde{\mathbf{n}}^{\mathrm{d}}_{\alpha}$, the *flow velocity* $\tilde{\mathbf{u}}^{\mathrm{d}}_{\alpha}$ and the *pressure tensor* $\tilde{\mathbf{P}}^{\mathrm{d}}_{\alpha}$ which can be obtained from the formulas (A.1.2a), (A.1.2b) and (A.1.2c) of Appendix A.1 (where $\tilde{\mathrm{f}}^{\mathrm{k}}_{\alpha}$ is replaced by $\tilde{\mathrm{f}}^{\mathrm{d}}_{\alpha}$). The condition of quasi-neutrality $\tilde{\rho}^{\mathrm{d}} \equiv 0$ gives rise to the relation (2.2.18) on the quantities $\tilde{\mathbf{n}}^{\mathrm{d}}_{\alpha}$. On the other hand, the macroscopic quantities are governed by (A.1.5). In the stationnary case, when $(\tilde{\mathbf{E}},\tilde{\mathbf{B}}) \equiv (0,0)$, this yields:

$$m_{\alpha}\ \tilde{\mathbf{n}}^{\mathrm{d}}_{\alpha}\ (\tilde{\mathbf{u}}^{\mathrm{d}}_{\alpha}\cdot\nabla_{\tilde{\mathbf{x}}})\tilde{\mathbf{u}}^{\mathrm{d}}_{\alpha} + \nabla_{\tilde{\mathbf{x}}}\cdot\tilde{\mathbf{P}}^{\mathrm{d}}_{\alpha} = \tilde{\jmath}^{\mathrm{d}}_{\alpha}\times\tilde{\mathbf{B}}_e\,. \tag{3.2.20}$$

The introduction of $\tilde{\mathbf{u}}^{\mathrm{d}}_{\alpha}(\cdot)$ is motivated in the framework of tokamaks by the presence of some toroidal plasma current $\tilde{\jmath}^{\mathrm{d}}_{\alpha}$. A common assumption [8, 19] that is consistent with Assumption 3.2.2 is to take $\tilde{\mathbf{u}}^{\mathrm{d}}_{\alpha}(\cdot)$ of the form:

$$\tilde{\mathbf{u}}^{\mathrm{d}}_{\alpha}(\tilde{\mathbf{x}}) := \tilde{\rho}\ \Omega_{\alpha}\ e_{\tilde{\varphi}}\,, \qquad \Omega_{\alpha}\in\mathbb{R}_+\,. \tag{3.2.21}$$

In (3.2.21), the number Ω_α is the angular rotation frequency. It is easy to see that:

$$(\tilde{\mathbf{u}}^{\mathrm{d}}_\alpha \cdot \nabla_{\tilde{\mathbf{x}}})\tilde{\mathbf{u}}^{\mathrm{d}}_\alpha = -\,\tilde{\rho}\;\Omega^2_\alpha\;e_{\tilde{\rho}}\,. \tag{3.2.22}$$

This accounts for the centrifugal force density. Moreover, as pointed out by Lemma A.1.1, in an isotropic medium, the matrix $\tilde{\mathbf{P}}^{\mathrm{d}}_\alpha$ is diagonal, of the form $\tilde{\mathbf{P}}^{\mathrm{d}}_\alpha(\tilde{\mathbf{x}}) = \tilde{\mathrm{p}}^{\mathrm{d}}_\alpha(\tilde{\mathbf{x}})\,Id$ where $\tilde{\mathrm{p}}^{\mathrm{d}}_\alpha$ is the scalar pressure of the α^{th} species. With (3.2.20) and (3.2.22), we obtain that $\tilde{\mathrm{p}}^{\mathrm{d}}_\alpha$ is linked to Ω_α and to the current density $\tilde{\jmath}^{\mathrm{d}}_\alpha$ of the α^{th} species through:

$$\nabla_{\tilde{\mathbf{x}}}\tilde{\mathrm{p}}^{\mathrm{d}}_\alpha = \tilde{\jmath}^{\mathrm{d}}_\alpha \times \tilde{\mathbf{B}}_e + m_\alpha\;\tilde{\mathbf{n}}^{\mathrm{d}}_\alpha\;\tilde{\rho}\;\Omega^2_\alpha\;e_{\tilde{\rho}}\,, \qquad \tilde{\jmath}^{\mathrm{d}}_\alpha = e_\alpha\;\tilde{\mathbf{n}}^{\mathrm{d}}_\alpha\;\tilde{\mathbf{u}}^{\mathrm{d}}_\alpha\,. \tag{3.2.23}$$

Now, consider the total scalar pressure $\tilde{\mathrm{p}}^{\mathrm{d}} := \tilde{\mathrm{p}}^{\mathrm{d}}_1 + \cdots + \tilde{\mathrm{p}}^{\mathrm{d}}_N$. Due to the axisymmetric hypothesis, the function $\tilde{\mathrm{p}}^{\mathrm{d}}(\cdot)$ depends only on $(\tilde{\rho}, \tilde{z})$. Then, summing the equation (3.2.23) over α, we can infer that:

$$\nabla_{\tilde{\mathbf{x}}}\tilde{\mathrm{p}}^{\mathrm{d}} = \partial_{\tilde{\rho}}\tilde{\mathrm{p}}^{\mathrm{d}}\;e_{\tilde{\rho}} + \partial_{\tilde{z}}\tilde{\mathrm{p}}^{\mathrm{d}}\;e_{\tilde{z}} = \tilde{\jmath}^{\mathrm{d}} \times \tilde{\mathbf{B}}_e + \tilde{\rho}\left(\sum_{\alpha=1}^{N} m_\alpha\,\tilde{\mathbf{n}}^{\mathrm{d}}_\alpha\,\Omega^2_\alpha\right)\,e_{\tilde{\rho}}\,. \tag{3.2.24}$$

Using the decomposition $\tilde{\jmath}^{\mathrm{d}} = \tilde{\jmath}^{\mathrm{d}t} + \tilde{\jmath}^{\mathrm{d}p}$ of (3.2.18), it follows directly from (3.2.24) that:

$$\tilde{\jmath}^{\mathrm{d}p} \times \tilde{\mathbf{B}}^p_e = 0\,, \tag{3.2.25a}$$

$$\partial_{\tilde{\rho}}\tilde{\mathrm{p}}^{\mathrm{d}}\;e_{\tilde{\rho}} + \partial_{\tilde{z}}\tilde{\mathrm{p}}^{\mathrm{d}}\;e_{\tilde{z}} = \tilde{\jmath}^{\mathrm{d}p} \times \tilde{\mathbf{B}}^t_e + \tilde{\jmath}^{\mathrm{d}t} \times \tilde{\mathbf{B}}^p_e + \tilde{\rho}\left(\sum_{\alpha=1}^{N} m_\alpha\,\tilde{\mathbf{n}}^{\mathrm{d}}_\alpha\,\Omega^2_\alpha\right)\,e_{\tilde{\rho}}\,. \tag{3.2.25b}$$

From the MHD point of view expressed in (3.2.25), the centrifugal force is balanced by the magnetic and pressure forces at all points. In particular, inserting the expressions (3.2.12) and (3.2.18) of $\tilde{\mathbf{B}}^p_e$ and $\tilde{\jmath}^{\mathrm{d}p}$, the relation (3.2.25a) implies that $\nabla\tilde{\Psi}\cdot\nabla\tilde{g} = 0$. In particular, $\tilde{g}(\cdot)$ is constant along the curves $\mathscr{C}_\psi$, and therefore $\tilde{g}(\cdot)$ can be expressed in terms of $\tilde{\Psi}$, namely $\tilde{g} = \tilde{\mathrm{g}}(\tilde{\Psi})$ for some $\tilde{\mathrm{g}} \in \mathcal{C}^1(\mathbb{R};\mathbb{R})$. Then, (3.2.25b) together with (3.2.12) and (3.2.18) gives rise to the following vectorial equilibrium equation [22]:

$$\nabla\tilde{\mathrm{p}}^{\mathrm{d}} = -\frac{\epsilon_0\,c_0^2}{\tilde{\rho}^2}\;\Delta^*\tilde{\Psi}\;\nabla\tilde{\Psi} - \frac{\epsilon_0\,c_0^2}{\tilde{\rho}^2}\;\tilde{\mathrm{g}}(\tilde{\Psi})\;\tilde{\mathrm{g}}'(\tilde{\Psi})\;\nabla\tilde{\Psi} + \tilde{\rho}\left(\sum_{\alpha=1}^{N} m_\alpha\tilde{\mathbf{n}}^{\mathrm{d}}_\alpha\Omega^2_\alpha\right)e_{\tilde{\rho}}\,. \tag{3.2.26}$$

Moreover, the function $\tilde{\mathrm{p}}^{\mathrm{d}}(\cdot)$ can always be written in the form $\tilde{\mathrm{p}}^{\mathrm{d}} = \tilde{\mathrm{P}}(\tilde{\rho},\tilde{\Psi})$ for some function $\tilde{\mathrm{P}} \in \mathcal{C}^1(\mathbb{R}\times\mathbb{R};\mathbb{R})$. A first projection of equation (3.2.26) in the $e_{\tilde{\rho}}$ direction yields:

$$\left.\frac{\partial\tilde{\mathrm{P}}}{\partial\tilde{\rho}}\right|_{\tilde{\Psi}=cste} = \tilde{\rho}\left(\sum_{\alpha=1}^{N} m_\alpha\tilde{\mathbf{n}}^{\mathrm{d}}_\alpha\Omega^2_\alpha\right). \tag{3.2.27}$$

Then, a second projection of equation (3.2.26) in the direction of $\nabla\tilde{\Psi}$ gives the *extended Grad-Shafranov* equation:

$$\Delta^*\tilde{\Psi} = -\,\frac{\tilde{\rho}^2}{\epsilon_0\,c_0^2}\;\left.\frac{\partial\tilde{\mathrm{P}}}{\partial\tilde{\Psi}}\right|_{\tilde{\rho}=cste} - \tilde{\mathrm{g}}(\tilde{\Psi})\;\tilde{\mathrm{g}}'(\tilde{\Psi})\,. \tag{3.2.28}$$

The equation (3.2.28) has been extensively studied [11, 13, 14, 22] because it gives access to the geometry of the magnetic surfaces. It is scale invariant through:

$$\tilde{\Psi} \,/\, \alpha \; \tilde{\Psi}\,, \qquad \tilde{\mathrm{P}} \,/\, \alpha^2 \; \tilde{\mathrm{P}}\,, \qquad \tilde{\mathrm{g}} \,/\, \alpha \; \tilde{\mathrm{g}}\,, \qquad \alpha \in \mathbb{R}\,. \tag{3.2.29}$$

Note that the change (3.2.29) does not affect the shape of magnetic surfaces. Observe also that the number Ω_α plays only an indirect role at the level of (3.2.28). It expresses itself through (3.2.27). Lastly, under Assumption 3.2.3, the equation (3.2.28) reduces to:

$$\Delta^*\tilde{\Psi} = -\,\frac{\tilde{\rho}^2}{\epsilon_0\, c_0^2}\;\frac{\partial \tilde{\mathrm{P}}}{\partial \tilde{\Psi}}\bigg|_{\tilde{\rho}=cste}\,. \tag{3.2.30}$$

3.2.1.3. *Kinetic equilibria in magnetized plasmas.* The fluid theory that has been outlined in Paragraph 3.2.1.2 is the most common way to study tokamak equilibria. However, it faces significant challenges due to the well-known closure problem. In (3.2.20), the pressure tensor $\tilde{\mathbf{P}}^{\mathrm{d}}_\alpha(\cdot)$ is an unknown. Except under special restrictions (see Appendix A.1), it cannot be expressed in terms of $\tilde{\mathbf{u}}^{\mathrm{d}}_\alpha$. The equation (3.2.20) is not self-contained.

From that perspective, the kinetic framework offers a more consistent, thorough and precise approach. As a consequence, the study of tokamak equilibria through a kinetic approach has been the subject of intensive research over the last few years in both physics [8, 19] and mathematics [20]. In [8, 19], the purpose is to construct exact (or approximate) solutions to the stationary equation:

$$\tilde{\mathbf{p}}\cdot\nabla_{\tilde{\mathbf{x}}}\tilde{\mathrm{f}}^{\mathrm{d}}_\alpha + \,e_\alpha\;\big[\tilde{\mathbf{p}}\times\tilde{\mathbf{B}}_e(\tilde{\mathbf{x}})\big]\cdot\nabla_{\tilde{\mathbf{p}}}\tilde{\mathrm{f}}^{\mathrm{d}}_\alpha \;=\; 0\,. \tag{3.2.31}$$

To this end, the existence of constants of motion (or of adiabatic invariants) is useful. Obviously, in the case $\tilde{\mathbf{E}} \equiv 0$, the *kinetic energy*:

$$E_\alpha \equiv E_\alpha(\tilde{\mathbf{p}}) := \frac{1}{2\,m_\alpha}\;|\tilde{\mathbf{p}}|^2\,, \tag{3.2.32}$$

and more generally any funcion of $|\tilde{\mathbf{p}}|$ (or $|\tilde{\mathbf{v}}|$) is preserved by the flow associated to the Vlasov equation. It follows that the function $E_\alpha(\cdot)$ is a solution to (3.2.31).

Definition 3.2.1. *[angular momentum] The angular momentum is the quantity defined by:*

$$C_\alpha \equiv C_\alpha(\tilde{\mathbf{x}},\tilde{\mathbf{p}}) := m_\alpha\;(\tilde{\rho}\;\;\tilde{\mathbf{p}}\cdot e_{\tilde{\varphi}} + e_\alpha\;\tilde{\Psi})\,. \tag{3.2.33}$$

Under Assumption 3.2.2 (of axisymmetry), another invariant is available.

Lemma 3.2.1. *The angular momentum is a constant of motion. The function $C_\alpha(\cdot)$ is a solution to the equation (3.2.31).*

Proof. Decompose $\tilde{\mathbf{p}}$ into $\tilde{\mathbf{p}} = \tilde{\mathbf{p}}_{\tilde{\rho}}\,e_{\tilde{\rho}} + \tilde{\mathbf{p}}_{\tilde{\varphi}}\,e_{\tilde{\varphi}} + \tilde{\mathbf{p}}_{\tilde{z}}\,e_{\tilde{z}}$. Recall that $\tilde{\mathbf{B}}_e = \tilde{\mathbf{B}}^t_e + \tilde{\mathbf{B}}^p_e$ with $\tilde{\mathbf{B}}^t_e$ and $\tilde{\mathbf{B}}^p_e$ as in (3.2.12). The condition (3.2.31) tested with $\tilde{\mathrm{f}}^{\mathrm{d}}_\alpha \equiv C_\alpha$ amounts to the same thing as:

$$\Big[(\tilde{\mathbf{p}}_{\tilde{\rho}}\;\partial_{\tilde{\rho}} + \tilde{\rho}^{-1}\;\tilde{\mathbf{p}}_{\tilde{\varphi}}\;\partial_{\tilde{\varphi}})(\tilde{\rho}\;\tilde{\mathbf{p}}_{\tilde{\varphi}})\Big] + e_\alpha\,\Big[\tilde{\mathbf{p}}\cdot\nabla_{\tilde{\mathbf{x}}}\tilde{\Psi} + \big(\tilde{\mathbf{p}}\times(\nabla_{\tilde{\mathbf{x}}}\tilde{\Psi}\times e_{\tilde{\varphi}})\big)\cdot e_{\tilde{\varphi}}\Big] = 0\,. \tag{3.2.34}$$

In (3.2.34), the two parts inside brackets are zero. □

More generally, any function of E_α and C_α is a solution to (3.2.31). However, to avoid technicalities, we only consider functions of separate variables. Moreover, without any loss of generality, we restrict our attention to functions involving scales that come in handy when looking at the dimensionless version of the equations (see Paragraph 3.2.2.2). Such prototypes of (non-maxwellian) axisymmetric equilibria are highlighted below.

Definition 3.2.2. *[tokamak transient distributions] Any function* $\tilde{\mathrm{f}}^{\mathrm{d}}_\alpha(\tilde{\mathbf{x}},\tilde{\mathbf{p}})$ *having the form:*

$$\begin{aligned}\tilde{\mathrm{f}}^{\mathrm{d}}_\alpha(\tilde{\mathbf{x}},\tilde{\mathbf{p}}) &:= \frac{n^{\mathrm{d}}_\alpha}{(m_\alpha\, c_0\, \theta^{\mathrm{d}}_\alpha)^3}\; F^{\mathrm{d}}_\alpha\left(\frac{|\tilde{\mathbf{p}}|^2}{(m_\alpha\, c_0\, \theta^{\mathrm{d}}_\alpha)^2}\right)\; G^{\mathrm{d}}_\alpha\left(\frac{1}{e_\alpha\, L^2\, b_e}\cdot\left(\tilde{\rho}\;\tilde{\mathbf{p}}\cdot e_{\tilde{\varphi}} + e_\alpha\,\tilde{\Psi}\right)\right)\\ &= \frac{n^{\mathrm{d}}_\alpha}{(m_\alpha\, c_0\, \theta^{\mathrm{d}}_\alpha)^3}\; F^{\mathrm{d}}_\alpha\left(\frac{2\,E_\alpha}{m_\alpha\,(c_0\,\theta^{\mathrm{d}}_\alpha)^2}\right)\; G^{\mathrm{d}}_\alpha\left(\frac{1}{e_\alpha\, L^2\, b_e}\cdot\frac{C_\alpha}{m_\alpha}\right)\end{aligned} \tag{3.2.35}$$

with $F^{\mathrm{d}}_\alpha(\cdot)\in\mathcal{S}(\mathbb{R}_+;\mathbb{R})$ *and* $G^{\mathrm{d}}_\alpha(\cdot)\in\mathcal{C}^1(\mathbb{R};\mathbb{R})$ *is called a tokamak transient distribution.*

As long as the temperature $\theta^{\mathrm{d}}_\alpha$ (see Paragraph 2.2.2.1) is small enough, such that $\theta^{\mathrm{d}}_\alpha \leq 10^{-3}$, one can consider that the momentum $\tilde{\mathbf{p}}$ satisfies some usual statistical repartition around the toroidal flow velocity $\tilde{\mathbf{u}}^{\mathrm{d}}_\alpha(\cdot)$. Then, the choice of $\tilde{f}^{\mathrm{d}}_\alpha(\cdot)$ can be further specified.

Definition 3.2.3. *[shifted Maxwell-Boltzmann distribution] The notion of a shifted Maxwell-Boltzmann distribution refers to the special choice:*

$$\tilde{\mathrm{f}}^{\mathrm{d}}_\alpha(\tilde{\mathbf{x}},\tilde{\mathbf{p}}) = \frac{\tilde{\mathbf{n}}^{\mathrm{d}}_\alpha(\tilde{\mathbf{x}})}{m^3_\alpha\, c^3_0}\,\mathcal{M}^b_{\theta^{\mathrm{d}}_\alpha}\Big(\frac{|\tilde{\mathbf{p}}-m_\alpha\,\tilde{\mathbf{u}}^{\mathrm{d}}_\alpha(\tilde{\mathbf{x}})|}{m_\alpha\, c_0}\Big)\,,\qquad \mathcal{M}^b_\theta(r) := \frac{1}{\pi^{3/2}}\,\frac{1}{\theta^3}\,\exp\Big(-\frac{r^2}{\theta^2}\Big)\,. \tag{3.2.36}$$

In (3.2.36), the vector field $\tilde{\mathbf{u}}^{\mathrm{d}}_\alpha(\cdot)$ *represents the flow velocity of the* α^{th} *species, as it can be given by (3.2.21). On the other hand, the function* $\tilde{\mathbf{n}}^{\mathrm{d}}_\alpha(\cdot)$ *is determined by:*

$$\tilde{\mathbf{n}}^{\mathrm{d}}_\alpha(\tilde{\mathbf{x}}) := n^{\mathrm{d}}_\alpha\;\exp\left(\frac{1}{(c_0\,\theta^{\mathrm{d}}_\alpha)^2}\left[|\tilde{\mathbf{u}}^{\mathrm{d}}_\alpha(\tilde{\mathbf{x}})|^2 + \frac{2\,e_\alpha}{m_\alpha}\,\Omega_\alpha\,\tilde{\Psi}\right]\right)\,. \tag{3.2.37}$$

Remark that (3.2.36) is indeed some particular case of (3.2.35), with:

$$F^{\mathrm{d}}_\alpha(r) := \frac{1}{\pi^{3/2}}\;\exp(-r)\,,\qquad G^{\mathrm{d}}_\alpha(s) := \exp\left(\frac{2\,\Omega_\alpha\, e_\alpha\, L^2\, b_e}{m_\alpha\,(c_0\,\theta^{\mathrm{d}}_\alpha)^2}\;s\right)\,. \tag{3.2.38}$$

Recall (2.2.5) which says that $\tilde{\mathrm{f}}^{\mathrm{k}}_\alpha = \tilde{\mathrm{f}}^{\mathrm{d}}_\alpha + \nu\,\tilde{\mathrm{f}}^{\mathrm{s}}_\alpha$ with $\nu \ll 1$. The relativistic features come from the possible presence of energetic particles. As long as the fraction of such particles remains small, the relativistic effects are restricted to the perturbation $\tilde{\mathrm{f}}^{\mathrm{s}}_\alpha(\cdot)$. On the other hand, the part $\tilde{\mathrm{f}}^{\mathrm{d}}_\alpha$ can take into account cold, warm or hot aspects (see Paragraph 2.2.2.1). When adjusting $\tilde{\mathrm{f}}^{\mathrm{d}}_\alpha(\cdot)$, it is important to look at the physical data.

Discussion 3.2.2. *[about the dominant stationnary part* $\tilde{\mathrm{f}}^{\mathrm{d}}_\alpha$*] Tokamaks involve special values of temperatures. Two regions can be distinguished. The edge region implies a diluted plasma with* $T_e \simeq 50$ *eV, so that* $\theta^{\mathrm{d}}_1 \simeq 10^{-2}$ *whereas* $\theta^{\mathrm{d}}_\alpha \ll \theta^{\mathrm{d}}_1$ *for* $\alpha \neq 1$*. It separates the cooler vessel wall from the plasma core. The core region contains a hotter plasma, but not that much. We find* $T_e \simeq 5$ *keV, and we still have* $\theta^{\mathrm{d}}_\alpha \ll \theta^{\mathrm{d}}_1 \simeq 10^{-1}$ *for* $\alpha \neq 1$*.* ∘

Taking into account these observations, we can point out the following.

Assumption 3.2.5. *[ions in a state of local cold thermodynamic equilibrium] For all $\alpha \neq 1$, we impose (3.2.36) with $\theta_\alpha^{\rm d} \leq 10^{-3}$.*

The shifted Maxwell-Boltzmann distribution $\tilde{\rm f}_\alpha^{\rm d}(\cdot)$ of (3.2.36) is clearly subjected to (A.1.6). Therefore, for $\alpha \neq 1$, the pressure tensor $\tilde{\mathbf{P}}_\alpha^{\rm d}$ is diagonal. It is of the form $\tilde{\mathbf{P}}_\alpha^{\rm d} = \tilde{p}_\alpha^{\rm d}\ Id$, where $\tilde{p}_\alpha^{\rm d}$ is some scalar pressure. For $\alpha \neq 1$, the equation (3.2.23) is satisfied and the fluid approach of Paragraph 3.2.1.2 does make sense. Now, the model (3.2.36) is not sure to apply when dealing with electrons. As a matter of fact, as revealed by (2.2.2), electrons are much lighter than ions and neutral atoms. This has two main consequences:

- First, the electrons can faster reach high energies. Thus, a certain level of flexibility must be achieved concerning $\tilde{\rm f}_1^{\rm d}(\cdot)$. It is preferable to use (3.2.35) instead of (2.2.20) or (3.2.36). This allows to better localize the support or the properties of the function $\tilde{\rm f}_1^{\rm d}(\cdot)$;

- Secondly, the electrons are more sensitive to perturbations. Such disturbances are induced for instance by the injection of neutral beams or radio waves. They can induce anisotropic effects with respect to the variable $|\tilde{\mathbf{p}}|$ or with respect to the variable $|\tilde{\mathbf{p}} - m_\alpha\, \tilde{\mathbf{u}}_\alpha^{\rm d}(\tilde{\mathbf{x}})|$. The corresponding aspects are not detected by (2.2.20) which deals only with $|\tilde{\mathbf{p}}|$. They are not viewed by (3.2.36) which involves only $|\tilde{\mathbf{p}} - m_\alpha\, \tilde{\mathbf{u}}_\alpha^{\rm d}(\tilde{\mathbf{x}})|$. They can be taken into acount at the level of $\tilde{\rm f}_\alpha^{\rm s}(\cdot)$. They can also be incorporated (albeit partially) through (3.2.35).

Assumption 3.2.6. *[electrons in a state of transient kinetic equilibrium] The distribution function $\tilde{\rm f}_1^{\rm d}(\cdot)$ is chosen as indicated in (3.2.35), with expressions $F_1^{\rm d}(\cdot)$ and $G_1^{\rm d}(\cdot)$ adjusted in order to achieve the quasi-neutrality condition:*

$$e \int_{\mathbb{R}^3} \tilde{\rm f}_1^{\rm d}(\tilde{\mathbf{x}}, \tilde{\mathbf{p}})\ d\tilde{\mathbf{p}} \ = \ \sum_{\alpha=2}^{N} e_\alpha\ \tilde{\mathbf{n}}_\alpha^{\rm d}(\tilde{\mathbf{x}})\,, \qquad \forall\, \tilde{\mathbf{x}} \in \tilde{\Omega}\,. \tag{3.2.39}$$

For general choices of $\tilde{\rm f}_1^{\rm d}(\cdot)$, the pressure tensor $\tilde{\mathbf{P}}_1^{\rm d}$ is not at all diagonal. It follows that the equation (3.2.23) does not hold. On the other hand, the relation (3.2.18) can still be exploited. In particular, the second equation of (3.2.18) yields:

$$\Delta^* \tilde{\Psi} = \frac{\tilde{\rho}}{\epsilon_0\, c_0^2} \int_{\mathbb{R}^3} (-\sin\tilde{\varphi}\, \tilde{\mathbf{v}^1} + \cos\tilde{\varphi}\, \tilde{\mathbf{v}^2}) \left(\sum_{\alpha=1}^{N} e_\alpha\, \tilde{\rm f}_\alpha^{\rm d}(\tilde{\mathbf{x}}, \tilde{\mathbf{p}}) \right) d\tilde{\mathbf{p}}\,. \tag{3.2.40}$$

In view of (3.2.35) and (3.2.36)-(3.2.37), the expressions $\tilde{\rm f}_\alpha^{\rm d}(\cdot)$ are non linear functions of $\tilde{\Psi}$. Thus, the condition (3.2.40) can be interpreted as a non linear elliptic equation. The dependence of (3.2.40) on Ω_α can still appear through (3.2.38). However, the equation (3.2.40) cannot be scaled as in (3.2.29). There are clear differences between (3.2.28) and (3.2.40).

Under reasonable assumptions, that is with adequate (possibly free) boundary conditions, the equation (3.2.40) can be solved. We refer for instance to the appendix of [20] or to the sections III and IV of [19]. A realistic adjustment through $\tilde{\Psi}(\cdot)$ of the magnetic

flux surfaces is an important piece of information before looking at more refined aspects. In what follows, the function $\tilde{\Psi}(\cdot)$ is assumed to satisfy the condition (3.2.40), which is equivalent to (3.2.28) when the fluid approach is affordable. From now on, the external magnetic field $\tilde{\mathbf{B}}_e(\cdot)$ is fixed as indicated in (3.2.12), and the kinetic distribution functions $\tilde{\mathrm{f}}^{\mathrm{d}}_d(\cdot)$ are adjusted as in Assumptions 3.2.5 and 3.2.6.

3.2.2. **Dimensionless equations.** The approach here is similar to that of Section 2.2.6. The context however is distinct. In Paragraphs 3.2.2.1 and 3.2.2.2, additional terms appear. In Paragraph 3.2.2.3, the dimensionless parameters are adjusted somewhat differently. There are more singular parameters.

3.2.2.1. *Perturbation theory.* As in Section 2.2.1, a small term $\nu\, \tilde{\mathrm{f}}^{\mathrm{s}}_\alpha(\cdot)$ with $\nu \ll 1$ is added to the exact solution $\tilde{\mathrm{f}}^{\mathrm{d}}_\alpha(\cdot)$. In other words, the solution $\tilde{\mathrm{f}}^{\mathrm{k}}_\alpha(\cdot)$ to (3.2.1) is broken into:

$$\tilde{\mathrm{f}}^{\mathrm{k}}_\alpha(\tilde{\mathbf{t}}, \tilde{\mathbf{x}}, \tilde{\mathbf{p}}) = \tilde{\mathrm{f}}^{\mathrm{d}}_\alpha(\tilde{\mathbf{x}}, \tilde{\mathbf{p}}) + \nu\, \tilde{\mathrm{f}}^{\mathrm{s}}_\alpha(\tilde{\mathbf{t}}, \tilde{\mathbf{x}}, \tilde{\mathbf{p}})\,, \quad (\tilde{\mathbf{t}}, \tilde{\mathbf{x}}, \tilde{\mathbf{p}}) \in \mathbb{R}_+ \times \tilde{\Omega} \times \mathbb{R}^3\,. \tag{3.2.41}$$

With a dominant stationary part $\tilde{\mathrm{f}}^{\mathrm{d}}_\alpha(\cdot)$ given by the shifted Maxwell-Boltzmann distribution (3.2.36) or by the tokamak transient distribution (3.2.35), the extra part $\tilde{\mathrm{f}}^{\mathrm{s}}_\alpha(\cdot)$ is governed by:

$$\begin{aligned} &\partial_{\tilde{\mathbf{t}}} \tilde{\mathrm{f}}^{\mathrm{s}}_\alpha + \tilde{\mathbf{v}}_\alpha(\tilde{\mathbf{p}}) \cdot \nabla_{\tilde{\mathbf{x}}} \tilde{\mathrm{f}}^{\mathrm{s}}_\alpha + e_\alpha \left[\tilde{\mathbf{E}} + \tilde{\mathbf{v}}_\alpha(\tilde{\mathbf{p}}) \times (\tilde{\mathbf{B}} + \tilde{\mathbf{B}}_e) \right] \cdot \nabla_{\tilde{\mathbf{p}}} \tilde{\mathrm{f}}^{\mathrm{s}}_\alpha \\ &\qquad = - \frac{e_\alpha}{\nu} \left[\tilde{\mathbf{E}} + \tilde{\mathbf{v}}_\alpha(\tilde{\mathbf{p}}) \times \tilde{\mathbf{B}} \right] \cdot \nabla_{\tilde{\mathbf{p}}} \tilde{\mathrm{f}}^{\mathrm{d}}_\alpha\,. \end{aligned} \tag{3.2.42}$$

In view of (3.2.4), the Maxwell's equations give rise to:

$$\left\{ \begin{array}{l} \partial_{\tilde{\mathbf{t}}} \tilde{\mathbf{B}} + \nabla_{\tilde{\mathbf{x}}} \times \tilde{\mathbf{E}} = 0\,, \\ \partial_{\tilde{\mathbf{t}}} \tilde{\mathbf{E}} - c_0^2\, \nabla_{\tilde{\mathbf{x}}} \times \tilde{\mathbf{B}} = -\epsilon_0^{-1}\, \nu\, \tilde{\jmath}(\tilde{\mathrm{f}}^{\mathrm{s}}_1, \cdots, \tilde{\mathrm{f}}^{\mathrm{s}}_N)\,, \end{array} \right. \tag{3.2.43}$$

together with:

$$\nabla_{\tilde{\mathbf{x}}} \cdot \tilde{\mathbf{E}} = \frac{\nu}{\epsilon_0}\, \tilde{\rho}(\tilde{\mathrm{f}}^{\mathrm{s}}_1, \cdots, \tilde{\mathrm{f}}^{\mathrm{s}}_N)\,, \qquad \nabla_{\tilde{\mathbf{x}}} \cdot \tilde{\mathbf{B}} = 0\,. \tag{3.2.44}$$

3.2.2.2. *Dimensionless equations and straightening of the field lines.* We proceed here as in Section 2.2.6. Details are not provided. The dimensionless version $\mathbf{A}(\cdot)$ of $\tilde{\mathbf{A}}(\cdot)$ is:

$$\mathbf{A}(\mathbf{x}) := \frac{1}{L\, b_e}\, \tilde{\mathbf{A}}(L\, \mathbf{x})\,, \qquad \mathbf{x} := \frac{\tilde{\mathbf{x}}}{L} \in \Omega\,, \qquad \rho := \frac{\tilde{\rho}}{L} \in \mathbb{R}_+\,, \qquad z := \frac{\tilde{z}}{L} \in \mathbb{R}\,. \tag{3.2.45}$$

The dimensionless function $\Psi(\cdot)$ associated with the magnetic flux function $\tilde{\Psi}(\cdot)$ is:

$$\Psi(\rho, z) := \frac{1}{L^2\, b_e}\, \tilde{\Psi}(L\, \rho, L\, z)\,. \tag{3.2.46}$$

With the same dimensionless unknowns defined in Paragraph 2.2.6.1 and the notations from Paragraph 2.2.6.2, the new Vlasov equation is:

$$
\begin{aligned}
&\partial_{\mathbf{t}} f_\alpha + \frac{\theta_\alpha^{\mathrm{d}}}{\langle \theta_\alpha^{\mathrm{d}}\, r\rangle}\, O(\mathbf{x})\, p\cdot\nabla_{\mathbf{x}} f_\alpha + \frac{\theta_\alpha^{\mathrm{d}}}{\langle \theta_\alpha^{\mathrm{d}}\, r\rangle}\, Q(\mathbf{x},p)\cdot\nabla_p f_\alpha \\
&+\frac{\theta_1^{\mathrm{d}}}{\theta_\alpha^{\mathrm{d}}}\,\frac{\nu}{\varepsilon_\alpha}\left[E + \frac{\theta_\alpha^{\mathrm{d}}}{\langle \theta_\alpha^{\mathrm{d}}\, r\rangle}\, p\times B\right]\cdot\nabla_p f_\alpha \;-\; \frac{1}{\varepsilon_\alpha}\,\frac{\mathbf{b}_e(\mathbf{x})}{\langle \theta_\alpha^{\mathrm{d}}\, r\rangle}\,(-p_2\,\partial_{p_1} + p_1\,\partial_{p_2}) f_\alpha \\
&+\frac{\theta_1^{\mathrm{d}}}{\theta_\alpha^{\mathrm{d}}\,\varepsilon_\alpha}\left[E + \frac{\theta_\alpha^{\mathrm{d}}}{\langle \theta_\alpha^{\mathrm{d}}\, r\rangle}\, p\times B\right]\cdot\nabla_p\left(\mathrm{f}_\alpha^{\mathrm{d}}(\mathbf{x}, O(\mathbf{x})\, p)\right) = 0\,.
\end{aligned}
\tag{3.2.47}
$$

Combining (3.2.33), (3.2.35) and (2.2.38), we find that $\tilde{\mathrm{f}}_\alpha^{\mathrm{d}}(\cdot)$ must be transformed according to:

$$
\begin{aligned}
\mathrm{f}_\alpha^{\mathrm{d}}(\mathbf{x},p) &:= (n_\alpha^d)^{-1}\, m_\alpha\, c_0\, (\theta_\alpha^d)^3\; \tilde{\mathrm{f}}_\alpha^{\mathrm{d}}(L\,\mathbf{x}, m_\alpha\, c_0\, \theta_\alpha^d\; O(\mathbf{x})p) \\
&= F_\alpha^{\mathrm{d}}(|p|^2)\; G_\alpha^{\mathrm{d}}(\varepsilon_\alpha\; \theta_\alpha^{\mathrm{d}}\; \rho\; O(\mathbf{x})p\cdot e_\varphi + \Psi(\rho,z))\,.
\end{aligned}
\tag{3.2.48}
$$

On the other hand, the Maxwell's equations become:

$$
\partial_{\mathbf{t}}\mathbf{B} + \nabla_{\mathbf{x}}\times\mathbf{E} = 0\,, \qquad \nabla_{\mathbf{x}}\cdot\mathbf{B} = 0\,, \tag{3.2.49a}
$$

$$
\partial_{\mathbf{t}}\mathbf{E} - \nabla_{\mathbf{x}}\times\mathbf{B} = -\jmath(\mathrm{f}_\alpha)\,, \qquad \nabla_{\mathbf{x}}\cdot\mathbf{E} = \rho(\mathrm{f}_\alpha)\,. \tag{3.2.49b}
$$

In (3.2.49b), the expressions $\jmath(\mathrm{f}_\alpha)$ and $\rho(\mathrm{f}_\alpha)$ are as in (2.2.42a) and (2.2.42b):

$$
\rho(\mathrm{f}_1,\cdots,\mathrm{f}_N)(\mathbf{t},\mathbf{x}) \equiv \rho(\mathrm{f}_\alpha)(\mathbf{t},\mathbf{x}) := \sum_{\alpha=1}^{N} \frac{1}{\theta_1^{\mathrm{d}}}\,\frac{\mu_\alpha^2}{\varepsilon_\alpha}\int_{\mathbb{R}^3} \mathrm{f}_\alpha(\mathbf{t},\mathbf{x},\mathbf{p}_\alpha)\; d\mathbf{p}_\alpha\,, \tag{3.2.50a}
$$

$$
\jmath(\mathrm{f}_1,\cdots,\mathrm{f}_N)(\mathbf{t},\mathbf{x}) \equiv \jmath(\mathrm{f}_\alpha)(\mathbf{t},\mathbf{x}) := \sum_{\alpha=1}^{N} \frac{\theta_\alpha^{\mathrm{d}}}{\theta_1^{\mathrm{d}}}\,\frac{\mu_\alpha^2}{\varepsilon_\alpha}\int_{\mathbb{R}^3} \frac{\mathbf{p}_\alpha}{\langle \theta_\alpha^{\mathrm{d}}\,|\mathbf{p}_\alpha|\rangle}\; \mathrm{f}_\alpha(\mathbf{t},\mathbf{x},\mathbf{p}_\alpha)\; d\mathbf{p}_\alpha\,. \tag{3.2.50b}
$$

3.2.2.3. *The hierarchy between the dimensionless parameters.* We follow the same procedure as in Paragraph 2.2.6.3, but with data issued from tokamaks.

Discussion 3.2.3. *[about the size of ε] As indicated in (2.2.39), the number ε is defined as the ratio beween the reference frequency $1/T = c_0/L$ and the gyrofrequency ω_{ce}. This turns out to be a small parameter. For fusion devices like ITER [35], we find $\varepsilon \simeq 10^{-4}$.* ∘

The parameter ε is used as a reference factor unit. Keep in mind the relation (2.2.49):

$$
|\varepsilon_\alpha| \;=\; \frac{e}{|e_\alpha|}\,\frac{m_\alpha}{m_e}\,\varepsilon \simeq \frac{\varepsilon}{\iota_\alpha} \gtrsim \beta\;\varepsilon \simeq 1\,, \qquad \forall\,\alpha\in\{2,\cdots,N\}\,. \tag{3.2.51}
$$

Discussion 3.2.4. *[about the size of the coefficients $\theta_\alpha^{\mathrm{d}}$] In view of (2.2.15), the numbers $\theta_\alpha^{\mathrm{d}}$ increase with the temperatures T_α, see (2.2.14). They decrease with the masses m_α, see (2.2.2). The ratio $\theta_\alpha^{\mathrm{d}}/\theta_1^{\mathrm{d}}$, which is given by (2.2.17), remains relevant. The comparison of θ_1^{d} with 1 and of all the other coefficients $\theta_\alpha^{\mathrm{d}}$ for $\alpha\neq 1$ with ε seems acceptable.* ∘

Discussion 3.2.5. *[about the size of the coefficients μ_α] In view of (2.2.38)-(2.2.39), the access to μ_1 requires to evaluate b_e, m_e and $n_1^{\rm d}$. How to fix b_e and m_e has already been explained. As regards the electron density, we can take the value $n_1^{\rm d} \equiv n_\alpha^{\rm d} = 10^{20}\, electrons/m^3$ [24, 35]. Let us recall that:*

$$|\mu_\alpha| \,=\, \Big(\frac{n_\alpha^{\rm d}\; m_\alpha}{\epsilon_0}\Big)^{1/2}\; \frac{1}{b_e} \,=\, \Big(\frac{n_\alpha^{\rm d}\; m_\alpha}{n_1^{\rm d}\; m_1}\Big)^{1/2}\; |\mu_1| \gtrsim |\mu_1|\,, \qquad \forall\, \alpha \in \{1, \cdots, N\}\,. \tag{3.2.52}$$

The higher value $n_1^{\rm d} \simeq 10^{20}\, electrons/m^3$ is compensated by the presence of a stronger magnetic field $b_e \simeq 4,5\, T$. We can again assert that $|\mu_1| \simeq 1$. We also remind that:

$$\frac{\mu_\alpha^2}{\varepsilon_\alpha} \,=\, \frac{e_\alpha\, n_\alpha^{\rm d}}{e_1\, n_1^{\rm d}}\; \frac{\mu^2}{\varepsilon} \simeq \frac{\mu^2}{\varepsilon}\,, \qquad \forall\, \alpha \in \{1, \cdots, N\}\,. \tag{3.2.53}$$

∘

The discussion 2.2.5 still holds. Thus, we can adjust ν in such a way that $\nu \sim \varepsilon$.

3.2.3. **The hot asymptotic regime.** The framework specified below is intended to describe what happens in fusion devices. This requires to fix the size of the various parameters in function of ε. Of course, this can be done only under simplifying assumptions that make the model tractable. In the light of Paragraph 3.2.2.3, we can retain the following choices:

- *(Hp1)*: We have $\varepsilon_1 = -\varepsilon \ll 1$ together with $\varepsilon_\alpha = 1$ for all $\alpha \in \{2, \cdots, N\}$;
- *(Hp2)*: We have $\theta_1^{\rm d}(\varepsilon) = 1$ together with $\theta_\alpha^{\rm d}(\varepsilon) = \varepsilon$ for all $\alpha \in \{2, \cdots, N\}$;
- *(Hp3)*: For all $\alpha \in \{2, \cdots, N\}$, the dominant stationary part $\tilde{\rm f}_\alpha^{\rm d}(\cdot)$ is given by the shifted Maxwell-Boltzmann KDF (3.2.36);
- *(Hp4)*: For $\alpha = 1$, the dominant stationary part $\tilde{\rm f}_1^{\rm d}(\cdot)$ is given by (3.2.35) with (3.2.39);
- *(Hp5)*: The perturbation in (3.2.41) is such that $\nu = \varepsilon$;
- *(Hp6)*: We have $\mu := |\mu_1| = 1$ and $\mu_\alpha^2 = \varepsilon^{-1}$ for all $\alpha \in \{2, \cdots, N\}$.

In particular, this yields $|\varepsilon_\alpha|\, \theta_\alpha^{\rm d} = \varepsilon$ for all $\alpha \in \{1, \cdots, N\}$ so that:

$${\rm f}_\alpha^{\rm d}(\mathbf{x}, p) = F_\alpha^{\rm d}(|p|^2)\; G_\alpha^{\rm d}(\Psi(\mathbf{x})) + O(\varepsilon)\,, \qquad \forall\, \alpha \in \{1, \cdots, N\}\,. \tag{3.2.54}$$

By combining informations from Section 2.2.6 with the assumptions *(Hp1)*, $\cdots$, *(Hp6)*, we can simplify (3.2.47)-(3.2.49). For all $\alpha \in \{2, \cdots, N\}$, with $F_\alpha^{\rm d}(\cdot)$ and $G_\alpha^{\rm d}(\cdot)$ as in (3.2.38), we have to impose:

$$\begin{aligned} &\partial_{\mathbf{t}} f_\alpha + \frac{\varepsilon}{\langle \varepsilon\, r\rangle}\; O(\mathbf{x})\, p \cdot \nabla_{\mathbf{x}} f_\alpha + \frac{\varepsilon}{\langle \varepsilon\, r\rangle}\; Q(\mathbf{x}, p) \cdot \nabla_p f_\alpha \\ &+ \Big[E + \frac{\varepsilon}{\langle \varepsilon\, r\rangle}\, p \times B\Big] \cdot \nabla_p f_\alpha \;-\; \frac{\mathbf{b}_e(\mathbf{x})}{\langle \varepsilon\, r\rangle}\; (-p_2\, \partial_{p_1} + p_1\, \partial_{p_2}) f_\alpha \\ &+ \frac{1}{\varepsilon}\, \Big[E + \frac{\varepsilon}{\langle \varepsilon\, r\rangle}\, p \times B\Big] \cdot \nabla_p {\rm f}_\alpha^{\rm d} = 0\,. \end{aligned} \tag{3.2.55}$$

On the other hand, for $\alpha = 1$, the equation (3.2.47) yields:

$$
\begin{aligned}
&\partial_{\mathbf{t}} f_1 + \frac{1}{\langle r \rangle}\, O(\mathbf{x})\, p \cdot \nabla_{\mathbf{x}} f_1 + \frac{1}{\langle r \rangle}\, Q(\mathbf{x}, p) \cdot \nabla_p f_1 \\
&- \Big[E + \frac{1}{\langle r \rangle}\, p \times B \Big] \cdot \nabla_p f_1 \; + \; \frac{1}{\varepsilon}\, \frac{\mathbf{b}_e(\mathbf{x})}{\langle\, r \rangle}\, (-p_2\, \partial_{p_1} + p_1\, \partial_{p_2}) f_1 \\
&- \frac{1}{\varepsilon} \left[E + \frac{1}{\langle r \rangle}\, p \times B \right] \cdot \nabla_p \mathrm{f}_\alpha^{\mathrm{d}} = 0\,.
\end{aligned}
\tag{3.2.56}
$$

With $B(\cdot)$ and $E(\cdot)$ as in (2.2.44), the equation (3.2.49) becomes:

$$
O(\mathbf{x})\, \partial_{\mathbf{t}} B + \nabla_{\mathbf{x}} \times \big(O(\mathbf{x})\, E\big) = 0\,, \qquad \nabla_{\mathbf{x}} \cdot \big(O(\mathbf{x})\, B\big) = 0\,, \tag{3.2.57a}
$$

$$
O(\mathbf{x})\, \partial_{\mathbf{t}} E - \nabla_{\mathbf{x}} \times \big(O(\mathbf{x})\, B\big) = -\, \jmath(\mathrm{f}_\alpha)\,, \qquad \nabla_{\mathbf{x}} \cdot \big(O(\mathbf{x})\, E\big) = \rho(\mathrm{f}_\alpha)\,, \tag{3.2.57b}
$$

where $\rho(\mathrm{f}_\alpha)$ and $\jmath(\mathrm{f}_\alpha)$ can be specified by using *(Hp1)* and (3.2.53) in order to find:

$$
\rho(\mathrm{f}_\alpha)(\mathbf{t}, \mathbf{x}) \equiv \rho^{\mathrm{h}}(\mathrm{f}_\alpha)(\mathbf{t}, \mathbf{x}) := -\, \frac{1}{\varepsilon} \int_{\mathbb{R}^3} \mathrm{f}_1 \; d\mathbf{p} + \sum_{\alpha=2}^{N} \int_{\mathbb{R}^3} \mathrm{f}_\alpha \; d\mathbf{p}\,, \tag{3.2.58a}
$$

$$
\jmath(\mathrm{f}_\alpha)(\mathbf{t}, \mathbf{x}) \equiv \jmath^{\mathrm{h}}(\mathrm{f}_\alpha)(\mathbf{t}, \mathbf{x}) := -\, \frac{1}{\varepsilon} \int_{\mathbb{R}^3} \frac{\mathbf{p}}{\langle |\mathbf{p}| \rangle}\, \mathrm{f}_1 \; d\mathbf{p} + \sum_{\alpha=2}^{N} \varepsilon \int_{\mathbb{R}^3} \frac{\mathbf{p}}{\langle \varepsilon\, |\mathbf{p}| \rangle}\, \mathrm{f}_\alpha \; d\mathbf{p}\,. \tag{3.2.58b}
$$

3.3. Hot plasma dispersion relations

The dispersion relations inform about various properties of wave propagation. They say if a wave can propagate. More generally, by looking at complex frequencies, they can indicate if a wave is damped or amplified. They furnish the phase velociy. They give the group velocity. They yield the refractive index. They allow to determine the eikonal equation. They are crucial in reflectometry [15]. They are a prerequisite to understand turbulence phenomena [4, 5], ... And the list of potential applications goes on.

Based on the Vlasov theory of hot collisionless and magnetized plasmas, several approaches have been proposed in order to obtain the dispersion relations. Derivations can be found in Trubnikov [32] (1959), Bekefi [2] (1966), Krall and Trivelpiece [18] (1973), Davidson [9] (1983), Swanson [28] (1989), etc. They give access to a preliminary treatment of wave propagation. There are more recent works dealing with the relativistic features [12, 21] or with the numerical aspects [30, 36].

Most of these contributions [2, 9, 18, 32] are restricted to the case of a *constant* external magnetic field and also to the case of a *homogeneous* velocity distribution function. The improvements concerning the choice of more realistic functions $\tilde{\mathrm{f}}_\alpha^{\mathrm{d}}(\cdot)$ have been principally related to the dependence on $\tilde{\mathbf{p}}$ of $\tilde{\mathrm{f}}_\alpha^{\mathrm{d}}(\cdot)$. As a matter of fact, the behaviour of $\tilde{\mathrm{f}}_\alpha^{\mathrm{d}}(\cdot)$ in $\tilde{\mathbf{p}}$ can be of quasi-Maxwellian type [10] or of gyrotropic type [26]. One of the advantages of Section 3.2 is to incorporate through (3.2.35) realistic variations in $\mathbf{x}$ of $\tilde{\mathrm{f}}_\alpha^{\mathrm{d}}(\cdot)$

Now, many practical situations in space and laboratory plasmas [24] involve variations in position $\tilde{\mathbf{x}}$ of the distribution $\tilde{\mathrm{f}}^{\mathrm{d}}_{\alpha}(\cdot)$ but also of the function $\tilde{\mathbf{B}}_e(\cdot)$. These variations have an effect on the dispersion relations, and by this way they can modify the geometry of the propagation. They have an impact on ray tracing, and beyond they can induce caustics [3, 16]. The recent book [31] gives in the framework of plasma physics a detailed and comprehensive overview of modern ray-tracing techniques in nonuniform media. It explains the practical importance of the subject, with discussions about tunneling, mode conversion, weak dissipation, and so on.

The inhomogeneities have first been taken into account in the framework of the K*inetic* T*heory of* D*rift* W*aves* (KTDW), see for instance Paragraph 6.6.3 in [28]. This approach implies very specific assumptions (electrostatic approximation, modelling of the curvature effects through some gravitational potential, ...). In fact, the idea behind KTDW is to come back to the case of a constant external magnetic field $\tilde{\mathbf{B}}_e(\cdot)$ and to handle the variations in $\tilde{\mathbf{x}}$ as perturbations. This allows to expand the particle orbits around their trajectories, to integrate the unperturbed trajectories through explicit formulas, to perform a Fourier analysis of the linearized Vlasov equation, and to employ a fixed decomposition of the velocity $\tilde{\mathbf{p}}$ into two components $\tilde{\mathbf{p}}_{\parallel}$ and $\tilde{\mathbf{p}}_{\perp}$ which are respectively parallel and perpendicular to the magnetic field. These lines of reasoning are employed even when finite Larmor radius effects are incorporated [29]. Note however that the key reference [31] develops more sophisticated tools, with up-to-date phase space methods.

For many technical reasons, the preceding procedures [2, 9, 18, 28, 29, 32] do not apply appropriately in the presence of realistic inhomogeneities. On the one hand, they rely on hypotheses that could be questionable. On the other hand, they often use non local arguments in space or in time (especially when integrating the Vlasov equation), while the dispersion relations should emanate from a *local* space-time analysis. For all theses reasons, the approaches [2, 9, 18, 28, 29, 32] bring answers that need to be completed. As a matter of fact, they are not able to fully capture the underlying *geometry*, which is essential to really understand wave propagation.

Now, of course, a dielectric tensor is a macroscopic notion. In some ways, it summarizes the average macroscopic outcome of the underlying kinetic effects. Thus, it should depend on $\mathbf{t}$ and $\mathbf{x}$, but not on $\mathbf{p}$. In the end, the momentum variable $\mathbf{p}$ should disappear. Some *global* analysis is needed, but only in $\mathbf{p}$.

In contrast with [2, 9, 10, 18, 28], and as required by tokamak configurations, the modelling and the dimensional analysis of Section 3.2 takes into account the concrete dependence on $\tilde{\mathbf{x}}$ of both $\tilde{\mathbf{B}}_e(\cdot)$ and $\tilde{\mathrm{f}}^{\mathrm{d}}_{\alpha}(\cdot)$. They combine together the various physical data in order to evaluate their relative importance and to provide a coherent description of the phenomena. They allow to formulate the problem in terms of geometrical optics. This is a prerequisite which gives rise in this Section 3.3 to a complete understanding of the dispersion relations, valid in the presence of inhomogeneities.

From now on, we are interested in the asymptotic analysis (when $\varepsilon \ll 1$) of the oscillating solutions to the system (3.2.55)-(3.2.58). To this end, the framework which has been presented in Paragraph 2.2.8 is particularly well-suited. It is understood that the hypotheses and the notations of Paragraph 2.2.8 are retained. In particular, Assumption 2.2.6 about the non-stationary phase function $\phi(\cdot)$ is still valid.

Select a *macroscopic* phase $\phi(\cdot)$ depending only on $(\mathbf{t},\mathbf{x}) \in [0,T]\times\Omega$ (for some $T\in\mathbb{R}_+^*$) and profiles $\check{\mathscr{U}}_j(\cdot)$ such that:

$$\phi(\mathbf{t},\mathbf{x}) \in \mathcal{C}^\infty([0,T]\times\Omega;\mathbb{R})\,, \qquad \check{\mathscr{U}}_j(\mathbf{t},\mathbf{x},\mathbf{p},\theta) \in \mathcal{C}^\infty([0,T]\times\Omega\times\mathbb{R}^3\times\mathbb{T};\mathbb{R}^{N+6})\,.$$

We look for approximate solutions to the system (3.2.55)-(3.2.58) in the form of *monophase* representations. More precisely, for some $M\in\mathbb{N}$, we consider expansions of the form:

$$\begin{pmatrix} f^\varepsilon_{a,1}(\mathbf{t},\mathbf{x},\mathbf{p}) \\ \vdots \\ f^\varepsilon_{a,N}(\mathbf{t},\mathbf{x},\mathbf{p}) \\ B^\varepsilon_a(\mathbf{t},\mathbf{x}) \\ E^\varepsilon_a(\mathbf{t},\mathbf{x}) \end{pmatrix} = \sum_{j=0}^{M} \varepsilon^j\ \check{\mathscr{U}}_j\Big(\mathbf{t},\mathbf{x},\mathbf{p},\frac{\phi(\mathbf{t},\mathbf{x})}{\varepsilon}\Big)\,. \tag{3.3.1}$$

In (3.3.1), with $p = {}^tO(\mathbf{x})\,\mathbf{p}$ as in (2.2.44) and with $\tilde{\mathscr{U}}_j(\mathbf{t},\mathbf{x},p,\theta) := \check{\mathscr{U}}_j(\mathbf{t},\mathbf{x},O(\mathbf{x})p,\theta)$, the profiles $\check{\mathscr{U}}_j(\cdot)$ can be decomposed into:

$$\check{\mathscr{U}}_j(\mathbf{t},\mathbf{x},\mathbf{p},\theta) = \tilde{\mathscr{U}}_j(\mathbf{t},\mathbf{x},{}^tO(\mathbf{x})\mathbf{p},\theta) = \begin{pmatrix} \tilde{\mathscr{F}}_{j,1}\big(\mathbf{t},\mathbf{x},{}^tO(\mathbf{x})\mathbf{p},\theta\big) \\ \vdots \\ \tilde{\mathscr{F}}_{j,N}\big(\mathbf{t},\mathbf{x},{}^tO(\mathbf{x})\mathbf{p},\theta\big) \\ \mathscr{B}_j(\mathbf{t},\mathbf{x},\theta) \\ \mathscr{E}_j(\mathbf{t},\mathbf{x},\theta) \end{pmatrix}, \qquad \tilde{\mathscr{F}}_{j,k}(\mathbf{t},\mathbf{x},p,\theta)\,.$$

With p represented in spherical coordinates as in (2.2.45), the functions $\tilde{\mathscr{U}}_j(\mathbf{t},\mathbf{x},\cdot,\theta)$ and the functions $\tilde{\mathscr{F}}_{j,k}(\mathbf{t},\mathbf{x},\cdot,\theta)$ can be viewed as functions $\mathscr{U}_j(\mathbf{t},\mathbf{x},\cdot,\theta)$ and $\mathscr{F}_{j,k}(\mathbf{t},\mathbf{x},\cdot,\theta)$ of the variables $(\varpi,\omega,r)\in\mathbb{T}^2\times\mathbb{R}_+$. The spatial-velocity position is marked by $\mathbf{y}$ with:

$$\mathbf{y} := (\mathbf{x},\varpi,\omega,r) \in \Omega\times\mathbb{T}\times\mathbb{T}\times\mathbb{R}_+.$$

After substitution of (3.3.1) in (3.2.55)-(3.2.58), we get (2.2.59). Then, an approximate solution can be obtained by solving successively the conditions $\mathscr{G}_j = 0$ for $j=-1$, $j=0$, and so on. The discussion focuses on the *eikonal equation* which is issued from the constraint:

$$\mathscr{G}_{-1}(\mathbf{t},\mathbf{y},\theta;\mathscr{U}_0) = 0\,. \tag{3.3.2}$$

In Part 3.3.1, starting from (3.3.2), we give a precise definition of the characteristic variety sustaining wave propagation. Thus, we recover the classical form of the dielectric tensor which is highlighted in standard textbooks [27, 28]. The rest of the analysis is new. In Part 3.3.2, the rigorous analysis of the dielectric tensor is performed. Part 3.3.3 is devoted to the study of interesting special cases.

3.3.1. **Description of the characteristic variety.** The condition (3.3.2) is expressed in an abstract form. In Paragraph 3.3.1.1, we extract from (3.3.2) a simplified system of equations that is amenable to a sort of Fourier analysis, see Paragraph 3.3.1.2. Then, as explained in Paragraph 3.3.1.3 and in coherence with basic concepts of wave-particle interactions [17, 33], this yields a kinetic interpretation of electron cyclotron resonances. Finally, Paragraph 3.3.1.4 gives an overview of the conductivity tensor which has to be studied carefully.

3.3.1.1. *A reduced system of equations.* From (3.2.55)-(3.2.58), we can extract the equations composing (3.3.2). Since by assumption $\nabla_{\mathbf{p}}\phi \equiv 0$, the term coming with ε^{-1} in factor after substitution of (3.3.1) inside (3.2.56) furnishes:

$$\partial_{\mathbf{t}}\phi\ \partial_\theta \mathscr{F}_{0,1} + \frac{1}{\langle r\rangle}\ O(\mathbf{x})\, p\cdot\nabla_{\mathbf{x}}\phi\ \partial_\theta \mathscr{F}_{0,1} + \frac{\mathbf{b}_e(\mathbf{x})}{\langle r\rangle}\ \partial_\omega \mathscr{F}_{0,1} \tag{3.3.3}$$
$$- 2\, G_1^{\mathrm{d}}(\Psi(\rho,z))\, \partial_r F_1^{\mathrm{d}}(r^2)\ p\cdot\mathscr{E}_0 \ =\ 0\,.$$

For $\alpha \in \{2,\cdots,N\}$, the equations inside (3.2.55) give rise to:

$$\partial_{\mathbf{t}}\phi\ \partial_\theta \mathscr{F}_{0,\alpha} \ +\ 2\ G_\alpha^{\mathrm{d}}(\Psi(\rho,z))\ \partial_r F_\alpha^{\mathrm{d}}(r^2)\ p\cdot\mathscr{E}_0 = 0\,. \tag{3.3.4}$$

The Maxwell's equations (3.2.57) provide:

$$\partial_{\mathbf{t}}\phi\,\partial_\theta \mathscr{B}_0 \ +\ {}^tO(\mathbf{x})\nabla_{\mathbf{x}}\phi\times\partial_\theta\mathscr{E}_0 = 0\,, \tag{3.3.5a}$$
$$\partial_{\mathbf{t}}\phi\,\partial_\theta \mathscr{E}_0 \ -\ {}^tO(\mathbf{x})\nabla_{\mathbf{x}}\phi\times\partial_\theta\mathscr{B}_0 = \mathcal{J}_1\big(\mathscr{F}_{0,1}(\mathbf{t},\mathbf{x},\cdot)\big)\,, \tag{3.3.5b}$$

together with:

$${}^tO(\mathbf{x})\nabla_{\mathbf{x}}\phi\cdot\partial_\theta\mathscr{B}_0 = 0\,, \qquad {}^tO(\mathbf{x})\nabla_{\mathbf{x}}\phi\cdot\partial_\theta\mathscr{E}_0 = -\,\rho\big(\mathscr{F}_{0,1}(\mathbf{t},\mathbf{x},\cdot)\big)\,. \tag{3.3.6}$$

In view of (3.2.58), with $dp = r^2\, d\varpi\, d\omega\, dr$, we find that:

$$\mathcal{J}_1(\mathscr{F}_{0,1}) := \int_{\mathbb{R}^3} \frac{p}{\langle r\rangle}\ \mathscr{F}_{0,1}\, dp\,, \qquad \rho(\mathscr{F}_{0,1}) = \int_{\mathbb{R}^3} \mathscr{F}_{0,1}\, dp\,.$$

Consider the expansion in Fourier series of $\mathscr{U}_0(\mathbf{t},\mathbf{y},\cdot)$, as in (2.2.58). For the same reasons as in Section 2.3, only one Fourier coefficient is switched on.

Assumption 3.3.1. *[presence of a non-trivial monochromatic electromagnetic oscillation] There is some non-zero integer $l \in \mathbb{N}^*$ such that:*

$$(E_0^l, B_0^l) \equiv (\bar{E}_0^{-l}, \bar{B}_0^{-l}) \not\equiv 0\,, \qquad \mathcal{U}_0^\ell \equiv 0\,, \qquad \forall\, \ell \in \mathbb{Z}\setminus\{-l,l\}\,. \tag{3.3.7}$$

Recall the following notations (already introduced in Section 2.3.1):

$$\tau := l\ \partial_{\mathbf{t}}\phi(\mathbf{t},\mathbf{x}) \in \mathbb{R}\,, \qquad \xi := l\ {}^tO(\mathbf{x})\,\nabla_{\mathbf{x}}\phi(\mathbf{t},\mathbf{x}) \in \mathbb{R}^3\,.$$

Then, from equations (3.3.3) and (3.3.4), we can extract:

$$\Big[i\,\tau + i\,\frac{1}{\langle r\rangle}\,p\cdot\xi + \frac{\mathbf{b}_e}{\langle r\rangle}\,\partial_\omega\Big]\,\mathcal{F}_{0,1}^l = 2\,G_1^{\mathrm{d}}(\Psi(\rho,z))\ \partial_r F_1^{\mathrm{d}}(r^2)\ p\cdot E_0^l\,. \tag{3.3.8}$$

On the other hand, from equation (3.3.4), we get:

$$\forall\, \alpha \in \{2, \cdots, N\}\,, \qquad i\,\tau \mathcal{F}^l_{0,\alpha} = -\,2\; G^{\rm d}_\alpha(\Psi(\rho,z))\; \partial_r F^{\rm d}_\alpha(r^2)\; p\cdot E^l_0\,. \tag{3.3.9}$$

Moreover, the Maxwell's equations (3.3.5)-(3.3.6) reduce to:

$$\tau B^l_0 \,+\, \xi\times E^l_0 = 0\,, \qquad\qquad \xi\times B^l_0 - \tau E^l_0 = i\,\mathcal{J}_1(\mathcal{F}^l_{0,1})\,, \tag{3.3.10a}$$

$$\xi\cdot B^l_0 = 0\,, \qquad\qquad \xi\cdot E^l_0 = i\,\rho(\mathcal{F}^l_{0,1})\,. \tag{3.3.10b}$$

Lemma 3.3.1. *Fix $\tau\neq 0$ and assume that $(\mathcal{F}^l_{0,1}, E^l_0, B^l_0)$ satisfies (3.3.8) and (3.3.10a). Then, the two equations of (3.3.10b) are satisfied.*

Proof. Knowing that $\tau\neq 0$, the scalar product with ξ of the first equation in (3.3.10a) yields directly $\xi\cdot B^l_0 = 0$. Using the second equation of (3.3.10a), we get:

$$-\,\tau\;\xi\cdot E^l_0 = i\;\xi\cdot\mathcal{J}_1(\mathcal{F}^l_{0,1})\,. \tag{3.3.11}$$

Integrate (3.3.8) with respect to p in order to obtain:

$$\tau\,\rho(\mathcal{F}^l_{0,1}) + \xi\cdot\mathcal{J}_1(\mathcal{F}^l_{0,1}) = 0\,. \tag{3.3.12}$$

Combining (3.3.11) and (3.3.12), since $\tau\neq 0$, we get the second equation of (3.3.10b). □

In view of Lemma 3.3.1, we can forget about the condition (3.3.10b). On the other hand, we can eliminate B^l_0 from (3.3.10a) to retain:

$$\big[(\tau^2 - |\xi|^2)\,Id + \xi\,{}^t\xi\big]\,E^l_0 \;=\; -\,i\;\tau\;\mathcal{J}_1(\mathcal{F}^l_0)\,. \tag{3.3.13}$$

Observe that the functions $\mathcal{F}^l_{0,\alpha}$ with $\alpha\neq 1$ are not present at the level of (3.3.8)-(3.3.13). Thus, knowing what E^l_0 is, we can deduce the expressions $\mathcal{F}^l_{0,\alpha}$ from (3.3.9). The relation (3.3.9) just says that the presence of a non trivial electric field E^l_0 is associated with the production of oscillations at the level of the ions's kinetic distribution functions.

We now concentrate on the remaining system (3.3.8)-(3.3.13) on $(\mathcal{F}^l_{0,1}, E^l_0)$. To simplify the notations, like we did in Section 2.3.1, we drop the subscript 1. We use the notations $G^{\rm d}$, $F^{\rm d}$ and $\mathcal{F}^l_0$ instead of $G^{\rm d}_1$, F^d_1 and $\mathcal{F}^l_{0,1}$. Define $\xi_\perp := |\xi|\,\sin\varpi_\xi$ and $\xi_\parallel := |\xi|\,\cos\varpi_\xi$. The spherical coordinates which are associated with the direction $\xi\in\mathbb{R}^3$ are:

$$\xi = |\xi|\,(\cos\omega_\xi\sin\varpi_\xi\,,\,\sin\omega_\xi\sin\varpi_\xi\,,\,\cos\varpi_\xi) := (\xi_\perp\cos\omega_\xi\,,\,\xi_\perp\sin\omega_\xi\,,\,\xi_\parallel)\,.$$

Another preliminary step is to reduce the discussion to the case where $\omega_\xi = 0$. This can be done by rotation of both ξ and p. Let $R\in SO(3)$ be such that:

$$R\,\xi = (\xi_\perp, 0, \xi_\parallel)\,, \qquad \breve{p} := R\,p = |p|\,\big(\cos(\omega-\omega_\xi)\,\sin\varpi\,,\,\sin(\omega-\omega_\xi)\,\sin\varpi\,,\,\cos\varpi\,\big)\,.$$

Introduce:

$$\breve{\mathcal{F}}^l_0(\mathbf{t},\mathbf{x},\breve{p}) := \mathcal{F}^l_0(\mathbf{t},\mathbf{x},{}^t\!R\,\breve{p}) \equiv \mathcal{F}^l_{0,1}(\mathbf{t},\mathbf{x},{}^t\!R\,\breve{p})\,, \qquad \breve{E}^l_0(\mathbf{t},\mathbf{x}) := R\,E^l_0(\mathbf{t},\mathbf{x})\,. \tag{3.3.14}$$

Lemma 3.3.2. *The couple $(\breve{\mathcal{F}}^l_0, \breve{E}^l_0)$ is a solution to (3.3.8)-(3.3.13) with $\xi = (\xi_\perp, 0, \xi_\parallel)$.*

Proof. The equation (3.3.8) amounts to the same thing as:

$$\big[i\,\tau + i\,\frac{1}{\langle r\rangle}\,Rp\cdot R\xi + \frac{\mathbf{b}_e}{\langle r\rangle}\,\partial_\omega\big]\,\mathcal{F}_0^l(\mathbf{t},\mathbf{x},p) = 2\,G^{\mathrm{d}}\big(\Psi(\rho,z)\big)\;\partial_r F^{\mathrm{d}}(r^2)\;Rp\cdot RE_0^l\,.$$

Replace p by ${}^tR\,\breve{p}$ to recover (3.3.8) for $(\breve{\mathcal{F}}_0^l,\breve{E}_0^l)(\mathbf{t},\mathbf{x},\breve{p})$, this time with $\xi=(\xi_\perp,0,\xi_\parallel)$. On the other hand, apply the matrix R to the left of (3.3.13) to find:

$$\big[(\tau^2-|R\,\xi|^2)\,Id + (R\,\xi)\,{}^t(R\,\xi)\big]\,R\,E_0^l \;=\; -\,i\;\tau\;R\,\mathcal{J}_1(\mathcal{F}_0^l)\,.$$

Now, to obtain (3.3.13) for $(\breve{\mathcal{F}}_0^l,\breve{E}_0^l)$, it suffices to remark that:

$$R\,\mathcal{J}_1(\mathcal{F}_0^l) = \int_{\mathbb{R}^3}\frac{\breve{p}}{\langle|\breve{p}|\rangle}\;\mathscr{F}_{0,1}(\mathbf{t},\mathbf{x},{}^tR\,\breve{p})\;d\breve{p} = \mathcal{J}_1(\breve{\mathcal{F}}_0^l)\,. \qquad \square$$

The system (3.3.8)-(3.3.13) will be studied with $\xi=(\xi_\perp,0,\xi_\parallel)$. The general situation can be obtained by coming back from $(\breve{\mathcal{F}}_0^l,\breve{E}_0^l)$ to $(\mathcal{F}_0^l,E_0^l)$ through (3.3.14). From now on, we will assume that $\omega_\xi=0$.

3.3.1.2. *Fourier analysis through Jacobi-Anger identity.* Knowing that $\omega_\xi=0$, the equation (3.3.8) is translated into:

$$\Big[i\,\tau + i\,\frac{\mathbf{b}_e\,\zeta}{\langle r\rangle}\,\cos\omega + i\,\frac{r\,\xi_\parallel\,\cos\varpi}{\langle r\rangle} + \frac{\mathbf{b}_e}{\langle r\rangle}\,\partial_\omega\Big]\,\mathcal{F}_0^l = 2\,G^{\mathrm{d}}\big(\Psi(\rho,z)\big)\,\partial_r F^{\mathrm{d}}(r^2)\,p\cdot E_0^l\,. \tag{3.3.15}$$

This is a first order differential equation with respect to $\omega\in\mathbb{T}$. It can be analysed through a Fourier analysis in $\omega\in\mathbb{T}$. When doing this, the variables $\mathbf{x}$, ϖ, r, τ and ξ can be viewed as parameters. Define:

$$\zeta\equiv\zeta(\mathbf{x},r,\varpi,\xi_\perp) := r\;\xi_\perp\;\sin\varpi\;\mathbf{b}_e(\mathbf{x})^{-1}\,. \tag{3.3.16}$$

Now, we want to remove the variable coefficient in ω from the differential operator which in the equation (3.3.15) is inside brackets. This means concretely to eliminate the presence of "$\cos\omega$". This can be achieved by replacing $\mathcal{F}_0^l$ by

$$\mathfrak{F}_0^l(\mathbf{t},\mathbf{x},p) := \exp(i\,\zeta\,\sin\omega)\,\mathcal{F}_0^l(\mathbf{t},\mathbf{x},p)\,. \tag{3.3.17}$$

Then, the equation (3.3.15) becomes:

$$\Big[i\,\tau + \frac{i\,r\,\xi_\parallel\,\cos\varpi}{\langle r\rangle} + \frac{\mathbf{b}_e}{\langle r\rangle}\,\partial_\omega\Big]\,\mathfrak{F}_0^l = 2\,G^{\mathrm{d}}\big(\Psi(\rho,z)\big)\,\partial_r F^{\mathrm{d}}(r^2)\;p\cdot E_0^l\;\exp\left(i\,\zeta\,\sin\omega\right)\,. \tag{3.3.18}$$

By this way, we are reduced to the case of a linear differential equation in ω with constant coefficients. Now, we can deal with the equation (3.3.18) through a Fourier analysis like we did in Paragraph 2.3.1.1.b). Decompose $\mathfrak{F}_0^l(\cdot)$ according to:

$$\mathfrak{F}_0^l(\mathbf{t},\mathbf{x},\varpi,\omega,r) \;=\; \sum_{m\in\mathbb{Z}}\mathfrak{F}_0^{l,m}(\mathbf{t},\mathbf{x},\varpi,r)\;e^{i\,m\,\omega}\,.$$

The counterpart of the change (3.3.17) is that all the Fourier coefficients (with respect to ω) of the right hand side of (3.3.18) are non zero.

Lemma 3.3.3. *The condition (3.3.18) is satisfied if and only if, for all $m \in \mathbb{Z}$, we have:*

$$i\,[\tau+\tau_m]\,\mathfrak{F}_0^{l,m} = 2\,r\,G^{\mathrm{d}}(\Psi(\rho,z))\;\partial_r F^{\mathrm{d}}(r^2)\begin{pmatrix} m\;\zeta^{-1}\,J_m(\zeta)\,\sin\varpi \\ -\,i\,J_m'(\zeta)\,\sin\varpi \\ J_m(\zeta)\,\cos\varpi \end{pmatrix}\cdot E_0^l\,, \tag{3.3.19}$$

where:

$$\tau_m(\mathbf{x},p,\xi) \equiv \tau_m(\mathbf{x},r,\varpi,\xi) := \langle r\rangle^{-1}\,(r\,\xi_\parallel\,\cos\varpi + m\,\mathbf{b}_e) = -\,\tau_{-m}(\mathbf{x},r,\pi-\varpi,\xi)\,. \tag{3.3.20}$$

Proof. It suffices to compute the Fourier coefficient in ω of the right hand side of (3.3.18). To do so, recall the Jacobi-Anger identity:

$$\exp(i\,\zeta\,\sin\omega) = \sum_{m\in\mathbb{Z}} J_m(\zeta)\;e^{i\,m\,\omega}\,,\qquad \forall\,(\zeta,\omega)\in\mathbb{R}\times\mathbb{T}\,, \tag{3.3.21}$$

where $J_m(\cdot)$ denotes the m-th Bessel function of the first kind. The formula (3.3.19) is a consequence of (3.3.21) together with the wellknown relations:

$$J_{m+1}(\zeta) + J_{m-1}(\zeta) = 2\;m\;\zeta^{-1}\,J_m(\zeta)\,, \tag{3.3.22a}$$

$$J_{m+1}(\zeta) - J_{m-1}(\zeta) = -\,2\;J_m'(\zeta)\,. \tag{3.3.22b}$$

□

3.3.1.3. *Kinetic interpretation of electron cyclotron resonances.* Recall the definition (3.3.20) of τ_m. The expression $\tau+\tau_m$ depends on the position $\mathbf{x}\in\Omega$, the momentum $p\in\mathbb{R}^3$ with norm $r\in\mathbb{R}_+$ and pitch angle $\varpi\in[0,\pi]$, the direction $\xi\in\mathbb{R}^3$, the Fourier mode $m\in\mathbb{Z}$, and the time frequency $\tau\in\mathbb{R}$. The electrons gyrate with the local gyrofrequency $\mathbf{b}_e(\mathbf{x})$. On the other hand, their guiding centers move with the drift velocity $\mathbf{v}_G = r\,\cos\varpi\,e_3(\mathbf{x})$ where $e_3(\cdot)$ is the unit vector field pointing in the magnetic direction. Looking at ξ as a wave vector $\mathbf{k}\in\mathbb{R}^3$, we have $\mathbf{v}_G\cdot\mathbf{k} = r\;\xi_\parallel\;\cos\varpi$. Seen in this way, the function $\tau+\tau_m$ can be interpreted as a (relativistic) *gyroballistic dispersion function*, see [31]-chapter 7.

The important role of $\tau+\tau_m$ results naturally from the preceding asymptotic analysis. In view of (3.3.19), as long as $\tau+\tau_m\neq 0$, the expression $\mathfrak{F}_0^{l,m}$ can easily be expressed in terms of E_0^l. However, difficulties arise when $\tau+\tau_m = 0$. Below, such special values are set aside.

Definition 3.3.1. *[notion of resonance] Given $(\mathbf{x},p,\xi,m)\in\Omega\times\mathbb{R}^3\times\mathbb{R}^3\times\mathbb{Z}$, the resonant time frequency is given by $-\tau_m(\mathbf{x},r,\varpi,\xi)$. Equivalently, it is the time frequency τ satisfying the condition:*

$$\langle r\rangle\;\tau\;+\;r\;\xi_\parallel\;\cos\varpi\;+\;m\;\mathbf{b}_e(\mathbf{x})\;=\;0\,. \tag{3.3.23}$$

In (3.3.23), the quantity $\langle r\rangle\,\tau + r\,\xi_\parallel\,\cos\varpi$ can be viewed as a Doppler shifted frequency [17]. Since the right-hand term of (3.3.19) is divided by $\tau+\tau_m$ with $\tau+\tau_m\simeq 0$ near resonances, it can be said [33] that the interactions between the waves and the charged particles become strong when the particles sense the Doppler-shifted wave at its cyclotron frequency ($m=1$) or its harmonics ($m\in\mathbb{Z}$ with $m\neq 1$). The special case $m=0$ corresponds to the well-known Landau resonance.

Given $(\mathbf{x}, r, \varpi, \xi)$ and m, there exists obviously one and only one resonance, which is given by $\tau = -\tau_m(\mathbf{x}, r, \varpi, \xi) = 0$. Another issue is whether all values $\tau \in \mathbb{R}$ are resonant, and under what conditions.

Lemma 3.3.4. *[Infinite set of resonances] Fix $(\mathbf{x}, \xi) \in \Omega \times (\mathbb{R}^3 \setminus \{0\})$ as well as $\varpi \in [0, \pi]$ and $\tau \in \mathbb{R}$. There exists infinitely many $(m, r) \in \mathbb{Z} \times \mathbb{R}_+$ such that $\tau + \tau_m(\mathbf{x}, r, \varpi, \xi) = 0$.*

Proof. The condition $\tau + \tau_m = 0$ is equivalent to:

$$r^2\ (\tau^2 - \xi_\parallel^2\ \cos^2\varpi) - 2\ r\ m\ \mathbf{b}_e\ \xi_\parallel\ \cos\varpi + \tau^2 - m^2\ \mathbf{b}_e^2 = 0\,. \tag{3.3.24}$$

- First, if $\tau^2 = \xi_\parallel^2\ \cos^2\varpi = 0$, just take $m = 0$. Then, any value $r \in \mathbb{R}_+$ can be selected.

- Secondly, if $\tau^2 = \xi_\parallel^2\ \cos^2\varpi \neq 0$, to solve (3.3.24), it suffices to look at:

$$r(m) = \frac{\xi_\parallel^2\ \cos^2\varpi - m^2\,\mathbf{b}_e^2}{2\,m\,\mathbf{b}_e\,\xi_\parallel\ \cos\varpi} = -\,\frac{m\,\mathbf{b}_e}{2\,\xi_\parallel\ \cos\varpi} + O\Big(\frac{1}{m}\Big)\,.$$

Either for $m \to -\infty$ or for $m \to +\infty$, we find that $r(m) \geq 0$.

- Thirdly, if $\tau = 0$ and $\xi_\parallel^2\ \cos^2\varpi \neq 0$, the second order polynomial (3.3.24) has a double root which is given by:

$$r(m) = -\,\frac{m\,\mathbf{b}_e}{\xi_\parallel\ \cos\varpi}\,.$$

Again, either for $m \to -\infty$ or for $m \to +\infty$, we have $r(m) \geq 0$.

- Finally, assume that $\tau \neq 0$ and $\tau^2 \neq \xi_\parallel^2\ \cos^2\varpi$. The condition (3.3.24) can be seen as a quadratic equation to be solved for r, with discriminant:

$$\Delta = 4\ \tau^2\ (\xi_\parallel^2\ \cos^2\varpi + m^2\,\mathbf{b}_e^2 - \tau^2)\,.$$

Since, $\mathbf{b}_e(\mathbf{x}) > 0$, the number Δ is sure to become positive for all $m \in \mathbb{Z}$ sufficiently large. Then, the two roots $r_\pm(m)$ of (3.3.24) are:

$$r_-(m) := \frac{2\,m\,\mathbf{b}_e\,\xi_\parallel\ \cos\varpi - \sqrt{\Delta}}{2\,(\tau^2 - \xi_\parallel^2\ \cos^2\ \varpi)}\,, \qquad r_+(m) := \frac{2\,m\,\mathbf{b}_e\,\xi_\parallel\ \cos\varpi + \sqrt{\Delta}}{2\,(\tau^2 - \xi_\parallel^2\ \cos^2\varpi)}\,.$$

In particular, when $|m|$ goes to infinity, there remains:

$$r_\pm(m) := -\,\frac{m\,\mathbf{b}_e}{|\xi_\parallel\ \cos\ \varpi| \mp |\tau|} + O\Big(\frac{1}{m}\Big)\,.$$

For $m \to -\infty$, we find $r_-(m) \geq 0$, and the value $r_-(m)$ is suitable. Either for $m \to -\infty$ or for $m \to +\infty$, the selection of $r_+(m)$ is also relevant. □

A number of differences between the cold case (2.3.14) and the hot case (3.3.18) deserve to be emphasized. Theses aspects are commented below.

∘ *Cold situation.* At the level of (2.3.14), only three Fourier coefficients ($F_0^{l,-1}$, $F_0^{l,0}$ and $F_0^{l,1}$) are involved, and the set of resonances (namely $\tau = 0$ and $\tau = \pm\mathbf{b}_e$) is finite, simple and localized in the usual (time-space) cotangent space.

∘ *Hot situation.* When dealing with (3.3.18), all Fourier coefficients $\mathfrak{F}_0^{l,m}$ (with $m \in \mathbb{Z}$) make some non trivial contribution. Moreover, the structure of resonances is much more complicated. It is based on kinetic features, in the sense that the velocity p plays a role through special choices of ϖ and r. As revealed by Lemma 3.3.4, all values of τ are affected (for some p) by a (kinetic) resonance.

Technically, the implementation of all the coefficients $\mathfrak{F}_0^{l,m}$ comes from the change (3.3.17). In practice, this reveals the impact on the dispersion relations of fast (hot) beams of particles, as it can be achieved through the advection term $(\mathbf{v}\cdot\nabla_{\mathbf{x}})f$. For the same reasons, in the hot case, the time resonant frequency τ_m has come to depend on (r,ϖ). In some ways, the velocities $\mathbf{v}$ contribute to resonances that are dispatched in a continuum of time-space frequencies, instead of being focused on special positions.

The above discussion reveals that the resonances come from the interaction between an electromagnetic wave represented in (3.3.19) by $E_0^l(\mathbf{t},\mathbf{x})$ and a population of particles that is associated with $\mathfrak{F}_0^{l,m}(\mathbf{t},\mathbf{x},\varpi,r)$, where (m,r) is adjusted as in Lemma 3.3.4. This is consistent with the basic concepts of wave-particle interactions in collisionless plasmas [33].

In the hot case, as a consequence of the kinetic aspects, the approach of Section 2.3.1 cannot be implemented. Then, another method must be found. This starts below, in the next Paragraph 3.3.1.4, with formal computations. This continues in Section 3.3.2 with a rigorous work of justification.

3.3.1.4. *Formal resolution of the system (3.3.8)-(3.3.13).* In view of (3.3.17)-(3.3.18), the density coefficient $\mathcal{F}_0^l$ can be viewed as a linear function of E_0^l through:

$$\mathcal{F}_0^l(\mathbf{t},\mathbf{x},p) = \exp\left(-i\,\zeta\,\sin\omega\right)\ \mathfrak{F}_0^l(\mathbf{t},\mathbf{x},p) = V(\mathbf{t},\mathbf{x},p,\tau,\xi)\cdot E_0^l(\mathbf{t},\mathbf{x})\,, \tag{3.3.25}$$

where $V(\cdot)$ is the vector valued function which can be obtained by inverting the relations contained in (3.3.19). This furnishes:

$$\begin{aligned} V(\mathbf{t},\mathbf{x},p,\tau,\xi) \equiv V(\mathbf{x},r,\varpi,\tau,\xi_\perp,\xi_\parallel) &:= 2\,r\,G^{\mathrm{d}}\big(\Psi(\rho,z)\big)\ \partial_r F^{\mathrm{d}}(r^2) \\ &\times \sum_{(m,n)\in\mathbb{Z}^2} \frac{J_n(\zeta)}{i\,(\tau+\tau_m)} \begin{pmatrix} m\,\zeta^{-1}\,J_m(\zeta)\,\sin\varpi \\ -\,i\,J_m'(\zeta)\,\sin\varpi \\ J_m(\zeta)\,\cos\varpi \end{pmatrix} e^{i\,(m-n)\,\omega}\,. \end{aligned} \tag{3.3.26}$$

Due to the factor $(\tau+\tau_m)^{-1}$, it must be clear that the formula (3.3.26) has no sense at resonant time frequencies. Still, the relation (3.3.25) with $V(\cdot)$ as in (3.3.26) can be exploited in order to express $\mathcal{J}_1(\mathcal{F}_0^l)$ in terms of E_0^l.

Lemma 3.3.5. *The vector $\mathcal{J}_1(\mathcal{F}_0^l)$ can be determined through:*

$$\mathcal{J}_1(\mathcal{F}_0^l) = \sigma(\mathbf{x},\tau,\xi)\,E_0^l\,, \tag{3.3.27}$$

where the conductivity tensor $\sigma(\cdot)$ is given by:

$$\sigma(\mathbf{x},\tau,\xi) := -\,4\,\pi\,i\ G^{\mathrm{d}}\big(\Psi(\rho,z)\big)\sum_{n\in\mathbb{Z}}\int_0^{+\infty}\!\!\int_0^{\pi}\frac{r^4\ \partial_r F^{\mathrm{d}}(r^2)}{\langle r\rangle\,(\tau+\tau_n)}\ T_n\ dr\,d\varpi\,. \tag{3.3.28}$$

At the level of (3.3.28), with ζ and τ_n as in (3.3.16) and (3.3.20), the "T_n" symbol stands for the Hermitian matrix:

$$T_n := \begin{pmatrix} \dfrac{n^2\,J_n^2(\zeta)}{\zeta^2}\,\sin^3\varpi & \dfrac{i\,n\,J_n(\zeta)\,J_n'(\zeta)}{\zeta}\,\sin^3\varpi & \dfrac{n\,J_n^2(\zeta)}{\zeta}\,\cos\varpi\,\sin^2\varpi \\ -\dfrac{i\,n\,J_n(\zeta)\,J_n'(\zeta)}{\zeta}\,\sin^3\varpi & (J_n'(\zeta))^2\,\sin^3\varpi & -i\,J_n(\zeta)\,J_n'(\zeta)\,\cos\varpi\,\sin^2\varpi \\ \dfrac{n\,J_n^2(\zeta)}{\zeta}\,\cos\varpi\,\sin^2\varpi & i\,J_n(\zeta)\,J_n'(\zeta)\,\cos\varpi\,\sin^2\varpi & J_n^2(\zeta)\,\cos^2\varpi\,\sin\varpi \end{pmatrix}.$$

A first remark is about the general form of (3.3.28). There are some similarities with models already proposed. For instance, just replace $v_\perp$ and $v_\parallel$ respectively by $r\,\sin\varpi$ and $r\,\cos\varpi$ in the formulas (3.4) and (3.5) of [10]. But there are also some subtleties which for example are due to the factorization of $G^{\rm d}(\cdot)$ and to the relativistic context.

At this stage, the definition (3.3.28) of $\sigma(\cdot)$ is only formal. Indeed, the denominator $\tau+\tau_n$ vanishes at the resonances. At first sight, nothing guarantees that the improper integrals of (3.3.28) converge. On the other hand, in (3.3.28), the convergence (with respect to $n\in\mathbb{N}$) of the series could be problematic.

Proof. Recall that:

$$\mathcal{J}_1(\mathcal{F}_0^l) = \int_0^{+\infty}\!\!\int_0^{\pi}\!\!\int_{-\pi}^{\pi} \frac{r^3}{\langle r\rangle} \begin{pmatrix} \cos\omega\,\sin\varpi \\ \sin\omega\,\sin\varpi \\ \cos\varpi \end{pmatrix} \mathcal{F}_0^l(\mathbf{t},\mathbf{x},\varpi,\omega,r)\;\sin\varpi\;dr\,d\varpi\,d\omega\,.$$

With (3.3.22), (3.3.25) and (3.3.26), we get the result by direct calculation. □

Taking into account (3.3.27), the system (3.3.13) reduces to:

$$\mathfrak{N}(\mathbf{x},\tau,\xi)E_0^l = 0\,,\qquad \mathfrak{N}(\mathbf{x},\tau,\xi) := \xi\,{}^t\xi + (\tau^2-|\xi|^2)\,Id\, + i\,\tau\,\sigma(\mathbf{x},\tau,\xi)\,. \tag{3.3.29}$$

In accordance with what has been done in Chapter 2, we can now define the characteristic variety which is associated with hot magnetized plasmas.

Definition 3.3.2 (characteristic variety)**.** *The characteristic variety which is associated with hot magnetized plasmas is the subset $\mathscr{V}$ of the cotangent bundle T^*M composed of:*

$$\mathscr{V} := \big\{(\mathbf{t},\mathbf{x},\tau,\xi)\in[0,1]\times\Omega\times(\mathbb{R}^4\setminus\{0\})\,;\,\det\mathfrak{N}(\mathbf{x},\tau,\xi)=0\big\}\,. \tag{3.3.30}$$

The relation $\det\mathfrak{N}(\mathbf{x},\tau,\xi)=0$ depends on $\mathbf{x}\in\Omega$, on $\tau\in\mathbb{R}$, on $|\xi|\in\mathbb{R}_+$ and on the angle $\varpi_\xi\in[0,\pi]$. But, as in Chapter 2, it neither involves the time $\mathbf{t}\in[0,1]$ nor implies the angle $\omega_\xi\in[0,2\pi]$. For some subset $\mathrm{V}(\mathbf{x},\varpi)$ of the half-space $\mathbb{R}\times\mathbb{R}_+$, we have:

$$\mathscr{V} := \big\{\,(\mathbf{t},\mathbf{x},\tau,\xi)\in[0,1]\times\Omega\times(\mathbb{R}^4\setminus\{0\})\,;\,(\tau,|\xi|)\in\mathrm{V}(\mathbf{x},\varpi_\xi)\,\big\}\,. \tag{3.3.31}$$

Locally, in the neighbouhood of a regular point of $\mathscr{V}$, the characteristic variety can be parameterized as follows:

$$\mathscr{V} = \big\{\,(\mathbf{x},\tau,\xi)\in\Omega\times(\mathbb{R}^4\setminus\{0\})\,;\,D_M(\mathbf{x},\tau,\xi)=0\,\big\}\,,$$

where $D_M(\cdot)$ stands for the dispersion relation of electromagnetic waves. Note that the gyroballistic dispersion function $D_m=\tau+\tau_m$ is constitutive of the definition (3.3.28), and therefore of $D_M(\cdot)$.

There have been many interpretations of wave-particle interaction. A way of doing things is to suppose that the dispersion relation $D_M(\cdot)$ is given *a priori*. Then, it is to locate the positions $(\mathbf{x}, \tau, \xi)$ where $D_M(\mathbf{x}, \tau, \xi) = 0$ and $D_m(\mathbf{x}, p, \tau, \xi) = 0$ (for some p), and to consider that it is where the exchanges of energy take place through *gyroresonant wave conversion* [7]. We adopt here a different approach since the effects of $D_m(\cdot)$ are directly incorporated inside $D_M(\cdot)$. As a byproduct, when defining $D_M(\cdot)$, we are faced with new difficulties (of convergence and summability), which are solved in the next Part 3.3.2.

The questions about active power transfer will not be investigated in this article. It is the next step, related to the transport equations on the amplitudes. These equations could be obtained by looking at what appears with ε^0 in factor in the WKB hierarchy.

3.3.2. **Analysis of the conductivity tensor $\sigma(\cdot)$.** In the cold case [6], exact algebraic dispersion relations are available. In contrast, in the hot case, the formula (3.3.28) cannot be solved analytically. It is not clear whether the matrix $\sigma(\cdot)$ makes sense. In fact, in most texts on plasma physics, this last difficulty is simply avoided by working in the upper half of the complex plane, that is with $Im\,\tau > 0$. Then, the discussion provides information on the damping or the amplification of waves, but not on the geometry of propagation (which says how to send or receive signals).

In this Part 3.3.2, the matter is to show that, even when $\tau \in \mathbb{R}$, the coefficients of $\sigma(\cdot)$ are all well-defined. This means to verify that the improper integrals involved at the level of (3.3.28) are convergent for all $n \in \mathbb{Z}$, and also that (3.3.28) gives rise to a convergent series with respect to $n \in \mathbb{N}$. To our knowledge, the following analysis is new.

We consider here the general situation, that is when $\xi_\parallel \neq 0$ and $\xi_\perp \neq 0$. The discussion starts in Paragraph 3.3.2.1 with a change of variables allowing to transform (3.3.28) in a usable way. This allows to highlight the role of the Hilbert transform, which is introduced in Paragraph 3.3.2.2.

3.3.2.1. *A change of variables.* Consider the transformation:

$$\begin{array}{rccc} \Phi: &]0,+\infty[\times]0,\pi[& \longrightarrow & D \\ & (r,\varpi) & \longmapsto & (y,z) := \big(\, r\,\cos\varpi\,,\,\langle r\rangle\,\big)\,, \end{array}$$

where:

$$D := \Big\{\, z \in]1,+\infty[\ ,\ y \in \,]-\sqrt{z^2-1},\sqrt{z^2-1}[\,\Big\}\,.$$

The Jacobian of the transformation Φ is given by

$$J_\Phi(\Phi^{-1}(y,z)) := z^{-1}\,\sqrt{z^2-1}\,\sqrt{z^2-1-y^2}\,. \tag{3.3.32}$$

On the other hand, with $F^d(\cdot)$ as in (3.2.38) and $\mathrm{F}^{\mathrm{d}}(\cdot)$ as indicated below, we have:

$$2\,(\partial_r F^{\mathrm{d}})(r^2) = z^{-1}\,\partial_z \mathrm{F}^{\mathrm{d}}(z)\,, \qquad \mathrm{F}^{\mathrm{d}}(z) := F^{\mathrm{d}}(z^2-1) = F^{\mathrm{d}}(r^2)\,. \tag{3.3.33}$$

Using (3.3.32) and (3.3.33), the matrix $\sigma(\cdot)$ can be rewritten:

$$\sigma(\mathbf{x},\tau,\xi) := -2\,\pi\,i\;G^{\mathrm{d}}\big(\Psi(\rho,z)\big) \times \sum_{m\in\mathbb{Z}} \int_1^{+\infty} \left(\int_{-\sqrt{z^2-1}}^{\sqrt{z^2-1}} \frac{\mathcal{T}_m(y,z)}{\tau\,z+\xi_\parallel\,y+m\,\mathbf{b}_e}\;dy \right)\;\partial_z \mathrm{F}^{\mathrm{d}}(z)\;dz\,. \tag{3.3.34}$$

In (3.3.34), $\mathcal{T}_m(y,z)$ is the skew-symmetric matrix whose coefficients are given by:

$$\mathcal{T}_m^{1,1} := \frac{m^2\,J_m^2(\zeta)}{\zeta^2}\;(z^2-1-y^2)\,, \qquad \mathcal{T}_m^{1,2} := \frac{i\,m\,J_m(\zeta)\,J_m'(\zeta)}{\zeta}\;(z^2-1-y^2)\,, \tag{3.3.35a}$$

$$\mathcal{T}_m^{1,3} := \frac{m\,J_m^2(\zeta)}{\zeta}\;y\;\sqrt{z^2-1-y^2}\,, \qquad \mathcal{T}_m^{2,1} := \frac{-i\,m\,J_m(\zeta)\,J_m'(\zeta)}{\zeta}\;(z^2-1-y^2)\,, \tag{3.3.35b}$$

$$\mathcal{T}_m^{2,2} := J_m'(\zeta)^2\;(z^2-1-y^2)\,, \qquad \mathcal{T}_m^{2,3} := -i\,J_m(\zeta)\,J_m'(\zeta)\;y\;\sqrt{z^2-1-y^2}\,, \tag{3.3.35c}$$

$$\mathcal{T}_m^{3,1} := \frac{m\,J_m^2(\zeta)}{\zeta}\;y\;\sqrt{z^2-1-y^2}\,, \qquad \mathcal{T}_m^{3,2} := i\,J_m(\zeta)\,J_m'(\zeta)\;y\;\sqrt{z^2-1-y^2}\,, \tag{3.3.35d}$$

$$\mathcal{T}_m^{3,3} := J_m^2(\zeta)\;y^2\,. \tag{3.3.35e}$$

In (3.3.35), the symbol ζ must be viewed as a function of (y,z) as indicated below:

$$\zeta = \xi_\perp\;\mathbf{b}_e(\mathbf{x})^{-1}\;\sqrt{z^2-1-y^2}\,. \tag{3.3.36}$$

In view of (3.3.35) and (3.3.36), the functions $\mathcal{T}_m^{i,j}(\cdot)$ are locally bounded.

3.3.2.2. *The Hilbert transform.* Consider the improper integral which at the level of (3.3.34) is inside brackets, that is:

$$\int_{-\sqrt{z^2-1}}^{\sqrt{z^2-1}} \frac{\mathcal{T}_m(y,z)}{\tau\,z+\xi_\parallel\,y+m\,\mathbf{b}_e}\;dy = \int_{\mathbb{R}} \frac{\mathcal{T}_m(y,z)}{\tau\,z+\xi_\parallel\,y+m\,\mathbf{b}_e}\;\mathbb{1}_{]-\sqrt{z^2-1},\sqrt{z^2-1}[}(y)\;dy\,.$$

Changing y into $\tilde{y}$ with $\tau\,z+\xi_\parallel\,y+m\,\mathbf{b}_e = \xi_\parallel\,\tilde{y}$, this becomes:

$$\int_{-\sqrt{z^2-1}}^{\sqrt{z^2-1}} \frac{\mathcal{T}_m(y,z)}{\tau\,z+\xi_\parallel\,y+m\,\mathbf{b}_e}\;dy = \frac{1}{\xi_\parallel}\;\mathcal{I}_0(z)\,, \qquad \mathcal{I}_0(z) := \int_{\mathbb{R}} \frac{\mathbf{T}_m(\tilde{y},z)}{\tilde{y}}\;d\tilde{y}\,, \tag{3.3.37}$$

where we have introduced:

$$\mathbf{T}_m(y,z) := \mathcal{T}_m\Big(y-\frac{(\tau\,z+m\,\mathbf{b}_e)}{\xi_\parallel},z\Big)\;\mathbb{1}_{]-\sqrt{z^2-1},\sqrt{z^2-1}[}\Big(y-\frac{(\tau\,z+m\,\mathbf{b}_e)}{\xi_\parallel}\Big)\,. \tag{3.3.38}$$

We have to specify a prescription for dealing with the singular denominator in the integral on the right hand side of (3.3.37). To this end, a standard procedure is to push the singularity above the real $\tilde{y}-$axis, in order to recover a well-defined contour integral. Given a small parameter $\eta\in\mathbb{R}_+^*$, this amounts to look at:

$$\tilde{\mathcal{I}}_\eta(z) := \int_{\mathbb{R}} \frac{\mathbf{T}_m(\tilde{y},z)}{\tilde{y}-i\,\eta}\;d\tilde{y}\,, \qquad \tilde{\mathcal{I}}_0(z) := \lim_{\eta\,\longrightarrow\,0+}\;\tilde{\mathcal{I}}_\eta(z)\,.$$

The Plemelj formula allows to define $\tilde{\mathcal{I}}_0(z)$ as a complex number whose real part is:

$$\mathcal{I}_0(z) := Re\ \tilde{\mathcal{I}}_0(z) = \mathcal{H}((\mathbf{T}_m(\cdot, z))(0)\,, \tag{3.3.39}$$

where the linear operator $\mathcal{H}$ is determined as indicated below.

Definition 3.3.3 (Hilbert transform)**.** *Given $f : \mathbb{R} \longrightarrow \mathbb{R}$ in the Schwartz space $\mathcal{S}(\mathbb{R})$, the Hilbert transform $\mathcal{H}\,f(\cdot)$ of $f(\cdot)$ is the function given by:*

$$\mathcal{H}\,f(x) := \lim_{\varepsilon \longrightarrow 0+} \mathcal{H}_\varepsilon\,f(x)\,, \qquad \mathcal{H}_\varepsilon\,f(x) := \int_{|x-y|\geq\varepsilon} \frac{f(y)}{x-y}\ dy\,. \tag{3.3.40}$$

The quantity $\mathcal{I}_0(z)$ inside (3.3.39) is usually associated with a *phase*, whereas the imaginary part of $\tilde{\mathcal{I}}_0(z)$ could be interpreted as inducing some damping or amplification effect on the *amplitude* of the waves. Now, the perspective of our WKB hierarchy is to look successively at the terms with different powers of ε in factor. In this process, the *eikonal equation* (ε^{-1}) is listed first, whereas the *modulation* (transport) equation (ε^0) is displayed after. From this standpoint, the primary step is to identify the *geometry* of the phase. In this respect, the definition (3.3.39) with $\mathbf{T}_m$ as in (3.3.38) is what comes first. This is why it is selected in what follows.

Of course alternative definitions of $\mathcal{I}_0(z)$ may be considered. But they will be ignored here, because the aim of this article is to focus on *dispersion relations*. Furthermore, as will be seen below, the formula (3.3.39) makes perfectly sense.

As a matter of fact, the Hilbert transform of the function $f(\cdot)$ is well-defined provided the integral (3.3.40) exists as a Cauchy principal value. Intuitively, the contributions related to the negative and positive values of $\tilde{y}$ can compensate when determining $\mathcal{I}_0(z)$ through the integral of (3.3.37). On the one hand, the function $\mathbf{T}_m(\cdot, z)$ of (3.3.38) has compact support. It is piecewise continuously differentiable, with two possible jumps. On the other hand, the operator $\mathcal{H}$ is an isometry on $L^2(\mathbb{R})$. It also maps bounded functions to the Banach space of bounded mean oscillation classes, denoted by $BMO(\mathbb{R})$. Since $\mathbf{T}_m(\cdot, z) \in (L^2 \cap L^\infty)(\mathbb{R})$ both arguments can be used to define $\mathcal{I}_0(z)$.

Coming back to the initial formulation (3.3.34), with (3.3.37) and (3.3.39) in mind, we can rewrite (3.3.34) in the form:

$$\sigma(\mathbf{x}, \tau, \xi) := \frac{2\,\pi\,i\ G^{\mathrm{d}}(\Psi(\rho, z))}{\xi_\parallel} \int_1^{+\infty} \mathcal{H}\left(\mathbf{T}\left(\cdot, z\right)\right)(0)\ \partial_z \mathrm{F}^{\mathrm{d}}\ dz\,, \tag{3.3.41}$$

where:

$$\mathbf{T}(y, z) := \sum_{m\in\mathbb{Z}} \mathbf{T}_m(y, z)\,, \tag{3.3.42}$$

The discussion about a rigorous definition of the dielectric tensor $\sigma(\cdot)$ is not finished. Supplementary estimates on $\mathcal{H}\left(\mathbf{T}\left(\cdot, z\right)\right)(0)$ are needed to be sure that, inside (3.3.41), the integral with respect to z is convergent. A functional framework that is suitable for that purpose is exhibited below.

Lemma 3.3.6. *Fix $x \in \mathbb{R}$ and $\eta > 0$. Assume that the function $f(\cdot)$ is in $L^1(\mathbb{R})$ and that it is Lipschitz on the interval $[x-\eta, x+\eta]$ with Lipschitz constant:*

$$\|f\|_{Lip([x-\eta,x+\eta])} := \sup_{x-\eta \le s < t \le x+\eta} \frac{|f(s)-f(t)|}{|s-t|}\,.$$

Then, the improper integral $\mathcal{H}\, f(x)$ is well-defined. Moreover, we have:

$$|\mathcal{H}\, f(x)| \le 2\,\eta\, \|f\|_{Lip([x-\eta,x+\eta])} + \eta^{-1}\, \|f\|_{L^1(\mathbb{R})}\,. \tag{3.3.43}$$

Proof. The expression $\mathcal{H}_\varepsilon\, f(x)$ makes sense and we have $|\mathcal{H}_\varepsilon\, f(x)| \le \varepsilon^{-1}\, \|f\|_{L^1(\mathbb{R})}$. Using the fact that t^{-1} is an odd function, we can split the integral of (3.3.40) according to:

$$\mathcal{H}_\varepsilon\, f(x) = \int_{\varepsilon<|t|<\eta} \frac{f(x-t)-f(x)}{t}\, dt + \int_{|t|\ge\eta} \frac{f(x-t)}{t}\, dt\,.$$

Then a rough estimate gives rise to:

$$|\mathcal{H}_\varepsilon\, f(x)| \le \int_{\varepsilon<|t|<\eta} \|f\|_{Lip([x-\eta,x+\eta])}\, dt + \eta^{-1} \int_{|t|\ge\eta} |f(x-t)|\, dt\,.$$

By passing to the limit ($\varepsilon \to 0$), we easily get the result from Lemma 3.3.6. □

The series (3.3.42) is in fact finite, with a number of terms depending on y and z. For $m \in \mathbb{Z}$ and $1 \le i, j \le 3$, we denote by $\mathbf{T}_m^{i,j}$ the coefficient of index (i,j) inside $\mathbf{T}_m$. The matter in the next Paragraphs 3.3.2.3 and 3.3.2.4 is to show that, at least for $(m,i,j) \neq (0,3,3)$, the functions $\mathbf{T}_m^{i,j}(\cdot, z)$ satisfy the assumptions of Lemma 3.3.6 for $x = 0$ and $\eta = 1$. The more singular case of $\mathbf{T}_0^{3,3}$ is handled separately. It is addressed in Paragraph 3.3.2.4.

3.3.2.3. *Lipschitz estimates.* We focus here on the Lipschitz condition of Lemma 3.3.6.

Lemma 3.3.7. *For all $(m,i,j) \in \mathbb{Z} \times [\![1,3]\!]^2 \setminus \{(0,3,3)\}$ and $z \in]1,+\infty[$, the function $\mathbf{T}_m^{i,j}(\cdot, z)$ is Lipschitz on $\mathbb{R}$. For all $(i,j) \in [\![1,3]\!]^2 \setminus \{(3,3)\}$, there exists a polynomial $P^{i,j}(\cdot) \in \mathbb{R}[X]$ such that:*

$$\forall\, z \in]1,+\infty[\,, \qquad \sum_{m\in\mathbb{Z}} \|\mathbf{T}_m^{i,j}(\cdot, z)\|_{Lip([-1,1])} \le P^{i,j}(\sqrt{z^2-1})\,. \tag{3.3.44}$$

There exists also a polynomial $P^{3,3}(\cdot) \in \mathbb{R}[X]$ such that:

$$\forall\, z \in]1,+\infty[\,, \qquad \sum_{m\in\mathbb{Z}^*} \|\mathbf{T}_m^{3,3}(\cdot, z)\|_{Lip([-1,1])} \le P^{3,3}(\sqrt{z^2-1})\,. \tag{3.3.45}$$

Proof. Fix $z \in [1,+\infty[$ and $(m,i,j) \in \mathbb{Z} \times [\![1,3]\!]^2 \setminus \{(0,3,3)\}$. Then, the function $\mathbf{T}_m^{i,j}(\cdot, z)$ is Lipschitz on $\mathbb{R}$ if and only if the function $\mathcal{T}_m^{i,j}(\cdot, z)\, \mathbb{1}_{]-\sqrt{z^2-1},\sqrt{z^2-1}[}(\cdot)$ is Lipschitz on $\mathbb{R}$. This function is clearly $\mathcal{C}^1$ on $\mathbb{R} \setminus \{\pm\sqrt{z^2-1}\}$. Difficulties can arise at $\pm\sqrt{z^2-1}$, due to the Heaviside step function. The idea is to compensate for this by the behaviour (vanishing

when $m \neq 0$) of the functions $J_m(\cdot)$ or by the $\sqrt{z^2-1-y^2}$ factor that appears in almost all the coefficients of $\mathcal{T}_m$. The Taylor expansions near $\zeta = 0$ of the Bessel functions are:

$$J_0(\zeta) \underset{\zeta\to 0}{=} 1 + O\Big(\zeta^2\Big)\,, \tag{3.3.46a}$$

$$J_{\pm 1}(\zeta) \underset{\zeta\to 0}{=} \pm\frac{1}{2}\,\zeta + O\Big(\zeta^2\Big)\,, \tag{3.3.46b}$$

$$J_n(\zeta) \underset{\zeta\to 0}{=} O\Big(\zeta^2\Big)\,, \qquad \forall\, n \in \mathbb{Z}\setminus\{0,\pm 1\}\,. \tag{3.3.46c}$$

It follows that, except for $(m,i,j) = (0,3,3)$, all the coefficients $\mathcal{T}_m^{i,j}(\cdot,z)$ of (3.3.35) vanish at the points $\pm\sqrt{z^2-1}$. The functions $\mathbf{T}_m^{i,j}(\cdot,z)$ are therefore continuous on $\mathbb{R}$. To see why the functions $\mathbf{T}_m^{i,j}(\cdot,z)$ are Lipschitz and why we have both (3.3.44) and (3.3.45), we need to be more specific. The corresponding verifications are carried out separately, in Appendix C, see Section C.1. □

3.3.2.4. L^1-*estimates.* We focus here on the L^1-bound required by Lemma 3.3.6.

Lemma 3.3.8. *Fix $(m,i,j) \in \mathbb{Z}\times[\![1,3]\!]^2$ and $z \in]1,+\infty[$. Then, $\mathbf{T}_m^{i,j}(\cdot,z) \in L^1(\mathbb{R})$. More precisely, we have:*

$$\forall\, z \in]1,+\infty[\,, \qquad \sum_{m\in\mathbb{Z}} \|\mathbf{T}_m^{i,j}(\cdot,z)\|_{L^1(\mathbb{R})} \leq 2\ (z^2-1)^{3/2}\,. \tag{3.3.47}$$

Proof. The function $\mathbf{T}_m^{i,j}(\cdot,z)$ is bounded on $\mathbb{R}$ with compact support. It is therefore integrable on $\mathbb{R}$. Moreover:

$$\|\mathbf{T}_m^{i,j}(\cdot,z)\|_{L^1(\mathbb{R})} = \int_{-\sqrt{z^2-1}}^{\sqrt{z^2-1}} \Big|\mathcal{T}_m^{i,j}(y,z)\Big|\ dy\,. \tag{3.3.48}$$

Observe that the matrix T_m has the following structure:

$$T_n = \begin{pmatrix} a^2\,\sin^3\varpi & i\,a\,b\,\sin^3\varpi & a\,c\,\cos\varpi\,\sin^2\varpi \\ -\,i\,a\,b\,\sin^3\varpi & b^2\,\sin^3\varpi & -\,i\,b\,c\,\cos\varpi\,\sin^2\varpi \\ a\,c\,\cos\varpi\,\sin^2\varpi & i\,b\,c\,\cos\varpi\,\sin^2\varpi & c^2\,\cos^2\varpi\,\sin\varpi \end{pmatrix},$$

with:

$$(a,b,c) = \big(\,m\,\zeta^{-1}\,J_m(\zeta)\,,\,J_m'(\zeta)\,,\,J_m(\zeta)\,\big)\,.$$

Thus, using the elementary case of Young's inequality, the off-diagonal coefficients can be controlled by the diagonal ones:

$$\forall\,(i,j) \in [\![1,3]\!]^2\,, \qquad \|\mathbf{T}_m^{i,j}(\cdot,z)\|_{L^1(\mathbb{R})} \leq 2^{-1}\Big(\|\mathbf{T}_m^{i,i}(\cdot,z)\|_{L^1(\mathbb{R})} + \|\mathbf{T}_m^{j,j}(\cdot,z)\|_{L^1(\mathbb{R})}\Big)\,. \tag{3.3.49}$$

To get (3.3.47), it suffices to prove the result for $\|\mathbf{T}_m^{i,i}(\cdot,z)\|_{L^1(\mathbb{R})}$ with $1 \leq i \leq 3$. To do so, recall the following addition theorem on the Bessel functions of the first kind ([34], p.358):

$$\forall\,(r,s,\theta) \in \mathbb{R}^2\times\mathbb{T}\,, \qquad \sum_{m\in\mathbb{Z}} J_m(r)\,J_m(s)\,e^{-im\theta} = J_0\Big(\sqrt{r^2+s^2-2\,r\,s\,\cos\theta}\Big)\,. \tag{3.3.50}$$

Looking at (3.3.50) for $r = s$ and $\theta = 0$, taking two derivatives of (3.3.50) with respect to θ at $r = s$ and $\theta = 0$, and then applying ∂_r and ∂_s at $r = s$ and $\theta = 0$, we find successively:

$$\forall\, r \in \mathbb{R}\,, \qquad \sum_{m\in\mathbb{Z}} J_m^2(r) = 1\,, \qquad \sum_{m\in\mathbb{Z}} m^2\, J_m^2(r) = \frac{r^2}{2}\,, \qquad \sum_{m\in\mathbb{Z}} J_m'(r)^2 = \frac{1}{2}\,. \tag{3.3.51}$$

Combining (3.3.35) and (3.3.51), we get:

$$\forall\, i \in [\![1,3]\!]\,, \qquad \forall\, y \in \,]-\sqrt{z^2-1}, \sqrt{z^2-1}[\,, \qquad \sup_{|y|\le\sqrt{z^2-1}} \sum_{m\in\mathbb{Z}} \Big|\mathcal{T}_m^{i,i}(y,z)\Big| \le z^2-1\,.$$

In view of (3.3.48), this estimate leads directly to (3.3.47). □

3.3.2.5. *Study of the most singular coefficient.* Of course, the expression $\mathbf{T}_0^{3,3}(y,z)$ does contribute at the level of (3.3.41). However, it cannot be treated as before. As a matter of fact, since $J_0(0) = 1$, for all $z > 1$, the function issued from (3.3.35e) and (3.3.38), say:

$$y \longmapsto \mathbf{T}_0^{3,3}\Big(y + \frac{\tau\, z}{\xi_\parallel}, z\Big) = y^2\; J_0^2\left(\frac{\xi_\perp}{\mathbf{b}_e}\sqrt{z^2-1-y^2}\right)\; \mathbb{1}_{]-\sqrt{z^2-1},\sqrt{z^2-1}[}(y)\,,$$

is discontinuous at the points $\pm\sqrt{z^2-1}$. In this particular case, another argument must be put forward.

Lemma 3.3.9. *Except possibly for two values of $z \in [1,+\infty[$, the expression $\mathcal{H}(\mathbf{T}_0^{3,3}(\cdot,z))(0)$ makes sense. Moreover, it is locally integrable with respect to $z \in [1,+\infty[$.*

Proof. The idea is to remove from $\mathbf{T}_0^{3,3}(\cdot,z)$ the singular part. To this end, introduce the following decomposition:

$$\mathbf{T}_0^{3,3}(y,z) = \mathfrak{T}_0^{3,3}(y,z) + (z^2-1)\; \mathbb{1}_{]-\sqrt{z^2-1},\sqrt{z^2-1}[}\left(y - \frac{\tau z}{\xi_\parallel}\right),$$

where:

$$\mathfrak{T}_0^{3,3}(y,z) := \mathbf{T}_0^{3,3}(y,z) - (z^2-1)\; \mathbb{1}_{]-\sqrt{z^2-1},\sqrt{z^2-1}[}\left(y - \frac{\tau z}{\xi_\parallel}\right).$$

In view of (3.3.46a), the function $\mathfrak{T}_0^{3,3}(\cdot,z)$ is continuous on $\mathbb{R}$ with compact support. The information (C.1.2f), (C.1.9) and (C.1.11) indicates that $\partial_y \mathcal{T}_0^{3,3}(\cdot,z)$ is bounded on the interval $]-\sqrt{z^2-1}, \sqrt{z^2-1}[$. It follows that $\mathfrak{T}_0^{3,3}(\cdot,z)$ is Lipschitz on $\mathbb{R}$. Moreover, there exists a polynomial $P_0^{3,3}(\cdot) \in \mathbb{R}[X]$ such that:

$$\forall\, z \in [1,+\infty[\,, \qquad \|\mathfrak{T}_0^{3,3}(\cdot,z)\|_{Lip([-1,1])} \le P_0^{3,3}(\sqrt{z^2-1})\,. \tag{3.3.52}$$

From Lemma 3.3.8, we know that $\mathfrak{T}_0^{3,3}(\cdot,z)$ belongs to $L^1(\mathbb{R})$. Thus, to define $\mathcal{H}(\mathfrak{T}_0^{3,3}(\cdot,z))(0)$, we can apply Lemma 3.3.6. We now turn to the remaining (more singular) part.

The Hilbert transform of the characteristic function $\mathbb{1}_{[a,b]}(\cdot)$ is given by:

$$\forall\, t \in \mathbb{R}\setminus\{a,b\}\,, \qquad \mathcal{H}(\mathbb{1}_{[a,b]}(\cdot))(t) \;=\; \ln\left|\frac{t-a}{t-b}\right|\,.$$

Thus, for almost every $z \in]1,+\infty[$, we have:

$$\mathcal{H}\Big((z^2-1)\,\mathbb{1}_{]-\sqrt{z^2-1},\sqrt{z^2-1}[}\,(\cdot-\frac{\tau z}{\xi_\parallel})\Big)(0) = (z^2-1)\ \ln\left|\frac{\xi_\parallel^{-1}\,\tau\,z+\sqrt{z^2-1}}{\xi_\parallel^{-1}\,\tau\,z-\sqrt{z^2-1}}\right|. \tag{3.3.53}$$

More precisely, (3.3.53) is well-defined for all $z \in]1,+\infty[$ when $|\tau| > \sqrt{2}\ |\xi_\parallel|$. On the contrary, when $|\tau| \le \sqrt{2}\ |\xi_\parallel|$, only the two values $z_\pm = \pm\,\xi_\parallel^{-1}\sqrt{\tau^2-\xi_\parallel^2}$ can be problematic. However, the logarithmic behaviour near the (potentially) singular points $z_\pm$ is compatible with L^1_{loc}-estimates. Retain also that the asymptotic behaviour of (3.3.53) when $z \to \pm\infty$ is controlled by $C\,(z^2-1)$ for some constant $C \in \mathbb{R}_+$.

□

Using (3.3.41), it is now possible to define rigorously the conductivity tensor $\sigma(\cdot)$.

Lemma 3.3.10. *In (3.3.41), the Lebesgue integral*

$$\int_1^{+\infty} \mathcal{H}(\mathbf{T}(\cdot,z))(0)\ \partial_z \mathrm{F}^{\mathrm{d}}(z)\ dz \tag{3.3.54}$$

is well-defined and finite.

Proof. For $(i,j) \neq (3,3)$, applying the inequality (3.3.43) with Lemmas 3.3.7 and 3.3.8, we obtain that $\mathcal{H}(\mathbf{T}^{i,j}(\cdot,z))(0)$ is locally bounded with respect to $z \in]1,+\infty[$, and therefore it is locally integrable. In view of (3.3.45) and Lemma 3.3.9, the coefficient $\mathcal{H}(\mathbf{T}^{3,3}(\cdot,z))(0)$ is also locally integrable.

Now, recall that $\mathrm{F}^{\mathrm{d}}(\cdot) \in \mathcal{S}(\mathbb{R}_+;\mathbb{R})$. Thus, the controls (3.3.44), (3.3.45), (3.3.47) and (3.3.52), by at most some polynomial growth in z is compensated by the rapid decreasing of $\partial_z \mathrm{F}^{\mathrm{d}}(\cdot)$. The integrand inside (3.3.54) is in $L^1(]1,+\infty[)$. □

3.3.3. **Interesting case studies.** It was shown in Section 3.3.2 that the matrix $\sigma(\cdot)$ is well-defined for all ξ such that $\xi_\parallel \neq 0$ and $\xi_\perp \neq 0$. The case of a parallel propagation ($\xi_\perp = 0$) is considered in Paragraph 3.3.3.1. The case of a perpendicular propagation ($\xi_\parallel = 0$) is studied in Paragraph 3.3.3.2. From the viewpoint of the number of resonances to be taken into account, that is the number of nonzero terms in the sum (3.3.28), the following may be noted. There is a growing complexity when passing from the parallel case (involving the choices $m=-1$, $m=0$ and $m=1$), to the generic case of Section 3.3.2 (implying a finite number of m), up to the perpendicular case (giving rise to the selection of an infinite number of $m \in \mathbb{Z}$).

3.3.3.1. *Parallel propagation ($\xi_\perp = 0$ and $\xi_\parallel \neq 0$).* When $\xi_\perp = 0$, as indicated in (3.3.36), we simply find $\zeta = 0$. Now, in many formulas such as (3.3.26) or (3.3.35), the term ζ^{-1} appears in factor. However, this singularity is compensated by $m\,J_m(\zeta)$. Indeed, the relation (3.3.22a) is valid for all values of $m \in \mathbb{Z}$ and $\zeta \in \mathbb{R}$. The function $\chi_m : \zeta \mapsto m\,\zeta^{-1}\,J_m(\zeta)$ can be extended to some analytic function on $\mathbb{R}$ satisfying:

$$\chi_{\pm 1}(0) = \frac{1}{2}\,, \qquad \chi_m(0) = 0\,, \qquad \forall\, m \in \mathbb{Z} \setminus \{-1,+1\}\,. \tag{3.3.55}$$

It follows that the matrices T_n of Lemma 3.3.5 are zero except if $n \in \{-1, 0, +1\}$. We find:

$$\begin{aligned}\sigma(\mathbf{x},\tau,\xi) &= -4\,\pi\,i\;G^{\mathrm{d}}\big(\Psi(\rho,z)\big)\;\sum_{|n|\le 1}\int_0^{+\infty}\!\!\int_0^{\pi}\frac{r^4\;\partial_r F^{\mathrm{d}}(r^2)}{\langle r\rangle\,(\tau+\tau_n)}\;T_n\;dr\,d\varpi\,.\\ &= -4\,\pi\,i\;G^{\mathrm{d}}\big(\Psi(\rho,z)\big)\;\int_0^{+\infty}\!\!\int_0^{\pi}r^4\;\partial_r F^{\mathrm{d}}(r^2)\;T(\mathrm{par})\;dr\,d\varpi\,,\end{aligned}\tag{3.3.56}$$

with:

$$T(\mathrm{par}) := \begin{pmatrix} \dfrac{\big(\langle r\rangle\tau + r\xi_\parallel\cos\varpi\big)\sin^3\varpi}{2\Big[\big(\langle r\rangle\tau + r\xi_\parallel\cos\varpi\big)^2 - \mathbf{b}_e^2\Big]} & \dfrac{-i\,\mathbf{b}_e\sin^3\varpi}{2\Big[\big(\langle r\rangle\tau + r\xi_\parallel\cos\varpi\big)^2 - \mathbf{b}_e^2\Big]} & 0\\ \dfrac{i\,\mathbf{b}_e\sin^3\varpi}{2\Big[\big(\langle r\rangle\tau + r\xi_\parallel\cos\varpi\big)^2 - \mathbf{b}_e^2\Big]} & \dfrac{\big(\langle r\rangle\tau + r\xi_\parallel\cos\varpi\big)\sin^3\varpi}{2\Big[\big(\langle r\rangle\tau + r\xi_\parallel\cos\varpi\big)^2 - \mathbf{b}_e^2\Big]} & 0\\ 0 & 0 & \dfrac{\cos^2\varpi\,\sin\varpi}{\langle r\rangle\tau + r\xi_\parallel\cos\varpi}\end{pmatrix}.$$

When $\xi_\perp = 0$, the condition $\det\mathfrak{N}(\mathbf{x},\tau,\xi) = 0$ defining the characteristic variety can be computed according to:

$$\Lambda_L\;\Lambda_T^-\;\Lambda_T^+ \;=\; 0\,.\tag{3.3.57}$$

To simplify, note $\kappa \equiv \kappa(\mathbf{x}) := 4\,\pi\,G^{\mathrm{d}}\big(\Psi(\rho,z)\big)$. We can distinguish three conditions:

$$\Lambda_L(\mathbf{x},\tau,\xi_\parallel) := \tau^2 + \kappa\,\tau\int_0^{+\infty}\!\!\int_0^{\pi}\frac{r^4\partial_r F^{\mathrm{d}}(r^2)\cos^2\varpi\sin\varpi}{\langle r\rangle\tau + r\xi_\parallel\cos\varpi}\;dr\,d\varpi = 0\,,\tag{3.3.58a}$$

$$\Lambda_T^-(\mathbf{x},\tau,\xi_\parallel) := \tau^2 - \xi_\parallel^2 - \kappa\,\tau\int_0^{+\infty}\!\!\int_0^{\pi}\frac{r^4\partial_r F^{\mathrm{d}}(r^2)\sin^3\varpi}{2\Big[\langle r\rangle\tau + r\xi_\parallel cos\varpi - \mathbf{b}_e\Big]}\;dr\,d\varpi = 0\,,\tag{3.3.58b}$$

$$\Lambda_T^+(\mathbf{x},\tau,\xi_\parallel) := \tau^2 - \xi_\parallel^2 - \kappa\,\tau\int_0^{+\infty}\!\!\int_0^{\pi}\frac{r^4\partial_r F^{\mathrm{d}}(r^2)\sin^3\varpi}{2\Big[\langle r\rangle\tau + r\xi_\parallel cos\varpi + \mathbf{b}_e\Big]}\;dr\,d\varpi = 0\,.\tag{3.3.58c}$$

Recall (3.3.31). In the case of parallel propagation where $\varpi_\xi = \xi_\perp = 0$, the set $\mathrm{V}(\mathbf{x},0)$ is usually separated into two parts, corresponding to the different possibilities marked above.

a) Transverse waves. We find two components $\mathrm{V}_T^+(\mathbf{x},0)$ and $\mathrm{V}_T^-(\mathbf{x},0)$ which are respectively defined by:

$$\mathrm{V}_T^-(\mathbf{x},0) \;=\; \Big\{\,(\tau,|\xi|)\in\mathbb{R}\times\mathbb{R}_+\,;\,\Lambda_T^-(\mathbf{x},\tau,|\xi|) = 0\,\Big\}\,,\tag{3.3.59a}$$

$$\mathrm{V}_T^+(\mathbf{x},0) \;=\; \Big\{\,(\tau,|\xi|)\in\mathbb{R}\times\mathbb{R}_+\,;\,\Lambda_T^+(\mathbf{x},\tau,|\xi|) = 0\,\Big\}\,.\tag{3.3.59b}$$

b) Longitudinal waves. We find only one component:

$$\mathrm{V}_L(\mathbf{x},0) \;=\; \Big\{\,(\tau,|\xi|)\in\mathbb{R}\times\mathbb{R}_+\,;\,\Lambda_L(\mathbf{x},\tau,|\xi|) = 0\,\Big\}\,.\tag{3.3.60}$$

3.3.3.2. *Perpendicular propagation ($\xi_{\|} = 0$ and $\xi_{\perp} \neq 0$).* The content of Paragraph 3.3.2.1 is still valid in the case $\xi_{\|} = 0$. However, the interpretation of $\sigma(\cdot)$ as in (3.3.41) does not hold. To get around this difficulty, the idea is to use Fubini's theorem at the level of (3.3.34) in order to recognize some Hilbert transform issued from an integration with respect to z (instead of y). The equation (3.3.34) then becomes:

$$\begin{aligned}\sigma\,(\mathbf{x},\tau,(\xi_{\perp},0,0)) &:= -\,2\,\pi\,i\;G^{\mathrm{d}}(\Psi(\rho,z))\\ &\times\sum_{m\in\mathbb{Z}}\int_{1}^{+\infty}\!\!\left(\int_{-\sqrt{z^2-1}}^{\sqrt{z^2-1}}\frac{\mathcal{T}_m(y,z)}{\tau\,z+m\,\mathbf{b}_e}\;dy\right)\partial_z\mathrm{F}^{\mathrm{d}}(z)\,dz \qquad (3.3.61)\\ &=\;2\,\pi\,i\;G^{\mathrm{d}}(\Psi(\rho,z))\;\frac{1}{\tau}\;\sum_{m\in\mathbb{Z}}\mathcal{H}\,(\mathscr{T}_m)\left(-\,\frac{m\,\mathbf{b}_e}{\tau}\right),\end{aligned}$$

where:

$$\mathscr{T}_m(z) := \mathbb{1}_{]1,+\infty[}(z)\;\frac{\partial_z\mathrm{F}^{\mathrm{d}}(z)}{z}\;\int_{-\sqrt{z^2-1}}^{\sqrt{z^2-1}}\mathcal{T}_m(y,z)\;dy\,, \qquad (3.3.62)$$

and $\mathcal{T}_m(y,z)$ is the skew-symmetric matrix given by (3.3.35).

Lemma 3.3.11. *For all $m \in \mathbb{Z}$, the function $\mathscr{T}_m(\cdot)$ is Lipschitz on $\mathbb{R}$. Moreover, there exists a constant $C > 0$ such that:*

$$\forall\, m\in\mathbb{Z}\,,\qquad \|\partial_z\mathscr{T}_m\|_{\infty} := \sup_{z\in\mathbb{R}}\;\sup_{1\leq i,j\leq 3}\;|\partial_z\mathscr{T}_m^{i,j}(z)| \leq C\;(m^2+1)\,. \qquad (3.3.63)$$

Proof. Fix $m \in \mathbb{Z}$ and $(i,j) \in [\![1,3]\!]^2$. Then:

$$\mathscr{T}_m^{i,j}(z) = \mathbb{1}_{]1,+\infty[}(z)\;\partial_z\mathrm{F}^{\mathrm{d}}(z)\;\int_{-1}^{1}\sqrt{z^2-1}\;\mathcal{T}_m^{i,j}(\sqrt{z^2-1}\,\mathrm{y},z)\;d\mathrm{y}\,. \qquad (3.3.64)$$

Note that $\mathscr{T}_m^{i,j}(1-) = \mathscr{T}_m^{i,j}(1+) = 0$. The function $\mathscr{T}_m^{i,j}(\cdot)$ is therefore continuous on $\mathbb{R}$. The rest of the proof is postponed to Appendix C, Section C.2. □

Lemma 3.3.12. *For all $m \in \mathbb{Z}$ and for all $(i,j) \in [\![1,3]\!]^2$, the functions $\mathscr{T}_m^{i,j}(\cdot)$ is in $L^1(\mathbb{R})$. For all $(i,j) \in [\![1,3]\!]^2$, there exists a polynomial $Q^{i,j} \in \mathbb{R}[X]$ such that:*

$$\sum_{m\in\mathbb{Z}} m^4\;\|\mathscr{T}_m^{i,j}\|_{L^1(\mathbb{R})} \leq \int_{1}^{+\infty} Q^{i,j}(\sqrt{z^2-1})\;\partial_z\mathrm{F}^{\mathrm{d}}(z)\;dz < +\infty\,. \qquad (3.3.65)$$

Proof. Use again (3.3.49) to reduce the discussion to the case $i = j$. At the level of (3.3.50), apply the derivatives ∂_θ, ∂_r and ∂_s. Then, take $r = s$ and $\theta = 0$. By this way, we can obtain the existence of polynomials $(P_i)_{1\leq i\leq 3} \in \mathbb{R}[X]^3$ such that, for all $r \in \mathbb{R}$ and $j \in \{2,3\}$:

$$\sum_{m\in\mathbb{Z}} m^{2\,j}\;J_m^2(r) = P_j(r)\,, \qquad \sum_{m\in\mathbb{Z}} m^4\,(J_m'(r))^2 = P_4(r)\,. \qquad (3.3.66)$$

Combining (C.2.3) and (C.2.5), we can see that:

$$\exists\, C\in\mathbb{R}_+\,;\qquad |\mathscr{T}_m^{i,j}(z)| \leq C\;\mathbb{1}_{]1,+\infty[}(z)\;|\partial_z\mathrm{F}^{\mathrm{d}}(z)|\;(1+m^3+z^3)\,.$$

Knowing that $\mathrm{F}^{\mathrm{d}}(\cdot) \in \mathcal{S}(\mathbb{R})$, this gives $\mathscr{T}_m^{i,j}(\cdot) \in L^1(\mathbb{R})$. Then, it suffices to exploit (3.3.66) together with (C.2.5) in the sum of (3.3.65) in order to recover (3.3.65). □

In view of Lemmas 3.3.11 and 3.3.12, for all $\eta \in \mathbb{R}_+^*$, we can apply Lemma 3.3.6. This yields:

$$|\mathcal{H}(\mathscr{T}_m^{i,j})(-\frac{m\,\mathbf{b}_e}{\tau})| \leq 2\ \eta\ \|\partial_z \mathscr{T}_m^{i,j}\|_\infty + \eta^{-1}\,\|\mathscr{T}_m^{i,j}\|_{L^1(\mathbb{R})}\,. \tag{3.3.67}$$

In (3.3.67), select $\eta = (m^4+1)^{-1}$. Take the sum over $m \in \mathbb{Z}$. In view of (3.3.63) and (3.3.65), the corresponding series is absolutely convergent. Coming back to (3.3.61), this implies that the matrix $\sigma\big(\mathbf{x}, \tau, (\xi_\perp, 0, 0)\big)$ is well-defined.

3.3.4. **Perspectives.** The analysis of Sections 3.3.2 and 3.3.3 shows that the definition of the characteristic variety $\mathscr{V}$ given in (3.3.31) makes sense. It says nothing about the decomposition of $\mathscr{V}$ in connected components, or how it could be visualized. A study as thorough as the one conducted in Chapter 2 seems difficult to implement since equation $\det \mathfrak{N}(\mathbf{x}, \tau, \xi) = 0$ cannot be solved analytically, as opposed to the cold case. However, an interesting perspective could be to study $\mathscr{V}$ through numerical computations. There are some recent works dealing with the numerical aspects [30, 36]. But these contributions are restricted to the rough case where the external magnetic field is constant and where the Maxwell-Boltzmann distribution function depends only on $\mathbf{p}$. More realistic numerical studies taking into account the inhomogeneities of the external magnetic field and the equilibrium distribution function through our refined model would be of much interest. This could also help to produce representations of $\mathscr{V}$, similar to the ones obtained in Chapter 2.

Besides, the analysis of Chapter 3 is a prerequisite for further developments. It would be mathematically interesting to complete the WKB analysis for times $t \sim 1$, and possibly for long times $t \sim \varepsilon^{-1}$. From a physics point of view, questions about wave-particle interactions [17, 33], anomalous transport [5], or confinement properties could thereby benefit from new perspectives.

References

[1] F. B. Argomedo, E. Witrant, and C. Prieur. *Safety Factor Profile Control in a Tokamak*. SpringerBriefs in Electrical and Computer Engineering, 2014.

[2] G. Bekefi. *Radiation processes in plasmas*. Wiley, 1966.

[3] Rémi Carles. Geometric optics with caustic crossing for some nonlinear schrödinger equations. *Indiana University Mathematics Journal*, 49(2):475–551, 2000.

[4] C. Cheverry. Can One Hear Whistler Waves? *Comm. Math. Phys.*, 338(2):641–703, 2015.

[5] C. Cheverry. Anomalous transport. *J. Differential Equations*, 262(3):2987–3033, 2017.

[6] C. Cheverry and A. Fontaine. Dispersion relations in cold magnetized plasmas. *Kinet. Relat. Models*, 10(2):373–421, 2017.

[7] D. R. Cook. *Wave Conversion in Phase Space and Plasma Gyroresonance.* PhD thesis, UNIVERSITY OF CALIFORNIA, BERKELEY., 1993.

[8] C. Cremaschini and M. Tessarotto. Kinetic description of rotating tokamak plasmas with anisotropic temperatures in the collisionless regime. *Physics of Plasmas (1994-present)*, 18(11):112502, 2011.

[9] R. C. Davidson. *Handbook of plasma physics*. North-Holland, 1983.

[10] H. Fichtner and S. R. Sreenivasan. Exact algebraic dispersion relations for wave propagation in hot magnetized plasmas. *J. Plasma Physics*, 49, 1993.

[11] J-P. Goedbloed, R. Keppens, and S. Poedts. *Advanced Magnetohydrodynamics. With applications to laboratory and astrophysical plasmas.* Cambridge University Press, 2010.

[12] G. Granata and Fidone I. A new representation of relativistic wave damping above the electron-cyclotron frequency. *J. Plasma Physics*, 45:361–369, 1991.

[13] J. W. Haverkort. *Magnetohydrodynamic waves and instabilities in rotating tokamak plasmas*. Eindhoven : Technische Universiteit Eindhoven, 2013.

[14] Y. Hu. *Notes on Tokamak Equilibrium*. 2015.

[15] Lise-Marie Imbert-Gérard. *Mathematical and numerical problems of some wave phenomena appearing in magnetic plasmas*. Theses, Université Pierre et Marie Curie - Paris VI, September 2013.

[16] Jean-Luc Joly, Guy Métivier, and Jeffrey Rauch. Nonlinear oscillations beyond caustics. *Communications on Pure and Applied Mathematics*, 49(5):443–527, 1996.

[17] R. Koch. Wave-particle interactions in plasmas. *Plasmas Phys. Control Fusion*, 48, 2006.

[18] N. A. Krall and A. W. Trivelpiece. *Principles of plasma physics*. McGray-Hill, 1973.

[19] A. Kuiroukidis, G. N. Throumoulopoulos, and H. Tasso. Vlasov tokamak equilibria with shearad toroidal flow and anisotropic pressure. *Physics of Plasmas*, 22(8):082505, 2015.

[20] Z. Lin and W. A. Strauss. Linear stability and instability of relativistic Vlasov-Maxwell systems. *Comm. Pure Appl. Math.*, 60(5):724–787, 2007.

[21] R. A. Lopez, P. S. Moya, V. Munoz, A. F. Vinas, and J. A. Valdivia. Kinetic transverse dispersion relation for relativistic magnetized electron-positron plasmas with maxwell-juttner velocity distribution functions. *Physics of Plasmas*, 21, 2014.

[22] E. K. Maschke and H. Perrin. Exact solutions of the stationary mhd equations for a rotating toroidal plasma. *Plasma Physics*, 22(6):579, 1980.

[23] G. Métivier. The mathematics of nonlinear optics. In *Handbook of differential equations: evolutionary equations. Vol. V*, Handb. Differ. Equ., pages 169–313. Elsevier/North-Holland, Amsterdam, 2009.

[24] A. Piel. *Plasma physics: an introduction to laboratory, space and fusion plasmas*. Springer, 2010.

[25] J. Rauch. *Hyperbolic Partial Differential Equations and Geometric Optics*. Graduate Studies in Mathematics. American Mathematical Society, 2012.

[26] R. Schlickeiser. General properties of small-amplitude fluctuations in magnetized and unmagnetized collision poor plasmas. i. the dielectric tensor. *Physics of Plasmas*, 17, 2010.

[27] T. H. Stix. *Waves in plasma*. American Institute of Physics, 1992.

[28] D. G. Swanson. *Plasma waves*. Academic, 1989.

[29] W. Sy and M. Cotsaftis. Wave propagation in hot nonuniform magnetized plasma. *Plasma Physics*, 21:985–998, 1979.

[30] A. Tomori. Numerical plasma dispersion relation solver. *WDS'15 Proceedings of Contributed Papers - Physics*, pages 206–211, 2015.

[31] E. R. Tracy, A. J. Brizard, A. S. Richardson, and A. N. Kaufman. *Ray Tracing and Beyond: Phase Space Methods in Plasma Wave Theory*. Cambridge University Press, 2014.

[32] B. A. Trubnikov. *Plasma Physics and the Problem of Controlled Thermonuclear Reactions*, volume 3. Pergamon, 1959.

[33] B. T. Tsurutani and Lakhina G. S. Some basic concepts of wave-particle interactions in collisionless plasmas. *Reviews of Geophysics*, 35:491–502, 1997.

[34] G. N. Watson. *A treatise on the theory of Bessel functions*. 1922.

[35] J. Wesson. *Tokamaks*. Clarendon Press-Oxford, 2004.

[36] H. Xie and Y. Xiao. Pdrk: a general kinetic dispersion relation solver for magnetized plasma. *Plasma Science and Technology*, 18(2), 2016.

APPENDIX A

About the fluid approach

The *dispersion relations* are aimed to capture the geometrical features of electromagnetic wave propagation. They turn out to be very sensitive to the properties of the underlying medium, in the present case, magnetized plasmas. At a scale larger than the particle mean free path, fluid theories such as magnetohydrodynamics (MHD) are found to be suitable. They contain the central aspects in view of ray tracing. Precisely, the purpose of this Appendix (and to some extent the purpose of Chapter 2) is to clarify what can be obtained through fluid considerations.

In this perspective, Part A.1 deals with the case where the plasma is close to the Coulomb collisional equilibrium. It explains what happens when the lowest order repartition of the charged particles is given by a Maxwellian distribution function. In this framework, it points out how averages over velocity space can be taken in order to extract from the relativistic Vlasov equation fluid moment representations. The technicalities of Part A.1 are useful in Chapter 3, when discussing the Grad-Shafranov equation.

In this perspective, Part A.2 investigates some MHD descriptions of magnetized plasmas, obtained by neglecting many kinetic subtleties, but by taking into account the effects of the fast rotations induced by the strong external magnetic field. By this way, a link can be made with more standard results in geometrical optics.

Now, in the case of many astrophysical and laboratory applications, the Knudsen number is near or greater than one. Then, the electromagnetic fluctuations become more sensitive to the microscopic physics, and non thermal structures in velocity space must be taken into account. With this in mind, Chapters 2 and 3 are concerned with the procedures which can be used to progress from the approximate (but easy to implement) fluid models of this Appendix to more precise and more relevant (but more complicated) descriptions of the electromagnetic wave propagation, based on kinetic features.

A.1. Fluid description in the non relativistic framework

When studying magnetized plasmas, there are three embedded levels of investigation: the *microscopic* description, the *kinetic* theory, and the *fluid* approach. In the microscopic point of view, the motion of each charged particle is taken into account. After applying the Fundamental Equation of Dynamics (the Lorentz Force Law), this yields a complex system of ordinary differential equations. On this basis, a variety of statistical models of plasma dynamics have been developed.

By averaging out the microscopic information, kinetic equations can be derived. Assume that some electric field $\tilde{\mathbf{E}}(\tilde{\mathrm{t}}, \tilde{\mathbf{x}})$ and some magnetic field $\tilde{\mathbf{B}}(\tilde{\mathrm{t}}, \tilde{\mathbf{x}}) + \tilde{\mathbf{B}}_e(\tilde{\mathbf{x}})$ are prescribed. Then, the time evolution of the distribution functions $\tilde{\mathrm{f}}^{\mathrm{k}}_\alpha(\cdot)$ introduced in Section 3.2 is governed by the Vlasov equation (3.2.1). The associated conservative form yields:

$$\partial_{\tilde{\mathrm{t}}} \tilde{\mathrm{f}}^{\mathrm{k}}_\alpha + \nabla_{\tilde{\mathbf{x}}} \cdot (\tilde{\mathbf{v}}_\alpha(\tilde{\mathbf{p}})\, \tilde{\mathrm{f}}^{\mathrm{k}}_\alpha) + e_\alpha \nabla_{\tilde{\mathbf{p}}} \cdot \Big(\big[\tilde{\mathbf{E}}(\tilde{\mathrm{t}}, \tilde{\mathbf{x}}) + \tilde{\mathbf{v}}_\alpha(\tilde{\mathbf{p}}) \times (\tilde{\mathbf{B}}(\tilde{\mathrm{t}}, \tilde{\mathbf{x}}) + \tilde{\mathbf{B}}_e(\tilde{\mathbf{x}})) \big]\, \tilde{\mathrm{f}}^{\mathrm{k}}_\alpha \Big) = 0\,. \tag{A.1.1}$$

The complexity of (A.1.1) is greatly reduced by averaging over the velocity coordinates of the distribution function. The averaged quantities are called macroscopic quantities. They depend only on the time variable $\tilde{\mathrm{t}} \in \mathbb{R}$ and on the spacial variable $\tilde{\mathbf{x}} \in \mathbb{R}^3$, but not on the momentum $\tilde{\mathbf{p}} \in \mathbb{R}^3$.

The non relativistic limit corresponds to the case where $\tilde{\mathbf{p}}(\tilde{\mathbf{v}}_\alpha) = m_\alpha\, \tilde{\mathbf{v}}_\alpha$, see for instance [1]. Then, for $\alpha \in \{1, \cdots, N\}$, we can define the *density* $\tilde{\mathbf{n}}_\alpha$, the *flow velocity* $\tilde{\mathbf{u}}_\alpha$ and the *pressure tensor* $\tilde{\mathbf{P}}_\alpha$ of the α^{th} species as indicated below:

$$\tilde{\mathbf{n}}_\alpha \equiv \tilde{\mathbf{n}}_\alpha(\tilde{\mathrm{f}}^{\mathrm{k}}_\alpha)(\tilde{\mathrm{t}}, \tilde{\mathbf{x}}) := \int_{\mathbb{R}^3} \tilde{\mathrm{f}}^{\mathrm{k}}_\alpha(\tilde{\mathrm{t}}, \tilde{\mathbf{x}}, \tilde{\mathbf{p}})\; d\tilde{\mathbf{p}}\,, \tag{A.1.2a}$$

$$\tilde{\mathbf{u}}_\alpha \equiv \tilde{\mathbf{u}}_\alpha(\tilde{\mathrm{f}}^{\mathrm{k}}_\alpha)(\tilde{\mathrm{t}}, \tilde{\mathbf{x}}) := \frac{1}{\tilde{\mathbf{n}}_\alpha(\tilde{\mathrm{t}}, \tilde{\mathbf{x}})} \int_{\mathbb{R}^3} \tilde{\mathbf{v}}_\alpha\; \tilde{\mathrm{f}}^{\mathrm{k}}_\alpha(\tilde{\mathrm{t}}, \tilde{\mathbf{x}}, \tilde{\mathbf{p}})\; d\tilde{\mathbf{p}}\,, \tag{A.1.2b}$$

$$\tilde{\mathbf{P}}_\alpha \equiv \tilde{\mathbf{P}}_\alpha(\tilde{\mathrm{f}}^{\mathrm{k}}_\alpha)(\tilde{\mathrm{t}}, \tilde{\mathbf{x}}) := m_\alpha \int_{\mathbb{R}^3} (\tilde{\mathbf{v}}_\alpha - \tilde{\mathbf{u}}_\alpha) \otimes (\tilde{\mathbf{v}}_\alpha - \tilde{\mathbf{u}}_\alpha)\; \tilde{\mathrm{f}}^{\mathrm{k}}_\alpha(\tilde{\mathrm{t}}, \tilde{\mathbf{x}}, \tilde{\mathbf{p}})\; d\tilde{\mathbf{p}}\,. \tag{A.1.2c}$$

Always in the non relativistic limit [1], macroscopic transport equations can easily be deduced from (A.1.1), like the *continuity equation* (for the conservation of mass):

$$\partial_{\tilde{\mathrm{t}}} \tilde{\mathbf{n}}_\alpha + \nabla_{\tilde{\mathbf{x}}} \cdot (\tilde{\mathbf{n}}_\alpha\, \tilde{\mathbf{u}}_\alpha) = 0\,. \tag{A.1.3}$$

Introduce the *charge density* $\tilde{\rho}_\alpha := e_\alpha\, \tilde{\mathbf{n}}_\alpha$ and the *current density* $\tilde{\jmath}_\alpha := e_\alpha\, \tilde{\mathbf{n}}_\alpha\, \tilde{\mathbf{u}}_\alpha$. The equation (A.1.3) is equivalent to:

$$\partial_{\tilde{\mathrm{t}}} \tilde{\rho}_\alpha + \nabla_{\tilde{\mathbf{x}}} \cdot \tilde{\jmath}_\alpha = 0\,. \tag{A.1.4}$$

On the other hand, multiplying (A.1.1) by $\tilde{\mathbf{v}}_\alpha$ and integrating with respect to $\tilde{\mathbf{p}}$, we can extract the *momentum transport equation* (for the conservation of momentum):

$$m_\alpha\, \tilde{\mathbf{n}}_\alpha \left[\partial_{\tilde{\mathrm{t}}} \tilde{\mathbf{u}}_\alpha + (\tilde{\mathbf{u}}_\alpha \cdot \nabla_{\tilde{\mathbf{x}}}) \tilde{\mathbf{u}}_\alpha \right] + \nabla_{\tilde{\mathbf{x}}} \cdot \tilde{\mathbf{P}}_\alpha = \tilde{\rho}_\alpha\, \tilde{\mathbf{E}} + \tilde{\jmath}_\alpha \times (\tilde{\mathbf{B}} + \tilde{\mathbf{B}}_e)\,. \tag{A.1.5}$$

Lemma A.1.1. *Assume that the distribution function $\tilde{\mathrm{f}}^{\mathrm{k}}_\alpha(\cdot)$ is of the form:*

$$\forall\, (\tilde{\mathrm{t}}, \tilde{\mathbf{x}}, \tilde{\mathbf{p}}) \in \mathbb{R} \times \mathbb{R}^3 \times \mathbb{R}^3\,, \qquad \tilde{\mathrm{f}}^{\mathrm{k}}_\alpha(\tilde{\mathrm{t}}, \tilde{\mathbf{x}}, \tilde{\mathbf{v}}) = \tilde{\mathcal{F}}^{\mathrm{k}}_\alpha(\tilde{\mathrm{t}}, \tilde{\mathbf{x}}, |\tilde{\mathbf{p}} - m_\alpha \tilde{\mathbf{u}}_\alpha(\tilde{\mathrm{t}}, \tilde{\mathbf{x}})|)\,, \tag{A.1.6}$$

where $\tilde{\mathcal{F}}^{\mathrm{k}}_\alpha(\cdot) \in \mathcal{S}(\mathbb{R} \times \mathbb{R}^3 \times \mathbb{R}_+; \mathbb{R})$. Then, for some scalar function $\tilde{\mathrm{p}}_\alpha(\cdot)$, the pressure tensor $\tilde{\mathbf{P}}_\alpha$ takes the form:

$$\tilde{\mathbf{P}}_\alpha(\tilde{\mathbf{x}}) = \tilde{\mathrm{p}}_\alpha(\tilde{\mathbf{x}}) Id\,. \tag{A.1.7}$$

Proof. The integral over a symmetric domain of an odd function is equal to zero. Therefore, for $i \neq j$, with the change of variable $\tilde{P}_\alpha := \tilde{\mathbf{p}} - m_\alpha \tilde{\mathbf{u}}_\alpha$, we have:

$$\int_{\mathbb{R}^3} ((\tilde{\mathbf{v}}_\alpha - \tilde{\mathbf{u}}_\alpha) \otimes (\tilde{\mathbf{v}}_\alpha - \tilde{\mathbf{u}}_\alpha))_{ij} \ \tilde{\mathrm{f}}^{\mathrm{k}}_\alpha(\tilde{\mathrm{t}}, \tilde{\mathbf{x}}, \tilde{\mathbf{p}}) \ d\tilde{\mathbf{p}} = \frac{1}{m_\alpha^2} \int_{\mathbb{R}^3} \tilde{P}^i_\alpha \tilde{P}^j_\alpha \ \tilde{\mathcal{F}}^{\mathrm{k}}_\alpha(\tilde{\mathrm{t}}, \tilde{\mathbf{x}}, |\tilde{P}_\alpha|) \ d\tilde{P}_\alpha = 0 \,.$$

On the other hand, for $i \neq 1$, changing $\tilde{P}^i_\alpha$ into $\tilde{P}^1_\alpha$, we get:

$$\tilde{\mathrm{p}}_\alpha(\tilde{\mathrm{t}}, \tilde{\mathbf{x}}) := \frac{1}{m_\alpha^2} \int_{\mathbb{R}^3} (\tilde{P}^1_\alpha)^2 \ \tilde{\mathcal{F}}^{\mathrm{k}}_\alpha(\tilde{\mathrm{t}}, \tilde{\mathbf{x}}, |\tilde{P}_\alpha|) \ d\tilde{\mathbf{p}} = \int_{\mathbb{R}^3} (\tilde{P}^i_\alpha)^2 \ \tilde{\mathcal{F}}^{\mathrm{k}}_\alpha(\tilde{\mathrm{t}}, \tilde{\mathbf{x}}, |\tilde{P}_\alpha|) \ d\tilde{\mathbf{p}} \,.$$

In view of these elements, we have (A.1.7). The function $\tilde{\mathrm{p}}_\alpha(\cdot)$ thus defined is called the *scalar pressure* of the α^{th} species. □

A.2. The cold dispersion relations from the perspective of magnetohydrodynamics: advantages and disadvantages

Equations (A.1.4)-(A.1.5) does not form a self-contained system of equations. In fluid dynamics, this difficulty is known as the *closure problem*, which explains why the dispersion relations cannot be derived in a consistent way by starting from (A.1.4)-(A.1.5). To rigorously extract the dispersion relations, it is necessary to get back to the kinetic model, as is done in Chapters 2 and 3.

Moreover, when dealing with magnetized plasmas, it is especially important to work with the nondimensional form (2.2.52) of the Vlasov equation, because it reveals the relevant hierarchy of powers of ε. The *eikonal equation* is what appears in factor of ε^{-1}. The *modulation equation* is what occurs in factor of ε^0.

The influence of the kinetic features can manifest itself in different ways. It depends mainly on the context, *hot* or *cold*. In Chapter 3 (hot case), it is evident with regard to the dispersion relations. On the contrary, in Chapter 2 (cold case), it does not appear at the level of the eikonal equation. This has been fully justified through the cold asymptotic regime of Paragraph 2.2.7. Note that kinetic aspects can be detected inside the modulation equation. But the related phenomena will not be studied here.

Now, the part A.2 of this Appendix gives another (less accurate but more direct) way to proceed. It explains how the dispersion relations can be recovered from a simplified fluid model issued from (2.2.52) by neglecting directly all the intricacies of the (small) transport terms. Recall that:

$$p = r \ (\cos\omega \ \sin\varpi, \sin\omega \ \sin\varpi, \cos\varpi) \,, \qquad r := |p| \,.$$

Given a distribution function $f(\mathbf{t}, \mathbf{x}, p) \equiv f(\mathbf{t}, \mathbf{x}, \varpi, \omega, r)$, define:

$$\begin{aligned} \mathcal{J}(f) \ (\mathbf{t}, \mathbf{x}) &:= \int_{\mathbb{R}^3} p \, f(\mathbf{t}, \mathbf{x}, p) \, dp \\ &= \int_0^{+\infty} \int_0^{\pi} \int_{-\pi}^{\pi} r^3 \begin{pmatrix} \cos\omega \ \sin\varpi \\ \sin\omega \ \sin\varpi \\ \cos\varpi \end{pmatrix} f(\mathbf{t}, \mathbf{x}, \varpi, \omega, r) \ \sin\varpi \ dr \, d\varpi \, d\omega \,, \end{aligned} \tag{A.2.1}$$

as well as:

$$\mathcal{M}(r) := \frac{1}{\pi^{3/2}}\ \exp(-r^2)\,.$$

A single particle basic system can be extracted from (2.3.6). Just consider:

$$\left\{\begin{array}{l} \partial_{\mathbf{t}} f - \dfrac{1}{\varepsilon}\ \mathbf{b}_e(\mathbf{x})\ \partial_\omega f = \dfrac{1}{\varepsilon}\ \mathcal{M}'(r)\ \dfrac{p\cdot E}{r}\,, \\ \partial_{\mathbf{t}} B + \nabla_{\mathbf{x}} \times E = 0\,, \\ \partial_{\mathbf{t}} E - \nabla_{\mathbf{x}} \times B = \dfrac{1}{\varepsilon}\ \mathcal{J}(f)\,. \end{array}\right. \tag{A.2.2}$$

At the time $t = 0$, impose the initial data:

$$f(0, \mathbf{x}, \varpi, \omega, r) = 0\,. \tag{A.2.3}$$

Lemma A.2.1. *The particle flux $\mathcal{J} \equiv \mathcal{J}(f)(\mathbf{t}, \mathbf{x})$ is related to the electric field E through:*

$$\mathcal{J} = -\frac{1}{\varepsilon}\ \int_0^{\mathbf{t}} \begin{pmatrix} +\cos\big(\frac{\mathbf{b}_e\,(\mathbf{t}-s)}{\varepsilon}\big) & \sin\big(\frac{\mathbf{b}_e\,(\mathbf{t}-s)}{\varepsilon}\big) & 0 \\ -\sin\big(\frac{\mathbf{b}_e\,(\mathbf{t}-s)}{\varepsilon}\big) & \cos\big(\frac{\mathbf{b}_e\,(\mathbf{t}-s)}{\varepsilon}\big) & 0 \\ 0 & 0 & 1 \end{pmatrix} \begin{pmatrix} E^1 \\ E^2 \\ E^3 \end{pmatrix}(s, \mathbf{x})\ ds\,. \tag{A.2.4}$$

It is subjected to $\mathcal{J}(f)(0, \mathbf{x}) = 0$ together with:

$$\partial_{\mathbf{t}} \mathcal{J} - \frac{1}{\varepsilon}\ \mathbf{b}_e(\mathbf{x})\ \Lambda\ \mathcal{J} = -\frac{1}{\varepsilon}\ E\,, \qquad \Lambda := \begin{pmatrix} 0 & -1 & 0 \\ 1 & 0 & 0 \\ 0 & 0 & 0 \end{pmatrix}. \tag{A.2.5}$$

Proof. The solution to the Vlasov equation (A.2.2) is:

$$f(\mathbf{t}, \mathbf{x}, \varpi, \omega, r) = \frac{1}{\varepsilon}\ \mathcal{M}'(r)\ \int_0^{\mathbf{t}} \begin{pmatrix} \cos\big(\omega + \frac{\mathbf{b}_e(\mathbf{x})\,(\mathbf{t}-s)}{\varepsilon}\big)\ \sin\varpi \\ \sin\big(\omega + \frac{\mathbf{b}_e(\mathbf{x})\,(\mathbf{t}-s)}{\varepsilon}\big)\ \sin\varpi \\ \cos\varpi \end{pmatrix} \cdot \begin{pmatrix} E^1 \\ E^2 \\ E^3 \end{pmatrix}(s, \mathbf{x})\ ds\,.$$

With $f(\cdot)$ as above, we can compute $\mathcal{J}(f)$ to find (with $d\mu = \sin\varpi\, d\varpi\, d\omega\, ds$):

$$\mathcal{J}(f) = -\frac{1}{\varepsilon}\ \frac{3}{4\,\pi}\ \int_0^{\mathbf{t}}\int_0^{\pi}\int_{-\pi}^{\pi} \begin{pmatrix} \cos\omega\ \sin\varpi \\ \sin\omega\ \sin\varpi \\ \cos\varpi \end{pmatrix} \begin{pmatrix} \cos\big(\omega + \frac{\mathbf{b}_e\,(\mathbf{t}-s)}{\varepsilon}\big)\ \sin\varpi \\ \sin\big(\omega + \frac{\mathbf{b}_e\,(\mathbf{t}-s)}{\varepsilon}\big)\ \sin\varpi \\ \cos\varpi \end{pmatrix} \cdot \begin{pmatrix} E^1 \\ E^2 \\ E^3 \end{pmatrix} d\mu$$

$$= -\frac{3}{4\,\varepsilon}\ \int_0^{\mathbf{t}}\int_0^{\pi} \begin{pmatrix} +\cos\big(\frac{\mathbf{b}_e\,(\mathbf{t}-s)}{\varepsilon}\big)\ \sin^2\varpi\ E^1 + \sin\big(\frac{\mathbf{b}_e\,(\mathbf{t}-s)}{\varepsilon}\big)\ \sin^2\varpi\ E^2 \\ -\sin\big(\frac{\mathbf{b}_e\,(\mathbf{t}-s)}{\varepsilon}\big)\ \sin^2\varpi\ E^1 + \cos\big(\frac{\mathbf{b}_e\,(\mathbf{t}-s)}{\varepsilon}\big)\ \sin^2\varpi\ E^2 \\ 2\ \cos^2\varpi\ E^3 \end{pmatrix} \sin\varpi\ d\varpi\, ds\,.$$

And we get the expression (A.2.4) for $\mathcal{J}$. From the formula (A.2.4), we can deduce (A.2.5). It should be noted that the equation (A.2.5) can also be obtained by following the same kind of procedure as in Part A.1. As a matter of fact, multiplying the first equation of (A.2.2) by p and integrating with respect to p yields directly (A.2.5). □

Thus, in the case of the very simplified model (A.2.2), we can replace (A.2.2) by a (closed) system of magnetohydrodynamic (MHD) type, namely:

$$\text{(A.2.6)} \qquad \left\{ \begin{array}{l} \partial_{\mathbf{t}} B + \nabla_{\mathbf{x}} \times E = 0\,, \\ \partial_{\mathbf{t}} E - \nabla_{\mathbf{x}} \times B = \dfrac{1}{\varepsilon}\, \mathcal{J}\,, \\ \partial_{\mathbf{t}} \mathcal{J} = -\dfrac{1}{\varepsilon}\, E + \dfrac{1}{\varepsilon}\, \mathbf{b}_e(\mathbf{x})\, \Lambda\, \mathcal{J}\,. \end{array} \right.$$

From (A.2.6), we can recover the dispersion relation of Chapter 2. This relation can be identified by looking at the eigenvalue problem:

$$\text{(A.2.7)} \qquad \left\{ \begin{array}{l} \tau\, B + \xi \times E = 0\,, \\ i\,\tau\, E - i\,\xi \times B = \mathcal{J}\,, \\ \Sigma(\mathbf{x}, \tau)\, \mathcal{J} = -\, E\,, \end{array} \right.$$

Multiplying the second line of (A.2.7) by $-i\,\tau\,\Sigma(\mathbf{x},\tau)$, we recover (2.3.21). Of course, this argument is only valid in the *cold* case and it works only after neglecting the $O(\varepsilon)$ terms inside (2.2.52). The study of (2.3.21) has been partially addressed in physics books. Before this dissertation, it had not yet been completed from a mathematical perspective.

With $\mathcal{V} := {}^t(B, E, \mathcal{J}) \in (\mathbb{R}^3)^3$, the system (A.2.6) can be put in the abbreviated form:

$$\text{(A.2.8)} \qquad \partial_{\mathbf{t}} \mathcal{V} + \sum_{j=1}^{3} A_j\, \partial_{\mathbf{x}^j} \mathcal{V} + \frac{1}{\varepsilon}\, L_0(\mathbf{x})\, \mathcal{V} = 0\,,$$

where the matrices A_j are symmetric, whereas $L_0(\cdot)$ is skew-symmetric:

$$\text{(A.2.9)} \qquad A_j = A_j^t\,, \qquad L_0(\mathbf{x}) := \begin{pmatrix} 0 & 0 & 0 \\ 0 & 0 & +I \\ 0 & -I & \mathbf{b}_e(\mathbf{x})\,\Lambda \end{pmatrix} = -\, L_0^t(\mathbf{x})\,.$$

Looking at (A.2.8)-(A.2.9), we recognize a standard form in *dispersive* geometric optics and indeed, the group and phase velocities which can be computed from the dispersion relations of Chapter 2 do not coincide. The asymptotic analysis of (A.2.8) when the parameter ε goes to zero (for times $t \sim 1$) should follow the same lines as in [2, 3, 4, 5]. In other words, as well as crystal optics, the Lorentz model or the Maxwell-Bloch equations, the *fluid* system (A.2.8)-(A.2.9) issued from the study of magnetized plasmas furnishes a basic model to perform some dispersive geometric optics.

Note however, that the model based on the relativistic Vlasov-Maxwell system is physically more relevant. It implies different features from the perspective of the corresponding asymptotic analysis. As a matter of fact, it contains more detailed information. It also involves kinetic effects which, in the cold case, could be revealed by looking at the higher order terms (ε^j with $j \geq 0$) in the WKB expansion. As seen in Chapter 3, in the hot case, these kinetic features crucially enter in the dispersion relations.

References

[1] James D. Callen. *Fundamentals of Plasma Physics*. University of Wisconsin, 2006.

[2] Phillipe Donnat and Jeffrey Rauch. Dispersive nonlinear geometric optics. *J. Math. Phys.*, 38(3):1484–1523, 1997.

[3] Jean-Luc Joly, Guy Metivier, and Jeffrey Rauch. Transparent nonlinear geometric optics and Maxwell-Bloch equations. *J. Differential Equations*, 166(1):175–250, 2000.

[4] David Lannes. Dispersive effects for nonlinear geometrical optics with rectification. *Asymptot. Anal.*, 18(1-2):111–146, 1998.

[5] Guy Métivier. The mathematics of nonlinear optics. In *Handbook of differential equations: evolutionary equations. Vol. V*, Handb. Differ. Equ., pages 169–313. Elsevier/North-Holland, Amsterdam, 2009.

APPENDIX B

Drawings of $\boldsymbol{\nu}(\mathbf{x},\tau)$ for different values of τ

Recall the definition of the set $\boldsymbol{\mathcal{V}}(\mathbf{x},\tau)$ studied in Paragraph 2.3.4.2 :

$\boldsymbol{\mathcal{V}}(\mathbf{x},\tau) := \{\, \xi \in \mathbb{R}^3 \,;\, (\tau,\xi) \in \mathscr{V}^*_{\mathbf{x}} \,\}$.

The aim of this appendix is to furnish a global vision of the evolution of the set $\boldsymbol{\mathcal{V}}(\mathbf{x},\tau)$ in function of τ, from small values of τ up to large values of τ. The purpose is to better illustrate some of the configurations that have been mentionned in Paragraph 2.3.4.2. We also explain how the transition takes place between these different configurations. To do so, we have to make the connection with the two-dimensionnal set $\mathrm{V}(\mathbf{x},\varpi)$ represented on Figures 15.(a) and 17. Retain that:

$$\mathrm{V}(\mathbf{x},\varpi) = \mathrm{V}_o^-(\mathbf{x},\varpi) \sqcup \mathrm{V}_o^+(\mathbf{x},\varpi) \sqcup \mathrm{V}_x^-(\mathbf{x},\varpi) \sqcup \mathrm{V}_x^+(\mathbf{x},\varpi)\,, \tag{B.0.10}$$

where:

$$\mathrm{V}_o^-(\mathbf{x},\varpi) := \{(\tau,r)\,;\, 0<\tau<\tau_\infty^-(\mathbf{x},\varpi)\,,\, 0\le r\,,\, r^2 = g_+(\mathbf{x},\varpi,\tau)\,\}\,, \tag{B.0.11a}$$

$$\mathrm{V}_o^+(\mathbf{x},\varpi) := \{(\tau,r)\,;\, \kappa(\mathbf{x})\le\tau\,,\, 0\le r\,,\, r^2 = g_+(\mathbf{x},\varpi,\tau)\,\}\,, \tag{B.0.11b}$$

$$\mathrm{V}_x^-(\mathbf{x},\varpi) := \{(\tau,r)\,;\, \tau_0^-(\mathbf{x})\le\tau<\tau_\infty^+(\mathbf{x},\varpi)\,,\, 0\le r\,,\, r^2 = g_-(\mathbf{x},\varpi,\tau)\,\}\,, \tag{B.0.11c}$$

$$\mathrm{V}_x^+(\mathbf{x},\varpi) := \{(\tau,r)\,;\, \tau_0^+(\mathbf{x})\le\tau\,,\, 0\le r\,,\, r^2 = g_-(\mathbf{x},\varpi,\tau)\,\}\,. \tag{B.0.11d}$$

The expressions of the cutoff frequencies $\tau_0^\pm(\cdot)$, the resonance frequencies $\tau_\infty^\pm(\cdot)$ and the functions $g_\pm(\cdot)$ are respectively given in Definitions 2.3.2, 2.3.3 and 2.3.4.

B.1. Overview of the evolution of $\boldsymbol{\mathcal{V}}(\mathbf{x},\cdot)$

In this paragraph, we give a global vision of the evolution of $\boldsymbol{\mathcal{V}}(\mathbf{x},\tau)$ in function of τ. Figures are included to illustrate the discussion. Details about some of the configurations highlighted below will be provided in Sections B.2 and B.3.

We assume that $\kappa(\mathbf{x}) < \sqrt{2}\ \mathbf{b}_e(\mathbf{x})$. This yields the most complex and varied situations. Depending on the simultaneous presence or not of the red and blue curves in Figure 30, six situations can be distinguished. They correspond to the selection of different frequency regions. These regions are represented by coloured frames in Figure 30, where it must be understood that $r = |\xi|$ is unbounded. Generally speaking, the occurrence in a given region of unbounded (in r) blue or red curves gives rise to resonance cones. On the contrary, the presence of only bounded curves (in r) means that spheres are involved. Moreover, the blue curves correspond to the ordinary component $\boldsymbol{\mathcal{V}}_o(\mathbf{x},\tau)$ of $\boldsymbol{\mathcal{V}}(\mathbf{x},\tau)$, while the red curves correspond to the extraordinary component $\boldsymbol{\mathcal{V}}_x(\mathbf{x},\tau)$ of $\boldsymbol{\mathcal{V}}(\mathbf{x},\tau)$.

∘ a) Ordinary resonance cone: $\tau \in [0, \tau_0^-(\mathbf{x})]$. This corresponds to the blue frame in the left of Figure 30. The set $\boldsymbol{\mathcal{V}}(\mathbf{x}, \tau)$ is just composed of $\boldsymbol{\mathcal{V}}_o(\mathbf{x}, \tau)$ which consists of an ordinary resonance cone. It is represented on Figure 31.

∘ b) Ordinary resonance cone together with an extraordinary sphere: $\tau \in [\tau_0^-(\mathbf{x}), \min(\mathbf{b}_e\,;\,\kappa)]$. This corresponds to the orange frame in Figure 30. The set $\boldsymbol{\mathcal{V}}(\mathbf{x}, \tau)$ contains the ordinary resonance cone $\boldsymbol{\mathcal{V}}_o(\mathbf{x}, \tau)$ and of the extraordinary sphere $\boldsymbol{\mathcal{V}}_x(\mathbf{x}, \tau)$. It is represented on Figures 32. Note that this configuration is specific to the case where $\kappa(\mathbf{x}) < \sqrt{2}\,\mathbf{b}_e(\mathbf{x})$. More details are given in Section B.2.

∘ c) Extraordinary sphere: $\tau \in [\min(\mathbf{b}_e\,;\,\kappa), \max(\mathbf{b}_e\,;\,\kappa)]$. When $\tau \geq \min(\mathbf{b}_e\,;\,\kappa)$, the ordinary resonance cone $\boldsymbol{\mathcal{V}}_o(\mathbf{x}, \tau)$ disappears. Inside the small purple frame of Figure 30, the set $\boldsymbol{\mathcal{V}}(\mathbf{x}, \tau)$ reduces to the extraordinary sphere $\boldsymbol{\mathcal{V}}_x(\mathbf{x}, \tau)$ displayed on Figures 33.

∘ d) Extraordinary resonance cone and ordinary sphere: $\tau \in [\max(\mathbf{b}_e\,;\,\kappa), \sqrt{\mathbf{b}_e^2 + \kappa^2}]$. Here, the extraordinary sphere is replaced by an extraordinary resonance cone. The transition between these two types of configurations occurs suddenly, at $\tau = \max(\mathbf{b}_e\,;\,\kappa)$. It will be further explained in Paragraph B.3.1. In the same time, the ordinary sphere $\boldsymbol{\mathcal{V}}_o(\mathbf{x}, \tau)$ appears. Then, when τ is in the frequency region delimited by the brown frame, the set $\boldsymbol{\mathcal{V}}(\mathbf{x}, \tau)$ is composed of the extraordinary resonance cone $\boldsymbol{\mathcal{V}}_o(\mathbf{x}, \tau)$ and of the ordinary sphere $\boldsymbol{\mathcal{V}}_x(\mathbf{x}, \tau)$. It is represented on Figures 34. More details about this configuration are given in Section B.3.2.

∘ e) Ordinary sphere: $\tau \in [\sqrt{\mathbf{b}_e^2 + \kappa^2}, \tau_0^+(\mathbf{x})]$. Above the value $\sqrt{\mathbf{b}_e^2 + \kappa^2}$, the extraordinary resonance cone is no longer present. In the region $\tau \in [\sqrt{\mathbf{b}_e^2 + \kappa^2}, \tau_0^+(\mathbf{x})]$ which corresponds to the turquoise frame, the set $\boldsymbol{\mathcal{V}}(\mathbf{x}, \tau)$ is just composed of the ordinary sphere. It is represented on Figures 35.

∘ f) Extraordinary sphere imbedded in an ordinary sphere: $\tau \in [\tau_0^+(\mathbf{x}), +\infty[$. Finally, when $\tau \geq \tau_0^+(\mathbf{x})$, that is in the frequency region delimited by the green frame in Figure 30, the extraordinary sphere appears inside the ordinary sphere. When the time frequency τ goes to $+\infty$, the blue curve and the red curve of Figure 30 issued respectively from $\mathrm{V}_o^+(\mathbf{x}, \varpi)$ and $\mathrm{V}_x^+(\mathbf{x}, \varpi)$, have the same asymptotic direction. As already highlighted in Figure 22, this corresponds to an asymptotic merge for large values of τ of the ordinary and extraordinary spheres. This situation is reproduced on Figures 37.

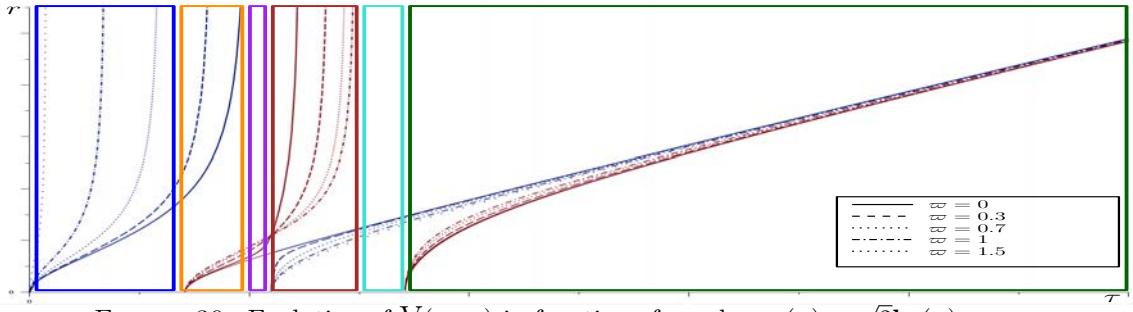

FIGURE 30. Evolution of $\mathrm{V}(\mathbf{x}, \varpi)$ in function of ϖ when $\kappa(\mathbf{x}) < \sqrt{2}\mathbf{b}_e(\mathbf{x})$.
From left to right: $\mathrm{V}_o^-(\mathbf{x}, \varpi)$, $\mathrm{V}_x^-(\mathbf{x}, \varpi)$, $\mathrm{V}_o^+(\mathbf{x}, \varpi)$ and $\mathrm{V}_x^+(\mathbf{x}, \varpi)$.

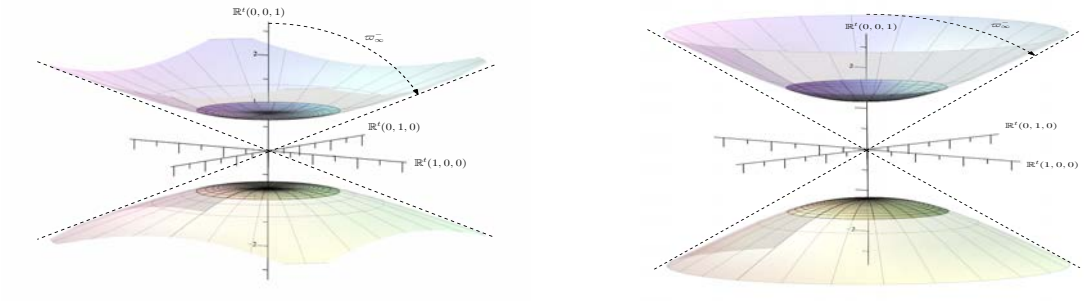

(a) $\tau = \tau_1$ (b) $\tau = \tau_2$

FIGURE 31. Ordinary resonance cone. Evolution in function of τ: (a) $\tau_1 \sim 0$; (b) $\tau_2 \sim \tau_0^-(\mathbf{x})$.

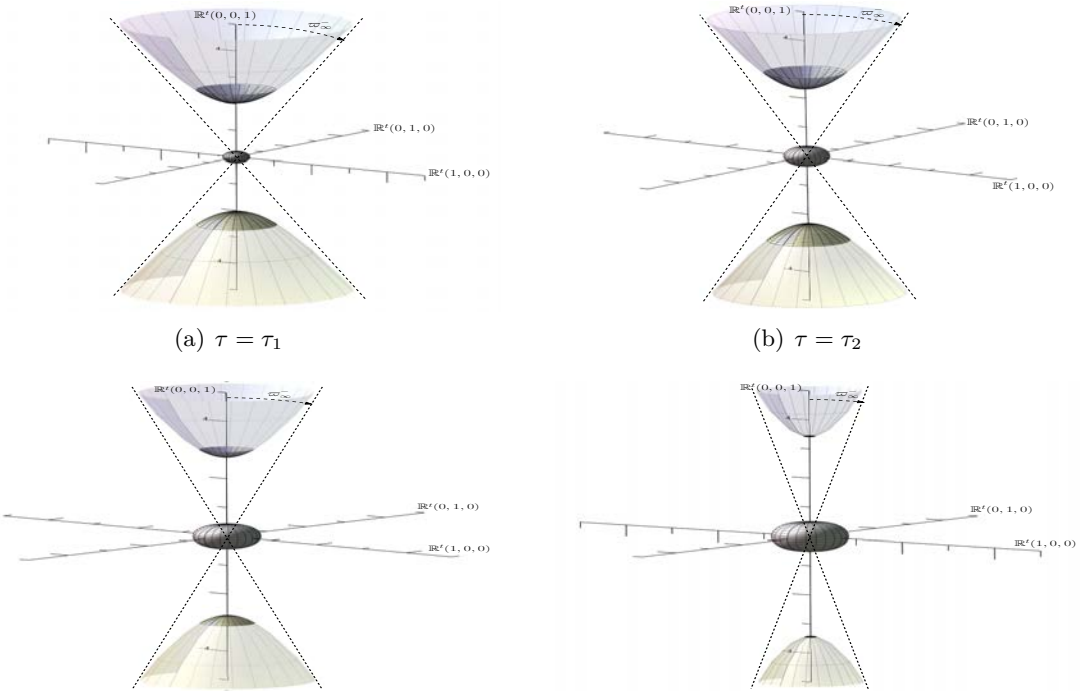

(a) $\tau = \tau_1$ (b) $\tau = \tau_2$

(c) $\tau = \tau_3$ (d) $\tau = \tau_4$

FIGURE 32. Ordinary resonance cone and extraordinary sphere. Evolution in function of τ: (a) $\tau_1 \sim \tau_0^-$; (b) $\tau_1 < \tau_2$; (c) $\tau_2 < \tau_3$; (d) $\tau_4 \sim \min\big(\mathbf{b}_e\,;\,\kappa\big)$.

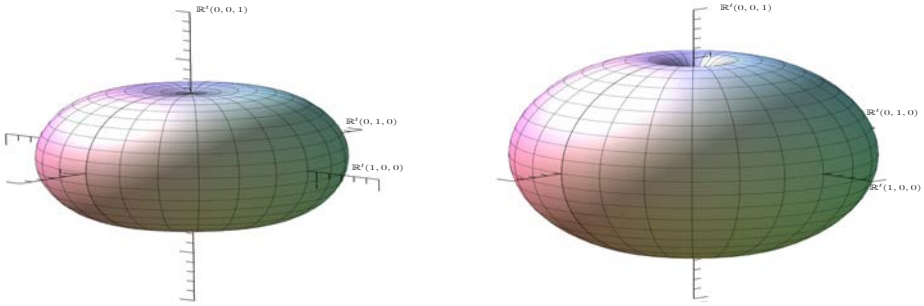

(a) $\tau = \tau_1$ (b) $\tau = \tau_2$

FIGURE 33. Extraordinary sphere. Evolution in function of τ:
(a) $\tau_1 \sim \min\big(\,\mathbf{b}_e\,;\,\kappa\,\big)$; (b) $\tau_2 \sim \max\big(\,\mathbf{b}_e\,;\,\kappa\,\big)$.

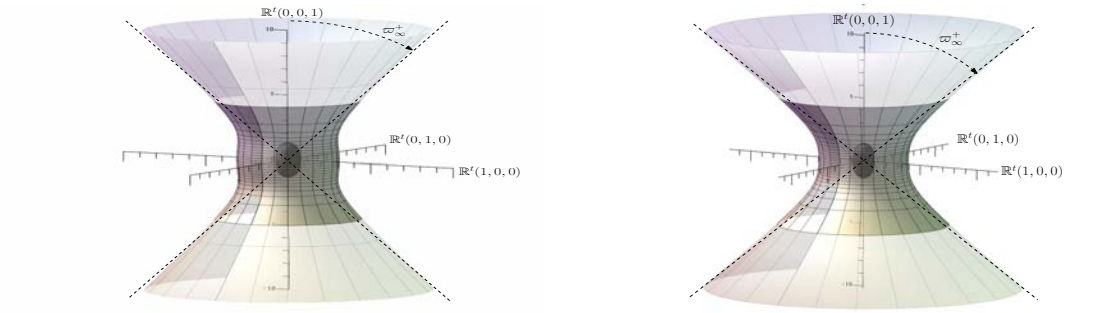

(a) $\tau = \tau_1$ (b) $\tau = \tau_2$

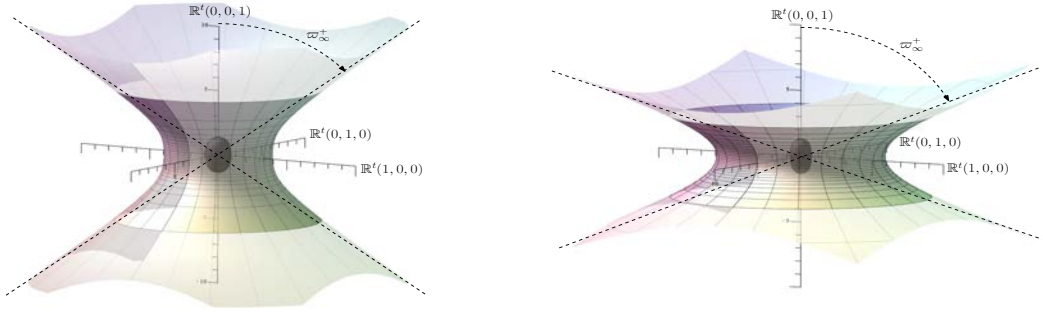

(c) $\tau = \tau_3$ (d) $\tau = \tau_4$

FIGURE 34. Extraordinary resonance cone and ordinary sphere. Evolution in function of τ: (a) $\tau_1 \sim \max\big(\mathbf{b}_e, \kappa\big)$; (b) $\tau_1 < \tau_2$; (c) $\tau_2 < \tau_3$; (d) $\tau_4 \sim \sqrt{\mathbf{b}_e^2 + \kappa^2}$.

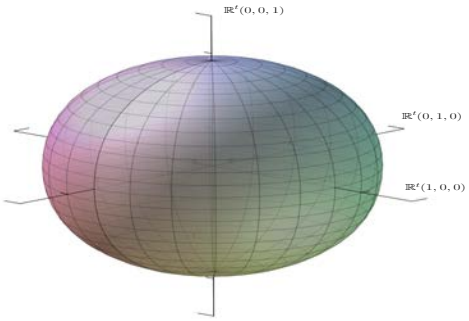

FIGURE 35. The ordinary sphere for $\tau \in \left[\sqrt{\mathbf{b}_e^2 + \kappa^2}, \tau_0^+(\mathbf{x})\right]$.

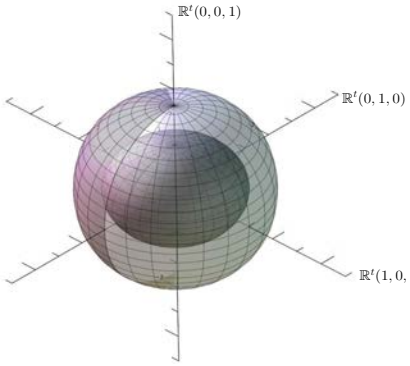

FIGURE 36. The extraordinary sphere nested into the ordinary sphere, for $\tau \gtrsim \tau_0^+(\mathbf{x})$.

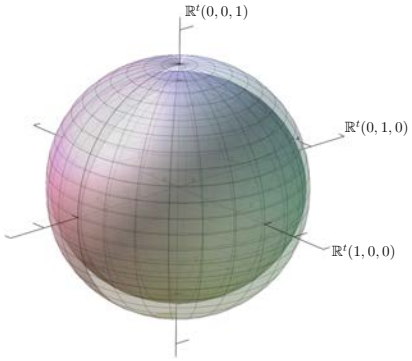

FIGURE 37. Asymptotic merge of the ordinary and extraordinary spheres, for $\tau \gg \tau_0^+(\mathbf{x})$.

B.2. Ordinary resonance cone together with an extraordinary sphere

This paragraph is concerned with the configuration that has been highlighted in Section B.1, paragraph d), see also Figure 32. From Lemma 2.3.15, case *ii)*, it is clear that when $\tau \in \left[\tau_0^-(\mathbf{x}), \max\left(\mathbf{b}_e(\mathbf{x})\,;\,\kappa(\mathbf{x})\right)\right]$, the set $\boldsymbol{\mathcal{V}}_x(\mathbf{x},\tau)$ is a bounded connected set, which is homeomorphic to a sphere. Similarly, when $\tau \in \left[0, \min\left(\mathbf{b}_e(\mathbf{x})\,;\,\kappa(\mathbf{x})\right)\right]$, we have already seen that the set $\boldsymbol{\mathcal{V}}_o(\mathbf{x},\tau)$ consists of an ordinary resonance cone, see Definition 2.3.9.

As already stated in Paragraph 2.3.4.2, these two situations can occur simultaneously. In fact, in the case where $\kappa(\mathbf{x}) < \sqrt{2}\,\mathbf{b}_e(\mathbf{x})$, we have $\tau_0^-(\mathbf{x}) < \min\left(\mathbf{b}_e(\mathbf{x})\,;\,\kappa(\mathbf{x})\right)$ (Lemma 2.3.10). Thefore, when $\kappa(\mathbf{x}) < \sqrt{2}\,\mathbf{b}_e(\mathbf{x})$ and $\tau \in \left[\tau_0^-(\mathbf{x}), \min\left(\mathbf{b}_e(\mathbf{x})\,;\,\kappa(\mathbf{x})\right)\right]$, the set $\boldsymbol{\mathcal{V}}(\mathbf{x},\tau)$ is composed of an ordinary resonance cone and an extraordinary sphere.

The simultaneous presence of the ordinary resonance cone $\boldsymbol{\mathcal{V}}_o(\mathbf{x},\tau)$ and the extraordinary sphere $\boldsymbol{\mathcal{V}}_x(\mathbf{x},\tau)$ is represented on Figure 32. Figure 32 is also interesting because it well illustrates the evolution of $\boldsymbol{\mathcal{V}}_o(\mathbf{x},\tau)$ and $\boldsymbol{\mathcal{V}}_x(\mathbf{x},\tau)$ in function of τ. On the one hand, the function $\varpi_\infty^-(\mathbf{x},\cdot)$ is a decreasing function of τ, which accounts for the narrowing from (a) to (d) of the ordinary resonance cone. On the other hand, since $g_-(\mathbf{x},\varpi,\cdot)$ is an increasing function, the radius of the extraordinary sphere is growing from (a) to (d).

B.3. From the extraordinary sphere to the simultaneous presence of the extraordinary resonance cone and the ordinary sphere

B.3.1. **Transition from the extraordinary sphere to the extraordinary resonance cone.** In this paragraph, we explain how the transition occurs between the extraordinary sphere and the extraordinary resonance cone. To do so, we rely on Figure 38 below.

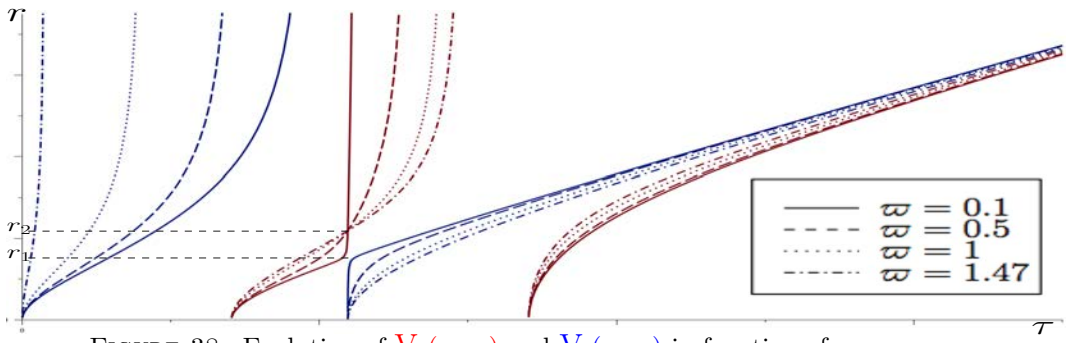

Figure 38. Evolution of $\mathrm{V}_x(\mathbf{x},\varpi)$ and $\mathrm{V}_o(\mathbf{x},\varpi)$ in function of ϖ. Asymptotic behaviour when $\varpi \to 0$ (see $\varpi = 0.1 \sim 0$) and $\varpi \to \pi/2$ (see $\varpi = 1.47 \sim \pi/2$)

On Figure 38, fix $\tau \lesssim \max(\mathbf{b}_e\,;\,\kappa)$ and consider a vertical half line with abscissa τ. Then, the limit when ϖ goes to 0 of the function $\sqrt{g_-}(\mathbf{x},\varpi,\tau)$ (represented by the red curve on Figure 38) is close to the value r_1. On the contrary, when ϖ is close to $\pi/2$, the function $\sqrt{g_-}(\mathbf{x},\varpi,\tau)$ is close to the value r_2. Therefore, since $r_1 < r_2$, the set $\boldsymbol{\mathcal{V}}_o(\mathbf{x},\tau)$ has a cavity in the direction $\varpi = 0$. This can clearly be seen on Figure 33(b). When $\tau = \max(\mathbf{b}_e\,;\,\kappa)$, this cavity degenerates into a vertical line which is composed of both ordinary and extraordinary component. This mixing has been studied more thoroughly in Paragraph 2.3.3.3. Finally, passing from $\tau = \max(\mathbf{b}_e\,;\,\kappa)$ to $\tau \gtrsim \max(\mathbf{b}_e\,;\,\kappa)$, the vertical segment between r_1 and r_2 disappears, whereas the half vertical line above r_2 gives rise to the extraordinary resonance cone.

B.3.2. **Extraordinary resonance cone together with an ordinary sphere.** The extraordinary resonance cone and the ordinary sphere occur when $\tau \in \big[\max(\mathbf{b}_e,\kappa), \sqrt{\mathbf{b}_e^2+\kappa^2}\,\big]$ and $\tau \in [\kappa(\mathbf{x}),+\infty[$ respectively. Therefore, for any value of the parameters $\mathbf{b}_e(\mathbf{x})$ and $\kappa(\mathbf{x})$ and $\tau \in \big[\max(\mathbf{b}_e,\kappa), \sqrt{\mathbf{b}_e^2+\kappa^2}\,\big]$, an ordinary sphere is located inside the extraordinary resonance cone. In the frequency region delimited by the brown frame on Figure 30, this corresponds to the simultaneous presence of the two branches $\mathrm{V}_x^-(\mathbf{x},\varpi)$ and $\mathrm{V}_o^+(\mathbf{x},\varpi)$.

As before, we can illustrate the evolution of $\boldsymbol{\mathcal{V}}_x(\mathbf{x},\tau)$ and $\boldsymbol{\mathcal{V}}_o(\mathbf{x},\tau)$ in function of τ. On the one hand, as τ approaches the value $\sqrt{\mathbf{b}_e^2+\kappa^2}$, the function $\varpi_\infty^+(\cdot)$ goes to $\frac{\pi}{2}$. As can be seen, this implies the enlargement of the extraordinary resonance cone. On the other hand, the function $g_+(\mathbf{x},\varpi,\cdot)$ is increasing. This corresponds in fact to a growth of the ordinary sphere radius. This second effect is not perceptible at the level of Figure 34. This is due to a change of scale when passing from the situations (a) to (d).

APPENDIX C

Various calculations

C.1. End of the proof of Lemma 3.3.7

To prove Lemma 3.3.7, we first establish the Lipschitz property.

Lemma C.1.1. *Fix* $(m,i,j) \in \mathbb{Z} \times [\![1,3]\!]^2 \setminus \{(0,3,3)\}$ *and* $z \in]1,+\infty[$. *Then:*

$$\|\mathbf{T}_m^{i,j}(\cdot,z)\|_{Lip(\mathbb{R})} < +\infty\,. \tag{C.1.1}$$

Proof. Recall (3.3.36), and note that

$$\sqrt{z^2-1-y^2}\ \partial_y\zeta = -\xi_\perp\ \mathbf{b}_e(\mathbf{x})^{-1}\ y\ , \qquad \xi_\perp \neq 0\,.$$

For $|y| < \sqrt{z^2-1}$, compute:

$$\partial_y \mathcal{T}_m^{1,1}(y,z) = -2\ m^2\ y\ \frac{J_m(\zeta)\ J_m'(\zeta)}{\zeta}\,, \tag{C.1.2a}$$

$$\partial_y \mathcal{T}_m^{1,2}(y,z) = -i\,m\,y\ \left[J_m'(\zeta)^2 + J_m(\zeta)\,J_m''(\zeta) + \frac{J_m(\zeta)\,J_m'(\zeta)}{\zeta}\right], \tag{C.1.2b}$$

$$\partial_y \mathcal{T}_m^{1,3}(y,z) = \frac{m\,\mathbf{b}_e}{\xi_\perp}\ J_m^2(\zeta) - \frac{2\,m\,\xi_\perp}{\mathbf{b}_e}\ y^2\ \frac{J_m(\zeta)\,J_m'(\zeta)}{\zeta}\,, \tag{C.1.2c}$$

$$\partial_y \mathcal{T}_m^{2,2}(y,z) = -2\ y\ \zeta\ J_m'(\zeta)\ J_m''(\zeta) - 2\ y\ J_m'(\zeta)^2\,, \tag{C.1.2d}$$

$$\begin{aligned}\partial_y \mathcal{T}_m^{2,3}(y,z) = &-i\ \frac{\mathbf{b}_e}{\xi_\perp}\ \zeta\ J_m(\zeta)\ J_m'(\zeta)\\ &+i\ \frac{\xi_\perp}{\mathbf{b}_e}\ y^2\ \left[J_m'(\zeta)^2 + J_m(\zeta)\,J_m''(\zeta) + \frac{J_m(\zeta)\,J_m'(\zeta)}{\zeta}\right],\end{aligned} \tag{C.1.2e}$$

$$\partial_y \mathcal{T}_m^{3,3}(y,z) = 2\ y\ \left[J_m^2(\zeta) - y^2\ \frac{\xi_\perp^2}{\mathbf{b}_e^2}\ \frac{J_m(\zeta)\ J_m'(\zeta)}{\zeta}\right]. \tag{C.1.2f}$$

Since the matrix $\partial_y \mathcal{T}_m$ is skew-symmetric, we have also:

$$\partial_y \mathcal{T}_m^{2,1} = \partial_y \bar{\mathcal{T}}_m^{1,2}\,, \qquad \partial_y \mathcal{T}_m^{3,1} = \partial_y \bar{\mathcal{T}}_m^{1,3}\,, \qquad \partial_y \mathcal{T}_m^{3,2} = \partial_y \bar{\mathcal{T}}_m^{2,3}\,.$$

As long as $m \neq 0$, in view of (3.3.46b) and (3.3.46c), all the quantities $\partial_y \mathcal{T}_m^\star$ remain bounded when ζ goes to zero, or equivalently when y goes to $(\mp\sqrt{z^2-1})^\pm$. When $m=0$, the same applies because $J_0'(\zeta) = O(\zeta)$. As a consequence, the following one sided limits exist and are finite:

$$\lim_{y \to (\mp\sqrt{z^2-1})^\pm}\ \partial_y \mathcal{T}_m^{i,j}(y,z)\ < +\infty\,. \tag{C.1.3}$$

On the other hand, from the definition (3.3.38), we can infer that:

$$\|\mathbf{T}_m^{i,j}(\cdot,z)\|_{Lip(\mathbb{R})} = \|\partial_y \mathcal{T}_m^{i,j}(\cdot,z)\|_{L^\infty(]-\sqrt{z^2-1},\sqrt{z^2-1}[)}\,. \tag{C.1.4}$$

Since the function $\mathcal{T}_m^{i,j}(\cdot,z)$ is of class $\mathcal{C}^1$ on the interval $]-\sqrt{z^2-1},\sqrt{z^2-1}[$, combining (C.1.3) and (C.1.4), we get (C.1.1). □

To complete the proof of Lemma 3.3.7, we have to show the upper bounds (3.3.44) and (3.3.45).

Lemma C.1.2. *We have (3.3.44) and (3.3.45).*

Proof. To get (3.3.44) and (3.3.45), an important argument is that only a finite number of integers $m \in \mathbb{Z}$ contribute in the series (3.3.44) and (3.3.45). As a matter of fact, for $m \in \mathbb{Z}$ sufficiently large, namely:

$$|m| \geq M(z) := \mathbf{b}_e^{-1}\,\Big(|\xi_\parallel|\,(1+\sqrt{z^2-1}) + |\tau|\,z\Big)\,, \tag{C.1.5}$$

we have:

$$\forall\, y \in [-1,1]\,, \qquad \left| y - \frac{\tau\, z + m\,\mathbf{b}_e}{\xi_\parallel} \right| \geq \sqrt{z^2-1}\,.$$

Retain that

$$\forall\, |m| \geq M(z)\,, \qquad \forall\, y \in [-1,1]\,, \qquad \mathbf{T}_m^{i,j}(y,z) = 0\,.$$

Therefore, for all $(i,j) \in [\![1,3]\!]^2 \setminus \{(3,3)\}$, we have:

$$\begin{aligned} \sum_{m\in\mathbb{Z}} \|\mathbf{T}_m^{i,j}(\cdot,z)\|_{Lip([-1,1])} &= \sum_{|m|\leq M(z)} \|\mathbf{T}_m^{i,j}(\cdot,z)\|_{Lip([-1,1])} \\ &\leq \sum_{|m|\leq M(z)} \|\partial_y \mathcal{T}_m^{i,j}(\cdot,z)\|_{L^\infty(]-\sqrt{z^2-1},\sqrt{z^2-1}[)}\,. \end{aligned} \tag{C.1.6}$$

Similarly:

$$\sum_{m\in\mathbb{Z}^*} \|\mathbf{T}_m^{3,3}(\cdot,z)\|_{Lip([-1,1])} \leq \sum_{0<|m|\leq M(z)} \|\partial_y \mathcal{T}_m^{3,3}(\cdot,z)\|_{L^\infty(]-\sqrt{z^2-1},\sqrt{z^2-1}[)}\,. \tag{C.1.7}$$

For all $m \in \mathbb{N}$, the Bessel function of the first kind can be defined over the integral:

$$J_{-m}(\zeta) = (-1)^m\, J_m(\zeta)\,, \qquad J_m(\zeta) = \frac{1}{2\,\pi} \int_0^{2\,\pi} \cos\left(\zeta\,\sin t - m\,t\right)\,dt\,. \tag{C.1.8}$$

From (C.1.8) for $k=0$ and from (3.3.22b) for $k \in \{1,2\}$, we easily get:

$$\forall\, m \in \mathbb{Z}\,, \qquad \forall\, \zeta \in \mathbb{R}\,, \qquad \forall\, k \in \{0,1,2\}\,, \qquad |J_m^{(k)}(\zeta)| \leq 1\,. \tag{C.1.9}$$

Then, using (3.3.22a), we can obtain:

$$\forall\, m \in \mathbb{Z}^*\,, \qquad \forall\, \zeta \in \mathbb{R}\,, \qquad \left|\zeta^{-1}\,J_m(\zeta)\right| \leq 1\,. \tag{C.1.10}$$

For $m=0$, looking at (C.1.8), we can assert that:

$$\left|\zeta^{-1}\,J_0'(\zeta)\right| \leq 1\,. \tag{C.1.11}$$

Combining (C.1.8), (C.1.9), (C.1.10) and (C.1.11) at the level of (C.1.2), we see that:

$$|\partial_y \mathcal{T}_m^{i,j}(y,z)| \leq C\ (1+\zeta^2+m^2+|y|^3)\,,$$

where the constant C is uniform with respect to the variables (ζ, m, y). On the domains under consideration, we have:

$$|y| \leq \sqrt{z^2-1}\,, \qquad |\zeta| \leq |\xi_\perp|\ \mathbf{b}_e(\mathbf{x})^{-1}\ \sqrt{z^2-1}\,, \qquad |m| \leq |M(z)| \leq C\ (1+\sqrt{z^2-1})^2\,.$$

Thus, looking at (C.1.6), we can recover (3.3.44) and (3.3.45). □

C.2. End of the proof of Lemma 3.3.11

To prove Lemma 3.3.11, it suffices now to prove what follows.

Lemma C.2.1. *For all $(m,i,j) \in \mathbb{Z} \times [\![1,3]\!]^2$ and $z \in]1,+\infty[$, the derivative $\partial_z \mathscr{T}_m^{i,j}(z)$ exists. Moreover, we have:*

$$\exists\, C \in \mathbb{R}_+\,; \qquad \forall\, m \in \mathbb{Z}\,, \qquad \sup_{z\in]1,+\infty[}\ \sup_{1\leq i,j\leq 3} |\partial_z \mathscr{T}_m^{i,j}(z)| \leq C\ (m^2+1)\,. \tag{C.2.1}$$

Proof. Recall (3.3.64). Consider the auxiliary function:

$$\begin{array}{rcl} \mathrm{f}_m^{i,j}\ :]1,+\infty[\times]-1,1[& \longrightarrow & \mathbb{R} \\ (z,\mathrm{y}) & \longmapsto & \mathrm{f}_m^{i,j}(z,\mathrm{y}) := \sqrt{z^2-1}\ \mathcal{T}_m^{i,j}(\sqrt{z^2-1}\,\mathrm{y},z)\,, \end{array} \tag{C.2.2}$$

so that:

$$\mathscr{T}_m^{i,j}(z) = \mathbb{1}_{]1,+\infty[}(z)\ \frac{\partial_z \mathrm{F}^{\mathrm{d}}(z)}{z}\ \int_{-1}^{1} \mathrm{f}_m^{i,j}(z,\mathrm{y})\ d\mathrm{y}\,. \tag{C.2.3}$$

With $y = \sqrt{z^2-1}\,\mathrm{y}$, we find:

$$\zeta \equiv \zeta(z,\mathrm{y}) = \xi_\perp\ \mathbf{b}_e(\mathbf{x})^{-1}\ \sqrt{z^2-1}\ \sqrt{1-\mathrm{y}^2}\,, \tag{C.2.4}$$

as well as:

$$\mathrm{f}_m^{1,1}(z,\mathrm{y}) = \frac{\mathbf{b}_e^2}{\xi_\perp^2}\ m^2\ J_m^2(\zeta)\ \sqrt{z^2-1}\,, \tag{C.2.5a}$$

$$\mathrm{f}_m^{1,2}(z,\mathrm{y}) = \frac{\mathbf{b}_e}{\xi_\perp}\ i\ m\ J_m(\zeta)\ J_m'(\zeta)\ (z^2-1)\ \sqrt{1-\mathrm{y}^2}\,, \tag{C.2.5b}$$

$$\mathrm{f}_m^{1,3}(z,\mathrm{y}) = \frac{\mathbf{b}_e}{\xi_\perp}\ m\ J_m^2(\zeta)\ (z^2-1)\ \mathrm{y}\,, \tag{C.2.5c}$$

$$\mathrm{f}_m^{2,2}(z,\mathrm{y}) = J_m'(\zeta)^2\ (z^2-1)^{3/2}\ (1-\mathrm{y}^2)\,, \tag{C.2.5d}$$

$$\mathrm{f}_m^{2,3}(z,\mathrm{y}) = -\,i\ J_m(\zeta)\ J_m'(\zeta)\ (z^2-1)^{3/2}\ \mathrm{y}\ \sqrt{1-\mathrm{y}^2}\,, \tag{C.2.5e}$$

$$\mathrm{f}_m^{3,3}(z,\mathrm{y}) = J_m^2(\zeta)\ (z^2-1)^{3/2}\ \mathrm{y}^2\,. \tag{C.2.5f}$$

Fix $(m,i,j) \in \mathbb{Z}\times[\![1,3]\!]^2$. We will drop the reference to (m,i,j) when it is not necessary to mention it. On the interval $]1,+\infty[$, the function $z \longmapsto z^{-1}\,\partial_z \mathrm{F}^{\mathrm{d}}(z)$ is of class $\mathcal{C}^\infty$. Thus,

at the level of (C.2.3), it suffices to look at the parameter-dependent integral:

$$]1,+\infty[\ni z\longmapsto\int_{-1}^{1}\mathrm{f}_m^{i,j}(z,\mathrm{y})\,d\mathrm{y}\,.$$

In order be able to apply the Leibniz's rule for differentiation under the integral sign, we can check the following conditions:

(i) For all $z>1$, the function $\mathrm{y}\longmapsto\mathrm{f}(z,\mathrm{y})$ is integrable on $]-1,1[$;
(ii) For all $\mathrm{y}\in]-1,1[$, the function $z\longmapsto\mathrm{f}(z,\mathrm{y})$ is of class C^1 on $]1,+\infty[$;
(iii) The function $(z,\mathrm{y})\longmapsto\partial_z\mathrm{f}(z,\mathrm{y})$ is bounded on every set of the form $K\times]-1,1[$, where K is a compact subset of $]1,+\infty[$.

Below, we perform the verification work step by step.

(i) Fix $z\in]1,+\infty[$. In view of (3.3.35) and (3.3.36), the function $\mathcal{T}_m^{i,j}(\cdot,z)$ is continuous on the interval $]-1,1[$. In view of (C.2.2), this also holds true for $\mathrm{f}_m^{i,j}(z,\cdot)$.

(ii) Fix $\mathrm{y}\in]-1,1[$. On the one hand, the function $\zeta(\cdot,\mathrm{y})$ is smooth. On the other hand, the Bessel function $J_m(\cdot)$ is analytic on $\mathbb{R}$. In view of (C.2.5), the function $z\longmapsto\mathrm{f}(z,\mathrm{y})$ is therefore of class C^1 on $]1,+\infty[$.

(iii) We have to compute $D_m^{i,j}(z,\mathrm{y}):=\partial_z\mathrm{f}_m^{i,j}(z,\mathrm{y})$. Since the matrix D is skew-symmetric, it is enough to compute $D_m^{i,j}$ when $i\leq j$. Use (C.2.4) and (C.2.5) in order to obtain:

$$D_m^{1,1}(z,\mathrm{y})=\frac{\mathbf{b}_e^2}{\xi_\perp^2}\,\frac{z}{\sqrt{z^2-1}}\,m^2\,J_m^2(\zeta)+2\,\frac{\mathbf{b}_e}{\xi_\perp}\,z\,m^2\,J_m(\zeta)\,J_m'(\zeta)\,\sqrt{1-\mathrm{y}^2}\,, \tag{C.2.6a}$$

$$\begin{aligned}D_m^{1,2}(z,\mathrm{y})&=2\,i\,\frac{\mathbf{b}_e}{\xi_\perp}\,z\,m\,J_m(\zeta)\,J_m'(\zeta)\,\sqrt{1-\mathrm{y}^2}\\&\quad+i\,z\,\sqrt{z^2-1}\,m\,\big[J_m'(\zeta)^2+J_m(\zeta)\,J_m''(\zeta)\big]\,(1-\mathrm{y}^2)\,,\end{aligned} \tag{C.2.6b}$$

$$D_m^{1,3}(z,\mathrm{y})=2\,\frac{\mathbf{b}_e}{\xi_\perp}\,z\,m\,J_m^2(\zeta)\,\mathrm{y} \tag{C.2.6c}$$

$$+2\,z\,\sqrt{z^2-1}\,m\,J_m(\zeta)\,J_m'(\zeta)\,\mathrm{y}\,\sqrt{1-\mathrm{y}^2}\,, \tag{C.2.6d}$$

$$\begin{aligned}D_m^{2,2}(z,\mathrm{y})&=3\,z\,\sqrt{z^2-1}\,J_m'(\zeta)^2\,(1-\mathrm{y}^2)\\&\quad+2\,\frac{\xi_\perp}{\mathbf{b}_e}\,z\,(z^2-1)\,J_m'(\zeta)\,J_m''(\zeta)\,(1-\mathrm{y}^2)^{3/2}\,,\end{aligned} \tag{C.2.6e}$$

$$\begin{aligned}D_m^{2,3}(z,\mathrm{y})&=-3\,i\,z\,\sqrt{z^2-1}\,J_m(\zeta)\,J_m'(\zeta)\,\mathrm{y}\,\sqrt{1-\mathrm{y}^2}\\&\quad-i\,\frac{\xi_\perp}{\mathbf{b}_e}\,z\,(z^2-1)\,\big[J_m'(\zeta)^2+J_m(\zeta)\,J_m''(\zeta)\big]\,\mathrm{y}\,(1-\mathrm{y}^2)\,,\end{aligned} \tag{C.2.6f}$$

$$\begin{aligned}D_m^{3,3}(z,\mathrm{y})&=3\,z\,\sqrt{z^2-1}\,J_m^2(\zeta)\,\mathrm{y}^2\\&\quad+2\,\frac{\xi_\perp}{\mathbf{b}_e}\,z\,(z^2-1)\,J_m(\zeta)\,J_m'(\zeta)\,\mathrm{y}^2\,\sqrt{1-\mathrm{y}^2}\,.\end{aligned} \tag{C.2.6g}$$

All these functions $D_m^{i,j}(\cdot)$ are clearly bounded on $K\times]-1,1[$, at least if K is compact which is contained in $]1,+\infty[$. Since the three conditions (i), (ii) and (iii) are satisfied, we

can assert that:

$$\partial_z \left(\int_{-1}^{1} \mathrm{f}_m^{i,j}(z,\mathrm{y})\ d\mathrm{y} \right) = \int_{-1}^{1} D_m^{i,j}(z,\mathrm{y})\ d\mathrm{y}\,. \tag{C.2.7}$$

It follows that:

$$\exists\, C \in \mathbb{R}_+\,; \quad \forall\, z \in]1,+\infty[\,, \quad |\partial_z \mathscr{T}_m^{i,j}(z)| \leq C \sup_{(z,\mathrm{y})\in]1,+\infty[\times]-1,1[} |D_m^{i,j}(z,\mathrm{y})|\,. \tag{C.2.8}$$

Exploit (C.1.9) to control the $J_m^{(k)}(\zeta)$ uniformy with respect to $m \in \mathbb{Z}$. In view of (C.2.6), as indicated in (C.2.1), the growth in m is at most m^2. When z goes to $1+$, the only term which may be problematic is $D_m^{1,1}(z,\mathrm{y})$, see (C.2.6a). For $m = 0$, there is nothing to do. For $|m| = 1$, exploit (3.3.46b) together with (C.2.4) to see that $|D_m^{1,1}(z,\mathrm{y})|$ remains bounded. For $|m| > 1$, the expression $|D_m^{1,1}(z,\mathrm{y})|$ simply tends to zero when z goes to $1+$. By this way, we recover (C.2.1). □

Résumé

Cette thèse décrit comment les ondes électromagnétiques se propagent dans les plasmas magnétisés, lorsque les fréquences sollicitées sont proches de la fréquence électron cyclotron. Elle porte sur l'analyse mathématique des variétés caractéristiques qui sont associées à des systèmes de type Vlasov-Maxwell relativiste avec paramètres rapides.

La première partie s'intéresse aux plasmas froids des magnétosphères planétaires. On explique comment obtenir les relations de dispersion dans le cas d'un dipôle magnétique. Cela conduit à l'étude détaillée de certaines variétés algébriques de l'espace cotangent : les cônes et les sphères dits ordinaires et extraordinaires. La description géométrique de ces cônes et de ces sphères donne accès à une classification complète des ondes électromagnétiques susceptibles de se propager. Diverses applications sont proposées, concernant l'équation eikonale et l'absence de propagation en mode parallèle, ou encore concernant la structure des ondes dites en mode siffleur.

La seconde partie porte sur la modélisation des plasmas chauds, typiquement ceux qui sont mis en jeu dans les tokamaks. On prouve dans un contexte réaliste que la propagation des ondes électromagnétiques s'effectue au travers d'un tenseur dielectrique. Ce tenseur est obtenu via une analyse fine des résonances cinétiques qui sont issues des interactions entre les particules (Vlasov) et les ondes (Maxwell). Il s'exprime comme une somme infinie d'intégrales singulières, faisant intervenir l'opérateur de Hilbert. Le sens mathématique de la formule donnant accès à ce tenseur est rigoureusement justifié.

Abstract

This thesis describes how electromagnetic waves propagate in magnetized plasmas, when the frequencies are in a range around the electron cyclotron frequency. It focuses on the mathematical analysis of the characteristic varieties which are associated with relativistic Vlaosv-Maxwell systems involving fast parameters.

The first part is concerned with cold plasmas issued from planetary magnetospheres. We explain how to obtain the dispersion relations in the case where the magnetic field is given by a dipole model. This leads to the detailed study of some algebraic varieties from the cotangent space: the so-called ordinary and extraordinary cones and spheres. The geometrical description of these cones and spheres gives access to a complete classification of the electromagnetic waves which can propagate. Various applications are proposed, concerning the eikonal equation and the absence of purely parallel propagation, or about the structure of whistler waves.

The second part focuses on the modelling of hot plasmas, typically like those involved in tokamaks. We prove in a realistic context that the propagation of electromagnetic waves is governed by some dielectric tensor. This tensor is obtain via some careful analysis of the kinetic resonances, which are issued from the interactions between the particles (Vlasov) and the waves (Maxwell). It can be expressed as an infinite sum of singular integrals, involving the Hilbert transform. The mathematical meaning of the formula defining this tensor is rigorously justified.